Cranfield University

Allison L. Bennington

Application of Multi-Spectral Remote Sensing for Crop Discrimination in Afghanistan

School of Applied Sciences

PhD Thesis

Cranfield University

School of Applied Sciences

PhD Thesis

Academic Year 2008

Allison L. Bennington

Application of Multi-Spectral Remote Sensing for Crop Discrimination in Afghanistan

Supervisor: Prof. Dr. J.C. Taylor

March 2008

Abstract

The spectral properties of poppy and other annual crops vary considerably throughout their growth and development. Until the publication of this research the spectral signature of poppy and its contrast with neighbouring crops in Afghanistan was undefined. The aim of this work was to investigate the application of remote sensing to discriminate poppy from other cover types using spectral signatures obtained from the analysis of multi-spectral imagery. The consistency of discrimination through time for different geographical regions was of particular interest.

A review of previous poppy studies identified weaknesses with existing methods used to monitor poppy and provide reference data to validate resulting maps. Weaknesses were in the main due to the limited availability of quantifiable knowledge on the spectral-temporal properties of cover types and the lack of accuracy measures necessary to validate poppy identification. To overcome the lack of quantitative knowledge this research characterises the spatial and temporal variability of poppy spectral response patterns.

A methodology was developed to acquire multi-temporal IKONOS images, aerial photographs and ground data covering two growth cycles across a range of sites in Afghanistan. Optimum techniques were developed to facilitate the collection of training pixels for each cover type to satisfy the assumptions of the supervised Maximum Likelihood classification (MLC). Spectral signatures of cover types were examined using the Jeffries Matusita distance measure to identify signature separability and predict classification accuracy. The accuracy of each MLC was assessed using error matrices, Kappa statistics and regression.

Results confirm that sufficient spectral contrast exists between poppy and other crops during poppy flowering which enables accurate discrimination. A relationship was found between overall spectral separability and classification accuracy, showing separability can be used to predict classification accuracy at flowering. At other times insufficient differences exist between the spectral reflectance of other crops and poppy. Multi-temporal image classifications achieved greater accuracy than their corresponding single date classifications in the majority of cases studied.

Acknowledgements

The work presented in this thesis could not have been undertaken without sponsorship and funding from the Ministry of Defence and the Foreign and Commonwealth Office for which I am very grateful.

I am indebted to both my supervisor Prof. Dr. John Taylor and to Dr. Simon Trigg for their guidance, support, invaluable advice, dedication and enthusiasm. I would also like to thank Dr. Toby Waine for his helpful comments on the first draft, his unwavering assistance, advice and support. I would also like to give my heartfelt thanks to Grahame Juniper and Dan Simms for their assistance, support and interest. I also wish to thank Hakan Demiburken from UNODC for his cooperation and support from Vienna and Afghanistan.

I would also like to thank my family and friends whose support and encouragement were invaluable throughout. Finally, I would like to express my sincere and deepest gratitude to my darling husband Ben, who encouraged me to complete my PhD against all the odds and inspired me to the very end. Without his dedication, enthusiasm and love, his patience, humour and kindness, I would not have had the courage to complete what I started so many years ago. I am deeply and forever in his debt and thank him for giving up so much to allow me to achieve my dream.

Abstract ..... **ii**

1. Introduction **1**

1.1 Background 1

1.2 Role of Remote Sensing 3

1.3 Poppy Detection Project (PDP) 4

1.3.1 Eradication Activities 5

1.4 Review of Opium Poppy Surveys 6

1.4.1 Key Points 7

1.4.2 Analysis of Surveys 18

1.5 Aims and Objectives 26

1.5.1 Areas of Investigation 27

1.6 Thesis Structure 28

2. Fundamentals of Multi-Spectral Remote Sensing **31**

2.1 Introduction 31

2.2 Concept of a Spectral Signature 33

2.3 General Spectral Characteristics of Vegetation and Bare Soil 35

2.3.1 Vegetated Surface 35

2.3.2 Spectral Reflectance Properties of Green Leaves 35

2.3.3 Spectral Characteristics of Bare Soil 41

2.3.4 Illumination Effects – Bidirectional Reflectance 44

2.4 Cropping Calendars 45

2.5 Visual Interpretation Fundamentals 46

2.5.1 Recognition Elements 46

2.5.2 Computer Processing for Photo Interpretation 48

2.5.3 Discussion of Photo-Interpretation 49
2.6 Digital Image Processing Fundamentals – Classification 50
2.6.1 Supervised Classification 52
2.6.2 Unsupervised Classification 56
2.6.3 Discussion 61
2.7 Factors Influencing Classification 62
2.7.1 Training/Evaluation Data 63
2.7.2 Assessing Training Data 66
2.7.3 Sensor Capabilities 73
2.7.4 The Ground Segment 77
2.8 Assessment of Classification 78
2.8.1 The Error Matrix 79
2.8.2 Kappa Statistic 81
2.8.3 Regression 82
2.9 Chapter Summary 83
3. Factors Influencing the Spectral Signature of Poppy 84
3.1 Afghan Environmental Factors 85
3.1.1 Topography 85
3.1.2 Climate 87
3.1.3 Hydrology 88
3.2 Agricultural Practices in Afghanistan 89
3.2.1 Irrigation 89
3.2.2 Preventing Disease and Pests 93
3.2.3 Application of Fertilisers 94

3.2.4 Mechanisation 95
3.2.5 Summary 95
3.3 Typical Afghan Crops 96
3.3.1 Cropping Calendars - Sowing and Harvesting Dates 103
3.4 Afghan Poppy Farming Practises 105
3.4.1 Thinning, Weeding, Nipping 105
3.4.2 Harvesting 106
3.5 The Poppy Growth Cycle 108
3.6 Experiences from UK Field Work 114
3.6.1 Plant Morphology and Soil Background 114
3.6.2 Local Environmental Factors 118
3.6.3 Farming Practise 121
3.6.4 Summary 122
3.7 Discussion 124
3.8 Chapter Summary 125
4. Acquisition and Pre-processing of Multi-temporal Datasets 127
4.1 Selection of Suitable Study Areas 127
4.2 Data Collection Plan 130
4.2.1 Summary of 2004 Data Collection Plan 133
4.3 Data Acquired - 2004 134
4.3.1 Forecasting Crop Growth Cycles using MODIS Imagery 139
4.4 Data Collection Plan - 2005 142
4.4.1 Data Acquired 2005 143
4.5 Collection Gaps – Revision of Training Sites 145

4.5.1 Summary of Study Areas 148
4.6 Data Preparation 148
4.6.1 Identification of Ground Data Errors 149
4.6.2 Development of a UN Field Data Collection Manual 155
4.6.3 Identification of Unknown Field Parcels 156
4.6.4 Surrogate Ground Data 161
4.6.5 IKONOS image-to-image Registration 161
4.6.6 Multi-temporal Image Datasets 163
4.7 Chapter Summary 163
5. Selection of Training and Evaluation Pixels 166
5.1 Investigation into Spatial Autocorrelation 167
5.2 Revised Experimental Methodology – Training Area Expansion 173
5.2.1 Identification and Removal of Mixed Pixels 174
5.2.2 Summary of Training and Evaluation Data Selection 178
5.3 Determining Spectral Separability and Classification Accuracy 179
5.3.1 Spectral Separability Measures 179
5.3.2 Determining Classification Accuracy 180
5.3.3 Multi-temporal Classification Accuracy 180
5.3.4 Determining a Link between Separability and Classification Accuracy 181
5.4 Chapter Summary 181
6. Results 183
6.1 Imagery Acquired 183
6.2 Spectral Separability 185
6.2.1 Visual Analysis – SCPs 185

6.2.2 Statistical Analysis – JM Distance 193
6.2.3 Summary of Spectral Separation 199
6.3 Classification 199
6.3.1 Classification Accuracy 202
6.3.2 Overall Classification Accuracy 204
6.3.3 Significance of Single Image Classifications 213
6.3.4 Poppy Users Accuracy 215
6.4 Relationship between Spectral Separability and Classification Accuracy 221
6.4.1 Chapter Summary 225
7. Multi-temporal Results 227
7.1 Visual Analysis 227
7.2 Overall Multi-temporal Classification Accuracy 229
7.2.1 Summary 231
7.2.2 Kappa Statistic 231
7.3 Multi-temporal Poppy User's Accuracy 234
7.3.1 Poppy User's Accuracy Summary 235
7.4 Chapter Summary 236
8. Summary and Discussion 237
8.1 Factors Influencing Data Collection 237
8.1.1 Site Selection 237
8.1.2 Image Collection 239
8.1.3 Ground Data Acquisition 240
8.1.4 Surrogate Ground Data 240
8.1.5 Predicting Data Acquisition Times 241

8.1.6 Summary 241
8.2 Factors Influencing Image Processing 241
8.2.1 Image Registration 241
8.2.2 Choice of Classifier 242
8.2.3 Use of Multi-temporal Imagery 243
8.3 Causes of Spectral Variability and their Consequences 244
8.3.1 Crop Maturity 244
8.3.2 Farming Practice 245
8.3.3 Disease and Drought 247
8.3.4 Number of Different Varieties of Crops Grown 247
8.3.5 Chapter Summary 248
9. Conclusions, Limitations and Recommendations 249
9.1 Objective 1 249
9.2 Objective 2 251
9.3 Objective 3 252
9.4 Objective 4 252
9.5 Limitations 253
9.6 Recommendations for Future Work 254
9.7 Summary of Key Points 256
References 258
Appendix A Technical Details 267
Appendix B UN Ground Survey Instructions 272
Appendix C Spectral Separability Data 297
Appendix D Supervised Classifications 346

Appendix E Classification Accuracy 347

List of Figures

Figure 1-1 - Annual Opium Poppy Estimates - US v UN. Sources: Wikipedia 2010/ UNODC, 2005. 2

Figure 1-2 - UNODC's Classification Methodology, after UNODC, 2005 15

Figure 2-1 – Typical Spectral Response Curves of Basic Cover Types (Lillesand and Kiefer, 1987) 34

Figure 2-2 – Typical reflectance and absorption characteristics of green vegetation (Adapted from Swain and Davis, 1978) 37

Figure 2-3 - Chlorophyll in Leaves (George State University, 2010) 37

Figure 2-4 - Spectral reflectance curves for Chelsea sand in three moisture-content groupings (Hoffer, 1978) 42

Figure 2-5 – Example of a Spectral Coincidence Plot. Blue (Band 1), green (Band 2), red (Band 3), near infrared (Band 4) displayed using 2 Standard Deviations. Class Ranges indicated by 68

Figure 2-6 – Example of a bi-spectral plot of different land cover classes with ellipses drawn around two distinct and separate classes 69

Figure 2-7 - Relationship between the spectral bands of the IKONOS and Zeiss sensors being considered and general vegetation spectral profile (after Swain and Davis, 1978).... 74

Figure 3-1 - Map of the internal provincial boundaries in Afghanistan. 85

Figure 3-2 – Flood irrigation used in individual plots within a flat field, Nangahar District, Afghanistan (courtesy of UNODC) 91

Figure 3-3 - Ground photos of raised soil embankments in Achin District, Afghanistan, courtesy of UNODC 91

Figure 3-4 - Ground photo of permanent within-field irrigation bunds in Nangahar Province, Afghanistan courtesy of UNODC 92

Figure 3-5 - Wheat at emergence (a) at leaf production (b) 96

Figure 3-6 – Wheat - stem elongation (a) heading (b) at anthesis (c) 96

Figure 3-7 – Wheat at senescence 97
Figure 3-8 - Barley (a) tillering (b) stem elongation 98
Figure 3-9 - Barley at flowering 98
Figure 3-10 - Barley at senescence 98
Figure 3-11 - Maize (a) emergence (b) leaf production (c) stem extension 99
Figure 3-12 - Maize at (a) flowering and (b) at senescence 99
Figure 3-13 – Onion at a mature growth stage 100
Figure 3-14 – Watermelon at an early growth stage 100
Figure 3-15 – Courgette at flowering 101
Figure 3-16 - Alfalfa 102
Figure 3-17 – Vineyard 102
Figure 3-18 - Afghan labourer lancing a capsule, photograph courtesy of UNODC 106
Figure 3-19 - Afghan lancing equipment, photograph courtesy of UNODC 106
Figure 3-20 - Scored poppy capsules in Afghanistan. Photograph courtesy of UNODC .. 107
Figure 3-21 - Dried capsule, photograph courtesy of UNODC 108
Figure 3-22 - Poppy at the cabbage stage (a-c) (PDP) 111
Figure 3-23 - Poppy at (a) stem elongation and flower bud development (b) hook stage and (c) at flowering (PDP) 112
Figure 3-24 - Poppy at (a) Maturing capsule, (b) start of Senescence, and (c) end of senescence (PDP) 113
Figure 3-25 - Poppy growth cycle (not to scale) Photos: PDP 113
Figure 3-26 - Cabbage stage - (a) ground photograph and (b) aerial photograph acquired in Field 34 on 11 Jun 2004 (PDP) 115
Figure 3-27 - Flowering stage - ground photograph acquired looking across Field 34 on 28 Jun 2004 (PDP) 115

Figure 3-28 - Flowering stage - (a) ground photograph and (b) aerial photograph acquired in Field 34 on 28 Jun 2004 (PDP) 116

Figure 3-29 - Mature Capsule stage - (a) ground photograph and (b) aerial photograph acquired in Field 34 on 13 Jul 2004 (PDP) 117

Figure 3-30 - Senescence - (a) ground photograph and (b) aerial photograph acquired in Field 34 on 06 Aug 2004 (PDP) 117

Figure 3-31 - Generalised vegetation NDVI profile through time with approximate timings of poppy growth stages (after PDP, 2004) 120

Figure 3-32 – Field 34 on 28 Jun 2004. Poppy flowering (a) normal planting density and (b) high planting density (PDP) 121

Figure 3-33 - Influence of linear soil features - tractor tram-lines - on poppy spectral signature in Field 34 (a) ground photography at poppy flowering, (b) ADP at poppy senescence (PDP) 122

Figure 4-1 - Afghanistan Opium Poppy Cultivation - Source UNODC, 2003 128

Figure 4-2 - Approximate locations of UK imagery survey sites in Afghanistan 129

Figure 4-3 - Locations of three 250m x 250m ground data segments with field boundaries overlaid onto a 10 km x 10 km 4m resolution IKONOS image, acquired on 28 Apr 04 in Musa Quala District, Helmand Province. The image is displayed in true colour, i.e. RGB = bands 3, 2 and 1. 130

Figure 4-4 – MODIS NDVI profile of Nade-Ali District, Helmand Province. The green line indicates vegetation activity in the 2004 growth cycle; the red line indicates activity at the beginning of the 2005 growth cycle. 141

Figure 4-5 – Approximate locations of eventual UK study sites in Afghanistan 147

Figure 4-6 -IKONOS image of Held87 acquired 25 Apr 04 with ground data acquired on 11 Apr 04 overlaid. The image is displayed in true colour, i.e. RGB = bands 3, 2 and 1 at 4m spatial resolution. 150

Figure 4-7 - Nan11 S2 IKONOS image acquired on 29 Apr 04 at mid-end flowering with UN ground photographs acquired on 12 Apr 04 overlaid. 151

Figure 4-8 - Nan 2_S4 Dara-e-Nur District, Nangahar Province. Ground photographs acquired late in the growth cycle on 07 Jun 04 are overlaid onto an IKONOS image acquired 11 May 04. 153

Figure 4-9 – IKONOS image from Kand 073_S4, Daman District, Kandahar Province acquired on 26 Mar 05. Field labels are missing from the ground data. 154

Figure 4-10 - IKONOS image from Kand 073_S4, Daman District, Kandahar Province acquired on 26 Mar 05. Field labels have been photo-interpreted. 156

Figure 4-11 – Held87_S1 Nade-Ali District, Helmand Province. True colour Zeiss photography acquired on 17 Apr 04 from 20,000' at 60cm resolution. 157

Figure 4-12 - Held87_S1 Nade-Ali District, Helmand Province IKONOS imagery acquired on 25 Apr 04. True colour photography (3, 2, 1) at 4m resolution 158

Figure 4-13 Held87_S1 Nade-Ali District, Helmand Province. 1m resolution Panchromatic IKONOS image, 25 Apr 04 159

Figure 4-14 - Held87_S1 Nade-Ali District, Helmand Province. (a) Pan-sharpened IKONOS image, 25 Apr 2004 (b) un-sharpened true-colour IKONOS image. 160

Figure 5-1- Variogram illustrating the effects of spatial autocorrelation on IKONOS pixels, after PDP, 2005. Light blue–100% independence, red–95%, navy blue-90%, black dots, 85% and 75%, pink line 62%. 168

Figure 5-3 – FCC of a 4m IKONOS image of Held87 S2 25 Apr 04 with dot grid overlaid. 1 in 6 pixels selected by the dot grid matrix are enclosed within white circles giving a spacing of 24m between the centres of each selected pixel. 170

Figure 5-2 - True colour (bands 3, 2,1) and false colour (bands 4, 3, 2) composites of a 4m IKONOS image acquired on 25 Apr 04 showing the 250m x 250m Held87 S2 segment training area. 170

Figure 5-4 – FCC of a 4m IKONOS image of Held87 S2 25 Apr 04 with overlaid training and evaluation poppy pixels spaced 24m apart 171

Figure 5-5 - FCC 4m IKONOS sub-set of Held87 S2 25 Apr 04 with poppy evaluation pixels overlaid 172

Figure 5-6 – True and False Colour Composites of 17 May 04 IKONOS imagery showing the original Held87 S2 250m by 250m segment training area on true colour imagery (yellow square) - and the expanded 1000m by 1000m training area on false colour imagery. 174

Figure 5-7 - Mixed soil/poppy pixels highlighted in a FCC subset of a 4m IKONOS image from Held87 S2 25 Apr 04 176

Figure 5-8 - FCC subset of a 4m IKONOS image of Held87 S2 25 Apr 2004. Enlargement on the right shows wheat training pixels identified on the edge of wheat and poppy fields. 176

Figure 5-9 - Histogram of Poppy Training Pixels from Held115 S2 177

Figure 6-1 - 10 km by 10 km sites in (a) Nangahar Province, (b) Helmand Province and (c) Kandahar Province 184

Figure 6-2 - MODIS NDVI Profile for Held87 indicating the dates and approximate growth stages reached by the crops at the time of imaging 186

Figure 6-3 - Spectral Coincidence Plot from IKONOS imagery, Held87 on 16 Feb 05 at Stem Elongation (Band 1-blue, band 2–green, band 3–red and band 4–NIR). Class ranges indicated by 187

Figure 6-4- Spectral Coincidence Plot Held 87 on 21 Mar 05 at Beginning-mid Flowering, blue (Band 1), green (Band 2), red (Band 3), NIR (Band 4) displayed using 2 Standard Deviations. Class ranges are indicated by 189

Figure 6-5 - Spectral Coincidence Plot Held 87 on 25 Apr 04 at Mid-end of Flowering (Band 1-blue, band 2–green, band 3–red and band 4–NIR). Class ranges indicated by 191

Figure 6-6- Spectral Coincidence Plot Held 87 on 17 May 04 at end of Senescence (Band 1-blue, band 2–green, band 3–red and band 4-NIR band). Class ranges indicated by 192

Figure 6-7 - Supervised Classification of Nan25 from imagery dated 11 Apr 04 at mid-end flowering. Segment S1 enlargement is below the main image..... 200

Figure 6-8 - Supervised Classification of Nan25 from imagery dated 25 Apr 04 at end-flowering - beginning senescence with S4 subsets included below 201

Figure 6-9 % Overall Classification Accuracy and corresponding average JM Distance in Nangahar Province during the 2004 growth cycle 206

Figure 6-10 – Regression Analysis: Spectral Separability and % Overall Classification Accuracy for Nangahar Province, 2004 206

Figure 6-11- % Overall Classification Accuracy and corresponding average JM Distance in Helmand Province during the 2005 growth cycle 208

Figure 6-12 - Regression Analysis: Weak positive relationship between Spectral Separability and % overall Classification Accuracy in Helmand Province, 2005 209

Figure 6-13 - % Overall Classification Accuracy and corresponding average JM Distance in Helmand Province during the 2004 growth cycle 211

Figure 6-14- Regression Analysis: Strong positive relationship between Spectral Separability and % Overall Classification Accuracy in Helmand Province, 2004 212

Figure 6-15 – Single Date % Poppy Users Accuracy Results and Spectral Separability results, Nangahar Province, 2004 216

Figure 6-16 - Regression Analysis: Spectral Separability and % Poppy Users Accuracy for Nangahar Province, 2004 217

Figure 6-17 – Average JM Distance and Single Date % Poppy User's Accuracy Results, Helmand Province, 2005 218

Figure 6-18 – Regression Analysis: Spectral Separability and % Poppy User's Accuracy for Helmand Province, 2005 218

Figure 6-19– Single Date % Poppy User's Accuracy Results, Helmand Province, 2004 .. 219

Figure 6-20 – Regression Analysis: Spectral Separability and % Poppy User's Accuracy for Helmand Province, 2004 220

Figure 6-21 - Relationship between Spectral Separability and % Overall Classification Accuracy at Mid flowering–Beginning Senescence in Nangahar and Helmand Provinces, 2004 223

Figure 6-22 - Relationship between Spectral Separability and % Overall Classification Accuracy at Beginning-End Senescence in Nangahar and Helmand Provinces, 2004 224

Figure 6-23 - Relationship between JM Distance and % Overall Classification Accuracy at Stem Elongation-Mid Flowering in Helmand and Kandahar Provinces, 2005 225

Figure 7-1 - Multi-temporal classification of (a) Held115 05 with S3 location; (b) Held115 S3 05 classification, (c) Held115 S3 10 Feb 05 and (d) Held115 S3 21 Mar 05 228

List of Tables

Table 1-1 - Summary of Poppy Studies 7

Table 1-2 - Example of a logical post-classification look-up table (Shortepa District, Balkh Province), reproduced with permission from UNODC, 2005 17

Table 2-1 – Steps in Image Classification (Lu and Weng, 2007) 51

Table 2-2 - Range Indicators of Separability 72

Table 2-3 - Spectral bands of sensors used in the UK Poppy Detection Project 74

Table 2-4 - Spatial resolutions of sensors used in the UK Poppy Detection Project 75

Table 2-5 - Temporal and Radiometric Resolution of IKONOS and Zeiss Imagery 76

Table 2-6 - Radiometric Resolution Limitations and Advantages of 8-bit versus 11-bit 77

Table 3-1 - Afghan diseases and pests affecting poppy fields, after UNODC, 2005 93

Table 3-2 - Afghan autumn-sowing cropping calendar, after Dennis, Trutmann and Diab, 2002 103

Table 3-3 – Afghan spring-sowing cropping calendar, after Dennis, Trutmann and Diab, 2002 104

Table 3-4 - Flowering maturity, estimated from relative proportions of hooks, flowers and capsules 120

Table 4-1 - 2004 Imagery and Ground Survey Collection Plan 134

Table 4-2 - 2004 IKONOS Imagery Collection Received 136

Table 4-3 – 2004 Zeiss Collection Received 137

Table 4-4 -2004 Ground Survey Date per Segment per District Site 138

Table 4-5 - 2005 IKONOS Imagery Collection Requested (source: UNODC, 2005) and Received. 143

Table 4-6 – 2005 Zeiss Collection Requested and Received 144

Table 4-7 - 2005 Ground Survey Date per Segment per District Site 145

Table 4-8 – Data collected in Kandahar Province, 2005 148

Table 4-9 – IKONOS Images used in 2004 and 2005. 148

Table 5-1 – Comparison of Proportional Semi-variance against sampling rate achieved. 169

Table 5-2 – Number of training pixels collected per cover type in Nade-Ali (Held87) and Garmser (Held115) Districts, Helmand Province. 172

Table 5-3 – Comparison of the number of training pixels selected in Held87 in the new and old training areas 174

Table 5-4 - Training and Evaluation Pixels per Cover Type per District 178

Table 6-1 – Growth stages reached at the time of imaging in all locations 184

Table 6-2 - Growth stages reached at the time of image acquisitions in Held87 186

Table 6-3 - Summary of average JM distance between poppy and other classes in nine selected sites across Afghanistan in 2004 and 2005 194

Table 6-4 –Poppy Separability Ranking - results by growth stage 195

Table 6-5 - JM distance between poppy and other cover types 196

Table 6-6 - Error matrix for Nan25 11 Apr 04 – Mid-end Flowering 203

Table 6-7 - Error matrix for Nan29 11 Apr 04 – Mid-end Flowering 204

Table 6-8 - Summary of Overall Classification Accuracy and corresponding average JM Distance in Nangahar Province during the 2004 growth cycle. 205

Table 6-9 - Summary of Overall Classification Accuracy and corresponding Kappa coefficient in Helmand Province during the 2005 growth cycle 208

Table 6-10- Summary of Overall Classification Accuracy and corresponding Kappa coefficient in Helmand Province during the 2004 growth cycle 210

Table 6-11 - Summary of average JM Distance, overall Classification Accuracy and Kappa coefficient in Kandahar Province during the 2005 growth cycle 212

Table 6-12 – Results of Kappa Analysis – Test of Significance for Individual Image Classifications 214

Table 6-13 – Average JM Distance and Single Date % Poppy Users Accuracy Results, Nangahar Province, 2004 216

Table 6-14 – Average JM Distance and Single Date % Poppy Users Accuracy Results, Helmand Province, 2005 217

Table 6-15 – Single Date % Poppy User's Accuracy Results, Helmand Province, 2004 .. 219

Table 6-16 – Single Date % Poppy User's Accuracy Results Kandahar Province, 2005 .. 221

Table 6-17 – Spectral Separability and Classification Accuracy at Mid-flowering-Beginning Senescence in Helmand and Nangahar Provinces, 2004 222

Table 6-18 – Spectral Separability and Classification Accuracy at Beginning Senescence-End Senescence in Nangahar and Helmand Provinces, 2004 223

Table 7-1 - Mean Spectral Separability and Overall Classification Accuracy - Multi-Temporal Classification..... 230

Table 7-2 -– Results of Kappa Analysis – Test of Significance for Individual Error Matrices from Single and Multi-date Image Classifications 232

Table 7-3 – Results of Kappa Analysis for Comparison between Single versus Multi-temporal classifications 233

Table 7-4– Poppy User's Accuracy Results after Multi-temporal Classification 235

Abbreviations and Acronyms

ADP – Aerial digital photography

AOI – Area of interest

ASPRS – American Society of Photogrammetry and Remote Sensing

BH distance – Bhattacharyya distance

BRDF – Bidirectional Reflectance Distribution

DAP - Diammonium Phosphate

DN – Digital Number

DMC - Disaster Monitoring Constellation

EMR – Electromagnetic radiation

EMS – Electromagnetic spectrum

FCCs – False Colour Composites

FCO – Foreign and Commonwealth Office

IFOV – Instantaneous Field of View

JM distance – Jeffries-Matusita Distance

LANDSAT MSS – Landsat Multispectral Scanner

LANDSAT TM – Landsat Thematic Mapper

MDM – Minimum Distance to Means Classification

MLC - Maximum Likelihood Classification

MODIS - Moderate Resolution Imaging Spectroradiometer

NDVI – Normalised Difference Vegetation Index

NIR – Near Infrared

ONCB – Office of Narcotics Control Board

PDP – Poppy Detection Project

PI – Photographic Interpretation

SCP – Spectral Coincidence Plot

SPOT – *Satellite Pour l'Observation de la Terre*

SPOT HRV - *Satellite Pour l'Observation de la Terre* High Resolution Visible

SSP/TSP - Single super-phosphate/triple super-phosphate

SWIR – Shortwave Infrared

UK – United Kingdom

US – United States

USGS – United States Geological Service

UNODC – United Nations Office on Drugs and Crime

VI – Vegetation Indices

1. Introduction

This chapter provides background information on the requirement to improve existing remote sensing techniques for measuring opium poppy cultivation in Afghanistan. It demonstrates that an accurate methodology to monitor opium poppy cultivation in Afghanistan is necessary in order to monitor the impact of poppy cultivation reduction methods. It includes a critique of other poppy surveys to highlight key findings associated with using remote sensing for poppy detection. It closes with the aims and objectives of this research and the thesis structure.

1.1 Background

Although many different varieties of poppy exist throughout the world, opium producing poppy is grown in certain key areas; illicitly in SW Asia (in Afghanistan, Pakistan and Iran for example), SE Asia (in Myanmar, Laos, Thailand, southern China and NW Vietnam), Lebanon, Guatemala, Columbia and Mexico; and licitly in Australia, Tasmania, India, Turkey, Spain, France and the UK – grown legally for the pharmaceuticals industry.

Opium poppy has a growth cycle lasting approximately 3-4 months. It is usually planted in autumn/winter and flowers approximately three months after it has germinated. After the petals have fallen away seed capsules are exposed and an opaque, milky sap is contained within. In Afghanistan, the seed capsules are lanced, allowing opium resin to seep out for collection once it has dried to a black tar-like substance. The opium sap is then refined into opiate-based products. In countries where poppies are grown on a commercial scale for the pharmaceuticals industry the whole plant is processed to extract morphine.

Most of the heroin consumed in the UK originates from opium poppy grown illicitly in Afghanistan (Home Office, 2003). The UK Government has clearly established links between drugs misuse and crime (Home Office, 2003). With around three-quarters of heroin users in the UK committing crime to feed their habit (Home Office, 2003), the drugs problem over the last decade in the UK has been worsening. In 2001, the then British Prime Minister Tony Blair claimed that 90% of the heroin sold on British streets originated from Afghanistan (The Guardian, 2001), a country where heroin is produced

from illicit opium poppy cultivation and where links between the opiate trade and international terrorist activities have been proven by the US Government. By 2003, the Secretary of State for the Home Office estimated that 95% of the UK's heroin came from Afghanistan (Rammell, 2003).

Because of the impact of Afghan heroin on UK crime the UK is the lead nation assisting the Afghan Government to reduce the amount of heroin being manufactured, in support of its National Drug Control Strategy to eliminate opium poppy cultivation by 2013 (Rammell, 2003). This was in line with the UK Government's own 10-year drugs strategy to reduce the supply of Class A drugs in the UK by 2008 (Rammell, 2003).

Reduction of heroin is monitored through surveys of the Afghan opium poppy crop to produce annual cultivation figures. This monitoring activity is conducted independently using remote sensing techniques on satellite imagery by two international organisations - the United Nations Office on Drugs and Crime (UNODC) and the United States (US) Government. Annual US and UNODC opium poppy estimates from 1994 to 2005 are shown in Figure 1-1 as are 2006-2009 figures from UNODC. US data was not available in the public domain from 2006 onwards. Unfortunately, neither survey party provided accuracy estimates to indicate margins of error in any year.

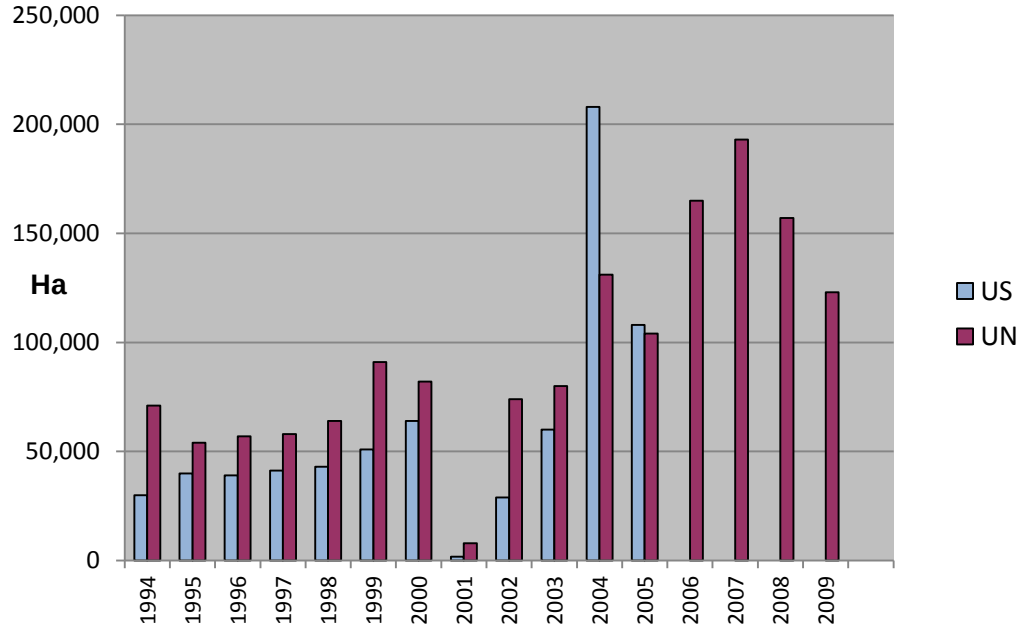

Figure 1-1 - Annual Opium Poppy Estimates - US v UN. Sources: Wikipedia 2010/ UNODC, 2005.

Several observations can be drawn from this graph:

- UN and US figures were consistently different between 1994 and 2004.
- UN figures were consistently higher than US figures until 2004.
- Both show an increase in opium cultivation between 1994 and 2004 (excluding the decrease in opium cultivation in 2001 due to the Taliban veto on poppy cultivation in late 2000), (Farrell and Thorne, 2005).
- UN recorded a fall in opium cultivation in 2005. However, opium cultivation then rose in 2006 and peaked in 2007 according to UN figures.
- The UN reported a decline in opium cultivation in 2008 and 2009, mainly due to a number of provinces becoming poppy-free.

Unfortunately, the differences in the figures and uncertainties surrounding the accuracy of the figures have complicated monitoring opium cultivation trends, which in turn have made measuring the success of the Afghan Drug Control Strategy even more difficult. The uncertainty in these figures has meant that research is needed.

1.2 Role of Remote Sensing

The basis for using remote sensing to identify different surface features is the supposition that each surface has a specific appearance on satellite imagery and aerial photography, depending on the type of sensor used (Schowengerdt, 2007). Many different remote sensing satellites and cameras are available for identifying land cover types and different remote sensing techniques exist to facilitate interpretation and analysis of the resulting imagery. For example, in vegetation studies cameras mounted on aircraft and sensors on satellites can be used to record subtle spectral characteristics about an object that may help differentiate between one vegetation species and another. The information may be collected over very small areas to measure crown diameters of oak trees (Jensen, 2007) or systematically across large areas of interest (i.e. at a regional scale) over multiple dates (days, weeks or months apart) to monitor the pheneological (growth) cycles of different crop species (Murakami *et al.*, 2001).

Over the past 40 years vast amounts of research effort has centred on increasing data supply at different resolutions and revisit frequencies, according to user requirements. For example, certain satellite sensors are able to image at very high resolutions (i.e.

between 0.5m and 4m) to help discriminate between different vegetation species and monitor vegetation health but across only relatively small swathes of land (i.e. 10-100 km). For example, IKONOS is capable of imaging at 1m resolution in the panchromatic band and 4m resolution in its 4 multi-spectral bands across a 10 km swathe of land.

Sensors with the most frequent, regular collections generally have coarser resolutions and a limited number of spectral bands. For example, the medium resolution sensors such as the Moderate Resolution Imaging Spectroradiometer (MODIS) with its two spectral bands at 250m spatial resolution have the capability of imaging very large areas of land at any one time (MODIS senses across 2000 km) with frequent, regular collections across the entire Earth's surface every one to two days for global vegetation monitoring studies.

In instances where regions or continents are to be mapped at resolutions sufficient for vegetation identification (i.e. using the high resolution sensors), it will be impossible to collect imagery or photography over every land parcel because of the considerable amount of land to be surveyed, the costs involved, time constraints and sensor limitations. Instead, area frame sampling surveys are used so that representative samples of images or photographs are acquired across selected areas. Notably, agricultural statistics have improved through the use of these sampling surveys (Lobo *et al.*, 1996) because they offer an efficient statistical means of acquiring data at national levels without the need for studying an entire area (Cochran, 1977).

In both the UN and the US surveys, independent area frame sampling techniques are used to acquire samples of high spatial resolution imagery (the UN use 4m resolution IKONOS images and the US use classified sub-metre sensors) to identify fields of opium poppy across Afghanistan's agricultural areas. The locations of images are selected from area frames overlaid onto independently-derived agricultural base maps. Potentially, most of the differences in their annual opium poppy cultivation estimates can be explained by their use of differing sampling techniques and agricultural base maps, and their different types of remotely sensed data and processing techniques.

1.3 Poppy Detection Project (PDP)

This research was initiated in 2003 to investigate the potential causes of the differences in the UN and US satellite image-derived survey figures. To do this, the UN's digital

image processing techniques and the US's visual interpretation techniques were to be assessed against high spatial resolution multi-spectral imagery, colour aerial photography and ground survey data. Of particular interest was the determination of the spectral variability of the poppy crop and the degree that it could be discerned from other crops throughout the annual crop growth cycle. This was to improve the accuracy with which poppy crops can be identified and quantified through digital image classification techniques.

Shortly after the start of this research it became apparent that other areas of interest would greatly assist the review of the UN and US remote sensing surveys. Consequently, Cranfield University was provided with funding to set up the Poppy Detection Project (PDP) which met with the approval of both the UN and the US.

The PDP focussed on the following areas:

- The design of the sampling surveys used by the UN and the US to acquire satellite imagery and the possible introduction of statistical sampling errors in the surveys.
- The appropriateness of MODIS to identify and monitor agricultural areas (refer to Appendix A for technical details on MODIS).
- The use of MODIS and medium resolution multi-spectral Disaster Monitoring Constellation (DMC) imagery for mapping and monitoring opium cultivation (refer to Appendix A for technical details on DMC).

In contrast, this study focuses towards improving the identification of poppy crops using high resolution image data. It is written for imagery analysts employed by the end used (the MOD) to assist in Afghan poppy identification using digital image classifications and visual image interpretation.

1.3.1 Eradication Activities

In addition to the requirement to quantify the amount of poppy being grown to measure the success of the Afghan Drug Control Strategy, the locations of the poppy crop were also of interest to enable eradication activities to take place.

In the lead up to this study, the Afghan government conducted eradication activities in a number of locations in Helmand Province. Eradication was conducted by farmers using

sticks to remove the poppy heads prior to the opium harvest, in return for financial compensation. It was hoped that this eradication would reduce the amount of opium available to make heroin. Farmers were also gifted wheat seeds and seeds for other crops with the intention that these would be planted in place of poppy in future years.

In the early stages of this research, the International Community was asked to scope the feasibility of assisting with the eradication activities. For the UK this meant potentially using the British Army to eradicate poppy, using whatever means available. Large areas of poppy fields would therefore have to be identified prior to the troops going on the ground in order to allow Commanders to plan their operations. The poppy fields would therefore have to be identified as early as possible in order to allow maximum preparation time, and certainly prior to the opium harvest. This study was therefore conducted with this in mind, to determine amongst other things, whether poppy could be identified early in its growth cycle.

1.4 Review of Opium Poppy Surveys

Over the last three decades, although remote sensing techniques have been used to map many of the earth's cover types (Agrawal *et al.*, 2003; Wang *et al.*, 2004) these have not been widely used for mapping illicit narcotics crops. However, with increasing advances in satellite technology and more analytical tools becoming available, remote sensing of illicit crops is becoming an effective weapon in the "war on drugs" (Lee *et al.*, 2001) and has led to greater identification accuracies (Dekeyne, 1988).

These improvements have taken place in part due to the abundance of higher resolution, more readily available satellite images developed as a result of increased competition among commercial vendors (Lee *et al.*, 2001). For example, the launch of IKONOS by Space Imaging provided higher resolution images than previously available, offering the possibility of enhanced discrimination of cover types (Wang *et al.*, 2004).

As early as 1991, Sader reported that very few articles were available in the public domain on the subject of identifying illicit narcotics crops using remote sensing technology. Unfortunately, much of the information exists within internal documents printed by the UN, the US State Department and agencies within some of the countries in which illicit narcotics crops are grown (Sader, 1991). The lack of published material

may be due to authors or organisations preserving their anonymity because of the secrecy and sensitivity required for monitoring illicit narcotics activities.

Of the information available in the public domain, very few studies give details of the remote sensing methodologies used, provide full details of results or quantify accuracy. As a result, the following review of opium poppy surveys does not examine the remote sensing methodologies in detail but seeks to highlight key findings subsequently used to underpin the methodology developed in this research. Table 1-1 gives a summary of published poppy studies.

Table 1-1 - Summary of Poppy Studies

Reference	Location	Sensor Used	Classification Method	Accuracy Reported?
Prapinmongkolkarn *et al.* (1980) Chuinsiri *et al* (1997)	Thailand	Landsat MSS	Digital	No
Dekeyne (1988) /Galtier *et al* (1990)	Thailand	SPOT 1	Digital	No
Chamnivikaipong (1992)	Thailand	Spot HRV	Digital	Yes - unclear
Chuinsiri *et al* (1997)	Thailand	Panchromatic Aerial Photographs	PI	No
Chuinsiri *et al.*, (1997)	Thailand	Landsat TM	Digital and PI	Yes
SPOT Image (2000)	Thailand	SPOT 5	PI	No
Srinivas *et al.*, (2004)	India	23.5m IRS-1D LISS-III	Digital	Yes
UNODC (2004 and 2005)	Afghanistan	IKONOS and SPOT 5	Digital	Yes - unclear

PI – Photographic Interpretation

The review considers methods used to survey poppy crops in Thailand, India and Afghanistan. It identifies key points drawn from each survey and details how this research investigates the recommendations made.

1.4.1 Key Points

Thailand

In Thailand, poppy has been identified using remote sensing since the early 1970's when remote surveys of poppy were performed by the Asian Institute of Technology, the National Research Council and the Office of Narcotics Control Board (ONCB), (Chuinsiri *et al.*, 1997).

In particular, a remote sensing feasibility study by Prapinmongkolkarn *et al.*, (1980) identified poppy fields in northwest Thailand using Landsat Multi-Spectral Scanner (MSS) images (Appendix A gives technical details on Landsat MSS). Two rectified Landsat MSS images were acquired over the poppy growing areas in November 1975 (when poppy plants were emerging) and again in February 1976 (when poppy plants were in flower) plus aerial photographs and ground survey data. A 1:50,000 map was used to rectify the images and to produce a digital terrain model to aid the subsequent digital classification procedures adopted.

Although Prapinmongkolkarn *et al.*'s (1980) method was vague and the results unclear they made two useful recommendations; they recommended that the accuracy of their digital image classifications could be improved by having accurate ground data for the different cover types and by analysing the temporal changes of the land covers. Similarly, many other studies have shown that multi-temporal images can successfully be used for monitoring seasonal vegetation change, for example to characterise cropping trends in Japan (Murakami *et al.*, 2001), for crop monitoring in Australia (Van Niel and McVicar, 2004) and for mapping rice fields in Africa (Turner and Congalton, 1998).

Other authors also reviewed Prapinmongkolkarn *et al.*'s 1980 work and drew out key points. For example, Chuinsiri *et al.*, (1997) commented that:

- The 80m spatial resolution of the Landsat MSS imagery was too poor to permit successful identification of Thai poppy because it was insufficient for recording the reflectivity values of the poppy crop within the small poppy fields. Although no further details were provided on field size by these authors a later survey conducted in 2000 by Spot Image/ONCB reported that poppy field sizes in Thailand averaged 0.18 hectare (more details provided later in this section).
- Imagery should be obtained at the end of the rainy season (November to December in Thailand) to reduce the chances of cloud cover obscuring the poppy fields on the imagery.
- Imagery should be superimposed onto a topographic map of the foothill zone in Thailand in order to eliminate other crops grown at a height where poppy fields were not.

Chuinsiri *et al.*, (1997) also cited a subsequent ONCB poppy survey in northern Thailand which was conducted with the assistance of the US Consulate in Chiang Mai.

From 1983 onwards, poppy crops were identified through visual Photo-Interpretation (PI) of regular acquisitions of 1:6,000 panchromatic aerial photographs. They reported that this PI approach was used by the ONCB for many years but then progressively declined after more advanced sensors became available in 1986 onboard SPOT 1 (see Appendix A for technical details). The programme was eventually stopped sometime after 1986 (no date provided) due to economic reasons.

Chuinsiri *et al.* suggested that their PI approach was more accurate than the digital image classification of satellite imagery documented previously. However, no further details were provided to justify this assertion.

Another approach to poppy surveying was described by Dekeyne (1988) and Galtier *et al.* (1990) based on SPOT 1 imagery. This approach was also briefly cited by Chuinsiri *et al.,* 1997. They reported that 10m panchromatic and 20m multispectral image data acquired by SPOT 1 was used to identify poppy fields in Thailand (no further details were provided) and the aerial extent of poppy was automatically computed (again, no further details were provided).

Chuinsiri *et al.,* (1997) reported that poppy fields could only be identified from SPOT 1 imagery at the end of the growing season in Thailand (December to February), and that the poppy spectral signature alone was "not sufficient for an adequate interpretation of the classifications born of digital image analysis" (Chuinsiri *et al.,* 1997).

Chuinsiri *et al.,* (1997) also noted that the spectral signature of poppy was strongly affected by directional effects such as slope, exposure, solar elevation and also by shadows. Although not described, these effects may have caused variations in brightness values being recorded by the Landsat Thematic Mapper (TM) sensor, as objects look differently when viewed from different angles and when illuminated in different directions. For example, when both the sun and viewing orientation are similar, objects are illuminated and shadows are hidden; therefore higher brightness values will be recorded. Conversely, when the sun and viewing orientation is opposite, shadows are visible and lower brightness values from shaded areas are expected. Similarly, the same vegetation type could have very different reflectance values as a result of different directional effects if imagery were acquired over the same site on different dates and at different times of day. To reduce the impact of directional effects the bidirectional reflectance distribution function (BRDF) is used to calibrate image

data for each wavelength being considered. This is often necessary when a quantitative study involving field measurements is undertaken. BRDF is explained in more detail in Section 2.3.4 of Chapter 2.

In their own survey of poppy fields in Chiang Mai Province in northern Thailand conducted for ONCB, Chuinsiri *et al.* investigated the use of different remote sensing techniques on two geo-rectified and radiometrically corrected Landsat TM images acquired over the same area using its six 30m resolution bands (refer to Appendix A for Landsat TM technical details). One Landsat TM image was acquired in February 1993, reportedly when the dry poppy crop residue remained in the field after the poppy harvest. A second image was also acquired two years later in January 1995, reportedly prior to the poppy harvest.

In conjunction with the satellite imagery, other data was used including aerial photographs at 1:6,000 scale collected in December 1992, a 1:1,000,000 soil map and two base maps at 1:50,000 and 1:250,000 scales. The base maps were used to extract height data so that areas below 800m - where poppy was not cultivated, could be excluded from the analysis – similar to recommendations made by Prapinmongkolkarn *et al.* in their 1980 survey.

Specifically, Chuinsiri *et al.*'s methodology was developed to compare the total amount of poppy calculated from visual PI of the Landsat TM imagery before and after digital enhancements had been conducted to results achieved using both a Maximum Likelihood digital image classification (MLC) and Minimum Distance to Means classifier (MDM).

In their PI analysis, results improved when digital enhancements were employed to the red part of the electro-magnetic spectrum (EMS) - Landsat TM band 3, the near-infrared (NIR) - Landsat TM band 4 and the mid-infrared (MIR) – TM band 5; however, no accuracy assessment was given.

In the digital classification investigation the MLC technique was reported to have produced better results than the MDM. In both cases spectral confusion was found between poppy and the 'various crops' class (barley and vegetables), grassland, bush, shadow and two forest classes in the January 1995 classified image acquired before the poppy was harvested. In the February 1993 classified image acquired when only the poppy residue remained spectral confusion was found between poppy and the 'various

crops' class and bare land. Less confusion was found between poppy and the grassland and bush classes than had been seen in the January imagery. Very little confusion was found between poppy and shadow, and unlike the January imagery, no confusion was found between poppy and secondary forest.

When the PI results were compared to the digital classification results Chuinsiri *et al.* found that the PI results improved upon those achieved by either the MLC or MDM. They attributed this to the fact that additional data could be included in the PI such as:

- Textural information - poppy fields were found to have a smooth texture on imagery during flowering.
- Geographical information - poppy fields were found to be located in isolated areas in places where small patches of forest had been logged and burned prior to poppy planting, often on steep mountainous areas on the crests of hills, between 1000-2000m in altitude with many small tracks crossing the areas.
- Cropping calendars - crops that were planted and harvested at different times of the year to poppy could easily be excluded from the analysis.

Another important finding in Chuinsiri *et al.'s* work was that the best time for cloud-free image acquisition could be determined using cropping calendars in conjunction with meteorological data. They found that the best chance for satellite data acquisition was during the cool and dry November to February winter season when the crops were maturing. However, they found that this time was not coincident with the best time for poppy identification in all areas studied. For example, very low reflected energy returns were found in mountainous areas during the winter months because the low winter sun angles cast long shadows over the agricultural areas. In these instances they recommended that shaded areas on imagery be avoided unless the shadow effects are corrected or are imaged from February onwards when the shadows are less extensive. In other locations Chuinsiri *et al.* found that some poppy fields were too immature to be identified during the dry winter months because later-maturing varieties had been grown (no further details provided). These crops were harvested between March and May at the beginning of the rainy season when collection of cloud-free data was considerably more difficult.

In their conclusions Chuinsiri *et al.* recommended using multi-temporal images obtained from at least two different satellites over two or three dates during the same growing season (Chuinsiri *et al.*, 1997). This was based on the difficulty found with collecting cloud-free single-date images, the impact of shadows and the use of later-maturing poppy varieties in their study area.

Chuinsiri *et al.*, (1997) also cited another Thailand poppy survey which was conducted by Chamnivikaipong in 1992 (reference not found) who used Spot HRV (see Appendix A). They reported that digital image classification accuracy improved by 5-10% (no further details provided) when 10m resolution panchromatic and 20m resolution true colour multi-spectral images from SPOT HRV were combined. They subsequently concluded from their own and Chamnivikaipong's 1992 work that PI of 10m resolution imagery was optimum for identifying poppy, supported by good local knowledge and aerial photography (Chuinsiri *et al.*, 1997).

Spot Image also conducted remote sensing surveys for poppy detection in collaboration with ONCB in Thailand over several years. Similar to the approach used in Chamnivikaipong's 1992 survey with SPOT HRV data, Spot Image used merged panchromatic and multi-spectral SPOT 5 image data (details in Appendix A) for poppy identification from 2000 onwards. In addition, they developed software to handle multiple layers of image data collected across the poppy growth cycle which could be integrated with map and field data (Spot Image, 2000b).

Unlike Chamnivikaipong's image classification approach on the merged digital imagery Spot Image used PI techniques on the 2.5m image product to identify the poppy fields. Specifically, they argued that the automatic recognition of crops (i.e. using a digital image classification) was not as accurate as their PI approach because of the diverse cultivation patterns present in Thailand (Spot Image, 2000a). Unfortunately, no accuracy assessment details were provided. They concluded that a PI approach was the most efficient and reliable method for identifying poppy fields (Spot Image, 2000a).

Spot Image provided useful information on the Thai poppy fields, namely that they:

- Averaged just 0.18 hectare in size, were often intercropped and were widely scattered over 2,000,000 hectares.

- Were frequently located on steep slopes in isolated and inaccessible mountain regions in the heart of primary forests and far from any infrastructure.
- Were irrigated and fertilised throughout the year by a minority of farmers for year-round poppy production.
- Contained poppies which reached different stages of maturity within the same field.

India

In 2000, the Indian Express reported that digital processing of satellite imagery was used to identify poppy in north-eastern and central states of India with 80-90% accuracy (no further details known). Although no information was provided on the techniques used, it was reported that farmers tried to avoid their poppy fields being detected during the January-March growing season by cultivating small areas of poppy alongside other crops and away from roads (The Indian Express, 2000).

More recently, Srinivas *et al.*, (2004) used 23.5m IRS-1D LISS-III image data (details in Appendix A) to distinguish opium poppy from other crops in India. The images were collected between 2000 and 2003 at two stages of the poppy lifecycle, during the winter months when only bare soil was visible and during a period of peak vegetative cover during poppy flowering when the poppy canopy was dense (Srinivas *et al.*, 2004). To enhance canopy reflectance a Weighted Difference vegetation index was applied (using algebraic combinations of the near infrared and red spectral bands) to two atmospherically corrected images of the same area. The end result was that poppy was successfully discriminated from other cover types with a user's accuracy of 94.8% and a Kappa statistic of 0.93 (Srinivas *et al*, 2004). Significantly, poppy was more discriminable at flowering than at any other growth stage (Srinivas *et al*, 2004).

Afghanistan

Between the early 1990's and the early 2000's the United Nations Office on Drugs and Crime (UNODC) used socio-economic data as the basis for their annual Afghanistan poppy survey. In 2002 UNODC introduced an additional remote sensing-based element to monitor the extent of poppy cultivation in the main poppy growing areas of Afghanistan (UNODC, 2005b). By 2004 digital image classifications of IKONOS images (details provided in Chapter 2 and Appendix A) acquired over ten provinces

were used to estimate the amount of opium poppy being grown. In 2005 images from fifteen provinces were analysed alongside socio-economic data collected in other provinces, which, when added to the results obtained from the analysis of satellite imagery, enabled cultivation estimates for the whole of Afghanistan to be made. This research considers only the remote sensing-based element of the overall poppy estimate.

Figure 1-2 shows various steps used by UNODC to identify poppy in their 2004 and 2005 remote sensing-based poppy surveys. Each step is described in detail in the ensuing paragraphs.

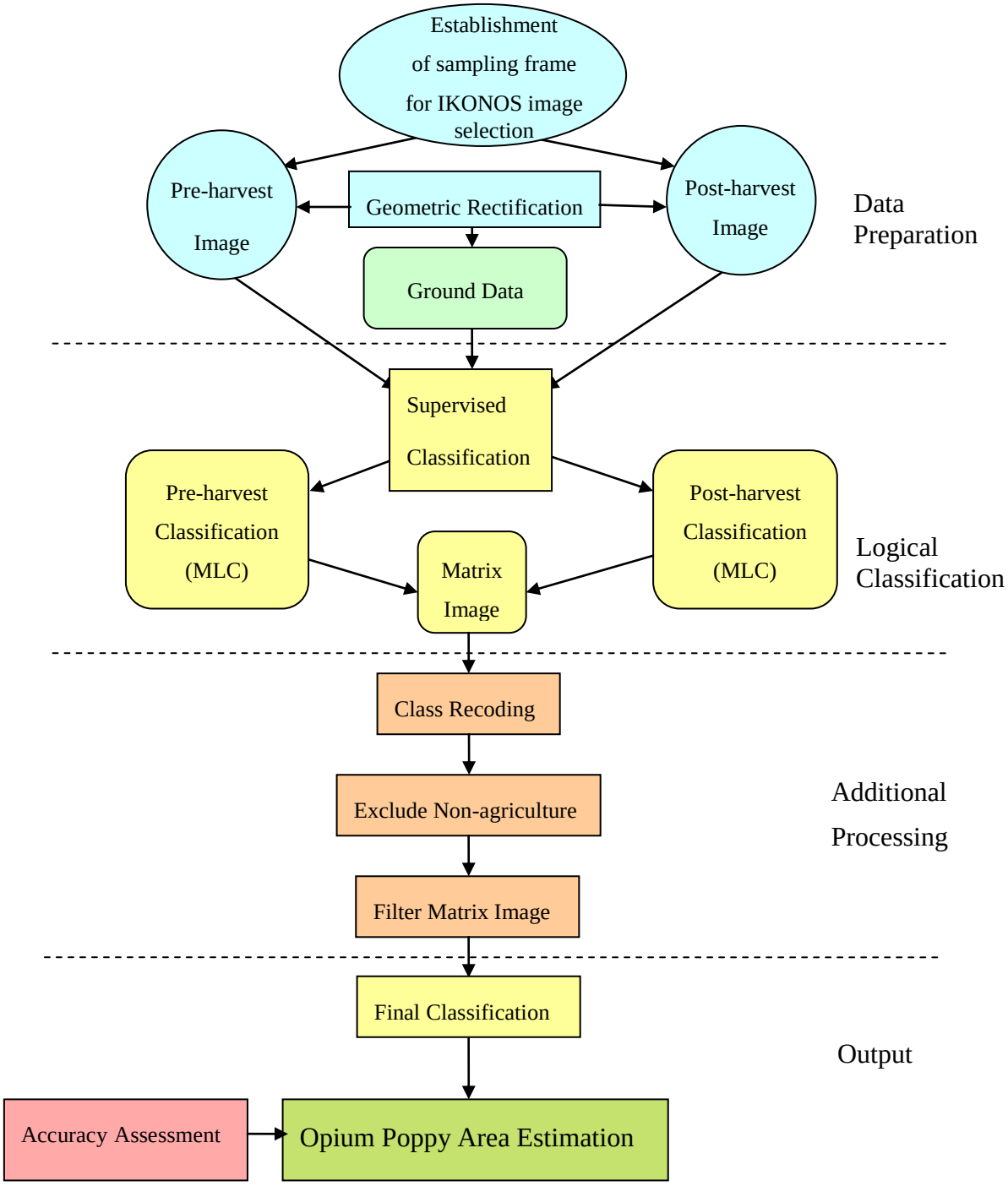

Figure 1-2 - UNODC's Classification Methodology, after UNODC, 2005

In the data preparation stage Landsat 7 images (details in Appendix A) from 2002-2003 were used to identify all major agricultural areas in each of the 15 provinces selected for the remote sensing-based survey. A systematic sampling frame made up of a grid of 10 km x 10 km areas (the size of each IKONOS image) was then overlaid onto the

agricultural areas. From this grid, 79 pairs of 4m resolution multi-spectral IKONOS images were randomly selected, each covering a 10 km x 10 km ground area.

Each IKONOS image selected from the sampling frame was then collected as one part of a pair of IKONOS images acquired over the same location a month apart; the first during the poppy growth cycle prior to the poppy harvest and the second post-poppy harvest, based on harvest dates from the previous year (UNODC, 2005b). Once collected the post-harvest images were geo-rectified to their coincident pre-harvest images as necessary for image comparison.

Simultaneously, up to four randomly-selected 250m x 250m ground segment training areas were chosen from within each 10 km x 10 km image area for ground data acquisition (collected by trained Afghan surveyors). The ground data was used to identify cover types in the image areas to help train the subsequent digital classifier used and for accuracy assessment purposes (UNODC, 2005b). As far as possible collection of ground data simultaneously took place with the acquisition of the first of each image pair. In total, data was collected from 178 segment training areas in 2004 and 230 areas in 2005 (UNODC, 2005b).

In the logical supervised classification stage, the Maximum Likelihood Classifier (MLC) was performed separately on each of the pre- and post-harvest images to identify areas of poppy, cereals, other crops and fallow. A logical classification look-up table was then created for each image pair to cross-tabulate classification results from both image dates. The rows of the look-up table indicated classification results for each cover type in the first image acquired pre-poppy harvest with the results post-poppy harvest (the columns). An example look-up table taken from UNODC's 2005 Afghanistan opium survey is reproduced in Table 1-2 with permission to demonstrate how the logical classification was used.

Using the uppermost row in Table 1-2 as an example, UNODC indicated that during the classification of image 1 (pre-poppy harvest), fields were assigned different colours. Image 2 was then classified. If the colour assigned to the fields had changed after the post-poppy harvest image had been classified, *i.e.* from red, green or pink to dark green, the field was classified as poppy. Similarly, red, green or pink to yellow/brown was classified as cereal, as was dark green to pink for example.

Table 1-2 - Example of a logical post-classification look-up table (Shortepa District, Balkh Province), reproduced with permission from UNODC, 2005

		Class post-harvest			
		Dark Green	**Green**	**Yellow/Brown**	**Pink**
Class pre-harvest	**Red**	Poppy	Other	Cereal	Other
	Green	Poppy	Other	Cereal	Cereal
	Dark Green	Fallow	Other	Other	Cereal
	Pink	Poppy	Other	Cereal	Other

Each look-up table was modified on a regional basis to account for differences in the appearance of cover types according to the influence of local environmental conditions and differences in the growth stages reached by the crops during image acquisition (UNODC, 2005b).

If there were any conflicts in the classifications, ground data was used to resolve these, after which the cover types in each image were subsequently recoded. Non-agricultural areas were then excluded from the output classified thematic maps. The thematic maps were subsequently filtered using a 3x3 low-pass filter to remove classification outliers and to simplify the output maps (UNODC, 2005b). A final thematic map was produced for each 10 km x 10 km area to indicate areas where poppy was grown. Area statistics were then used to calculate the total amount of poppy identified in each image.

Finally, confusion matrices (discussed in Chapter 2) were used to test the accuracy of each digital classification using the ground data collected. Bias corrections were subsequently performed to reduce area estimation bias (UNODC, 2005b). Overall, UNODC report that 80% of pixels classified as poppy on the ground were correctly classified as poppy in the imagery (UNODC, 2005b).

In addition to using IKONOS imagery, UNODC also trialled the use of SPOT 5 images (10m spatial resolution) across six provinces in 2005. Of significance was that UNODC attempted to collect imagery during ‘the ideal time for poppy identification’ - at the cabbage and lancing stages (UNODC, 2005b). Of 70 images collected, 15 were acquired at the cabbage stage, 15 were acquired in early March which were ‘still found useful for poppy identification’ (UNODC, 2005b) and the remainder were collected during the poppy flowering stage, which was ‘not ideal for discriminating poppy from other crops’ (UNODC, 2005b).

UNODC concluded that SPOT 5 images were inappropriate for identifying poppy fields because the low revisit capability (10-15 days) ‘does not take into account variations in

the poppy growth cycle within and between provinces' (UNODC, 2005b). They cited one example from Helmand Province where there was a 15-20 day difference in harvest time between lower and upper Helmand. No further details were provided.

UNODC also reported that single date SPOT 5 images 'did not provide enough confidence to depict poppy fields' (UNODC, 2005b) (no further details were provided). They also concluded that the poppy crops exhibited a high degree of spectral variability on SPOT 5 imagery due to different growth stages being imaged and different agro-climates and topographic conditions (UNODC, 2005b).

Additionally in their 2005 report, UNODC illustrated spectral reflectance curves for poppy, wheat, alfalfa, vegetables and fallow using normalised difference vegetation index values (no further details were provided). Significantly, they summarised that differences in the reflectance curves for poppy and wheat were more pronounced 'in the earlier [growth] stages' but more similar between March and June (no location specified) (UNODC, 2005b).

Notably, rather than exploit the spectral differences observed at the earlier poppy growth stages, UNODC reported that they identified poppy [on IKONOS imagery] on the basis of spectral differences brought on by a farming practise 'unique' to poppy grown in Afghanistan (UNODC, 2005b). This is that as all winter-planted crops (including poppy) simultaneously progress through their growth stages, poppy crops are the first to be harvested - whilst still green. Consequently, poppy becomes the first crop to be removed from the fields whilst the other crops begin to undergo senescence *in situ*. Therefore, no crop is identified until the second image has been acquired - when poppy fields have been harvested *and* removed from fields, and only bare soil remains (plus a small amount of poppy stalks). These bare fields are therefore identified as poppy. The remainder of the fields are labeled cereal if still under senescence or other crops.

1.4.2 Analysis of Surveys

This section critically appraises the surveys investigated by highlighting their agreements, contradictions and ambiguities and by examining what they have achieved. It also comments on how this research has used and tested their recommendations.

Optimum Timing of Image Acquisitions

Two factors were consistently reported to influence the optimum time of imagery acquisition in the studies reviewed - climatic conditions and the growth stage reached by the poppy crop. For example, in Thailand cloud cover was the most often cited climatic factor affecting the timing of image collection. Prapinmongkolkarn *et al*., (1980) identified that there were more opportunities for acquiring cloud-free images during the cool dry months of November and December than at any other time in the Thai poppy lifecycle and thus recommended these months for imagery acquisition. In Afghanistan, although UNODC reported that poor weather conditions prevented SPOT 5 imagery from being collected at the cabbage and lancing stages it did not directly influence IKONOS image acquisition times. This was perhaps because IKONOS revisit times (1-5 days at 4m x 4m resolution) were higher than SPOT 5's 10-15 day revisit times.

In a more recent study Lu and Weng (2007) described how dust and haze could affect image collection - particularly dust storms during spring months when crops are maturing as temperature and day light hours increase. Although UNODC did not mention this to be a limiting factor, it was considered that reduced visibility brought on by the presence of airborne dust in Afghanistan could delay the capture of aerial photography and satellite imagery. As such, it was decided that meteorological forecast data would be used to identify when atmospheric conditions were optimal for image collection. In addition, although windows of image collection opportunity would be submitted no other action could be taken to prevent collection being delayed. Chapter 3 examines the Afghan climate in more detail.

A second factor reported to affect the optimum time for image acquisition concerned the best time to identify poppy on imagery. In all poppy surveys, poppy was identified on the basis of its visual appearance, and/or its spectral properties, at one or various stages in its growth and development cycle. In UNODC's survey, poppy was identified on the basis of a farming practice unique to poppy. Although this may be a valid way to identify poppy, its success rests on farmers always harvesting poppy before any other crop.

Chuinsiri *et al.*, (1997) reported from studies conducted by Dekeyne (1988) and Galtier *et al*. (1990) that poppy fields could only be identified from SPOT 1 imagery in

Thailand at the end of the growing season (December to February). UNODC partially contradict this by reporting that both the poppy cabbage stage (an early stage in the growth cycle) and the opium harvest (which occurs towards the end of the growth cycle) were the best times to discriminate between Afghan poppy and other crops (UNODC, 2005b). In contrast, Srinivas *et al*, (2004) reported that poppy in India was more discriminable at flowering than at any other growth stage.

In a separate study in New South Wales, Australia, Van Niel and McVicar (2004) investigated temporal windows for crop discrimination using Landsat TM imagery. In addition, they compared results from three different classifications approaches; single-date Maximum Likelihood classifications (MLCs); standard multi-date MLCs (which combine image data from various dates to form a single multi-date image prior to classification) and multi-step classifications (which iteratively combines single classes, post-classification) (Van Niel and McVicar, 2004). Their results showed that the highest overall single-date classification accuracy achieved for the four major summer crops grown (rice, maize, sorghum and sorbean) was late February to mid March (Van Niel and McVicar, 2004). This differed to the best time found for discriminating the individual crops (rice – November to early December; maize – mid February to mid March; sorghum – early April until early May and soybeans late February to early March), (Van Niel and McVicar, 2004). The multi-step classification resulted in higher accuracies than the standard multi-date image stack (Van Niel and McVicar, 2004). They concluded that the identification of temporal windows for crop discrimination and the use of a multi-step classification approach greatly improved overall crop classification (Van Niel and McVicar, 2004).

In light of this, it was clear that imagery of Afghanistan should be obtained across as wide a range of dates as possible in order to determine if and when poppy is most discriminable from other cover types. As such, this study aimed to investigate the appearance of poppy and other major crops at their different growth stages in Afghanistan, from both the ground and air in order to determine suitable dates for image collection. As other studies suggested, the Afghan cropping calendar would also be used in conjunction with meteorological data to determine when poppy crops would be mature enough in the growth cycle for successful identification on imagery. As such,

Chapter 3 explores the appearance of poppy in detail at its different growth stages, and examines the Afghan poppy cropping calendar.

Finally, a recommendation made in a number of surveys was that more than one image at each site should be collected in order to overcome the difficulties of obtaining cloud-free data at one specific time in the poppy lifecycle. For example, Chuinsiri *et al.*, (1997) recommended multi-temporal image acquisitions in order to maximise the chances of acquiring cloud-free data. Both UNODC (2005b) and Prapinmongkolkarn *et al.* (1980) used multi-temporal image acquisitions to monitor temporal changes. Moreover, UNODC reported that single date SPOT 5 images 'did not provide enough confidence to depict poppy fields' (UNODC, 2005b) and concluded that the poppy crops exhibited a high degree of spectral variability on SPOT 5 imagery due to different growth stages being imaged and different agro-climates and topographic conditions (UNODC, 2005b). As a consequence, single-date and multi-date classification approaches were also to be tested to determine whether a multi-temporal classification approach achieved improved accuracies over a single-data approach for discriminating between poppy and other crops in Afghanistan in Chapter 7.

Ground Data

Prapinmongkolkarn *et al.* (1980) recommended that ground data should be acquired at a time coincident with image acquisition to limit the chances of crops changing in appearance between image acquisition and ground data capture, in order to improve the accuracy of the subsequent image analysis.

In the poppy survey by Chuinsiri *et al.*, (1997) the standard remote sensing practise of PI of aerial photography was used as a surrogate for ground data as inaccessibility and security issues prevailed. Unfortunately, as found with the ground surveys, the Chuinsiri *et al.*, (1997) study made no reference to the accuracy of its surrogate ground data. Future studies should be conducted with ground and surrogate ground data acquired over the same area to determine whether surrogate ground surveys can produce results of a similar/better accuracy to a ground survey when there are variable security conditions (in Afghanistan for example), and/or if the level of expertise of ground surveyors is inconsistent.

For this study, it was important therefore that investigations would be conducted to determine:

- How time-lags between ground and imagery data acquisitions influence the accuracy and consistency of PI and digital classifications.
- How PI and digital classifications are influenced by inaccurate or inconsistent ground data.
- How the accuracy of surrogate ground data compares to the accuracy of actual ground data.

The results of this investigation are discussed in Chapter 8.

Spatial Resolution

A major drawback reported in the study conducted by Prapinmongkolkarn *et al*., (1980) was the spatial resolution of the Landsat MSS sensor used. At 80m it was not able to directly record the amount of energy reflected from each poppy field and so was deemed to be inadequate for poppy identification (Chuinsiri *et al.*, 1997). As advances in satellite technology occurred, progressively higher spatial and spectral resolution sensors were used in later Thai surveys to monitor the poppy fields. For example, from 1983 the US Consulate with ONCB used aerial photographs at 1:6,000 scale, Dekeyne (1998) and Galtier *et al*. (1990) used 10m panchromatic and 20m multi-spectral SPOT 1 imagery, Chuinsiri *et al.* (1997) used 30m resolution Landsat TM with 6 spectral and one thermal band and Spot Image/ONCB (2000) used a 2.5m merged image product from the SPOT 5 sensor.

Although the technological advances have improved the spatial resolutions of the images, none of the papers reviewed provided detailed accuracy assessments. As such, comparisons of the results produced from each successive sensor could not be made. It was therefore not possible to determine whether an increase in spatial resolution brought about an increase in the accuracy of poppy identification, as found in other vegetation studies. For example, Mumby *et al.*,(1997) compared the performance of three sensors; the digital airborne remote sensing sensor CASI (1m resolution), SPOT XS (20m) and Landsat TM (30m) for mapping coral, mangrove and seagrass habitats of the Caicos Bank, British West Indies. Overall, they found that the results from the 1m CASI were significantly more accurate than those obtained from SPOT XS and Landsat TM. Similarly, Frank and Tweddale (2006) investigated the effect of three different spatial resolutions (0.6m, 1m and 2m) on the detection of shrubs in the Mojave Desert of California using a computerized airborne multi-camera imaging system (CAMIS)

mounted on a fixed wing aircraft. They found that vegetation cover measurements were most accurate at spatial resolutions ranging from 0.6-1m, and that as pixel size increased beyond 1m, less than 50% of the individual shrubs could be identified.

Accuracy Assessment

For poppy identification, building on from the work conducted by UNODC in 2005 it was important that the accuracy of poppy identification using satellite imagery was to be tested so that it could be used as a benchmark for future poppy studies. Accuracy measures used in this study included error matrices, Kappa statistics and regression analysis – each of which are discussed in Section 2.8 of Chapter 2. Sections 6.3 - 6.4 of Chapter 6 and Sections 7.1 - 7.27 of Chapter 7 present the results of the accuracy assessments performed in this study.

Influence of Slope

Chuinsiri *et al.* (1997) reported that Landsat TM reflectance was affected by directional effects including slope, exposure and solar elevation, but particularly by low sun angles in variable terrain which caused shadows. This concurred with similar observations made by Dekeyne (1988) and Galtier *et al*. (1990) when SPOT 1 imagery was used. UNODC did not report any shadow effects on their Afghan images acquired during the spring and summer months, presumably because the sun was high in the sky during these months. This concurs with Chuinsiri *et al.*'s recommendation that imagery should be acquired from high sun angles to reduce the size of shadows and their effect on imagery, but no mention was made of whether the UN determined if and by how much their imagery was affected by shadow, particularly in any mountainous agricultural areas.

A review of the likely locations for image acquisition in Afghanistan revealed that flat agricultural areas abounded. Whilst the effects of slope were therefore not considered in this research their influence would be considered in future research.

Accuracy of Poppy Identification Methodology - Photo-Interpretation vs. Digital Image Classification

The most successful remote sensing technique used to identify poppy in the surveys reviewed appeared to be the visual PI approach using either aerial photography or satellite imagery. Unfortunately, even as the source imagery and photography improved

through time with the introduction of more advanced sensors, measures to formally assess the accuracy of the PI or digital classifications conducted were not provided in the majority of cases. Most results were expressed as opinions rather than as quantitative measurements.

Fortunately, Chuinsiri *et al*.'s 1997 study directly compared their results obtained using PI to those obtained using both the supervised digital MLC procedure and the supervised Minimum Distance to Means Classifier (MDM). Although the MLC technique was reported to produce better results than the MDM, their visual PI method produced comparatively better results than the MLC. They reasoned this was because the analysts conducting the PI were able to use auxiliary data such as cropping calendar information and meteorological information to positively identify the poppy crop.

The overall lack of accuracy assessments using an independent analyst to cross-check interpretation results for consistency made it impossible to identify which methodology (digital classifications or PI) produced the most accurate results. As an alternative, qualitative accuracy assessments could have been conducted using a different set of ground data/surrogate ground data set aside from the training data to check whether the PI or digital classifications correctly identified known land cover types. In this study it was considered important that an investigation be carried out into the consistency and accuracy of the ground data used in this study. Chapter 4 describes this investigation and shows how errors were subsequently corrected.

Use of Ancillary Data

In the Spot Image study of Thai poppy fields ancillary data was used to modify the PI, based on rules that were established by experienced analysts. For example, poppy was frequently found to grow on steep slopes in isolated and inaccessible mountain regions in forests and located away from roads. In India, poppy was planted within fields of other crops and again located away from roads (the Indian Express, 2000). In this study of Afghan poppy fields, if specific farming practices were found to be unique to poppy and could be identified on imagery, attempts would be made to use them in a PI approach to assist in the training data collection stage of the digital classifications. Moreover, as Lu and Weng (2007) suggested, they potentially could also be used to modify any classification results and correct classification confusions based on specific knowledge of poppy farming practices, terrain characteristics and topographic features.

Other studies used texture to assist in poppy identification. In one Thai poppy field study Chuinsiri *et al.* (1997) reported that poppy fields in flower had a smooth texture on Landsat TM images. The Spot Image PI study concurred with this (on Spot imagery) – and used software to exploit the textural information present in their imagery (although no further details were provided). In essence, none of the standard spectral classifiers described in the literature were able to exploit the textural information available – only analysts using a PI approach could. Although the main aim of this study was to investigate the discrimination of poppy using spectral signatures, PI techniques were used in this research to assist in the identification of training datasets.

Summary

This literature review examined the recommendations, observations and lessons learned from these studies. It concurs with observations made by Sader (1991) that little has been formally reported on narcotic crop identification using remote sensing technology. Of the small number of published studies conducted in Thailand, India and Afghanistan, few provided solid, quantifiable evidence concerning the accuracy of detection of poppy crops using remote sensing means.

The review recognises that more research needs to be conducted into determining the best time(s) of image acquisition for poppy identification. It confirmed that cropping calendars, meteorological data and *a priori* knowledge of poppy and other crop growth cycles (Jensen, 2007) should be used to determine the optimum time of image acquisition.

It recognises that accurate ground data has to be acquired at, or as close to, the time of image acquisition. It observed how classification accuracy was affected by the spatial resolution of the sensor used and discussed the influence of slope, the accuracy of PI versus digital classifications and the use of ancillary data.

Only Chamnivikaipong (1992), Chuinsiri *et al.* (1997) and Srinivas *et al*'s (2004) surveys indicated that accuracy measures were employed, but only Chuinsiri *et al.* and Srinivas succeeded in providing robust quantitative accuracy figures.

Altogether, the surveys provided a departure point for the research conducted in this thesis and helped shape the aims and objectives for this study. Knowledge gaps listed in Section 1.5.1 were used to underpin the methods developed in this research.

1.5 Aims and Objectives

The aim of this research was to investigate the application of remote sensing for discriminating poppy from other land cover types in Afghanistan using spectral signatures obtained from the analysis of multi-spectral imagery. The consistency of discrimination through time and for different geographical regions was of particular interest. As such, although PI techniques were used to assist in the identification of training datasets for use in a digital classification, they were not formally investigated.

In meeting this aim, a review of previous poppy surveys developed the argument that in Afghan poppy, inadequacies in the quantitative understanding of the spectral and temporal properties of opium poppy have led to studies which would have benefited from improved methods to both enhance poppy discrimination and validate results. This thesis argues that quantitative knowledge of the spectral-temporal properties of poppy and the factors which influence classification accuracy positively contribute towards improving remote detection of poppy and provides solid, quantifiable evidence of the accuracy of poppy identification from remote sensing.

The following objectives were set to meet this hypothesis:

1. Identify factors that may influence the spectral properties of the opium poppy crop and investigate their influence with respect to accuracy of identification using multi-temporal and multi-spectral image analysis.
2. Investigate the spectral separability of cover types to determine:
    a. The presence or otherwise of a stable spectral signature of poppy that contrasts with the signatures of surrounding crops in Afghanistan.
    b. The most appropriate time(s) in the growth cycle for discriminating poppy from other crops.
3. Quantify the relationship between spectral separability and classification accuracy.
4. Investigate whether a single or multi-date classification approach improves classification accuracy.

1.5.1 Areas of Investigation

This section identifies knowledge gaps which this research aims to fill and draws together several areas of investigation which were explored to help characterise the spectral signature of poppy in Afghanistan.

Biophysical and Environmental Factors – Chapter 3:

- Determine the diversity of growing conditions and agricultural practices in Afghanistan.
- Investigate the Afghan poppy growth cycle and regional Afghan cropping calendars to determine the accuracy of simultaneous and predictive crop growth forecasts across Afghanistan created using MODIS imagery.
- Determine which factors are most significant for determining the optimum timing of image acquisition including; climatic constraints such as cloud cover, dust and haze as temperatures and daylight hours increase; biophysical parameters and cropping calendars.

Optimum timing of image acquisition – Chapter 4:

- Determine whether MODIS imagery can be used to develop a regional Afghan cropping calendar forecast based on the greening-up of vegetation.
- Determine the feasibility of acquiring good quality multi-temporal images in an operational context within specific collection time lines to coincide with key poppy growth stages, and with flexibility to bring collections forward or allow them to slip according to unforeseen local climatic conditions or local variations in sowing and harvest dates – all to be delivered on time and as cost-effectively as possible.

Improved spatial resolution – Chapter 4:

- Determine whether an increase in spatial resolution brings about an increase in the accuracy of poppy identification by conducting qualitative comparisons of 4m resolution multi-spectral IKONOS imagery with 60cm resolution Zeiss colour aerial photography.

- Investigate how the addition of the higher resolution panchromatic band with its added textural information improves the PI of different cover types, following on from research conducted by the PDP.

Single or multi-date approach – Chapters 6 and 7:

- Determine whether one image acquired at the optimum time in the cropping growth cycle for poppy identification is sufficient.
- Determine whether multi-temporal acquisitions can be used when accurate image rectification and geo-registration are required, particularly in areas where significant topographic changes occur or in areas where inadequate digital elevation data exist.
- Determine the identification accuracies that can be achieved using both single and multi-dated approaches.

Spectral signature – Chapter 6:

- Identify whether crops have a unique signature at a specific time in their growth cycle.

Feasibility – Chapter 8:

- Determine whether an operational poppy detection programme can be used by a non-specialist which integrates imagery, ground and auxiliary data.

1.6 Thesis Structure

This first chapter provided background information on the commitment made to improve on existing remote sensing techniques for measuring opium poppy cultivation in Afghanistan. It showed that an accurate methodology to monitor opium poppy cultivation in Afghanistan is necessary to quantify the impact of poppy cultivation reduction methods. It included a critical account of past and current poppy surveys to highlight key elements associated with using remote sensing for poppy detection, which led to the clarification of the aims and objectives of this thesis.

Chapter 2 introduces the fundamentals of remote sensing in the context of crop identification. It begins by describing the general spectral characteristics of vegetation and bare soils. It describes how their different reflectance and absorption properties

result in different spectral characteristics - which visual PI and digital image processing techniques attempt to identify. It then describes how visual interpretation and digital image processing techniques can be used to identify crops.

Chapter 3 details how environmental factors affect agriculture and cropping patterns in Afghanistan and then suggests ways in which crop spectral signatures may be influenced by agricultural practices used. It then describes in detail the poppy growth cycle and discusses how a range of poppy biophysical and morphological factors and Afghan farming practices may affect the spectral appearance of the poppy crop at various growth stages.

Chapter 4 presents methods developed to measure the spectral characteristics of poppy using multi-temporal and multi-spectral imagery acquisitions over selected sites in Afghanistan. It outlines the methodology used to select locations and dates for ground, imagery and aerial photographic data capture, provides details of the data collection bid and describes pre-processing required on the datasets before they could be used to measure the spectral characteristics of poppy.

Chapter 5 describes how training and evaluation data were collected and how spectral separability between poppy and other Afghan cover types and classification accuracy was determined.

Chapter 6 displays the results of the spectral separability and classification accuracy examination.

Chapter 7 presents the results of the multi-temporal image classifications.

Chapter 8 identifies the temporal and spatial variations found in the data and identifies factors which were found to influence the spectral signature of poppy and other cover types in Afghanistan. It also describes the consequences of the spectral variation on classification accuracy.

Chapter 9 presents the conclusions of this study with reference to the objectives listed in Chapter 1. It also discusses the study limitations and makes recommendations for future studies.

The Appendices provide: (A) technical details on the sensors discussed in this research, (B) Ground data collection instructions for surveyors, (C) JM Distance worksheet and Spectral Coincidence Plots (D) Supervised Classifications and (E) Error Matrices.

Altogether this thesis describes research that developed a systematic and rigorous methodology to investigate the spectral characteristics of poppy in Afghanistan. This study is unique in that it investigates and records the temporal and spatial variability of the poppy crop over two growth years across a range of growing conditions and attempts to identify the factors which influenced the spectral separability of poppy from other cover types during this time.

2. Fundamentals of Multi-Spectral Remote Sensing

This chapter describes how remote sensing techniques are used to discriminate crop types based on differences in their spectral signatures. It begins by describing how spectral information gathered by satellites and aircraft can be used to identify different earth surface features based on their individual spectral characteristics. It then explains how the complex structures of leaves influence the reflectance and absorbance characteristics of vegetation, to produce different spectral characteristics.

The chapter also describes how visual Photographic Interpretation (PI) is used to identify crop types remotely by using recognition elements that are visible to the naked eye. It then describes digital image processing techniques used to categorise the spectral characteristics of different cover types into classes. It illustrates how image classification techniques can be used to identify and quantify land cover types and how certain factors may influence the performance of the classification procedure. It then provides information on how spectral separability is assessed using graphical and statistical measures and how classification accuracies are measured using error matrices and Kappa statistics.

This chapter attempts to provide a basic but detailed theoretical background of the fundamentals of remote sensing for imagery analysts employed by the end-user (the MOD), who have no previous knowledge of either multi-spectral images or digital image classifications.

2.1 Introduction

Remote sensing is the measurement or acquisition of information about the Earth's surface and atmosphere using specialised instruments without physically being in contact with the object of interest (Mather, 2004; Richards and Jia, 1999; Lillesand and Kiefer, 2000; Jensen, 2007; Schowengerdt, 2007). Data can be gathered within a wide range of discreet wavelengths including the ultraviolet, visible, near-infrared (NIR), thermal infrared and microwave regions of the electromagnetic spectrum (EMS) using sensors such as detectors and scanning mirrors, linear arrays, cameras, lasers and radars located on aircraft and spacecraft (Jensen, 2007).

Some types of electromagnetic radiation (EMR) easily pass through the atmosphere whilst others do not. Gases in the atmosphere (i.e. water vapour, CO_2 and ozone) absorb EMR in

certain wavelengths (absorption bands). Absorption by these gases results in only portions of EMR reaching the Earth through atmospheric windows and these windows are present in the visible and the infrared regions of the EMS. Therefore, most remote sensing instruments operate in these atmospheric windows, where EMR easily passes through the atmosphere to the Earth's surface.

Data can be collected using either passive or active remote sensing systems. Active sensors such as radar generate their own active radiation and direct it towards objects of interest and then record the amount of energy scattered back towards the sensor (Jensen, 2007). Passive sensors measure radiation that is naturally reflected or emitted (at temperatures above absolute zero) from the ground, atmosphere and clouds (Schowengerdt, 2007).

Passive sensors can be configured to record radiant energy simultaneously in hundreds of spectral bands of the EMS (hyperspectral), in multiple bands (multi-spectral) or in a single band (panchromatic). For example, hyperspectral sensors are configured to acquire data in hundreds of individual narrow bands in parts of the EMS (Jensen, 2005). Multi-spectral sensors have been optimised to acquire data in several optimal bands, normally configured to collect data about specific parameters of objects (Jensen, 2005). For instance, data is usually collected in the visible (blue, green and red) and NIR part of the EMS if data on the biological and physical (bio-physical) characteristics of vegetation is required – this is because most vegetation activity affects the spectral reflectance factors of these bandwidths (Murakami *et al.* 2001). Although each sensor's spectral bandwidths are refined to record information in specific regions of the EMS, gaps between the spectral sensitivities exist (Jensen, 2005). This is because it is difficult to create a detector that has extremely sharp bandpass boundaries (Jensen, 2005).

The actual data gathered by the passive sensors in the EMS is the amount of electromagnetic radiation (EMR) reflected, back-scattered or emitted from an object or geographic area at one point in time (Lillesand and Kiefer, 2000; Jensen, 2005) which is used as a surrogate for the object under investigation (Jensen, 2005). Any changes in the properties or changes in the amounts of electromagnetic radiation detected by a sensor from an object or geographic area may be a valuable source of data for interpreting important properties of the object (Jensen, 2007). These changes are used in visual interpretation as information or modelled mathematically in digital image processing.

2.2 Concept of a Spectral Signature

For any given material its chemical, biological and physical composition (internal and external structures) plus viewing geometry, illumination geometry, atmospheric conditions and other extraneous factors determine the amount of EMR reflected from the object, transmitted or absorbed by chemical bonds (Jensen, 2007).

In an ideal world, each object reflects, emits, transmits or absorbs its own characteristic wavelengths of light (i.e. different proportions of energy in different ranges of the EMS) which would result in every object having its own unique EMR signature. However, in reality this is not the case because there is no guarantee that different materials will exhibit measurably different signatures in the natural environment (Schowengerdt, 2007). Instead of an object's individual spectral reflectance characteristics being termed spectral "signatures", Lillesand and Kiefer, (2000) recommend that the term spectral "response patterns" should be used because the term *signature* tends to imply a pattern that is absolute and unique. This is not the case with the spectral patterns observed in the natural world - they may be distinct but they are not necessarily unique (Lillesand and Kiefer, 2000).

By plotting on a graph the percentage of incident energy reflected by an object at specific wavelengths, spectral response patterns can be examined. These patterns show each object's absorption/reflection profiles as a function of wavelength and give an insight into their spectral characteristics (Lillesand and Kiefer, 2000). In particular, an object's pattern may indicate subtle spectral characteristics which differ from that of other objects, depending on the spatial and spectral resolution of the sensor used (Schowengerdt, 2007). It is therefore on the basis that landscape features have different reflectance properties in different ranges of the EMS that they appear different on remotely sensed images (Gibson and Power, 2000).

The utility of remote sensing therefore depends on sensors recording in wavelength regions of the EMS where detectable differences in reflected and emitted radiation occur for specific features of interest which are large enough to permit individual identification. In vegetation studies where the spectral characteristics of plants change through time according to variables such as growth stage, phenology, atmospheric conditions and illumination conditions (Carvalho *et al.*, 2004) the utility of remote sensing also depends on imagery being obtained at times of the year that maximise the spectral contrast between different crops. The ability to obtain multi-temporal image acquisitions within and between growing seasons is therefore

advantageous for detecting and monitoring vegetation cycles (Murakami *et al.*, 2001; Agrawal *et al.*, 2003).

Figure 2-1 shows typical spectral response patterns for three basic types of land cover; healthy green vegetation, dry bare soil and clear lake water. The wavelength of incident energy is shown on the horizontal axis and the percentage of incident energy reflected at the different wavelengths is indicated on the vertical axis.

The generic spectral response pattern for soil in Figure 2-1 climbs evenly to high reflectance in the longer wavelengths. Reflectance of clear water is higher at the blue end of the EMS and decreases with increasing wavelength. Overall, clear water reflects very little irradiance. The spectral response pattern of green vegetation is much more varied than that of soils or water and is perhaps the most variable in nature as it changes completely during the seasonal lifecycle of many plants (Schowengerdt, 2007). It has an undulating shape with localised reflectance peaks in the 0.55µm (green part of the EMS) and 0.75µm (NIR) regions and a high plateau which begins at 0.8µm after which it gradually descends.

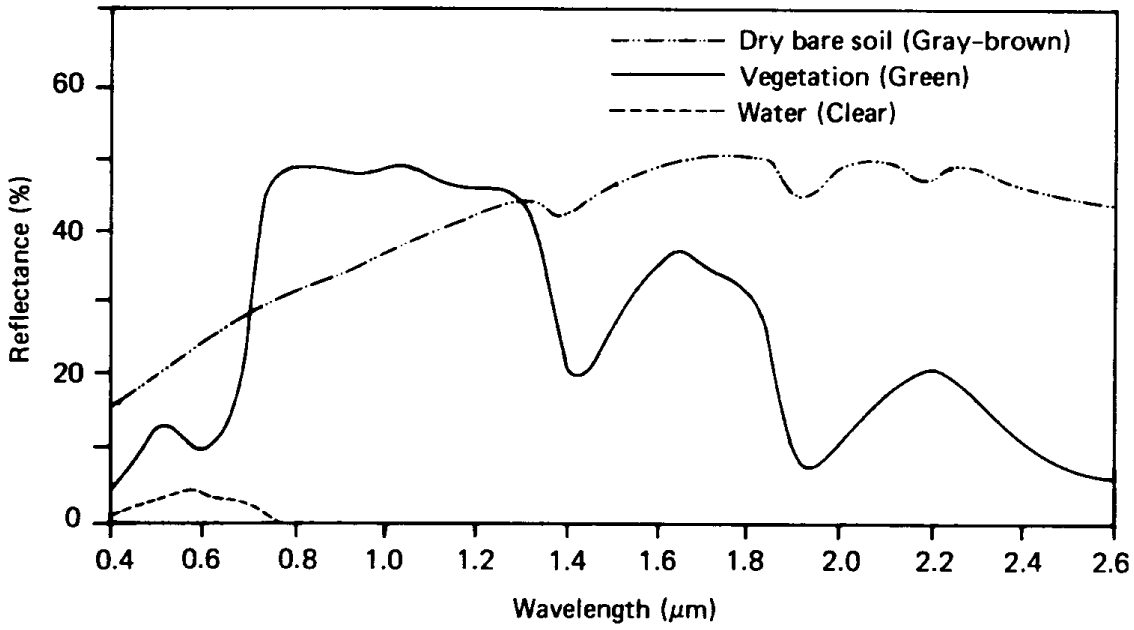

Figure 2-1 – Typical Spectral Response Curves of Basic Cover Types (Lillesand and Kiefer, 1987)

Whilst the response patterns for some vegetation types may visually appear similar at first, a multi-spectral sensor may be able to record subtle differences in absorption and reflectance spectra - which may be indicative of different species, depending on the spectral and spatial

resolution of the sensor used. It is therefore these subtle spectral features that multi-spectral remote sensing analysts try to identify in order to discriminate between different crops.

2.3 General Spectral Characteristics of Vegetation and Bare Soil

A plant's spectral response is determined by how its chemical and physical composition interacts with electro-magnetic energy (Richards and Jia, 1999 and Jensen, 2005). These physical structures therefore have a direct impact on how a plant appears spectrally when recorded using a multi-spectral remote sensing instrument. In the following sections these influences are discussed, beginning with a plant's external structure – its vegetative surface.

2.3.1 Vegetated Surface

For the purpose of this work a vegetated surface consists of many elements, which include all components of the plant and its background, such as: its canopy made up of flower buds, flowers, seed heads and leaves; the canopies' shadows; the gaps in the canopy; the stems and most significantly, the soil background.

As a result, spectral reflectance from the vegetated surface will depend on:

- Its canopy geometry, morphology, total leaf area, absorption and scattering properties.
- How much bare soil is visible, which will depend on the age of the plant, i.e. the stage it has reached in its growth cycle.
- Shadows contained within the canopy.
- Additional environmental factors including site and plant stress, illumination and angles of observation.

In the following paragraphs, factors influencing the appearance of vegetated surfaces are discussed aided by the use of a more detailed vegetation spectral response curve illustrated in Figure 2-2.

2.3.2 Spectral Reflectance Properties of Green Leaves

As solar radiation comes into contact with different plant species the amount of radiation reflected, internally absorbed, emitted, transmitted or scattered changes according to variations in the leaf structures, pigments and moisture content of the plants (Richards and Jia, 1999). It is the reflected and emitted radiance component that is detected by remote

sensing systems and depending on variables such as species, foliage age and environmental conditions during growth, the absolute reflectance of leaves is highly variable (Jensen, 2005).

A leaf comprises several discrete structural layers (Schowengerdt, 2007). Reflection and absorption of EMR is controlled by factors such as leaf pigments, internal light scattering and the amount of moisture in a plant (Jensen, 2005). These influences can be monitored throughout the life-cycles of crops by investigating spectral response patterns. A typical spectral response pattern for vegetation is shown in Figure 2-2, adapted from Swain and Davis (1978).

The next section describes how the reflectance and absorption characteristics of green vegetation in the region from 0.35 to 2.6 μm are influenced by leaf pigments in the visible region, cell structure in the NIR and leaf water content in the MIR.

Influence of Leaf Pigments in the Visible Region

In the visible portion of the EMS, chlorophyll (the green pigment that is chiefly responsible for the green colour of vegetation) controls much of the spectral response of the leaf (Schowengerdt, 2007). Chlorophyll enables the plant to absorb sunlight which makes photosynthesis possible. Additionally, carotenoids - orange pigments, also make photosynthesis possible, but to a lesser extent. Carotenoids and anthocyanins (pink, purple and red pigments) also help to protect the leaf by dissipating excess energy (and therefore avoid leaf damage).

Chlorophyll molecules do not absorb all sunlight equally - they preferentially absorb as much as 70-90% of blue (0.45μm) and red light (0.65μm) for use in photosynthesis (Schowengerdt, 2007) and much smaller quantities of green light. The vegetation response curve in Figure 2-2 confirms this.

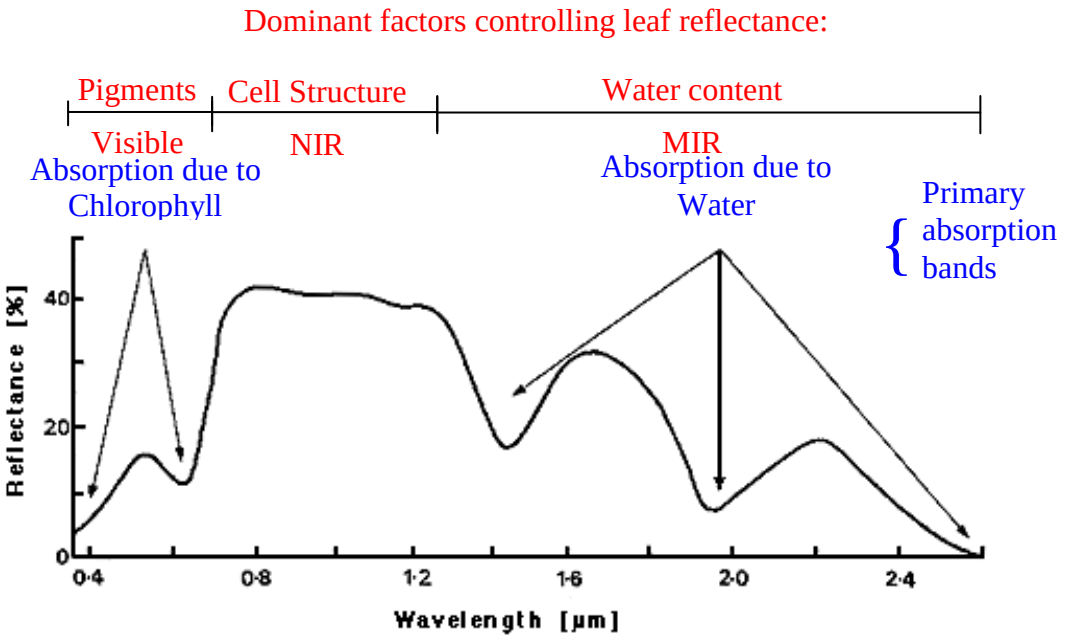

Figure 2-2 – Typical reflectance and absorption characteristics of green vegetation (Adapted from Swain and Davis, 1978)

Significantly, chlorophyll pigments *a* and *b* are the most important plant pigments for absorbing blue and red light - chlorophyll *a* at wavelengths of 0.43µm and 0.66µm and chlorophyll *b* at wavelengths of 0.45µm and 0.65µm (Curran, 1985; Jensen, 2005) – hence the low reflectivity visible on the graph in the blue and red regions. Chlorophyll resides in the membranes of chloroplasts and can be seen in Figure 2-3 below:

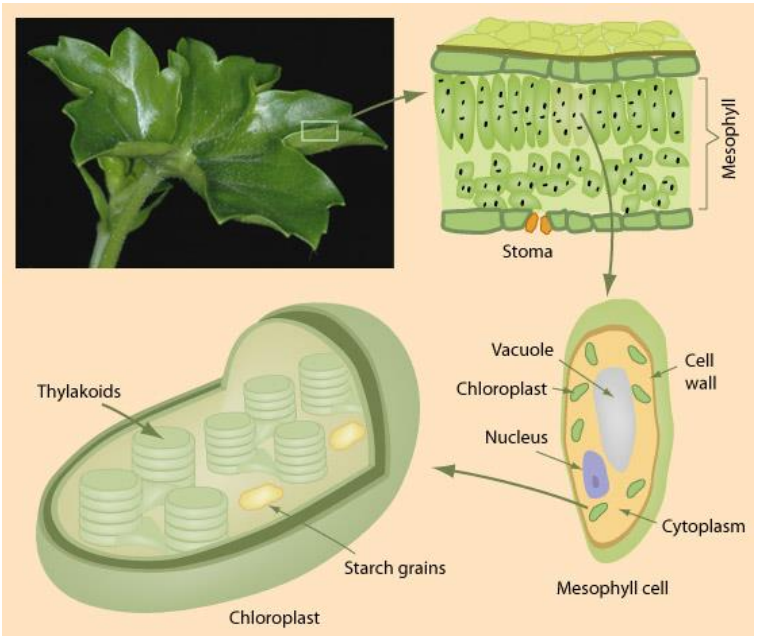

Figure 2-3 - Chlorophyll in Leaves (George State University, 2010)

In contrast, the localised peak identifiable in the visible green part of the EMS in Figure 2-2 indicates that green light is reflected at 0.55µm by chlorophyll pigments. Although blue and red light is also reflected in the visible part of the EMS these are reflected at smaller amounts to green reflectance. This explains why healthy leaves appear green to the naked eye.

Other pigments also present in plant cells are usually masked by the chlorophyll pigments whilst the plant is developing and producing chlorophyll. When crops undergo senescence (die off) or encounter environmental stress caused by drought or disease the chlorophyll pigment may disappear, allowing other pigments to become dominant (Jensen, 2005). In particular, as the crops age and enter senescence the yellow colouration of carotenes and other pigments become more visible to the naked eye (Jensen, 2005).

Influence of Internal Leaf Structure in the NIR Region

In the NIR region, reflection of the leaf is controlled by the structure of the spongy mesophyll tissue, which consists of irregularly shaped cells separated by interconnected openings (Schowengerdt, 2007). At the edge of the visible spectrum at the point where the absorption of red light by chlorophyll pigments begins to decline, reflectance rises sharply (Schowengerdt, 2007). Figure 2-2 shows this simultaneous sharp rise in reflectance and decrease in absorption in the 0.68µm to 0.75µm region.

Peak reflectance in vegetation occurs in the NIR plateau between 0.75µm and approximately 1.35µm where very weak absorption occurs (Srinivas *et al.*, 2004). This is because plants have adapted their internal leaf structure to ensure that very little NIR energy is absorbed (5-10%) to prevent a plant from overheating, particularly in a region where absorption of the bulk of the sun's energy would irreversibly denature a plant's proteins (Jensen, 2005). As a result, the spongy mesophyll layer reflects approximately 40-60% of the incident NIR energy and the remaining 40-60% is transmitted through the leaf onto the underlying leaves where it can be reflected once again by leaves below it (Jensen, 2005).

Theoretically, the greater the number of leaf layers in a healthy mature canopy, the greater the NIR reflectance (Jensen, 2005). This is because vegetation canopies can contain many leaf layers which transmit NIR energy through the leaves - and then reflect them back. This process is called leaf additive reflectance. Conversely, if a canopy is composed of a single, sparse leaf layer the NIR reflectance will be reduced because the energy transmitted through the leaf layer will be absorbed by the soil beneath, rather than being reflected back (Jensen, 2005).

When the reflectance of plants under stress is plotted against wavelength, the often reported "red edge shift" is seen (Jensen, 2005). Red-edge is found in the region from 0.65-0.70µm, at the edge of the visible spectrum at the point where the absorption of red light by chlorophyll pigments begins to decline and reflectance rises sharply (Schowengerdt, 2007). The "red edge shift" occurs when the red-edge moves towards shorter wavelengths when plants become stressed (Jensen, 2005).

This is because as a plant reaches senescence or becomes stressed due to moisture shortages, disease or pest attack, the abundance and effectiveness of chlorophyll declines and so an increase in brightness in the blue and red regions of the EMS occurs (Jensen, 2005). This is accompanied by a distinct decline in NIR reflectance due to a deterioration of cell walls (Schowengerdt, 2007).

Although senescing or stressed plants have a much higher reflectance in the visible region of the EMS as senescence progresses (Jensen, 2005), changes in the NIR are often more noticeable (Schowengerdt, 2007). Therefore, any changes in NIR reflectance may reveal the rate of growth of a crop, and/or when crops have matured, or assist in the detection and subsequent mapping of the spread of disease (Schowengerdt, 2007). It should therefore be possible to identify these changes on multi-spectral and multi-temporal imagery. However, unlike some bio-physical variables which are measured directly by remote sensing systems, vegetation stress is a hybrid variable because it can only be modelled after other biophysical variables are systematically analysed. Therefore, by recording a plant's chlorophyll absorption characteristics in addition to other remotely sensed data, modelling can be used to detect plant stress, yield and other hybrid variables (Jensen, 2005).

Influence of Leaf Moisture Content in the MIR Region

In the MIR region, a leaf's reflectance is controlled by its moisture content. A plant obtains its water via its roots, stems and veins which then carry water into the spongy mesophyll layer. The degree to which incident energy in the middle IR (MIR) region is absorbed by a plant is a function of the total amount of water present in the leaf and the leaf thickness (Jensen, 2005). The greater a plants water content the lower the MIR reflectance (Jensen, 2005). This is because water is a good absorber of MIR energy and so a fully turgid plant (holding as much water as it can) has a lower MIR reflectivity than one that is dehydrated. If a plant becomes dehydrated the amount of water in the intercellular air spaces decreases and

so incident MIR becomes intensely scattered. This results in an increase in MIR reflectance from the leaf (Jensen, 2005).

Five major absorption bands in the atmosphere exist at 0.97μm and 1.19μm (NIR), and at 1.45, 1.94 and 2.7μm in the MIR (Jensen, 2005). Between these bands plants absorb incident energy with increasing strength at longer wavelengths. Therefore, troughs in vegetation reflectance are particularly evident in Figure 2-2 at 1.45μm and 1.9μm owing to moisture content (Richards and Jia, 1999). Figure 2-2 also shows two vegetation reflectivity peaks in the MIR at 1.6 and 2.2μm. According to Jensen, the ranges 1.5–1.8μm and 2.1–2.3μm appear to be more sensitive to changes in moisture content in plants than the visible or NIR portions of the EMS (Jensen, 2005). Some remote sensing platforms like Landsat TM and Landsat 7 ETM have been made sensitive to some of the water bands in the MIR so that canopy moisture content can be examined (Jensen, 2005). Unfortunately, none of the sensors used in this research are able to detect radiance in the MIR region and so the reflectance and absorption characteristics of green vegetation in this portion of the EMS could not be examined in this work.

Measuring Photosynthetic Activity - NDVI

The relationship between red and NIR vegetation reflectance has resulted in many remote sensing vegetation indices (VIs) being developed (Jensen, 2005) to extract information about vegetation biophysical variables. In particular, VIs have been extensively used for monitoring and detecting vegetation and land cover changes (Agrawal *et al.*, 2003) because they produce digital quantitative measures which can be used as an indicator of percentage cover, chlorophyll content, leaf area index and structure, which thereby also indirectly help in the identification of a vegetation type and its state of health (Srinivas *et al.*, 2004). In general, the higher the VI value, the higher the probability that the corresponding area on the ground has a dense coverage of healthy green vegetation (Gibson and Power, 2000).

VI's should be used with caution, however, as quantitative applications necessitate given levels of accuracy which could be affected by errors and uncertainties. If these are not addressed, the results could be misleading. Moreover, as different sensors have their own radiometric, temporal, spatial and spectral characteristics, a single formula will yield different results and so VI results from different sensors will not be directly comparable.

One of the most popular VI's to represent vegetation activity is the Normalized Difference Vegetation Index (NDVI) (Takeuchi and Yasuouka, 2004) which uses a simple

transformation based on the ratio of the NIR band to the red band to highlight differences in the amount of green biomass and chlorophyll content of vegetation (Jensen, 2000). The NDVI equation is shown in Equation 2-1 as:

Equation 2-1 – Normalised Difference Vegetation Index (Jensen, 2000)

$$NDVI = \frac{NIR - Red}{NIR + Red}$$

Where NIR = reflectance in NIR waveband and Red is reflectance in the Red band

Calculations of NDVI for a given pixel result in numbers ranging from -1 to +1, where increasing positive values indicate increasing densities of green vegetation due to strong absorption of red light by chlorophyll in plants and strong reflection of infrared by leaf cells (Murakami *et al.* 2001) and negative values indicate non-vegetative surfaces such as snow, ice, water and clouds.

The NDVI has been shown to be sensitive to crop cycles (Agrawal *et al.*, 2003) and so, if NDVI values are calculated on multiple dates throughout a crop's growth cycle and plotted against time on a graph, seasonal photosynthetic activity trends can be identified and measurements of the length of the growth cycle can be made (Jensen, 2005). Generally, at the beginning of a growth cycle, photosynthetic activity, and hence NDVI is very low. NDVI is higher half-way through the cycle when photosynthetic activity has increased to a maximum and then subsequently decreases as photosynthetic activity reduces towards the end of the growth cycle. In areas where unhealthy or sparse vegetation exist very small positive NDVI values may be found as a result of more visible light than NIR being reflected.

The results of work conducted by the PDP to record the NDVI profile of a field of licit poppy grown for the pharmaceutical industry in the UK are discussed in Chapter 4 to demonstrate how NDVI profiles were subsequently used for identifying poppy growth stages in Afghanistan for use in this research.

2.3.3 Spectral Characteristics of Bare Soil

The general spectral profile of soil is substantially different to the general vegetation profile shown in Figure 2-1. This is because a number of different, but interrelated, soil properties influence the spectral reflectance of a soil including its texture, moisture content, organic content, iron-oxide content, surface roughness and salinity (Jensen, 2007).

A relationship exists between two of the main influences on the reflectance characteristics of soil - texture and moisture holding capacity (Jensen, 2007). Soils which retain water strongly absorb more incident EMR than soils which have a low moisture holding capacity (Jensen, 2007). This means that wetter soils have a lower reflectivity than dry soils and so appear less bright on imagery. For example, clay soils which are made up of very fine and extremely closely packed particles and have very small air spaces between them, hold more water than larger sand particles. This is because the very fine clay particles carry electrical charges which bond a thin membrane of water to them during a rainfall event or when groundwater rises. The air spaces between the particles also fill with water. This means that large forces are required to remove the water from the clay soils in air dried conditions and so less water will drain away or be lost through evaporation. Therefore, fine clay soils have an excellent ability to hold and retain moisture, and as a result, absorb more incident radiant energy and reflect less energy (Jensen, 2007). Conversely, sandy soils drain more rapidly and dry out more rapidly than clay soils because their significantly larger silica particles are inert and so water does not bond to their surfaces. In addition, the air spaces between the large particles are also unable to retain moisture.

Figure 2-4 demonstrates how the reflectance properties of a soil are influenced by its moisture holding capacity. Spectral reflectance curves for Chelsea sand in three moisture-content groupings are shown.

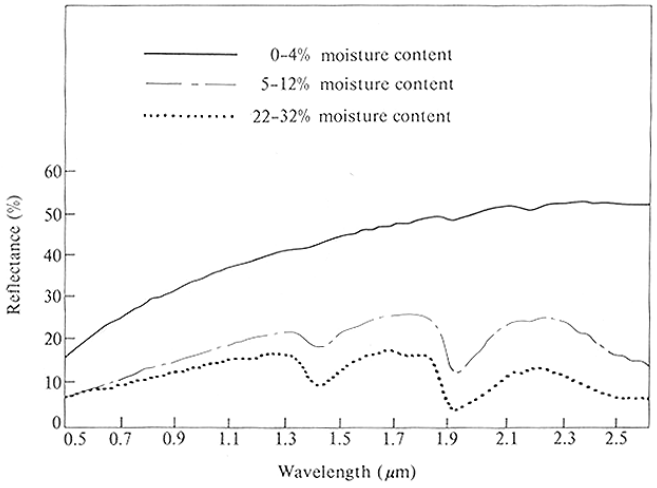

Figure 2-4 - Spectral reflectance curves for Chelsea sand in three moisture-content groupings (Hoffer, 1978)

In Figure 2-4 the curve for the driest soil (0-4% moisture content) shows a general rise in reflectivity as the wavelength increases throughout the region from 0.5μm -2.6μm (Jensen,

2007). The curves for the soils with moisture contents of 5-12% and 22-32% show dips at the 1.4μm, 1.9μm and 2.7μm atmospheric water absorption bands, indicating that incident EMR is strongly absorbed at these wavelengths (Jensen, 2007). This is similar to the dips in reflectance evident in the vegetation response curve in Figure 2-1 which are caused by leaf moisture. The curve for the soil with the highest moisture content has more dramatic dips in the water absorption bands and shows much lower reflectance than the other two curves. This shows that the amount of reflected energy noticeably decreases when moisture content increases.

One major influence on a soil's moisture content is climate. If a soil is located in a hot environment evapo-transpiration often exceeds precipitation. This causes a water deficiency in the soil. The soil will absorb less incident EMR and so will therefore reflect more light than if they were located in more temperate environments. If significant amounts of rain fall over a short period of time surface ponds will form - these also arise after specific irrigation practices are used. After an irrigation event or a rain storm a previously dry sandy soil will begin to absorb significant amounts of incident energy in the water absorption bands (Jensen 2007). As a consequence of this, if an image is acquired during or immediately after a rainfall event the sandy soil will appear much darker than normal until the soil has absorbed all the moisture.

Surface roughness, which is related to texture, also influences the spectral signature of soils - as particle size decreases the soil surface becomes much smoother. This smoothness causes more incoming energy to be reflected. Therefore, farming activities which cause soils to become compacted, such as trampling from the use of heavy machinery, will make the soil smoother, resulting in increased reflectivity. Conversely, ploughing activities could cause decreased levels of reflectance as a result of an increase in surface roughness.

The amount of organic matter in a soil also impacts the spectral reflectance characteristics of exposed soils (Jensen, 2007). Generally, the greater the build up of organic matter in the upper horizon of the soil, the greater the absorption of incident energy and the lower the spectral reflectance (Jensen, 2007).

Conversely, iron oxides in a soil cause an increase in reflectance in the red region of the EMS on imagery and the greater the soil salinity, the higher the spectral reflectance in the visible regions of the EMS (Jensen, 2007).

2.3.4 Illumination Effects – Bidirectional Reflectance

In addition to both soil background (texture, colour and moisture content) and the internal composition of a plant influencing the appearance of vegetated surfaces, the amount and spectral distribution of energy reflected from a vegetation canopy is also influenced by its external structure, illumination geometry and sensor geometry (Jensen, 2007). Each is discussed in turn.

As a plant matures, its canopy morphology, and therefore the percentage of canopy closure, will change. This means that at the early growth stages the spectral response of a canopy will comprise of mixtures of different amounts of energy reflected towards the sensor from its vegetated surfaces, the understory and/or the background soil. In addition, reflection of incident light towards a sensor will also depend on vegetation orientation (in the case of crops this will either be random or systematically arranged in rows), leaf-area-index and leaf-angle-distribution (which may change during the day as the plants orientate themselves towards the sun) (Jensen, 2007).

Even if it is possible to hold as many of these vegetation factors as constant as possible when attempting to compare spectral response patterns obtained over multiple dates, illumination geometry and sensor geometry may also have a significant impact on a plant's spectral response patterns (Jensen, 2007). The theoretical multi-dimensional reflecting characteristic of surfaces is called the Bidirectional Reflectance Distribution Function (BRDF) and focuses on the relationship between the amount of reflected radiance, the geometric characteristics of the sun's irradiance and the sensor viewing properties (Jenson, 2007). When vegetated surfaces are illuminated by the sun from different directions (illumination geometry) or when they are viewed from different angles by a sensor (sensor geometry) they may look different on imagery. This is because the brightness of plant leaves and canopies change as the view direction changes relative to the angle of incident radiation for a given wavelength (ASPRS, 1997). For example, the reflectance of a surface material (as a function of illumination geometry and viewing geometry) is highest when the angle of illumination and the sensor viewing angle are nearly identical and in the same plane, producing bright regions (hotspots) where all shadows are hidden on imagery (Jensen, 2007).

If information can be obtained on the bidirectional reflectance characteristics of illumination and sensor geometry, the remotely sensed data can be calibrated so that useful biophysical information can be extracted (Jensen, 2007). Put simply, the Bidirectional Reflectance

Distribution Function (BRDF) is needed in remote sensing studies for the correction of view and illumination angle effects. Certain wavebands are impacted greatest by BRDF effects. In low reflecting wavelengths (blue and red – in the chlorophyll absorption bands) BRDF effects are enhanced, whilst in the high reflecting green and NIR bands, BRDF effects are small (Jensen, 2007).

Instruments such as spectrometers have been developed by the remote sensing community to measure the BRDF of various surfaces to reveal when the effects are most pronounced. In particular, the Goddard Space Flight Center developed the PARABOLA, a sphere-scanning radiometer for field measurements of the BRDF of natural surfaces. BRDF can also be modelled by computer, such as the Lamertian reflectance model which represents perfectly diffuse surfaces by a constant BRDF.

2.4 Cropping Calendars

The crop calendar is the cycle of crops grown during the year, determined by local climate, local farming practices and economic incentives (Schowengerdt, 2007). It includes the cycle of ploughing, planting, emergence, growth, maturity, harvest and fallow (Gibson and Power, 2000).

Crop identification, classification and interpretation are often improved by knowledge of cropping calendars and individual crops growth cycles (Gibson and Power, 2000). Therefore, by acquiring several images collected at different times throughout the growing season different crops may be discriminated. Moreover, by having an intimate knowledge of the appearance of each crop at the field level at each growth stage, the likelihood of accurate crop discrimination using remote sensing methods increases (Avery and Berlin, 1992).

In this research therefore, local Afghan cropping information will be used in conjunction with an intimate knowledge of the poppy and other crop growth cycles in Afghanistan acquired during this study so that crop discrimination can be performed. In addition, cropping information will also be used to determine the likely rate of growth of each crop to predict when peak vegetative cover, and possible maximum spectral contrast, exists to aid discrimination. The information will also be used to predict when crops may first be visible on imagery so that the earliest appropriate time for image acquisition can be determined.

Information on the Afghan cropping calendar and the appearance of poppy and other crops at key growth stages have been included in Chapter 3.

2.5 Visual Interpretation Fundamentals

As outlined in the Literature Review, visual PI of colour or panchromatic aerial photographs or imagery was found to be sufficient for identifying poppy in Thailand in some of the surveys reviewed (Chuinsiri *et al.*, 1997; Spot, 2000). In these instances its success depended largely on the quality, scale and time (in the growth cycle) of the photographic acquisition and the analyst's experience and ability (Chuinsiri *et al.*, 1997; Spot, 2000a). Sun angle and clouds were also found to affect the identification of poppy. This next section describes the general visual PI techniques that are applicable to crop surveying using both aerial photography and satellite imagery.

2.5.1 Recognition Elements

A number of different generic recognition elements can be used for crop identification. They include: tonal contrast and colour (including black and white); elements concerned with the geometry of crops including their relative shapes, sizes, maximum heights and shadows; the spatial arrangement of crops including their different textures and patterns according to growth stages reached and farming practices used; and the relationships between objects including site, association, time and farming practise (Avery and Berlin, 1992; Jensen, 2007). If used together a higher crop identification accuracy should result.

Tone and Colour

When different objects are imaged or photographed the differences in spectral reflectance and emissivity appear as tonal differences on panchromatic imagery or colour differences on multi-spectral imagery (Jensen, 2007). The edges that are formed by these tonal or colour differences enable the detection of objects. Although colour is not always a critical recognition element it is generally preferred because grey tones often do not correspond to an analyst's perception of an object (ASPRS, 1997).

In panchromatic imagery, the tonal renditions closely resemble the brightness of the scene being imaged and are expressed as various shades of grey between the end values of black and white. Generally, the brighter the tone from a vegetated surface the greater the amounts of biomass present (Jensen, 2007). In colour imagery tone is expressed as various combinations of hue, saturation and intensity.

Geometry of Objects – Size, Shape, Height and Shadow

Descriptions of size, shape, height and shadow are each defined by tonal boundaries. Without tonal differences no perceptions of an object's size, height, shape relative to another object or its shadow can be made. The size of an object is a very distinguishing characteristic (Jensen, 2007) and can be used to rule out many possible alternatives.

Familiarity of the shape of an object from a recognisable side view on the ground and particularly from a plan view is also very important for accurate crop identification. This is because the shape of an object may be very different when viewed in plan or obliquely from aerial photography and imagery. In view of this, Chapter 3 provides examples of crops shown side-on from the ground and from plan views.

Spatial Arrangement of Tonal Boundaries – Texture and Pattern

Unlike size, shape, height and shadow, texture and pattern are not directly defined by tonal boundaries (ASPRS, 1997). Texture (the relationships, dependencies and context between objects (Richards and Jia, 1999) depends on photographic scale and relates to the spatial arrangement and frequency of tonal boundaries of objects. High spatial resolution imagery or photography provides more detail than coarser resolutions and so mapping of surface features should be more accurate (Dikshit, 1994) with fine resolution imagery.

Scale is very important in crop remote sensing studies – it determines how much textural information is available. Even with high resolution imagery textural averaging of small canopy geometries will take place, leading to a certain amount of degradation. Terms to describe texture such as fine, medium, coarse, smooth and rough are therefore relative to a particular scale.

Pattern is the spatial arrangement of objects in a landscape (Jensen, 2007). In an agricultural context, farming practices such as the use of irrigation bunds, the sowing of crops into rows or the division of fields into smaller units create easily discernable and regular patterns. Experience gained through PI of crops may provide a useful insight into the varied farming practices used on each crop - which may help in the discrimination of spectrally similar crops (Sader, 1991).

Context of Objects – Site, Association and Time

Site, association and time are concerned with the relationships between objects and their environment. Site is the relationship of objects to their geographic locations or terrain conditions such as topography, geology, soils, water, vegetation and cultural features (ASPRS, 1997) and has unique physical characteristics (e.g., elevation, aspect etc.) and/or socio-economic characteristics (land value, adjacency to water etc.), Jensen (2007). For example, if trees are to be mapped in a particular area it is useful to find out whether they grow above a certain altitude. This information can then be used to help constrain the number of areas to be interpreted, as recommended by Chuinsiri *et al.*, (1997) in the Literature Review.

Association is the spatial relationship of objects in their environment, which again can help a possible interpretation if certain objects are always known to be within close proximity (Jensen, 2007). For example, Spot Image recognised that Thai poppy fields were often located on steep slopes in inaccessible mountain regions.

Time relates to the temporal relationship of objects which can be established from sequential or multi-date coverage of objects. Knowledge of the time of occurrence can be useful, particularly if some objects can only be detected at certain times. For example, depending on the spatial resolution of the photograph or image, crops will only be visible once their green biomass has been given time to build up. Differences in planting, maturity and harvesting dates for various crops are therefore used to assist in their identification from satellite images or aerial photography. For example, in the Literature Review it was revealed that an indicator used by UNODC to discriminate poppy from other crops is its early harvest time which occurs whilst the crops are green and not when they have senesced like all other crops.

2.5.2 Computer Processing for Photo Interpretation

Photo-interpretation may be aided substantially when image data is available in digital form if a degree of digital processing is applied to image data before PI is used – which makes the spectral and spatial data more meaningful to photo-interpretations (Jensen, 2007 and (Richards and Jia, 1999). This was found to be the case in Chuinsiri *et al.*'s 1997 work where digital enhancements were found to improve PI results.

For instance, geometric enhancements can establish a new brightness value for a pixel by using the existing brightness values of pixels over a specified neighbourhood of pixels

(Richards and Jia, 1999). These enhancements are often used to smooth noise in the data so that large area features become more apparent, or to enhance and highlight edges so that roads or field boundaries become more visible, to aid recognition. In addition, radiometric enhancements, which alter the contrast range occupied by the pixels in an image, can be used to amplify an image's spectral character (Jensen, 2007). For example, when analysts were able to incorporate additional textural and contextual information into their PI approach, Chuinsiri *et al.*, (1997) reported higher identification successes.

In this study, Afghan poppy crops may be distinguished from other crops on satellite imagery if the imagery is acquired at an appropriate time in the cropping calendar, and if digital enhancements can be performed. PI of imagery and aerial photography may at least prove to be as good as, if not more successful than digital image classifications, especially if poppy does not have a unique spectral signature.

2.5.3 Discussion of Photo-Interpretation

Whilst PI of panchromatic or three-band colour photography or imagery may be effective and sufficient for many applications, particularly when a small number of pixels are to be analysed, there are occasions where a PI approach is inadequate – principally if large areas of land are imaged at high resolutions or where more spectral bands could provide additional information on vegetation characteristics. Given that there were approx 100,000 acres of land under poppy cultivation in Afghanistan in 2005 (UNODC, 2005b) a PI approach may be limited due to the immense number of pixels that have to be analysed and the time constraints imposed on operational poppy detection in Afghanistan, unless considerable resources are available.

In this instance, computer processing may be preferable to PI methods because computers are able to handle huge quantities of information with ease and require less analytical input than PI techniques. Moreover, if computer processing techniques are used on image and aerial photographic data the multi-dimensional aspect of the data and its radiometric resolution will be fully taken into account by the computer (Richards and Jia, 1999). In addition, a computer is able to conduct quantitative analysis which can be used for area estimates once certain processing procedures have taken place, which a PI approach is unable to do as accurately.

In terms of very high resolution images (at resolutions of less than 1m) PI and digital classifications have their respective advantages and disadvantages. Very high resolution images enable fast visual interpretation by the human eye, particularly as the brain can

understand a very small object's context and function, which digital classifications cannot. Moreover, less time may be required to produce a useable product of a small area through PI. However, with very high spatial resolution data such as 4m IKONOS, its 10 km x 10 km image size means that a digital classification will produce much quicker results than a human photo-interpreting the whole image, and therefore it may be cost effective to digitally classify larger geographical areas (i.e. 10 km and upwards).

Even though high resolution images contain more detailed information, classification accuracies may not be improved by increasing the spatial resolution, as class spectral seperability may decrease. The consequence of this may be a rise in classification errors.

Another consideration for PI and digital classifications of high resolution imagery is the effect of shadows. In lower resolution imagery (i.e. spatial resolutions of 30m plus) these are not too problematic as a classification will 'smooth out' variations across ranges of individual pixels. However, in classifications of higher resolution images, shadows could create very misleading results - whilst the shadows can be useful in PI as they could provide better context to an object.

Given all of the above, PI of high resolution oblique aerial photographs and satellite images is used by the US Government to identify poppy cultivation in Afghanistan. Although the PI recognition elements described in Section 2.5.1 are used by US analysts it was not possible to review their imagery or analysis in this research because of classification restrictions. As a result no investigation could be conducted into the US poppy identification methodology. In this study PI is used to assist in the identification of land cover types for use in digital image classifications using high resolution three-band aerial photographs acquired from a Zeiss camera mounted onboard a fast jet aircraft, wherever possible. The results are discussed in Chapter 4.

2.6 Digital Image Processing Fundamentals – Classification

Traditional digital image classification uses processing software to separate different cover types in an image into classes based on their spectral characteristics (Richards and Jia, 1999). This procedure is particularly useful as a means of automating a change detection process or when millions of pixels have to be examined, rendering the PI procedure both time-consuming and expensive if many areas are to be examined (Richards and Jia, 1999). Moreover, in an agricultural context where a large number of sample areas with many small fields have to be analysed, the amount of time required to identify the contents of every field

parcel through visual interpretation would make the PI technique very manpower intensive. Digital image processing may be more cost-effective in these circumstances, particularly if sufficient differences exist in the spectral responses of the various cover types being mapped. Digital classification is also advantageous in instances when the resolution of the imagery or photography is too coarse for accurate photo-interpretation.

Image classification is a complex process and requires consideration of many factors (Lu and Weng, 2007). Table 2-1 shows the major steps in image classification (Lu and Weng, 2007):

Table 2-1 – Steps in Image Classification (Lu and Weng, 2007)

Step	Steps in Image Classification
1	Determination of a suitable classification system
2	Selection of a sufficient number of training samples
3	Image pre-processing
4	Feature extraction
5	Selection of suitable classification approaches
6	Post-classification processing
7	Accuracy assessment

Many potential variables can be used in image classification. For land cover mapping, numerous studies have demonstrated the applicability of spectral information to discriminate between different land cover types (Carvalho *et al.*, 2004). However, as previously discussed, some objects appear spectrally very similar on imagery and so other variables may also be used to enable accurate discrimination of spectrally similar cover types. For example, one approach is to use additional information related to textural or spatial measures, which may lead to an improvement in classification accuracy (Dikshit, 1996). Other approaches include using multi-temporal images, multi-sensor images and auxiliary data (Lu and Weng, 2007).

In general, image classification strategies can be grouped into supervised or unsupervised, parametric and non-parametric, hard and soft (fuzzy), per-pixel, sub-pixel and per-field amongst others (Lu and Weng, 2007). Selection of the most suitable classification approach for a particular area of interest is usually dependent on the user's need and the desired accuracy of the classification, the scale of the study area, the availability of auxiliary data, the analyst's skills, experience and the amount of involvement required by the analyst to train the

classifier, the availability of classification software, the amount of time available for image processing and the quality of the classification (Lu and Weng, 2007).

Traditionally, land cover mapping applications using remotely sensed data have employed supervised classification algorithms or unsupervised clustering algorithms (Friedl and Brodley, 1997) using variables most useful for separating vegetation classes such as spectral signatures (Lu and Weng, 2007). In recent years many advanced classification approaches have been applied for image classification (Lu and Weng, 2007) alongside the widely used traditional heritage classifiers. These newer methods are more sophisticated than traditional classifiers and have the advantage that they can handle complex relations among class properties (Friedl and Brodley, 1997). However, one drawback is that they are highly complex with regard to their algorithmic basis and therefore require substantial expertise, human interaction and interpretation (Friedl and Brodley, 1997). Similarly, with the ability of the newer methods to handle large data volumes the computational costs required may be a significant operational limitation (Carvalho *et al.*, 2004).

Sections 2.6.1 and 2.6.2 discuss the traditional classification approaches in detail. Recommendations for further work using other variables with the more advanced classifiers are considered in the recommendations section of the final chapter.

2.6.1 Supervised Classification

A supervised digital image classification involves considerable input from the analyst and a knowledge of the land covers found in the study area (Gibson and Power, 2007). The classification process is divided into three distinct stages – training, classification and output. In the training stage, pixels are identified and collected by the analyst from multiple training areas representative of each known land cover type (information classes) present in the image, to enable the image processing software to classify the remaining pixels. Multiple training sites are selected so that as many spectral responses as possible are identified in each information class in order to include the range of spectral variability in each class (Schowengerdt, 2007). This process is most effective when the analyst has ancillary data such as ground data and photographs to assist in the selection, and has experience of the spectral properties of each land cover class (Skidmore, 2002).

For the classification stage numerous strategies are available to assign unknown pixels to the classes defined in the training stage (Lillesand and Kiefer, 2000), including; Minimum Distance to Means (MDM) classifier, Parallelepiped classifier (sometimes referred to as a

box classifier), Maximum Likelihood Classifier (MLC), Artificial Neural Network and Decision Tree classifiers for example (Lu and Weng, 2007).

Depending on which classification algorithm is selected a statistical characterisation of the reflectance of each information class is developed from numerical descriptors specified by the analyst, for each information class. The statistical characterisation may be based on the means of all spectral responses collected for each information class or the range of reflectance for each band. Information class variance, mean and covariance over all spectral bands may also be used in the signature analysis. Once the statistical characterisation has been achieved for every information class, decision rules are used to recognise other pixels with similar characteristics in the image (Richards and Jia, 1999). This stage is referred to as image classification because unknown pixels are assigned to the information class which they resemble the most.

In the output stage after the pixels have been assigned classes the results may be presented in the form of either a thematic (class) map in which pixels are given a label represented by a colour to identify them, or a table which summarises the number of pixels in the image belonging to each class.

The next section describes three of the more commonly used traditional supervised classification strategies used for land cover mapping. This emphasis is based on the fact that they form the backbone of most multi-spectral classification activities (Lillesand and Kiefer, 2000). Section 2.6.2 discusses the unsupervised classification approach.

Minimum Distance to Means

One of the simpler classification strategies is the MDM method (Gibson and Power, 2000; Lillesand and Kiefer, 2000). Firstly, the coordinate values of each mean vector (mean spectral value for each class) is determined. Then a pixel of unknown identity is classified by computing the distance between it and the mean spectral values for each class. The unknown pixel is then assigned to the closest class. If a pixel is further from any class mean than an analyst has pre-defined, it is classified as ‘unknown’ (Lillesand and Kiefer, 2000).

The MDM strategy is mathematically the simplest, requires minimum user input and is computationally efficient (Lillesand and Kiefer, 2000; Jensen, 2005). It is also of particular use when the number of training pixels per class is limited because it depends only on the mean positions of the spectral classes. For a given number of samples this is very useful

because the mean positions of classes can be more accurately estimated than the covariances which the gaussian MLC uses (Richards and Jia, 1999) described in a later paragraph.

Significantly, however, the MDM has two limitations - it is neither sensitive to different degrees of variance in the spectral properties of the training data (Lillesand and Kiefer, 2000), nor sensitive to its direction from different class means (Richards and Jia, 1999). Both of these factors can lead to misclassification because the MDM assigns an unknown pixel to the nearest class mean vector regardless of its position adjacent to a small number of spectral values from another class with a wider range of spectral values. Because of this the MDM is not widely used in applications where spectral classes are close to one another in measurement space and have high variance (Lillesand and Kiefer, 2000). Consequently, the parallelepiped classifier outlined below is sometimes used because it is sensitive to variance.

Parallelepiped Classification

The Parallelepiped classifier is simple to use, fast and efficient and takes into account class spectral variance by considering the range of values in each class training set (Richards and Jia, 1999; Lillesand and Kiefer, 2000). This range, known as a decision region, is defined by the highest and lowest digital number (DN) values in each band, yielding rectangles (‘boxes’) around each training class data set (Lillesand and Kiefer, 2000). In multi-dimensional space these ranges are called Parallelepipeds. An unknown pixel is classified according to the class range, or decision region within which it lies. An ‘unknown’ classification would result if a pixel lies outside all of the class ranges.

Problems arise however, when the boxed ranges overlap, typically when classes with similar spectral properties have been chosen and/or there is a high degree of correlation between the spectral properties of objects in different wavebands (Richards and Jia, 1999). Covariance, which is the tendency of spectral values to vary similarly in two bands, results in elongated ‘clouds’ of DN’s which do not fit neatly into the class training data rectangles when plotted onto a scatter diagram (Lillesand and Kiefer, 2000). This results in incorrectly classified pixels because the Parallelepiped classifier is insensitive to correlation (Richards and Jia, 1999). To alleviate such problems, individual training class rectangles can be broken into a series of rectangles with stepped borders which more closely describe the elongated distributions. This process results in stepped decision boundaries.

Maximum Likelihood Classifier

A strategy that is potentially more accurate because it considers the most information (variance and correlation) is the MLC. The MLC approach is based on probability and is the algorithm of choice for many users because of its ready availability and the fact that it does not require an extended training process (Pal and Mather, 2003).

The MLC works by first calculating the mean vector, variance and correlation of each land cover class in the training data, on the assumption that the distribution of the data for each class is gaussian (normally distributed) (Jensen, 2005), which gives rise to good mathematical descriptions of the supervised classification process (Richards and Jia, 1999). The assumption of normality is generally reasonable for common spectral response distributions and means that the distribution of pixel values can be completely described by the mean vector and the covariance matrix (Lillesand and Kiefer, 2000).

The statistical probability of a pixel belonging to any land cover class can be viewed on a three-dimensional scatter diagram, where the vertical axis shows the probability of a pixel value being a member of one of the classes. The resulting bell-shaped curves are known as probability density functions, one for each class, and can be used to allocate unidentified pixels to the class with which they have the highest probability of membership (Lillesand and Kiefer, 2000). As every spectral response has a probability of representing a class, no pixels will be left out unless the probability value is below a threshold set by the user. In this case a pixel will be labelled as ‘unknown’ (Lillesand and Kiefer, 2000). The probabilities can also be viewed as ellipsoid equiprobability contours on a two-dimensional scatter diagram, and, similar to the Parallelepiped classifier, their shape expresses the sensitivity of the MLC to covariance (Lillesand and Kiefer, 2000).

In the MLC each spectral class is described by a multivariable probability distribution in multi-spectral space (Richards and Jia, 1999), where the number of variables is determined by the number of spectral bands used. The MLC is appropriate for normally distributed data and generally provides higher classification accuracy than the MDM and Parallelepiped classification strategies (Richards and Jia, 1999). As classification accuracy is not overly sensitive to violations of the assumptions that the classes are normally distributed, the MLC is said to be robust (Richards and Jia, 1999).

2.6.2 Unsupervised Classification

An alternative method to the supervised classification is an unsupervised classification, where natural groups are identified within the multi-spectral data (Campbell, 2006). Unsupervised classification (also commonly referred to as clustering) normally requires only a minimal initial input from the analyst because the classification does not normally require training data (Jensen, 2005). Instead, the processing software uses an algorithm to separate unknown pixels into a number of spectral classes based on natural groupings of the reflectance values in an image (Lillesand and Kiefer, 2000). It operates on the basic premises that the DN values in a given class should be close together in spectral space with little variance but widely separated from other classes.

Numerous clustering algorithms can be used to determine the natural spectral groupings present in the dataset (Lillesand and Kiefer, 2000). In the "K-means" approach an analyst defines the desired number of clusters to be located in the data and the computer algorithm then arbitrarily selects this number of cluster centres in the image space. Distances between pixels are subsequently calculated and the pixels are then assigned to the nearest class. The computer then iteratively re-positions the cluster centres until they are optimally separated, and the revised positions are used to reclassify the image data (Lillesand and Kiefer, 2000). When there are no further significant changes in the locations of the class mean vectors the analyst determines the identity of each class using reference data. The end result is a set of spectrally distinct classes of image data (Lillesand and Kiefer, 2000).

Other unsupervised classification approaches use algorithms that incorporate image texture as a basis for establishing cluster centres (Lillesand and Kiefer, 2000). Texture is defined by the multi-dimensional variance observed in a moving window (using a 3x3 kernal for example) passed through an image. A variance threshold is set by an analyst, below which a window is considered smooth (homogenous), and above which is considered rough (heterogeneous). Cluster centres are selected according to the mean of the first, second, third etc. smooth windows encountered until an analyst-specified maximum number of cluster centres is reached (Lillesand and Kiefer, 2000). Then the distances between all previously-defined cluster centres are considered by the algorithm and the two closest centres are merged and their statistics defined. This process of combining the closest two clusters is repeated across the image until the entire image is analysed (Lillesand and Kiefer, 2000).

One major advantage of using an unsupervised classification is that the results can be obtained very quickly because the analyst does not spend time inputting training data. Additionally, the small amount of involvement required by the analyst to specify the number of classes desired (or minimum and maximum number of classes required) means that the opportunity for human error is minimised (Campbell, 2006).

An additional advantage is that an unsupervised classification can be used when an analyst has little extensive prior knowledge or reference data to help determine class composition. However, knowledge of the region is required to interpret the meaning of the results produced by the classification process (Campbell, 2006).

One other advantage is that a class with a very small areal extent can be recognised as a distinct unit in an unsupervised classification, which could otherwise be inadvertently incorporated into other classes in a supervised classification (Campbell, 2006).

Some disadvantages and limitations of unsupervised classifications exist. For example, the reliance on natural groupings means that the classifier may identify a spectral class that is not of interest to the user. In addition, if reference information is not available the analyst will experience difficulty determining the identity of the classes. One other disadvantage is that the spectral properties of vegetative classes will change over time, both seasonally and over a period of years. As a result, relationships between classes are not constant and relationships defined for one image may not be extended to other images (Campbell, 2006).

Alternative Types/Names of Classifiers

Per-pixel Classifiers

The traditional supervised and unsupervised classification approaches described above plus the Artificial Neural Network (ANN), Decision Tree (DT) classifier, evidential reasoning, and Support Vector Machine (SVM) classifiers label unknown pixels on the basis of their spectral properties alone. They are often referred to as per-pixel classifiers because they use pixels as the basic processing unit, and each pixel is classified into one of several mutually exclusive classes (Lu and Weng, 2007).

One overarching disadvantage of per-pixel classifiers is that the resulting class signatures will contain contributions from all the materials present in the same training set, and therefore, classification results may be ‘noisy’. Furthermore, with the increased availability of high resolution images (0.5-4m spatial resolution) the number of detectable classes and sub-classes

has increased, and as a result, within-class variance will be higher (Wang *et al.*, 2004) than that found with medium resolution sensors (i.e. 30m plus). This means that pixel-based classification methods may be unfavourable when very high spatial resolution images are used because separation of spectrally mixed land cover types may be very difficult (Wang *et al.*, 2004). For example, in a study of mangrove canopies in Panama, Wang *et al.*, (2004) reported that although the pixel-based MLC retained the spectral information within the high resolution IKONOS images used, the high spatial scale did not result in good differentiation between two different species of mangrove trees.

Non-parametric Classifiers

The ANN, DT classifier, evidential reasoning, SVM and expert system classifiers highlighted above are non-parametric because no assumption about the data is required as they do not employ statistical parameters to calculate class separation (Lu and Weng, 2007). Therefore, their ability to cope with non-normal distributions and intra-class variation found in a variety of spectral data means that non-parametric classifiers frequently yield higher classification accuracies than parametric classifiers (Carpenter *et al.*, 1999).

Other advantages of non-parametric classifiers are that they are insensitive to missing values, are capable of handling numerical and categorical input (Carvalho *et al.*, 2004) and are especially suitable for the incorporation of non-remotely sensed data into the classification procedure (Lu and Weng, 2007).

ANNs are computer programs that are designed to simulate human learning processes through establishment and reinforcement of linkages between input data (for example multi-temporal and multi-spectral data) and output data (classes of interest), (Campbell, 2006). In the literature, ANNs have been found to produce small accuracy improvements when their performance has been compared to the traditional statistical classifiers (Campbell, 2006). For example, in their land cover inventory of a complex rural area in central Italy, Bruzzone *et al.*, (1997) demonstrated that the non-parametric ANN approach provided more satisfactory accuracies than a parametric MLC approach, even though the MLC had been modified to include nonparametric *a priori* possibilities to make the classification more effective in the presence of non-Gaussian spectral distributions (Bruzzone *et al.*, 1997).

A DT is a classification procedure that repeatedly partitions a dataset into smaller subdivisions on the basis of a set of tests defined at each branch (or node) in the tree (Friedl

and Brodley, 1997). For example, water might be separated from all other classes based on a simple threshold set in a NIR band (Lillesand and Kiefer, 2000)

Rogan *et al.*, (2002) compared the MLC with DT classification techniques to identify changes in vegetation cover in a forested ecosystem in California and found that the DT classifier outperformed the MLC approach by approximately 10%. Similarly, Friedl and Brodley (1997) compared accuracies achieved by three DT algorithms with both MLC and linear discriminant function classifiers. They found that DTs in general and the hybrid decision tree in particular, produced consistently higher classification accuracies than either the MLC or LDF algorithms (Friedl and Brodley, 1997).

The SVM has become an effective tool for pattern recognition, machine learning and data mining in recent years (Dixon and Candade, 2008). In a study of land use in South West Florida, Dixon and Candade (2008) found that the ANN and SVM significantly outperformed the MLC. However, their study also showed that the ANN training was time-consuming, cumbersome, and compared to the SVM, was slow and more difficult to implement (Dixon and Candade, 2008).

Sub-pixel Classifiers

Due to the complexity of a landscape high spectral variation may be found within class training datasets (Lu and Weng, 2007). As a result, mixed pixels are common in remotely sensed data because each pixel represents a spatial average over the ground-projected constant instantaneous field of view of the sensor (Schowengerdt, 2007). Sub-pixel classification approaches such as IMAGINE's sub-pixel classifier, the fuzzy classifier and spectral mixture analysis classifiers have therefore been developed to overcome the mixed pixel problem.

Contextual Classifiers

In contrast, an object or segment is the basic processing unit of contextual classifiers, where a pixel is considered in the context of its neighbouring pixels. For example, if the features on a desert island are to be mapped, a pixel would only be assigned to a 'beach' class if it had the spectral signature of the beach class training data and it was within a specified distance of the water (Gibson and Power, 2000).

Contextual classifiers such as the iterated conditional modes, point-to-point contextual correction and frequency-based contextual classifier investigate the relationships, dependencies and context between an object and its neighbour - each of which are useful

information sources that are not exploited by the more traditional classifiers (Richards and Jia, 1999). They have been developed to cope with the problem of intra-class spectral variations (Lu and Weng, 2007). Pre-smoothing classifiers may be used to incorporate contextual information (additional bands for example) before a spectral classification is performed. Post-classification, post-smoothing is then conducted. By including context these classifiers exploit spatial information, and because of their sensitivity to the correct spatial context of a pixel, they can be used to identify pixel labelling errors that might result from noisy data or unusual classifier performance (Richards and Jia, 1999). A thematic map can be produced which is consistent both spectrally and spatially.

One object-oriented classifier, eCognition, uses an image segmentation approach to merge pixels into objects. Criteria can be set by the analyst to control the measures that are used to assess homogeneity and distinctiveness, and the thresholds that apply to a specific classification (Campbell, 2006). A classification is then subsequently performed on these objects (instead of individual pixels) using nearest neighbour or fuzzy classification algorithms. Unlike the per-field classifiers no GIS vector data are used.

Object-oriented classification has been found to give better classification results than per-pixel approaches when fine-resolution data has been used (Lu and Weng, 2007; Campbell, (2006) because they avoid intra-class spectral variation by using land parcels as the basic processing unit (Lu and Weng, 2007) and so noise prevalent in the per-pixel classifiers is averaged out. One major disadvantage of these classifiers is that they are often affected by poor definition of field boundaries (Lu and Weng, 2007).

In spectral-contextual classifications both spectral and spatial information is used. Spectral-contextual schemes tend to work best when an image scene consists of relatively homogenous objects of at least several pixels (Schowengerdt, 2007). One example is the ECHO algorithm, where initially, adjoining pixels are aggregated into small cells based on the similarity of their spectral vectors (Schowengerdt, 2007). If a pixel crosses a spatial boundary it is detected by a threshold on the pixel variance and is then discarded. The homogenous cells are then aggregated further if they are spectrally similar to neighbouring cells (Schowengerdt, 2007), and eventually the resulting spatially homogenous areas are classified in their entirety as single spectral samples, rather than pixel-by-pixel (Schowengerdt, 2007).

Knowledge-based Classification Approaches

A knowledge-based expert system represents an expert's knowledge-base as data and rules within the computer (Jensen, 2005). GIS is used extensively for developing knowledge-based classifications because their capabilities include managing multi-source data and spatial modelling (Lu and Weng, 2007). Ancillary data, such as a digital elevation model, temperature and precipitation data, soil maps and road networks may be incorporated into the classification approach (Lu and Weng, 2007).

One critical step is to build rules that can be used to examine the relationships between multi-source data. For example, Chuinsiri *et al.*, (1997) and Spot Image (2002a) noted that the distribution of poppy fields in the mountainous areas of Thailand was related to elevation, slope, logging activity and inaccessibility. By effectively using these relationships in classification procedure, classification accuracy may be improved (Lu and Weng, 2007). Rules for classification may be built by explicitly eliciting knowledge and rules from experts, by implicitly extracting variables and rules using cognitive methods, or by empirically generating rules from observed data with automatic induction methods (Lu and Weng, 2007). Pollution, erosion and flood risk mapping are all applications that take advantage of digital maps integrated within a GIS (Delenne *et al.*, 2008).

2.6.3 Discussion

It is not possible to state which classifier is "best" because each has its own strengths and limitations. Accurate classification of land cover types is a challenge because many factors, such as the complexity of the landscape in a study area, the spatial and temporal resolution of the remote sensing data used and the classification approach used may affect the success of the classification (Lu and Weng, 2007). Conventional classification methods such as the MLC are widely regarded in the remote sensing community as being an effective method for classifying individual land cover types (Wang *et al.*, 2004) if sufficient training samples are available and land cover features are normally distributed (Lu and Weng, 2007). Conversely, more complex classifiers have the potential to produce more accurate classification results than the MLC, particularly if the information contained in the relationships between each pixel and those that neighbour it are also exploited, in addition to the spectral information gathered (Campbell, 2007). However, some trade-offs between conventional and modern classifiers exist, such as simplicity and economy *versus* time consumption, software availability, analytical skills and experience required.

Of the traditional heritage classifiers (MDM, parallelepiped and MLC) the MLC is a promising choice. This is because it considers both the distance between means and variance, it assigns membership of an unknown pixel to one definitive class on the basis of the pixel's multivariate distribution and it generally provides more classification accuracy than the other hard, point classifiers described. However, it also assumes normally distributed data, which isn't always the case, and so the literature shows that the more recent classifiers have the potential to improve classification accuracy.

Careful consideration of these factors for this study led to the conclusion that the best classification approach to use in this research was a traditional supervised classification method using two variables: spectral signatures and multi-temporal data. This was principally based on the potential availability of imagery, the ready availability of the traditional classifiers, but more significantly, the total lack of experience of digital image classification by the image analysts that would be employed by the end-user.

Additionally, the choice of classification approach to be used was also influenced largely by the end-user's (the MOD) requirements that the classification software had to be easy to use, already available and would not require significant amounts of time for user training and subsequent image processing. It was crucial that these requirements were met because the skill-set required to use the chosen classification technique has to be easily and rapidly transferred to a broad group of analysts operationally employed in Afghanistan who had previously received formal training on PI techniques, but whom had obtained no professional qualifications in remote sensing and had no experience of multi-spectral image data.

As a consequence, despite recent advances in classification approaches, this research into the novel field of the multi-temporal, multi-spectral detection of poppy in Afghanistan uses the MLC, an established standard algorithm (Richards and Jia, 1999) which research has indicated is an effective method for classifying individual land cover types with traditional remotely sensed data (Wang *et al*., 2004).

2.7 Factors Influencing Classification

In order to avoid misleading or meaningless classification results several important factors were considered before the MLC approach was used in this research. These factors are described following Congalton (1991) and are detailed in subsequent sub-sections:

- Training and evaluation data must be independent, representative, free from the effects of spatial autocorrelation or spectral mixing and selected using optimum sampling parameters.
- The training data and classified image must be perfectly co-registered.
- The correct classification scheme is used.

A sensor's capabilities in terms of spectral, spatial, temporal and radiometric resolutions are also important factors influencing the accuracy of a digital image classification and are described in Section 2.7.3.

2.7.1 Training/Evaluation Data

Given that the quality of an image classification is only as good as the quality of the training data used to perform the classification (Poth *et al.*, 2001) it is critical that training and evaluation data is collected with care. If not, any errors present in the training data could lead to correctly classified pixels being incorrectly assessed and misclassified as a result. The following sub-sections outline the typical ways in which errors in training data are introduced and the steps that should be taken to avoid them.

Representativeness

For each class, samples of training and evaluation pixels should be collected from training areas dispersed throughout an image to ensure that each class set includes a representative sample of all pixels.

The number of pixels in each class selected for training and evaluation should be calculated based on the proportion of the cover type present in the image that they represent so that any possibility of bias in the subsequent classification process is reduced. It is also critical that a sufficiently large sample size is selected to allow statistically valid analysis, but this must be balanced against practical and economic considerations.

In order to obtain sufficient numbers of training pixels to allow accurate estimates of the elements of the mean vector and covariance matrix to be determined using the statistically-based MLC (Richards and Jia, 1999), Mather (2004) recommends that a sample size of at least 30p pixels per class should be used, where p is the number of spectral bands. Richards and Jia (1999), Lillesand and Kiefer (2000) and Swain and Davis (1978) recommend that a minimum of 10 n samples per spectral class be collected, where n is a pixel, with 100 n

training pixels being highly desirable if it can be attained. This is because the estimates of the mean vectors and covariance matrices employed in the MLC improve as the number of pixels in the training set increases (Lillesand and Kiefer, 2000).

Error-free Data – Minimising Selection of Mixed Pixels

Training data must represent the spectral variability of each cover type present, collected from different segments within an image. This is particularly important as classes are most likely to be heterogeneous mixtures of vegetative and soil matter, which frequently contain different spectral properties (Lillesand and Kiefer, 2000). The Literature Review revealed how different quantities of vegetation, soils, agricultural practices, aspect variations and different growth stages resulted in mixed spectral responses from poppy.

Although this mixing of spectral responses within vegetation classes cannot be avoided, the selection of mixed pixels - where a pixel falls across a boundary between two cover types - can be avoided if the training pixels are selected carefully. If mixed pixels are selected from the edges of linear features such as tracks and fields the sensor will measure the average response for the mixture under the pixel. As a result, the class will contain atypical values because the training data will be contaminated in a non-uniform way and could cause the cover type to be misclassified. The proportion of mixed pixels will also increase if the target size is close to the size of a pixel.

The presence of mixed pixels was of particular interest in this research - especially at different stages in the growth cycle. As such, a methodology was developed which enabled individual training class signatures to be carefully selected and examined. This methodology is described in Chapter 5.

Independent Data - Minimising Spatial Autocorrelation

For ease and rapidity, training data is frequently collected for each cover class by drawing polygons around the boundaries of homogenous land parcels to collect contiguous groups of pixels. Unfortunately, if the training data collected using this method is to be used in the MLC, this method will result in the data file values of each pixel selected within the polygon to be related to, or be dependent on the reflectance measured from its neighbouring pixels. This correlation between adjacent pixels is known as spatial autocorrelation, which is the tendency of measurements at one location to resemble those at nearby locations (Campbell, 2006). The presence of spatially autocorrelated training pixels will therefore invalidate one of

the assumptions made by the MLC, that training pixels are independent observations. As a result, the data values of the training pixels may affect the accuracy of any classification.

The degree of autocorrelation between pixels depends on the natural association between adjacent ground cover pixels, the dimensions of the pixels (as pixel size increases the autocorrelation distance decreases) and the effects of data pre-processing (Mather, 2004). Therefore, if the MLC is to be used, the degree of spatial autocorrelation between pixels must be calculated to determine how far apart training pixels must be in order to avoid the effects of spatial autocorrelation.

Its measurement involves the simultaneous consideration of both locational information (the pixels) and attribute information (the spectrally derived digital numbers) (Wulder and Boots, 1998). Spatial autocorrelation can be calculated by taking sequences of pixels that are spaced 1, 2, 3 etc. units apart and plotting the correlations between a set of pixels and its first, second, third and subsequent nearest neighbours in the form of a variogram.

Once the degree of spatial-autocorrelation is known a method which permits the collection of independent pixels from an image can be used. Campbell (1981) suggests taking random pixels from within a training area rather than using contiguous blocks. However, random selection does not altogether avoid adjacent pixels being selected.

A better method of pixel selection which does not result in contiguous pixels being selected was proposed by Labovitz and Masouka, (1984) who suggested that a systematic sampling scheme should be used where the spacing between samples is determined by the degree of positive spatial autocorrelation in the data. This method was subsequently adopted in this research using a dot grid matrix to select independent, non-spatially auto-correlated pixels.

Other Errors Introduced into Training Data

This section identifies ways to minimise other errors that can be introduced into training data, including the collection of separate evaluation data, the need for accurate image registration, the need to collect training data at the same time that the image data is collected, the need to minimise human labelling errors and the need for an appropriate classification scheme.

Separate evaluation data is ideally collected independently of the training data to allow an independent evaluation of map accuracy (Hammond and Verbyla, 1996). If the same pixels used to train the classification data are used to measure both the performance of the classification and estimate the classification accuracy overly-optimistic estimates of

classification accuracy will result (Hammond and Verbyla, 1996). Therefore, care must be taken to ensure that separate evaluation data is collected.

Even if images have been rectified to a certain level of tolerance the absolute location of any given pixel cannot be guaranteed. For example, when 4m resolution IKONOS images are rectified to within a root mean square error of 1 pixel, the average positional error of the rectification model will be to within +/- 4m. If the images are not rectified to within +- 4m this could lead to some correctly classified pixels being mis-located on the ground survey. Moreover, Foody (2002) reports that the mis-registration of datasets can act to significantly exaggerate or mask change and so may substantially limit the value of remote sensing for change detection purposes. Therefore, a classification error matrix used for accuracy assessment purposes could contain errors due to image mis-registration (Foody, 2002) and so care must be taken to ensure that the image rectification is performed as accurately as possible.

If ground data collection is hurried or if time has elapsed between ground data collection and image acquisition significant changes in the bio-physical parameters of the vegetation may have occurred which could result in parcels of land being incorrectly labelled.

If errors are made collecting and recording ground data or if class labels have been incorrectly assigned subsequent cross-referencing of ground data with the imagery will be difficult. Care should be taken to ensure that human errors are minimised.

The use of an appropriate classification scheme is also important for minimising errors in training data. Depending on the objectives of the project an existing system such as the U.S. Geological Survey Land-Use/Land-Cover Classification System (Anderson *et al*., 1976) can be used, or alternatively, a bespoke classification scheme could be used. In all situations consideration should be given to ensure that the classification scheme used is mutually exclusive, totally exhaustive and includes every area in the classification. As such, each class within the classification scheme must be logically explained so that misunderstandings about class delineations do not occur and any area to be classified falls into one single class. If not, considerable classification errors and extensive unclassifiable regions may result (Poth *et al.*, 2001).

2.7.2 Assessing Training Data

As the success of a supervised classification relies directly on the quality of the training procedure (Jensen, 2005) there are several graphical and statistical training aids that can be

used to examine the training data. For example, statistical separability measures are often used to estimate the expected errors in a classification (Murakami *et al.*, 2001) so that classification accuracy can be predicted on the assumption that high class separability translates into high classification accuracy. This next section describes various qualitative and quantitative methods used in this research to investigate the separability of spectral signatures and their effect on classification accuracy.

Gaussian Distribution

Measured brightness values (DNs) from each class can be plotted onto a histogram to check whether the training classes are spectrally characterised by a Gaussian distribution (Lillesand and Kiefer, 2000). If the DNs for each class lie on a bell curve at or near the middle of the peak with few extreme values at the ends of the curve, the data is said to be normally distributed. If the MLC is then subsequently performed high classification accuracies should result. However, if bi-modality is found in a class, when two different species, two different growth stages or different illumination conditions may have been recorded and included within the training data for one class (Schowengerdt, 2007) the class should be sub-divided into two different classes and each treated as a separate category. If this is carried out the classification accuracy will generally be improved (Lillesand and Kiefer, 2000).

Graphical Representations of Separability

Although histograms illustrate the distribution of individual training classes they do not show the spectral signatures of each class (as recorded by a sensor and displayed as DN values) for each image date. One simple method is to plot the mean spectral responses of each class onto a graph. Examples of response patterns for soil, water and vegetation were illustrated previously in Figure 2-1 and Figure 2-2.

One drawback of spectral response patterns is that they show only the mean value of the classes at various wavelengths - but not where class overlap exists (Lillesand and Kiefer, 2000). They therefore cannot be used to predict classification accuracy.

Instead, the spectral coincidence plot (SCP) can be used to visualise separability between classes. Although one of the main purposes of SCPs is to determine which band combinations are best for discrimination and which bands should be ignored, they are also useful for illustrating the range of spectral responses for each class and the amount of overlap between classes. A hypothetical SCP is illustrated in Figure 2-5.

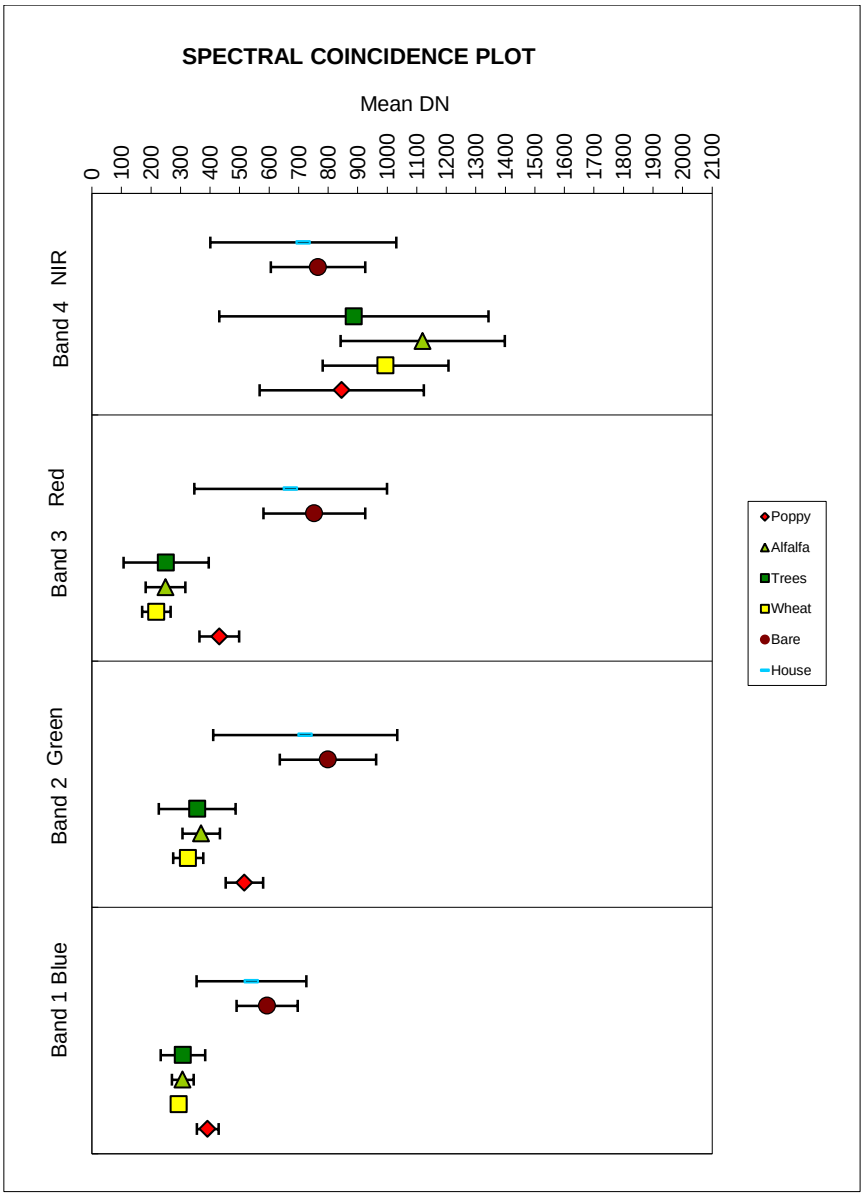

Figure 2-5 – Example of a Spectral Coincidence Plot. Blue (Band 1), green (Band 2), red (Band 3), near infrared (Band 4) displayed using 2 Standard Deviations. Class Ranges indicated by ⊢⊣

For each band, the mean spectral response for each class and the variance of the distribution (+/- 2 standard deviations) is displayed on the x-axis of the plot – which indicates the range of spectral responses for each class. The length of the upper and lower limits of each class range indicates the degree of variability within each class - the wider the class range the wider the spread of the cluster.

Where large overlaps exist between spectral response patterns in all spectral bands, classification accuracy may be reduced (Lillesand and Kiefer, 2000). But, if two or more bands are used in the classification, overlap may not have such a detrimental effect on

classification accuracy. SCP's therefore demonstrate how well separated different signatures are and so can be used to explain a good or poor classification accuracy.

A third type of graph, known as a bi-spectral plot provides a better representation of spectral response pattern distributions and shows between-class overlap more accurately but only two bands at a time.

Figure 2-6 shows an example of a bi-spectral plot of land cover classes.

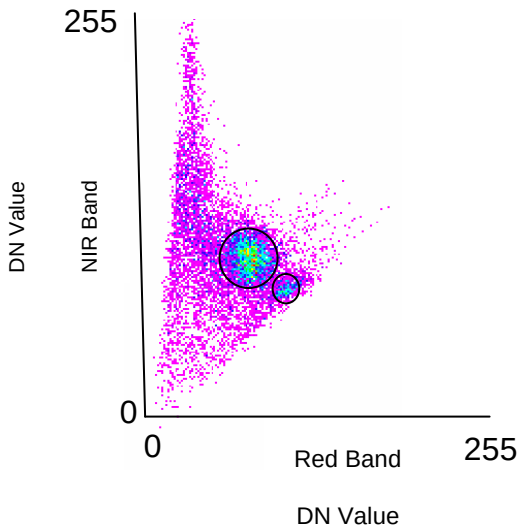

Figure 2-6 – Example of a bi-spectral plot of different land cover classes with ellipses drawn around two distinct and separate classes

By plotting pixel values for each class using the red band on the x-axis and the NIR band (for its sensitivity to vegetation biomass) on the y-axis, a two-dimensional scattergram is created. This illustrates the bi-variate distribution of the data and so can be used to reveal relationships in bi-spectral space and assess spectral distribution differences, particularly between vegetation classes.

The different colours evident on Figure 2-6 signify different densities of observations. The green and blue provide an indication of local concentrations of pixel values. The circles therefore indicate an increased frequency of occurrence of these values, showing two distinct and separate classes.

One drawback of the spectral response patterns, SCPs and bi-spectral plots is that they do not indicate the areal extent each cover type occupies on the thematic map and so therefore do not explain how each cover type influences classification accuracy. If training pixels are collected from a cover type which occupies only a small area in each training site there will be fewer spectral signatures for the classifier to use and therefore less information available.

The end result will be that the classification will calculate the statistical probability of a pixel belonging to that particular minority cover type based on a fewer number of cases and so the resultant classification accuracy could be reduced for that cover type.

The spectral response patterns, SCPs and bi-spectral plots described are all graphical representations of the training classes, and can be used to rapidly check if the training classes are separable and non-overlapping. However, none can be used to quantify the degree of separation or overlap between classes.

Statistical Measures of Separability – Divergence and JM Distance

An improved way to see if the training classes are separable and non-overlapping is by using quantitative statistical measures of separability. The M-statistic (Kaufman) for single bands, the Euclidean spectral distance or the Transform Divergence and Jeffries-Matusita (JM) distance between pairs of bands are just some of the available statistical measures of the distance between two features (Murakami *et al.* 2001).

Separability measures may also be used for feature selection purposes to determine the combination of bands that are most discriminating of the cover types of interest (Murakami *et al.* 2001). This is because certain band combinations have more power for discriminating between different cover types than others. Therefore, if sensors are used with several spectral bands, such as Landsat TM, or hyperspectral sensors are employed, statistical measures can be used to identify and remove feature combinations that are the least effective for discriminating cover types, based on the poorest separability of classes prior to classification. In this study, separability measures are used to indicate how successfully two classes will be discriminated in a classification based on their spectral properties, to estimate the expected classification error for various spectral band combinations (Swain and Davis, 1978).

Both divergence and the JM distance are statistical measures of the distance between pairs of class signatures (Richards and Jia, 1999). Divergence is a measure of the separability of a pair of normally distributed probability distributions (spectral classes) based on their degree of overlap (Richards and Jia, 1999). If there are more than two spectral classes, all pairwise divergences are checked to see whether a particular feature subset has sufficient separation. Then, an average indication of separability is shown by calculating the average divergence.

In general, the larger the transformed divergence, the greater the statistical distance between class means and the higher the probability of correct classification of classes (Lillesand and

Kiefer, 2000). However, one unsuitable and unsatisfactory problem with divergence is that it implies that as spectral classes become more separated from each other in multi-spectral space, further small increases will lead to vastly better classification accuracies (Richards and Jia, 1999). This is misleading because this is not the case in practice, and only very slight increases in classification accuracy occur (Richards and Jia, 1999). In addition, any outlying, easily separable classes will increase the average divergence in a misleading manner to the extent that less than optimal reduced feature sets may be selected (Richards and Jia, 1999). This problem makes divergence an unsuitable measure of separability. As the JM distance measure does not suffer from this weakness it is a more appropriate measure of the distance between class means for pairs of spectral bands. As a statistical measure of separability it indicates which classes are the most separable and therefore will be better identified in a classification.

The JM distance between a pair of probability distributions (spectral classes) is a measure of the average distance between the two class density functions (Richards and Jia, 1999) along the principle axis. Assuming multi-variate normal distributions, the JM distance is computed as follows:

Equation 2-2 – JM distance

$$\text{J - M}_{ub} = \sqrt{2(1 - e^{-\alpha})}$$

where:

$$\alpha = \frac{1}{8}(\boldsymbol{\mu}_u - \boldsymbol{\mu}_b)^T \left(\frac{\mathbf{C}_u + \mathbf{C}_b}{2} \right)^{-1} (\boldsymbol{\mu}_u - \boldsymbol{\mu}_b) + \frac{1}{2} \ln \left[\frac{\frac{1}{2}|\mathbf{C}_u + \mathbf{C}_b|}{\sqrt{|\mathbf{C}_u| \times |\mathbf{C}_b|}} \right]$$

and:

u and *b* (i.e. unburned and burned) are the two signatures (classes) being compared,

$\mathbf{C}_u$ is the covariance matrix of signature u,

$\boldsymbol{\mu}_u$ is the mean vector of signature u,

T is the transposition function.

Defined simply, the JM distance between two classes is the probabilistic distance between two distributions, indicating the probability of correct classification. Therefore, the larger the

separability values between classes, the better the classification results should be. For normally distributed classes, this distance becomes the Bhattacharyya (BH) distance, where a larger value indicates greater average distance (Richards and Jia, 1999). However, the BH distance does not indicate how successfully two classes will be discriminated.

In contrast, because the JM distance is asymptotic to the value of 1414, a scaled JM distance of 1414 between two spectral classes indicates perfect separation between the two classes, which implies 100% classification accuracy for these two classes. This saturating behaviour is highly desirable since it does not suffer from the difficulty experienced with divergence. Even though both the BH and JM distance measures can be used to predict the potential for correct classification of different cover types, only the JM distance statistic is described since it indicates how successfully two classes will be discriminated.

In order to present a means of quantifying separability using the JM distance, the measure is bounded by $\sqrt{2}$ (i.e. a value of ~ 1.41), presented as a scale in Erdas Imagine. Table 2-2 shows the range indicators of separability, where the minimum value for JM is 0 and the maximum value is 1414 (i.e. perfect separation).

Table 2-2 - Range Indicators of Separability

Measure of Separability between 2 classes	Equation	Distance Values
Good Separation (Minimum to Maximum)	$\sqrt{2.0} * 1000$	1378-1414
Poor separation (Minimum to Maximum)	$\sqrt{1.9} * 1000$	1000-1378
Very poor separation (Minimum to Maximum)		0-1000

Smaller JM distances show where there is difficulty in separating the classes. A JM distance of 0 between two spectral classes indicates inseparable classes and a JM distance of 1414 indicates perfect separation between classes. This implies that a classification would be 100% accurate.

As the JM distance statistic relates to spectral classes modelled by multi-variate normal distributions in preparation for the MLC (Richards and Jia, 1999) the JM distance was used in this study because of its equivalence to the MLC (Bruzzine *et al.*, 1997). In this study, JM distances were calculated to quantify the degree of separation/overlap between poppy and all other cover types identified from ground data in Afghanistan on each image date acquired, to determine the best date for spectrally separating poppy from other crops. In cases where the

JM distance indicates that good separability exists, the assumption that classification accuracy will also be high is tested, as per Objective 3. This test will subsequently determine the most appropriate time for poppy identification, as per Objective 2b.

In Chapters 5 and 6 a methodology was set up to investigate; the differences in spectral response patterns between poppy and other crops at different stages in the Afghan crop lifecycle; the amount of spectral variability; and the significance of the variability within and between the different Afghan crops, as per Objectives 2 and 3.

2.7.3 Sensor Capabilities

This next section describes how sensor capabilities may influence the performance of the classifier. Multi-spectral sensors can be characterised by their spectral, spatial, temporal and radiometric resolutions. Each of these characteristics can influence the accuracy of a classification which in turn can be used to assess the appropriateness of the imagery for crop discrimination. Each type of resolution is explained in the following sub-sections.

Spectral Resolution

A sensors spectral resolution refers to the number and dimension of specific wavelength intervals (referred to as bands) in the EMS to which the remote sensing instrument is sensitive (Jensen, 2005). Section 2.3 introduced the concept of using multi-spectral satellite sensors to record the amount of radiation reflected from an object at one point in time using specific bands covering the visible and NIR part of the EMS to derive information about the fundamental biophysical variables of different crop types.

A sensor will record reflected energy across the width of any waveband used. The nominal size of a band may be large, i.e., Landsat MSS NIR band detectors record a relatively large range of reflected NIR radiant flux between 0.8-1.1µm, or smaller, i.e., IKONOS NIR detectors record a much smaller range between 0.77-0.88µm. However, in reality, the spectral resolution of a sensor is a nominal spectral resolution, because it is difficult to create a detector that has extremely sharp band-pass boundaries (Jensen, 2005). The positioning and range of the visible and NIR bands of individual multi-spectral sensors therefore play a key part in influencing how well a classification performs because they determine whether a sensor's spectral resolution is sufficient to detect discrete spectral differences between different crops.

Figure 2-7 shows the approximate waveband positioning and width for the four discrete IKONOS bands used in this research covering the blue, green, red and NIR parts of the EMS. For comparison, the approximate wavelengths recorded by a Zeiss camera on film which were subsequently scanned to create digital images used in this research are also included in Figure 2-7. Note that the Zeiss survey camera is no longer being flown on MOD aircraft.

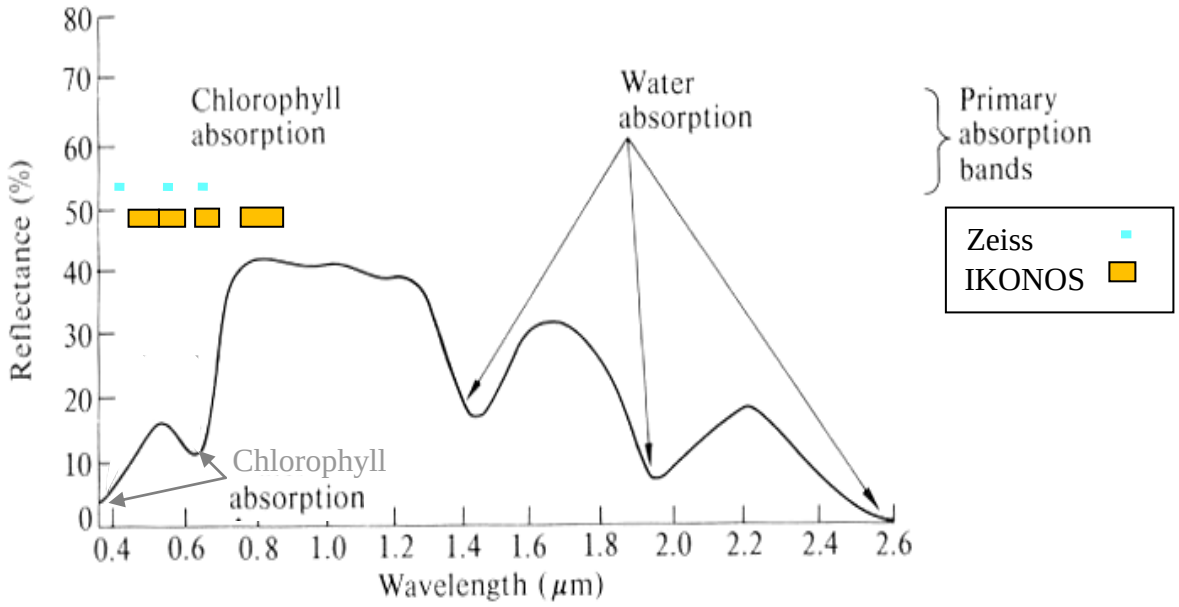

Figure 2-7 - Relationship between the spectral bands of the IKONOS and Zeiss sensors being considered and general vegetation spectral profile (after Swain and Davis, 1978)

The specific wavelengths covered by each spectral band of IKONOS and Zeiss are represented in Table 2-3.

Table 2-3 - Spectral bands of sensors used in the UK Poppy Detection Project

Sensor	Wavelength (μm)				
	Blue	Green	Red	NIR	Mid IR
Zeiss	0.4 (centre)	0.55 (centre)	0.65 (centre)	N/A	N/A
IKONOS	0.45-0.53	0.52-0.61	0.64-0.72	0.77-0.88	N/A

Spatial Resolution

The spatial resolution of a sensor is a measure of the smallest linear separation between two objects that can be resolved by a sensor (Jensen, 2005), and plays a key role in assisting in the discrimination between different crops.

A sensor's spatial resolution is normally described by the dimension in metres of the ground-projected constant instantaneous field of view (IFOV) (Jensen 2005). Table 2-4 shows the nominal resolutions of the IKONOS and Zeiss IFOV (when it was flown by the MOD in Afghanistan).

Table 2-4 - Spatial resolutions of sensors used in the UK Poppy Detection Project

Sensor	Spatial Resolution (m)
Zeiss	Approx 0.6
IKONOS	4

Some low spatial resolution remote sensors can be used to map single cover types within one pixel, e.g. over oceans or other large homogenous areas. However, in vegetation studies it is important that research objectives are met with an appropriate spatial resolution. Therefore, it is important that the characteristics of the vegetation being mapped are at scales commensurate to the size of a pixel (i.e. the more detail required the higher the spatial resolution).

In the case of crops, the brightness value of a pixel will not represent individual plants or components of a plant, rather it will represent the bulk properties of the vegetated surface, as discussed in Section 2.3.1. The degree of mixed responses is therefore directly related to the spatial resolution of the sensor used - the larger the IFOV the greater the spatial averaging of responses. Even in instances where the amount of energy reflected from a plant is recorded by an ultra-high resolution spectrometer, its spectral response will still include the combined spectral responses from all objects within the IFOV. To limit spatial averaging and mixed pixels, imagery could be acquired with as high a spatial resolution as possible. However, to do so will mean that more noise will be present which could lower classification accuracy.

Temporal Resolution

The temporal resolution of a remote sensing system refers to how often it is possible for a remote sensing system to collect imagery over a particular area, measured as the repeat cycle

of a sensor's orbit (Jensen, 2005). When investigating the timing of different crop growth stages a sensor's temporal resolution is particularly important. This is because, as described previously, different crop types reflect and absorb different proportions of visible and NIR energy at differing stages in their lifecycles. If a sensor's repeat cycle is sufficient for capturing imagery at key growth stages, a time-series approach can be used to determine how much energy is reflected from the different crops at specific times in their growth cycles. In addition, multi-temporal data is useful if a crop contrasts more strongly with its surroundings at different times of the year due to a different planting schedule, and so this will be useful to its detection.

A satellite's temporal resolution, as a function of its swath width and orbital parameters, is improved through the use of pointable sensors. This means that imagery can be acquired off-nadir, which provides greater revisit capabilities comparable in terms of a sensor's maximum off-nadir angle and the maximum latitude of an area of interest (AOI). For instance, the IKONOS sensor has a cross-track and along-track viewing capability which enables flexible and frequent image acquisitions. Table 2-5 shows the temporal resolution of IKONOS and Zeiss, the two sensors used in this study.

Table 2-5 - Temporal and Radiometric Resolution of IKONOS and Zeiss Imagery

Sensor	Radiometric Resolution	Revisit time in days	
		Off nadir	True nadir
IKONOS	11 bit	3-5*	144*
Zeiss (digital)	8 bit	On request**	On request**

* > 3 days @ 1x1m resolution for look angles >26° and 1-5 days at 4x4m spatial resolution.

** Constrained only by practicality and weather . No longer in service with the MOD.

Radiometric Resolution

Radiometric resolution refers to the sensitivity of a sensor to differences in signal strength as it records radiant flux reflected, back-scattered or emitted from the terrain (Jensen 2007). A sensor's radiometric resolution is defined by its range and discernable number of discreet brightness values used to quantize radiance. Radiometric resolution is expressed in terms of the number of binary digits (bits) necessary to represent the range of available brightness values, known as the dynamic range.

In general terms, a sensor with a high radiometric resolution records EMR with more sensitivity than others (Jensen, 2007). For example, more detail can be seen in an image if data is detected with a precision of 11-bits (which means data is collected in increments between 0-2048) than in 8-bit data which has less sensitivity with only 256 grey tones available (Jensen, 2007). If specialist software is available 11-bit IKONOS data can be stored as 16 bit data. If not, it is compressed to 8-bit by the vendor and rescaled to 256 values with a dynamic range of 0-255.

In classification terms the use of IKONOS's 11-bit data enables the detection of smaller differences in radiance received from different land cover types than 8-bit data. Unfortunately, direct comparisons of the radiometric sensitivity of the two sensors used in this study, IKONOS and Zeiss, cannot be performed because the photography acquired using Zeiss is collected as analogue data not as digital data. The advantages and limitations of 8-bit and 11-bit data are summarised in Table 2-6.

Table 2-6 - Radiometric Resolution Limitations and Advantages of 8-bit versus 11-bit

	Radiometric Resolution	
	8-bit	11-bit
Number of brightness values available	256	2048
File size	Small file sizes-easy to use and quick to process	Large file sizes require high-end hardware and software capable of viewing 16-bit data
Detail	Less tonal and intensity variation, limiting highlights and shadow detail	Increased tonal intensity variation and increasing highlights. More shadow detail is evident

2.7.4 The Ground Segment

The collection of ground data is an integral part of remote sensing because it is used to aid image interpretation, analysis and validation. Whilst Section 2.7.1 highlighted how the accuracy of an image classification can be affected by errors introduced into the training data this section gives a brief overview of ground data considerations and challenges.

The acquisition of ground data involves the collection of measurements or observations about an object, area or phenomena that is being remotely sensed and is both expensive and time

consuming. Costs associated with ground data collection could include the purchase or hire of vehicles, fuel and equipment plus the hire of labour and accommodation for example.

Many challenges may be encountered when collecting ground data including logistical problems, communications problems, equipment failure and inadequate maps. Moreover, if landowner permission has not been sought, or if survey teams are operating within areas of political unrest, or, in the case of poppy surveying in Afghanistan where farmers are growing illegal crops, danger could be present. Each of these challenges must be considered and alternative plans made in order to increase the chances of successful data collection.

One of the key components of this research was the collection of accurate ground segment data. This task was carried out by UN ground surveyors who faced many of the challenges outlined above, the most serious of which was the difficult and ever-changing security situation. To reduce the personal security risk to the surveyors and improve the chances of survey success, care was taken to ensure the safe passage of survey teams. It was key that surveyors local to the individual areas being surveyed were selected, as far as possible, as they were familiar with their region's geography, but more importantly, were able to diffuse any difficult situations if they arose as they had credibility with village elders. In some cases armed local Afghan police were called upon to escort survey vehicles and protect the surveyors whilst in each field when intelligence suggested the surveyors would face hostile villagers.

2.8 Assessment of Classification

Following on from the sensor capabilities described in Section 2.7.3 which may influence the accuracy of a classification, this section describes how the reliability and accuracy of a classification may be assessed. Classification accuracy assessment provides a meaningful quantification of the accuracy of a classification so that confidence in the results can be given. This in turn helps to indicate whether the study objectives have been achieved (Richards and Jia, 1999).

As described in Section 2.7.1 accuracy assessment should always be conducted using evaluation data which has been collected independently of the training data. Accuracy can be assessed qualitatively by field checks and comparisons with existing maps or, more commonly quantitatively using a more structured analysis of the field and map evaluation data through statistical analysis and confusion matrices.

In qualitative assessments a visual check of a sample of pixels from the classified thematic output can be compared with ground reference data or an existing map to judge the accuracy of classification results. However, these visual comparisons are qualitative and often misleading, and so quantitative assessments are generally preferred.

In quantitative assessments attempts are made to identify and measure the error of the remote sensing-based map. This is achieved by using the computer to estimate the percentage of correctly and incorrectly labelled pixels from each class. These results are displayed in tabular form, normally referred to as an error matrix. The error matrix is discussed in Section 2.8.1.

Accuracy assessment has been a topic of considerable debate for many years (Foody, 2002), and, as was discussed in the Literature Review in Chapter 1, there is a direct need for a standardisation of both the method of assessment and the style of reporting, to include target accuracy thresholds (Foody, 2002). In the Literature Review some studies provided no quantitative measure of accuracy, and while this may have been due to ignorance or laziness, it highlights a major limitation in the mapping and monitoring of land cover from remotely sensed data (Foody, 2002).

2.8.1 The Error Matrix

After a classification has been performed, one of the most common means of calculating and representing classification accuracy is through the use of an error matrix (Lillesand and Kiefer, 2000). The error matrix is generally accepted to be the standard descriptive reporting tool for accuracy assessments (Congalton, 1991; Foody, 2002) and can be used to assess the nature and frequency of erroneous labels, attach a degree of confidence to the classification results and indicate whether the analysis objectives have been achieved.

The error matrix is a square table of numbers organised in rows and columns which express the number of evaluation pixels that have been assigned to a particular class by the MLC, relative to the actual class on the ground (Congalton, 1991).

The error matrix represents both evaluation and classification data. The columns of the matrix represent the ground evaluation data acquired from the ground survey and the rows represent the predicted classes generated from the remotely sensed data. All correct classifications are indicated on the major diagonal of the error matrix.

The error matrix can also be used to assess the nature of erroneous misclassified labels which are displayed as the non-diagonal elements of the error matrix. Sometimes a distinction is made between errors of commission and errors of omission, particularly when only a small number of classes are of interest such as in the estimation of the area of a single agricultural crop (Richards and Jia, 1999). Errors of omission correspond to those pixels belonging to a class that the classifier failed to recognise (and have therefore been omitted from the correct class) and are shown in the columns of the error matrix. Errors of commission are those that correspond to pixels from other classes that the classifier has labelled as belonging to the class of interest and are shown in the rows of the error matrix. A misclassification error is therefore not only an omission from the correct class but is also a commission into another class.

The assumption that the error matrix is a true representation of the actual classification results achieved will only hold if an appropriate sampling scheme is used which enables adequate numbers of representative sample pixels to be chosen.

Overall Accuracy

Accuracy is simply a measure of the percentage of ground evaluation pixels in each class that have been labelled correctly by the classifier. The simplest descriptive measure is the overall accuracy, which is computed by dividing the total number of correctly classified pixels (i.e. the sum of the major diagonal in the error matrix) by the total number of sample pixels used. A benchmark accuracy of 85% is widely-used as an acceptable level of classification accuracy (Foody, 2002). However, the level of accuracy sought and obtained can be an arbitrary measure dependant on the size of the study area, the spatial resolution of the imagery used and the level of classification employed.

Unfortunately, this single measure of accuracy does not give an insight into how well a classifier has performed for each class. Because it only incorporates the major diagonal whilst ignoring omission and commission errors, the literal interpretation of percentage accuracies derived from an error matrix can be misleading (Mather, 2004). Therefore, if a classifier performs well for a class which accounts for a large proportion of the test data despite low class accuracies for the other classes, the overall accuracy will be biased. As a result overall accuracy should be used with caution.

Producer's Accuracy

The producer's accuracy is the probability of a reference pixel being correctly classified. It is calculated as the total number of correct pixels in a class (the diagonal element) divided by the total number of pixels of that class (the column total) derived from the ground reference data. Errors of omission (samples that have not been correctly classified and are therefore omitted from the correct category) can be measured using this method. For this accuracy measure to be of use it assumes that the ground data contains no errors. This measure is often called the 'producer's accuracy' because the producer of the classification is interested in how well the ground data were classified and how well a specific area can be mapped.

User's Accuracy

The 'user's accuracy' is computed by dividing the total number of correct pixels (the diagonal element) by the total number of pixels classified (the row total), and measures how well the classification identifies the correct class. It is referred to as the user accuracy because it is the accuracy experienced by the user of the map who is interested in the reliability of the map, i.e. how well the map represents the real cover types on the ground. User accuracy is thus the key indicator of classification accuracy.

2.8.2 Kappa Statistic

As the overall accuracy measure only incorporates information about the major diagonal, and neither producer's nor user's accuracies incorporates both off-diagonal errors, Fitzgerald and Lees (1994) and Congalton (1999) consider that a better measure of the accuracy of a classifier may be given when both omission and commission errors are incorporated. One such accuracy measure is Kappa, commonly recommended as an accuracy figure corrected for chance agreement. It is a discrete multivariate technique which indirectly incorporates both types of off-diagonal elements and can be used to perform statistical tests to determine classification accuracy (Congalton, 1999) minus chance agreement. Put simply, the Kappa statistic is a measure of how well the classifier agrees with the reference data (Murakami *et al.,* 2001), and has been shown to be a statistically more sophisticated measure of interclass agreement than the overall accuracy (Fitzgerald and Lees, 1994). It also gives better interclass discrimination than overall accuracy (Fitzgerald and Lees, 1994).

The result of performing a Kappa analysis is a KHAT statistic which is an estimate of Kappa. The equation for KHAT is given in Equation 2-3 as follows:

Equation 2-3 - KHAT

$$\hat{\kappa} = \frac{|\kappa_1 - \kappa_2|}{\sqrt{\text{var}(\kappa_1) + \text{var}(\kappa_2)}}$$

where k_1 and k_2 are estimated kappa statistics for two classifications and var(k_1) and var(k_2) are the sample variances of the respective kappa statistics.

Kappa is particularly useful because it measures the agreement between reference and evaluation data minus the chance agreement; the chance agreement being that which would occur between two sets of random numbers compiled into the error matrix (Foody, 2002). Not only can it be used to provide information about a single matrix but calculation of Delta Kappa can be used to statistically compare classification results from two error matrices generated from two different classification techniques conducted on the same image, or compare results from the same classification procedure used on two different image dates acquired from the same area (Foody, 2002).

During the course of this work Kappa statistics were computed from error matrices that were produced by the MLC to measure the accuracy of each single-date classified image. Delta Kappa was also used to compare classification accuracy results derived between single date classifications acquired over the same areas on different dates at each site with multi-temporal image classifications to determine whether any improvements to classification accuracy achieved were significant results or were due to random chance.

A worksheet produced by Taylor (2001) after Congalton (1999) was used to calculate the KHAT statistic for each image date and has been included in Appendix E. The Kappa statistic results are presented in Chapters 6 and 7 as percentages, characterised into three groups where; a value greater than 80% represents strong agreement between the reference data and classified data, 40-80% represents moderate agreement and below 40% represents poor agreement (Congalton, 1996).

2.8.3 Regression

Regression analysis can be used to establish whether a relationship exists between two variables, i.e. spectral separability and classification accuracy. The regression equation models the relationship and the r^2 value describes its fit, (i.e. the closer the r^2 value is to 1 the better the fit). If the two variables are plotted on a scatter plot a straight line will describe

how the response variable (i.e. classification accuracy) changes as an explanatory variable (i.e. spectral separability) varies (Moore and McCabe, 1998).

Whilst single linear regression assumes that the values for x or y can be of any value, the JM distance measure calculates bounded values. However, providing that the measurements are not very close to the limits of the measurement scale, (i.e. indicating perfect separation) regression can be applied (personal discussion with Bellamy, 2007). Therefore, in this study regression is used to determine whether a relationship exists between spectral separability and classification accuracy, as per Objective 3 in Chapter 1.

2.9 Chapter Summary

This chapter has examined how remote sensing techniques can be used to identify and discriminate various crops based on the ways in which their vegetative surfaces influence their reflectance and absorption properties. It has illustrated how spectral reflectance patterns may be indicative of different crop types and described the various classification methods available. It has given details of how errors can be introduced into the training data and demonstrated how classification accuracy can be assessed using error matrices and Kappa statistics.

The next chapter, Chapter 3, describes the Afghanistan environment and its agriculture. It illustrates the crops commonly grown in Afghanistan and makes particular reference to how poppy biophysical characteristics change during its growth cycle as it matures, which alters the spectral reflectance patterns recorded by a sensor.

3. Factors Influencing the Spectral Signature of Poppy

The literature review in Chapter 1 revealed that little had been formally reported on the spectral properties of poppy, how it changes through time and across diverse geographical regions in Afghanistan. Furthermore, little was found on how poppy farming practises such as thinning, weeding and irrigation could affect the spectral signature of poppy.

This chapter therefore begins by detailing how environmental factors such as topography and climate may affect agriculture and cropping patterns in Afghanistan. It then provides an insight into Afghan agricultural practices in terms of irrigation, disease and pest prevention, fertiliser use and mechanisation and suggests ways in which crop spectral signatures may be influenced by these practices.

Section 3.3 highlights the major crops grown alongside poppy in Afghanistan and Section 3.5 describes how the bio-physical characteristics of poppy, such as the number of flowers per plant, the timing of when plants flower and the length of time devoted to flowering, are influenced by Afghanistan's environmental conditions and determines how these may affect the spectral characteristics of the Afghan poppy.

The chapter then documents a systematic investigation undertaken in this research into the appearance of poppy at each of its growth stages. Defined terminology is used to describe the crops' appearance during its progressive growth and development stages in the context of remote sensing. The section is the first formal synthesis of the poppy growth cycle from ground and aerial photographs. It uses ground photographs acquired by both UNODC (from Afghan poppy fields) and from fieldwork obtained from UK poppy field trials conducted as part of the Poppy Detection Project (PDP) on poppy grown in the UK as well as aerial photographs also obtained by the PDP. It thus provides a useful insight into the inherent links between UK farming practises and environmental factors, and demonstrates how, without *a priori* knowledge of these influences, the accuracy of Afghan poppy identification using multi-spectral image analysis could be affected.

Predictions are made on whether visible differences apparent on ground photography would be identifiable on satellite imagery, and these were subsequently tested. It was hypothesised that if these differences are identifiable on imagery they could help to make the discrimination between poppy and other crops more robust, and ultimately, improve the accuracy of crop identification in Afghanistan.

The objective of this chapter therefore is to identify the factors influencing the spectral properties of the opium poppy crop so that their influence with respect to the accuracy of identification using multi-spectral imagery analysis can be investigated in the methodology chapters (Chapters 4 and 5).

3.1 Afghan Environmental Factors

This section examines a variety of growing areas in Afghanistan to determine how environmental factors affect the agricultural practices and cropping patterns used by Afghan farmers. This examination is conducted to identify the factors that have the potential to influence the spectral reflectance characteristics of poppy fields.

Figure 3-1 is a map of Afghanistan and illustrates its internal provincial boundaries. Three provinces in particular have been highlighted, where the importance of opium poppy cultivation to farmers is high – Nangahar in the eastern region, Helmand in the southern region and Badakshan in the north-eastern region.

Figure 3-1 - Map of the internal provincial boundaries in Afghanistan.

3.1.1 Topography

Afghanistan lies between 38° and 29° N and 61° and 75° E. Badakshan Province in the north-east lies on the Tajikistan and Chinese borders, Helmand Province in the South and Nangahar

Province in the East both lie on the Pakistan border. To the West of Afghanistan is Iran and to the North lie Turkmensitan and Uzbekistan. Of Afghanistan's population of 25 million people, 85% are engaged in agriculture (Sharif, 2002).

Afghanistan is characterised by rugged mountain ranges, extensive desert plains and scattered fertile valleys along its major rivers (Uhl, 2003). Its altitude ranges from 470m on its south-western border with Iran to over 6,000m in the eastern mountains. The Hindu Kush Mountain System dissects the country in half from north-east to south-west with average elevations ranging from 3,000m above mean sea level (amsl) in the north-east to 1,500m amsl in the south-west.

Although calcareous soils dominate the agricultural areas causing high pH levels, most of the cultivable soils do not have characteristics that could restrict rooting (ICARDA, 2002b). Cropping in Afghanistan is therefore not greatly influenced by soil type.

The upper zones of the mountains in the North-East (including Badakshan Province) have glaciers above 3,800m amsl, steep valleys, fast-flowing rivers and narrow valley floors. Lower down, valley floors broaden into basins at elevations of 500-700m amsl and once out of the foothills, flat plains and slow flowing rivers are found towards the West and South (including in Helmand Province). The snow line in the mountains in the summer varies between 3,000 - 4,600m and descends to approximately 1,800m in winter.

The South-Western region is the most arid zone comprised of deserts, steppe and high cropping intensity irrigated systems.

In Afghanistan a strong relationship exists between altitude, length of growing season and the amount of precipitation (ICARDA, 2002b). At high altitudes in the North and East precipitation is high but growing seasons are short due to frost hazard. On cooler, northern slopes crops may not be able to survive because of the lack of direct sunlight. On sunnier southern slopes crops may be able to survive because the direct sunlight will melt the snow and provide moisture and warmth to the plants. Aspect will therefore influence how long snow remains on the ground and will help determine whether a farmer can plant crops.

In the lower, flatter areas to the South and West precipitation is low but long growing seasons are supported wherever possible with irrigation water.

3.1.2 Climate

Afghanistan overall has a dry continental climate which varies according to elevation from moderately warm in the valleys to cold in the highest altitudes of the mountains (Uhl, 2003). Unique micro-climates can be found in valleys because of the influence of local mountain-valley winds that blow up in the valleys and mountains in the daytime and back at night.

In the higher altitudes in the North and East winter usually starts in November and finishes in April, characterised by very low temperatures ranging from -5 to -10°C during the day and drops of -20°C at night with cloudy skies. Precipitation mostly falls as snow in these areas and reaches an average snow cover of 0.5 - 1m deep which can persist in shaded valleys and mountain tops until August.

In the valleys and lower areas in the South and South-East winters are usually shorter, starting in December and finishing in February. They are characterised by drizzle with day time temperatures average between 2-6°C and descend down to -5°C at night.

Spring in the valleys and basins usually starts in March. In the mountains it usually begins around May and generally lasts in all areas until June. Spring is characterised by unstable weather patterns with warm days and short, heavy rains and cooler nights. Snow occasionally falls in the mountains in the spring.

In the lower areas of the West, East and South-East summer normally starts in late May with mostly warm, dry air from the north and north-east and ends in September. Daytime temperatures normally reach maximum values for the year between 25-30°C, occasionally peaking at 45°C. Night temperatures are usually between 18-22°C. In the highest altitudes of the mountains in the North and East summer usually starts in mid-June and ends at the end of August. Average day-time temperatures reach 10-15°C.

Autumn usually begins in October in the lower areas and September in the mountains. It normally lasts just one month due to early snow in the mountains and frosts in the low areas.

Winds across the country are predominantly from the north, with average wind speeds of 2-4 m per second. In the high exposed areas, particularly in the North and East the chill factor reduces average day and night-time temperatures by several degrees which can often kill immature and fragile seedlings before winter snows have had a chance to settle.

Precipitation

The amount of rainfall across Afghanistan directly correlates with altitude (Uhl, 2003). It varies from approximately 100mm per year in the South, North and West in areas less than 1000m in height to approximately 1000mm in higher altitudes above 3000m in the central region (FAO/WHP, 2004) and above 4000m in the north-east (Uhl, 2003). In mountainous areas where precipitation is sufficient agriculture is limited because of frost hazard and availability of suitable land due to the absence of soil on exposed rocks.

On average approximately 90% of the country's annual precipitation occurs during the winter months between December and April, mostly falling as snow (Uhl, 2003). This winter snow fall at the higher altitudes is particularly important for ensuring irrigation water availability during the spring and summer months (FAO/WFP, 2004). FAO/WFP (2004) indicate that the total precipitation for Afghanistan is approximately 180,000m³ in an average year broken down into approximately 150,000 million m³ from snow melt and approximately 30,000 million m³ from rainfall.

3.1.3 Hydrology

Afghanistan's rivers originate from the Hindu Kush mountain range in the centre of Afghanistan, approximately 100 km west of Kabul and flow towards its borders (Uhl, 2003). Maximum flow normally occurs in the spring and early summer months from snowmelt and lower flows are usually found in the autumn and winter months (Uhl, 2003). Dams have been built in several areas to collect and store rain water and snow-melt to regulate flows for down-river irrigation.

Afghanistan's perennial rivers originate from the Hindu Kush and include the Kabul River and its tributaries in the East, the River Helmand in the South/South-West and the rivers Arghandab, Hari Rud, Kunduz, Kokcha and Amu Darya in the North/North-West.

The Kabul River and its tributaries drain 10% of Afghanistan (Uhl, 2003). The Kabul River flows Eastwards through Kabul and Jalalabad and experiences peak flows during the spring months (March to April) as its drainage area encompasses the snow-covered central and North-Eastern parts of the Hindu Kush (Uhl, 2003). Low water levels occur from October to February with brief surges from storms occurring from November to May which result in water levels rising 1-2m more than normal. However, some of the water levels in the Kabul River depend on the release of water from the Naglu and Sorubi reservoirs (72 and 64 km

west of Jalalabad respectively) and the Danuntah reservoir. Double and triple cropping is common in eastern irrigated areas fed by the Kabul River and its tributaries (FAO/WHP, 2004).

The 1,300 km long Helmand River and its tributaries drain approximately 30% of Afghanistan (Uhl, 2003). It rises out of the central Hindu Kush Mountains and flows south-westerly and then westwards. Its flow is mainly supplied by its upper catchment areas which receive snow in the winter months.

In the North-East the perennial Kokcha River originates from the north-eastern part of the Hindu Kush and has substantial flows in the spring from snow melt. The Kokcha and Kunduz Rivers together with the upper drainage area of the Amu Darya cover about 15% of Afghanistan (Uhl, 2003).

3.2 Agricultural Practices in Afghanistan

Cereals, vegetables, spices, nuts and forage crops are also grown in addition to poppy in Afghanistan. The next sections (3.2.1-3.2.5) detail the irrigation practises used, how pests and diseases are controlled and the use of fertilisers. Section 3.3 provides an overview of other crops grown alongside poppy in Afghanistan.

3.2.1 Irrigation

As an arid/semi-arid country Afghanistan's agricultural production depends on either precipitation or irrigation. Of Afghanistan's total land area (63 million ha) approximately 8 million ha is under cultivation (ICARDA, 2002a). The rest of the land is given over to permanent pastures (46%), forests and woodland (3%) and other (39%) (FAO/WFP, 2004).

Poppy and other crops are grown predominantly within irrigated areas along the river valleys and basins. Crops are also grown in some rain-fed areas in the Northern Plains when enough precipitation falls for crops to survive. The intensity of cropping principally depends on the availability of irrigation water and the length of the growing season.

Approximately twelve per cent of Afghanistan's land area requires irrigating (CIA, 2006) but of this land just under half is irrigated annually, of which only a quarter has sufficient water to sustain double-cropping in one year and the remainder lie fallow due to water shortages (ICARDA, 2002a). A further 1.4 million ha of cultivated land is rain-fed (ICARDA, 2002a) predominantly in the Northern provinces.

In these rainfed areas water availability for irrigation is influenced by both rainfall and groundwater sources which are determined by the amount and distribution of precipitation. In the irrigated areas a farmer's choice of irrigation method largely depends upon the immediate water sources and irrigation systems available to him and his ability to pay for the water (ICARDA, 2002a). A survey of farmers conducted in several provinces found that at the field level a farmer's knowledge of crop water requirement is based on whether his soil appears dry on the surface, his memory of when it was last irrigated and whether the crops are showing plant stress indicators such as wilting for example (ICARDA, 2002a).

Several different types of traditional irrigation systems such as streams, rivers, shallow wells, springs and karezes together with modern systems with gates and sluices are used in different parts of the country depending on whether the water is available as groundwater or as surface water. This section describes only those systems which may influence the appearance of the poppy fields at the field level and includes canals, flood irrigation and permanent raised bunds which retain water once in the field.

The most commonly used irrigation method is flood irrigation supported by a canal irrigation system. Canal irrigation systems supply nearly 75% of irrigated land (ICARDA, 2002b), the majority of which lie in the North, West and South-West of Afghanistan. These are fed with waters from rivers supplied with snowmelt using gates and other similar structures to divert the water from the rivers into the irrigation canals. The water is then diverted into smaller irrigation channels which then further sub-divide into much smaller ditches running along the sides of fields.

When a farmer requires his fields to be irrigated a small break is made into one side of a man-made raised soil embankment adjacent to his fields to allow the water in the ditches to flood freely into the fields and be contained within. This practise is known as flood irrigation (Figure 3-2). Once the fields have received the water the bank is re-sealed. During and immediately after the water has flowed into the fields the colour of the exposed soil temporarily darkens until it has infiltrated or evaporated.

ICARDA noted that the practice of sub-dividing levelled fields into smaller plots achieved an improved crop, a uniform application of water and therefore a better water use efficiency. They noted that 50% of the farmers surveyed used this practice.

Figure 3-2 – Flood irrigation used in individual plots within a flat field, Nangahar District, Afghanistan (courtesy of UNODC)

If access to water is severely restricted due to a drought or if a farmer cannot afford to irrigate all his fields he will water only the most important cash crop (personal communication with UNODC staff, 2005). The presence of well-preserved raised soil embankments used at the edges of levelled fields to contain water (Figure 3-3a) or internally to sub-divide fields to retain the water (Figure 3-3b) may therefore provide an indication that important cash crops are being grown in these fields.

(a) (b)

Figure 3-3 - Ground photos of raised soil embankments in Achin District, Afghanistan, courtesy of UNODC

Grid patterns of raised banks within fields (furrow irrigation) are also used for growing vegetables where seeds are planted on the top of the soil bund to ensure that the plant's roots grow unhindered into the raked soil and have access to irrigation water when it is poured into the base of the bund (Figure 3-4). In a remote sensing context, this soil compaction activity makes the soil smoother, which results in increased spectral reflectivity, and so compacted soils will appear lighter on imagery. This increased reflectivity may also apply to soil paths

between rows of crops, particularly in poppy fields, where workers intensively weed and harvest the crops (as described in Chapter 2).

Figure 3-4 - Ground photo of permanent within-field irrigation bunds in Nangahar Province, Afghanistan courtesy of UNODC

ICARDA noted in their 2002 survey that the amount of water applied for irrigation bore no relevance to the actual crop's water requirement in the fields. Irrigation stopped when water reached the far end of a field, or when water covered all high spots in a field or when a certain depth was achieved (ICARDA, 2002b). They also noted that the number of times a field was irrigated was based on the availability of water and how much a farmer could pay. They also found that farmers who are fully dependent on canal waters tended to apply less water than those who had access to groundwater supplies.

ICARDA (2002b) noted that where farmers had not levelled their fields uneven water distribution produced patches of different infiltration rates which produced areas of high and low salinity within the same fields. This then affected the crops which reduced the crop yields. However, they reported that more than 60% of farmers did not have soil salinity issues. Of those that did, high water tables were blamed for the development of soil salinity with only a quarter using leaching and drainage to solve their salinity issues.

As found with the tractor wheeling in the soil in the UK field trials, it is expected that the majority of these drainage canals and ditches, perimeter embankments and within-field raised soil banks will be visible from sub-metre aerial and ground photography. It is anticipated that these soil features will have an influence on the spectral signature of all crops, regardless of crop maturity. Unless a severe drought causes farmers to use these irrigation systems only for their most important cash crop (i.e. poppy) it is highly unlikely that their identification on imagery can be claimed to be an absolute indicator of poppy.

3.2.2 Preventing Disease and Pests

Very little material exists on how Afghan farmers try to combat disease and pests. However, their presence and impact on poppy was documented by UNODC in their 2005 opium survey who found the majority of infestations in north-eastern Afghanistan - and in Badakshan in particular. The names and symptoms of each fungal and bacterial disease and pests identified in Afghan crops are listed in Table 3-1 (after UNODC, 2005b).

It was hoped that if any of the areas reported by UNODC surveyors to be infested fell within the sub-sample of areas investigated in this research it could be possible to identify the fields that were affected on imagery. This could only happen if; significant damage, discolouring or drying out occurred to most or all of the plants in a field at a particular growth stage; the plants had a much lower biomass content at a particular growth stage than normal (caused by growth retardation or damage); they prematurely senesced prior to the opium harvest.

It was anticipated that if the pests and diseases significantly damaged the majority of a field of crops the spectral signature would be affected. The methodology developed in Chapters 4 and 5 was subsequently used to investigate the extent of their influence on the spectral signature of poppy.

Table 3-1 - Afghan diseases and pests affecting poppy fields, after UNODC, 2005

Name	Disease or Pest	Location of attack	Symptoms
Powdery Mildew	Fungal disease	Immature shoots	Grey powder on shoots
Unknown	Fungal parasite	Upper sides of leaves/ stems	Black and brown spots
Blight	Fungal and bacterial diseases		Yellowing of leaves/ brown spots on leaves
Mosaic	Viral disease	Leaves/Capsule	Discoloured and deformed leaves/ stunted plant growth/ deformed capsules
Fusarium Wilt	Soil-borne fungal disease	Leaves and stems	Wilting and yellowing
Aphids	Pest	Leaves	Transmit viruses, suck sap and puncture foliage. Deposit a sticky, sweet liquid which forms a substrate for fungal and bacterial growth.

Name	Disease or Pest	Location of attack	Symptoms
Cut worms	Pest	Roots	Total destruction of poppy and other crop
White grub	Pest	Roots	Totally dried-out plant
Sun pest	Pest	Capsule	Destruction of plant
Capsule Caterpillars	Pest	Capsule	Destruction of plant
Root knot nematodes	Pest	Roots	Root deformation and inhibition of nutrient update.
Orobanche papaveris	Parasite Pest	Roots	Damage to plant
Beetle Larvae	Parasite Pest	Roots, leaves and capsules	
Locust Larvae	Parasite Pest	Roots, leaves and capsules	
Perenospora arborescens	Pest	Leaves and stems	Destruction of leaves and stems

3.2.3 Application of Fertilisers

The process of fertiliser application produces healthy, sturdy crops (Mansfield, 2001) that progress through their growth and development cycles without signs of distress, unless access to water is limited, diseases or pests are present, temperatures are not optimum or there are soil salinity issues, for example. The inclusion of fertilisers in this section was therefore to provide background information on farming practise only.

Fertilisers either in the form of animal manure or urea, diammonium phosphate (DAP) and single super-phosphate/triple super-phosphate SSP/TSP are generally used in all irrigated areas, with chemical fertilisers only being used by farmers who can afford them rather than on their availability. As a result FAO report that although fertilisers such as Urea, DAP and SSP/TSP are readily available from Pakistan, Iran and Turkmenistan many poor farmers are unable to purchase them. Instead many use natural manure from livestock or low quality fertilisers (FAO/WFP 1997). Unfortunately these lower quality fertilisers are usually diluted by the manufacturers (or the farmers themselves in the belief that a little fertiliser application is better than none) or infiltrated by the manufacturers, which reduces nutrient content and thus causes little improvement to crop yield (FAO/WFP, 2004).

On rainfed cereals particularly in northern areas mineral fertilisers are generally not used because of lack of water (and so no economic benefit), their cost and lack of credit available to the farmers.

3.2.4 Mechanisation

Before Afghanistan was besieged by war, oxen used to be the primary source of field power. Since then throughout the country oxen have gradually been replaced by tractors, particularly in Helmand Province (ICARDA, 2002b). In 2003 more than 48% of irrigated and rainfed land was cultivated using tractors, both owned and rented (FAO/WFP, 2004). However, despite their widespread availability, the sowing and harvesting of crops is still conducted exclusively by manual labour, with tractors being used for threshing of grain crops and for preparing fields for future planting (ICARDA, 2002b).

It is anticipated that obvious signs of the use of tractors will be evident on high resolution imagery, including tractor wheel marks in crop residues after they have been threshed or in newly ploughed fields. In remote sensing terms it is anticipated that fields of freshly ploughed soils will appear darker than normal for 10-15 minutes (personal communication with UNODC) because the higher moisture content of the up-turned soil will cause more incident energy to be absorbed, as discussed in Chapter 2.

3.2.5 Summary

Section 3.2 discussed different farming practices with reference to how they may impact the spectral signature of different cover types (including poppy) at various times in the poppy lifecycle. It was discovered that during an irrigation event the colour of exposed soil temporarily darkens until it has infiltrated or evaporated which could take approximately 5 minutes at temperatures over 30 degrees Celsius (personal communications with UNODC staff). In addition, soil compaction activity along soil paths between rows of well-tended crop, or raised soil beds used to contain irrigation water both make the soil smoother, which results in increased spectral reflectivity, and so compacted soils will appear lighter on imagery.

Rather than being viewed in isolation their impacts must also be assessed in conjunction with the environmental factors outlined in Section 3.1 because these factors are intrinsically linked to the geographical distribution of the cultivation areas and the cropping calendars of the different crops.

3.3 Typical Afghan Crops

The following paragraphs describe the typical crops grown in Afghanistan alongside poppy. Poppy is described later in Section 3.5. Wherever possible, ground photographs have been included to demonstrate the similarities and differences in the appearance of each crop compared with the opium poppy.

Wheat *Triticum aestivum*

Wheat is both the most important food crop and the most widely grown crop in Afghanistan - accounting for approximately 70% of total cereal consumption (FAO/WFP, 2004). 80% of wheat fields are sown as a winter crop in all regions, with only 20% from rainfed production ICARDA, 2002b). Figure 3-5a shows wheat at emergence and Figure 3-5b shows wheat at leaf production.

(a) (b)

Figure 3-5 - Wheat at emergence (a) at leaf production (b)

During stem elongation (Figure 3-6a) the growing head of the wheat plant is pushed out of its leaf sheaf - a stage referred to as 'heading' or ear stage (Figure 3-6b). After heading, flowering referred to as 'anthesis' begins (Figure 3-6c).

(a) (b) (c)

Figure 3-6 – Wheat - stem elongation (a) heading (b) at anthesis (c)

At physiological maturity the heads lose their green colour and internal moisture rapidly declines. With senescence the wheat plants have changed to a golden colour (Figure 3-7).

It is anticipated that wheat would be identifiable visually from imagery by its uniform golden appearance at senescence and possibly also during the green stages. This is because the texture and tone of wheat fields at these growth stages appears smooth. In comparison, poppy has a unique speckled texture during flowering made up of small tonal differences between the green leaves and stems which contrast starkly with the lighter colour of the petals. Section 3.6 outlines this in more detail.

Figure 3-7 – Wheat at senescence

Stand density may also be used to discriminate between poppy and wheat because wheat fields are usually densely planted whereas poppy tends to be not so tightly packed (as described in Section 3.4). In addition, it was thought that the identification of linear soil rows and gaps between plants would also be an aid to discriminate poppy from wheat.

Barley *Hordeum vulgare*

Barley is the second-most important crop in Afghanistan and is grown principally for animal feed. It is the most common crop in rain-fed areas. Because of its low tolerance to cold 80% is spring-planted. Of the autumn-planted barley, some are early-maturing, maturing up to 25 days before wheat is harvested (ICARDA, 2002a). In the early growth stages barley appears similar to wheat (Figure 3-8a barley at ‘tillering’ and b at stem elongation).

(a) (b)

Figure 3-8 - Barley (a) tillering (b) stem elongation

Figure 3-9 shows barley at flowering.

Figure 3-9 - Barley at flowering

Figure 3-10 shows three examples of barley at senescence.

(a) (b) (c)

Figure 3-10 - Barley at senescence

Maize (Corn) *Zea mays*

Maize is the third most important crop.

Figure 3-11a, b and c illustrate maize at the early stages of growth. It is characteristically grown in regularly spaced rows, and once fully grown can reach a height of over two metres. Visually, it has more leaf matter than poppy and is much taller in appearance when mature. Figure 3-12 shows maize at flowering and senescence.

(a) (b) (c)

Figure 3-11 - Maize (a) emergence (b) leaf production (c) stem extension

(a) (b)

Figure 3-12 - Maize at (a) flowering and (b) at senescence

Vegetables and Fruit

Approximately 6% of the irrigated areas consist of vegetables including onions (Figure 3-13), potatoes, tomatoes, carrots and pumpkins – all of which are grown both for family consumption and as a cash crop (ICARDA, 2002b). They are commonly intercropped with other vegetables, poppy, wheat and barley.

From a remote sensing perspective, it may be difficult to discriminate between different vegetable and fruit crops if they are intercropped because mixed pixels might arise from the heterogonous mixtures of cover types. Moreover, if poppy is also intercropped with vegetables and fruit it will be extremely hard to accurately discriminate between poppy and the other cover types for the same reason.

Figure 3-13 – Onion at a mature growth stage

Winter vegetables include cauliflower, spinach, carrot, potato and lettuce (FAO/WFP, 2004). Summer vegetables include watermelon (Figure 3-14), tomatoes, aubergine (also known as eggplant), pumpkin, courgette (Figure 3-15), garlic and okra which are sown in spring and harvested in the summer.

Figure 3-14 – Watermelon at an early growth stage

Figure 3-15 – Courgette at flowering

Alfalfa (Lucerne) *Medicago sativa*

Alfalfa is a fodder crop found countrywide in arable areas. It is planted year-round and can be harvested up to six times per year. Its uniform dark green colour and its dense canopy (Figure 3-16) should make it readily identifiable and easily discriminable from poppy at visible wavelengths. Moreover, as its canopy is made up of many small leaves on different layers within the canopy structure, it is anticipated that alfalfa will have a greater biomass content than other crops, which would lead to a higher volume reflectance, making its dark, dense canopy distinguishable from other crops. This is because the leaves layered deep within the canopy will each reflect light that has been transmitted through the leaves near the upper canopy. This increased volume reflectance may assist in the identification of alfalfa from satellite imagery at visible wavelengths.

As it is harvested in sections when required the level of growth in any one field will vary as each harvested section grows back. Its harvesting pattern may therefore also be a key identifiable recognition feature. However, recently cut alfalfa may look like immature poppy due to similarities in size and reflectivity in visible wavebands. It is important, therefore, that the NIR wavelength is also used to discriminate between different crops because the addition of the NIR (to examine vegetation growth activity) may make each crop more discernable.

Figure 3-16 - Alfalfa

Fruit and Nut Orchards

According to FAO/WFP (2004) almost all farming households in rural areas have orchard crops which cover approximately 10% of the irrigated areas. Stone fruits, apple, vines (grape – (Figure 3-17) and raisin), citrus, pomegranate, apricot, almond, walnut and mulberry are grown in all regions (ICARDA, 2002). Orchards are regularly intercropped with alfalfa, pulses, vegetables or cereals (FAO/WFP, 2004).

Figure 3-17 – Vineyard

Weeds

This section has described indicators of cover type in generalised terms only. It has made the assumption that fields containing single crops will have a uniform, even appearance with little in-field variation. If a crop fails to grow well because of drought conditions or because a disease has affected the plants the field could appear atypical of that crop. It would therefore

not be possible to correctly identify which crop the field contains. As a result, this field should be labelled as weeds unless it matures to a stage where it can be positively identified.

3.3.1 Cropping Calendars - Sowing and Harvesting Dates

Cropping calendars detailing planting and harvesting dates for each of the major crops grown differ from region to region according to climate and farming practice. Only the most important crops have been listed in planting order in Table 3-2 and Table 3-3, described by ICARDA who used Dennis *et al.*, (2002) for reference.

Table 3-2 - Afghan autumn-sowing cropping calendar, after Dennis, Trutmann and Diab, 2002

AUTUMN SOWING			
Crop	**Location**	**Month of Planting**	**Month of Harvest**
Onion, clover and alfalfa	E, SE and SW	September	Onion and clover - mid-March to mid-April. Alfalfa - throughout year
Wheat	East central areas (Ghor, Bamyian, N Ghazni and Wardak)	Beg September to mid-October	Mid-May to mid-June
Wheat	NE (Baghlan, Kunduz and Takhar)	Mid-October to end-November	Mid-June to mid-July
Wheat	All other regions	Mid-October to end-November	Mid-May to mid-June
Barley and oilseed (mustard, flax, sunflower and sesame)	SE, E and SW	Mid-October to end-November	Oilseed in April Barley mid-May to mid-June
Poppy	E (in Kunar, Laghman and Nangahar), SW (Helmand, Kandahar, Zabol, Nimroz, Uruzgan)	Mid-October to end November	Mid-April to mid-May
Sugarcane	E, SE and SW	January	Mid-October to November (or biennial in lower elevations – NFD)
Potato	E and SE SW	February February to March	Mid-April to mid-May July to August

Table 3-3 – Afghan spring-sowing cropping calendar, after Dennis, Trutmann and Diab, 2002

SPRING SOWING			
Crop	**Location**	**Month of Planting**	**Month of Harvest**
Wheat	Rainfed areas: N and NE (Baghlan, Kunduz and Takhar)	March	Mid-June to mid-July
Wheat and barley	NE (Badakshan)	Mid-March to mid-April	August to September
Barley	Rainfed areas: N and NE (Baghlan, Kunduz and Takhar)	March	Mid-June to mid-July
Barley	Central (Kabul, Parwan, Kapisa, Logar and Wardak)	Mid-March to mid-April	August
Wheat and Barley	E Central	April	August
Poppy	NE (Badakshan)	Mid-March to mid-April	August to September
Poppy	Central (Kabul, Parwan, Kapisa, Logar and Wardak)	April	September
Oilseed	N	Mid-March to mid-April	September
Oilseed	E central	April	Mid-August to mid-September
Oilseed	Central	Mid-April to mid-May	September
Maize	N, NE and central	Mid-April to mid-May	Mid-August
Maize	SE E central	May Mid-May to mid-June	Mid-August October
Alfalfa	N, E central and central	Mid-April to May	Harvested all year
Clover	N, E central and central	Mid-April to May	Clover – N - mid-Jun to mid-July. E central mid-July to mid-August. Central - mid-August to October
Vetches –	N, E central and central	Mid-April to May	September
Pulses, potatoes, alfalfa and melons	N, NE, central and E-central	April to May	September to October
Rice	N (except Badakshan), NE, SE, E and SW	Mid-April to mid-May (in nurseries). Transplanted - mid-June to July	Central – September. N and NE - September to October. SE, E and SW - November

3.4 Afghan Poppy Farming Practises

The poppy cultivation practices used by Afghan poppy farmers may impact the spectral signature of poppy plants - which in turn may affect the accuracy of any subsequent digital classifications performed on imagery. These practices include using different methods to sow their poppy crop; manually weeding, thinning-out and nipping the immature plants, practising different irrigation methods, and in many cases not preventing pests and diseases affecting their poppy crops. Each of these different factors are discussed in the following paragraphs with reference to how they may impact the spectral signature of poppy.

3.4.1 Thinning, Weeding, Nipping

In Afghanistan seeds are either randomly sown by broadcast methods or fixed-dropped by hand into shallow holes dug by sticks. Farmers then employ labourers to thin out the poppy plants into rows to improve individual plants survivability. Labourers weed throughout the growth cycle to prevent competition for nutrients. The use of planted rows ensures that labourers do not accidentally trample on neighbouring plants when weeding and to give good access to each plant during harvesting without crushing others.

During the cabbage stage labourers ensure that poppy plants are thinned-out to leave approximately fifteen plants per m^2 remaining (personal communication with members of UNODC international staff). This allows the poppy roots to continue to grow outwards and downwards (to approximately one foot in depth) to prevent their root systems from intertwining. As the plants develop flower buds labourers also nip a number of each to allow the remainder to develop better.

From a remote sensing context, these Afghan practises of thinning, weeding and nipping expose proportionally more background bare soil than if a field were left untended. Moreover, different planting densities will also impact the spectral response of the crop, particularly as the Afghan poppy planting density of 15 plants per m^2 is much lower than for poppy grown commercially in other countries (i.e. 70 plants per m^2 in Australia (Chung, 1990) and up to 100 plants per m^2 in the UK poppy fields visited by the PDP. Any research objective therefore needs to be carefully examined to identify whether the spectral signatures of individual Afghan poppy plants are of interest, or of whole fields of Afghan poppy. In the former, ultra-high resolution sensors (i.e. sub 50cm) will be appropriate, as the spectral signatures of the immature plants will consist of proportionally more radiant energy from the soil rather than from the poppy canopy at the early growth stages. In the latter, 4m resolution

sensors such as IKONOS will be appropriate to Afghan field sizes ranging on average from 20m by 20m to 100m by 100m.

3.4.2 Harvesting

In Afghanistan, harvesting generally begins approximately two to three weeks after the petals have fallen from the capsules, when the mature capsules have swelled and the crowns on the top of the capsules have curved upwards. Not all poppies in one field will have reached maturity at the same time so harvesting may take place over two weeks. Harvesting takes place in two phases. The first phase is the incision of the capsule known as lancing (also known as scoring, tapping or incising) where labourers slice into the ovary wall to drain the opium sap contained within – see Figure 3-18.

Figure 3-18 - Afghan labourer lancing a capsule, photograph courtesy of UNODC

Farmers use blades bound tightly together on wooden handles - Figure 3-19 - to score the capsules on two to three sides in a diagonal or vertical direction. Approximately 95% of the poppy's opium will be secreted using this lancing method over several occasions. A depth of approximately one mm per incision is desired; if too deep the opium latex will flow too quickly from the pod and will drip into the ground; if too shallow the flow will be too slow and the opium will harden in the capsule.

Figure 3-19 - Afghan lancing equipment, photograph courtesy of UNODC

The desired time for lancing is late afternoon to allow the opium to slowly coagulate on the surface of the capsule overnight. As it oxidises the opium darkens and thickens in the cool night air taking up to fourteen hours to congeal – see Figure 3-20.

.

Figure 3-20 - Scored poppy capsules in Afghanistan. Photograph courtesy of UNODC

The second phase of harvesting is the collection of latex (the oxidised opium sap) which is scraped off the surface of the capsule early the following morning, timed to avoid the higher temperatures which would cause the latex to drip off the capsule. Although opium can be collected from each capsule up to seven times until the opium has run down, the percentage of morphine in the latex decreases with each successive collection. As a result the UN reports that on average farmers lance the capsules up to five times (UNODC, 2005b).

After harvesting the capsules are cut from the stems and left to dry – see Figure 3-21. Once dry the seeds are removed, dried in the sun and then are either carefully stored for the following year's planting or used in cooking or the manufacture of paints and perfumes (Opioids, 2006). The stems and any remaining foliage are then removed from the fields and used as an alternative fuel source.

Figure 3-21 - Dried capsule, photograph courtesy of UNODC

As an alternative to using seeds collected from sun-dried capsules from the previous year some farmers collect seeds from intentionally-left poppy capsules for the following year's crop because they believe that scoring diminishes seed quality.

As previously described, lancing activities cause dark brown latex to coagulate on the surface of the green capsules. Once the latex is collected, dark brown score marks remain. From a remote sensing context, it is not clear whether the overall spectral response of lanced capsules will be influenced by the dark brown colour of the latex, the number of dark brown score marks or the green colour of each capsule. The overall response will depend on the orientation of each capsule in relation to the sensor, the proportion of area affected by scoring each capsule and the spatial resolution of the sensor used. Even with ultra-high spatial resolution sensors which record spectral responses at sub-50cm, the brightness value of a lanced capsule will still represent the average response from the canopy, rather than that of the dark opium sap and score marks. Therefore, there should be no noticeable effect of a lanced poppy field on a 4m resolution image, as the brightness value recorded will represent the bulk properties of the vegetated surfaces in the fields.

3.5 The Poppy Growth Cycle

This section provides the first formal synthesis of the appearance of poppy during its growth cycle from both ground and aerial perspectives. It is the first time that the lifecycle of opium poppy has been documented in such detail using both ground and airborne images.

Some of the ground photographs used in this section were collected by UNODC staff during Afghan field visits. Additional ground and aerial photographs were collected as part of work conducted by the PDP in the UK poppy fields. The author's contribution to the UK field

studies included photographing and measuring the poppy crop at different stages in its growth cycle.

The Afghan opium poppy is one of many varieties of poppy which all belong to the *Papaver* genus of the *Papaveraceae* family (Poppies, 2001). The opium poppy derives its name *Papaver somniferum* from the latex produced within its seed capsules (Opiods, 2006).

Opium poppy is a self-pollinating and cross-pollinating plant and so has the capacity to grow in a variety of climates (Mansfield, 2001a). It is a hardy plant and so is also able to adapt to specific local conditions but grows best in temperate, warm climates with low humidity (Poppies, 2001). Although it is vulnerable to cold, wind and moisture (Mansfield, 2001a) it can be cultivated in extremely cold or frosty regions if there is a sufficient covering of snow to protect the seed and young plant (Mansfield, 2001a).

As a 'long-day' photo-responsive plant poppy requires long days of adequate sunshine and short nights (Srinivas *et al.*, 2004) with a moderate amount of water during the first two months of growth before flowers develop. Although growth is enhanced by moisture, if there is too much after a heavy rainfall on poorly drained soils poppy plants may become waterlogged and eventually die (Opiods, 2006). In addition, if there is heavy rainfall during sowing, germination and rapid vegetative growth stages nutrients may be leached from the soil, and spoil the opium harvest (Mansfield, 2001a). Moreover, too much water before the crop matures may cause poppy to be attacked by diseases which may inhibit subsequent growth and development (Mansfield, 2001a).

The opium poppy has adapted to a number of different types of soils including sandy, clay, sandy loam and sandy clay (Opiods, 2006). However, because sandy soils do not retain sufficient water or nutrients for proper plant growth and clay soils cannot readily be penetrated by the roots of a young poppy plant, poppy responds best to sandy loam (Opioids, 2006). This is because sandy loam has good moisture-retentive and nutrient-retentive properties and has a favourable structure for root development (Opioids, 2006).

In Afghanistan sowing occurs in autumn and/or spring depending on the prevailing local environmental conditions. The tiny round seeds of the opium poppy are sown almost exclusively by manual labour rather than by mechanical means (ICARDA, 2002a) using either broadcast methods (thrown randomly by hand) or fixed-dropped by hand into shallow holes dug by sticks. Wheat, barley, clover and alfalfa are also planted at the same time as poppy (ICARDA, 2002a).

Germination

Given sufficient warmth and moisture autumn-sown poppy seeds germinate quickly (Opiods, 2006), partially develop and then remain in a stable state protected under a snow-covering during the cold winter months. As temperatures increase in early spring, snow-melt releases moisture which ensures further development. However, if early snow has fallen in autumn the poppy seeds will lay dormant during the cold winter months. The seeds will then germinate and emerge once temperatures have increased sufficiently in early spring and moisture becomes available from snow melt and rain to permit rapid growth.

In either case, during winter the seeds are protected by snow. In spring they are exposed to rain which is then followed by a dry period as they mature. This exposure to alternate rainy and dry periods and alternate cold nights and warm days is optimal for the production of hardy plants with high yields.

Alternatively, farmers may sow poppy seeds in the spring once temperatures have warmed the fields and excess moisture has drained. The spring-sown poppies emerge soon after planting and grow rapidly whilst temperatures are not too high and moisture is still available. These spring-planted poppy crops are less hardy and have lower yields than the autumn-planted crops because they do not experience the ideal conditions of large temperature changes with alternate rainy and dry periods (Poppies, 2001).

Emergence and Leaf Production

After germination, the seeds simultaneously put out their roots and shoots. The first narrow bluish-green leaves of the seedling (the cotyledons) emerge. The first true leaves subsequently begin to grow with growth rate controlled by local light and temperature conditions - usually taking up to a month to reach the next growth stage. The roots are extremely sensitive at this stage to large amounts of moisture or periods of intense cold (unless protected by snow cover) – both of which may kill the plants.

Cabbage Stage

After approximately four-five weeks from emergence several true leaves become exposed (Opiods, 2006). Individual plants are locally said to resemble cabbage plants and hence this stage is often referred to as the cabbage stage (Figure 3-22 a-c). Other physical characteristics also vary from the number and shape of the leaves (elongated, globular, oblate, etc.).

Figure 3-22 - Poppy at the cabbage stage (a-c) (PDP)

Stem Elongation and Flower Bud Development

Approximately six-eight weeks from emergence given uninterrupted growth, stem elongation occurs (Figure 3-23a) where one long smooth stem grows vertically upwards to a plant height of between 30 and 150 cm or more (1-5 feet) owing to negative geotropism. The upper portion of this main stem is without leaves and develops into the peduncle (Opiods, 2006). Up to ten other stems (tillers) subsequently grow from the main stem.

As the plants grow taller the main stem and each tiller subsequently terminate in a green flower bud enclosed by leaves. At this stage the stems are typically soft and easily broken.

Hook Stage

Approximately one week prior to the onset of flowering positive geotropism causes the now extending peduncle portion of the main stem to bend over – forming the distinctive hook that lends its name to this stage in the growth cycle (Opiods, 2006), (Figure 3-23b). As the plants subsequently develop the peduncle straightens and the buds then grow upright.

At this stage, the stem hardens and becomes quite robust and the leaves on each plant mature into green, oblong-shaped leaves which may reach up to seven inches in length and four inches in width (Srinivas *et al.*, 2004). By this stage practically no background bare soil is exposed between the plants (Srinivas *et al.*, 2004).

Flowering

12-14 weeks after emergence and approximately one or two days after the buds begin to point upward the two outer segments of each bud (the sepals) fall away, exposing the flower petals.

At first the exposed petals are moist and have a crushed and wrinkled appearance but soon expand and dry out in the sun giving them a smooth appearance. The colours of the petals

vary widely from white to red, pink, purple, crimson and lilac as does their shape, number and arrangement (Figure 3-23c).

Individual petals will remain on a plant for between 30-40 hours each (UNODC, 2004) before falling away. Because plants may have several flower buds (depending upon the prevalent local environmental conditions and the species of poppy) whole poppy fields may progressively flower for two weeks or even longer.

Figure 3-23 - Poppy at (a) stem elongation and flower bud development (b) hook stage and (c) at flowering (PDP)

Maturing Capsule

After the petals have dropped small round green fruits are revealed, referred to in different publications as capsules, bulbs, heads or seed pods, which begin to swell and develop very quickly. These immature capsules are covered in a waxy coating which imparts a grey-blue tinge (Figure 3-24a). Within two to three weeks of flowering maximum volume and fresh weight is reached with full capsule maturity. The percentage of water content in the capsule remains high for approximately 6 weeks after flowering. As such, the MIR part of the EMS could potentially be valuable and therefore worth investigating because of the importance of water content in the MIR.

Externally the capsule remains green in colour, tinged with grey-blue. Internally the skin of the capsule encloses the wall of the capsule ovary which consists of an outer, middle and inner layer (Opioids, date unknown). Within the ovary wall the plant produces opium which drains into the middle layer through a system of vessels and tubes.

Senescence

At the onset of senescence nutrients are internally redistributed around the plant to assist in seed production. Seeds inside the capsule simultaneously start to develop, expand and harden. Like petal colour, colours of the seeds vary widely from white, yellow and brown through to black and grey. Simultaneously the lower leaves of each plant begin to undergo senescence, visibly wither and turn from green to yellow and then brown as they lose water content (Figure 3-24b).

Figure 3-24 - Poppy at (a) Maturing capsule, (b) start of Senescence, and (c) end of senescence (PDP)

As the leaves loose water most or all fall away from the plant. Finally both the stem and the capsule begin to change from green to brown and harden leaving just the capsules on the main stem and tillers (Figure 3-24c).

The poppy growth cycle is summarised in the time line below.

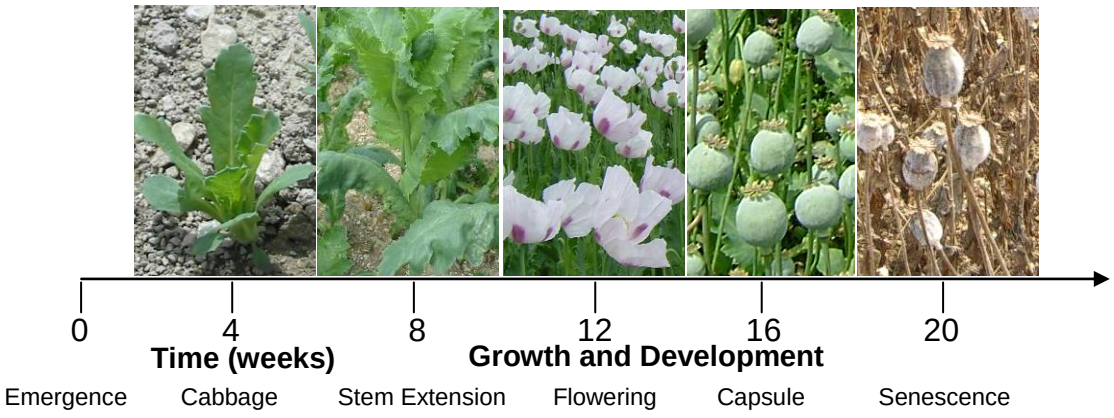

Figure 3-25 - Poppy growth cycle (not to scale) Photos: PDP

3.6 Experiences from UK Field Work

The previous section described the bio-physical changes that occur as individual poppy plants progress through each growth and development stage using ground photographs taken within poppy fields to illustrate their changing appearance.

This section continues with an examination of the appearance of the poppy crop by expanding the study up to an investigation of the appearance of an entire poppy field. To do so it draws on experiences gained from field trials conducted by the PDP in poppy fields in the UK, assisted by the author. It illustrates from a remote sensing perspective how the combined appearance of poppy plants in a field alters when viewed from above using digital aerial photography.

In 2004 simultaneous ground and aerial data were acquired over four occasions in two poppy fields grown for the pharmaceuticals industry in southern England. Within each field 1m sample locations were selected for the collection of biophysical and photographic data.

Aerial photography was acquired concurrently by the PDP using high resolution true-colour aerial digital photography (ADP) collected at a target ground pixel resolution of 0.6m by 0.6m from a Canon 10D 6.4 megapixel camera. This camera was mounted through the floor of a fixed wing Partenavia light aircraft flown at a flight height of 1200m (4,000 ft) across each field on each of the 4 dates selected.

3.6.1 Plant Morphology and Soil Background

Figure 3-26 illustrates two photographic examples of the UK poppy crop in Field 34 acquired on 11 Jun 04 at the cabbage stage. Photo (a) was acquired over a $1m^2$ area from a height of approximately 3m from the ground. Photo (b) is the corresponding aerial photograph acquired at a spatial resolution of 60cm from a height of 1200m over a portion of the same poppy field. Connecting lines indicate the approximate location from where the $1m^2$ photo in Figure 3-26a was acquired from. For reference, the spacing between sets of parallel tramlines in Field 34 was 28m. Although it is possible to estimate green leaf area index (i.e. the area of green leaves per unit area of ground) from multispectral reflectance measures this was not carried out by the PDP in their work in the UK poppy fields.

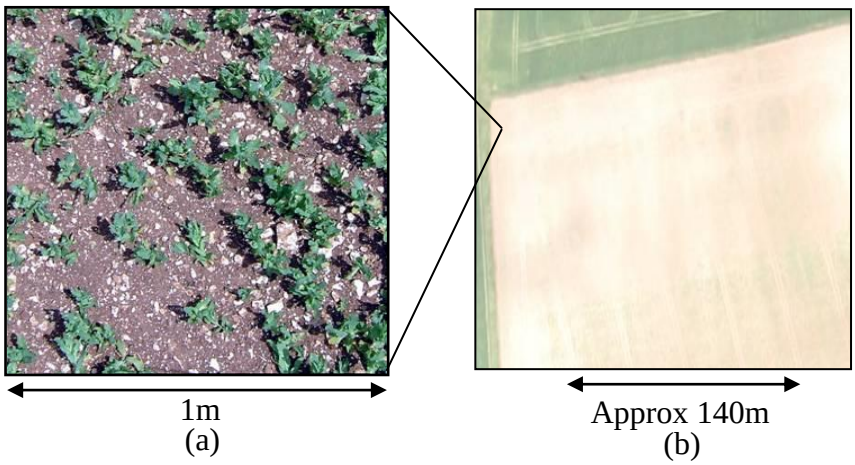

Figure 3-26 - Cabbage stage - (a) ground photograph and (b) aerial photograph acquired in Field 34 on 11 Jun 2004 (PDP)

In ground photograph (a) small green leaves on each poppy plant are clearly visible. The poppies are sparsely planted and so large gaps of bare soil and stones are evident. In aerial photograph (b) the light-toned sandy-coloured poppy field contrasts well with the adjacent green wheat field. This photograph reveals that because the plants had a low proportion of canopy cover at this immature stage the aerial camera recorded a mixed response of radiant energy from more of the background soil and stones than the plant canopy itself. The spectral response of the poppy field was therefore found to be influenced more by the colour of the soil and stones than the plant canopy itself at the cabbage stage. The same field was photographed a second time two weeks later on 28 Jun 04 at the flowering stage.

Figure 3-27 shows a ground photograph taken looking across Field 34 on this date and clearly shows white/lilac coloured petals visible on the poppy plants.

Figure 3-27 - Flowering stage - ground photograph acquired looking across Field 34 on 28 Jun 2004 (PDP)

Figure 3-28a is a ground photograph acquired over another 1m plot and shows that by flowering the poppy plants had developed a large and dense canopy which covered all of the

underlying background bare soil. In the aerial photography in Figure 3-28b, which shows the approximate location of the ground segment from Figure 3-28a, soil can be seen throughout the field where the poppy crop is not so dense, or where tractor wheels have evidently been. Overall, however, the ADP photography shows the combined contributions from the green poppy canopy and the hue of the lilac and white petals, which together, have brought about a distinct lilac/green/blue tone to the poppy field where, only two weeks previously, the brown of the soil had been the predominant colour. It is likely that the field would look similarly green/lilac on 1m and 4m satellite imagery, with the 4m imagery being easiest to handle in terms of image classification due to spatial averaging of mixed pixels.

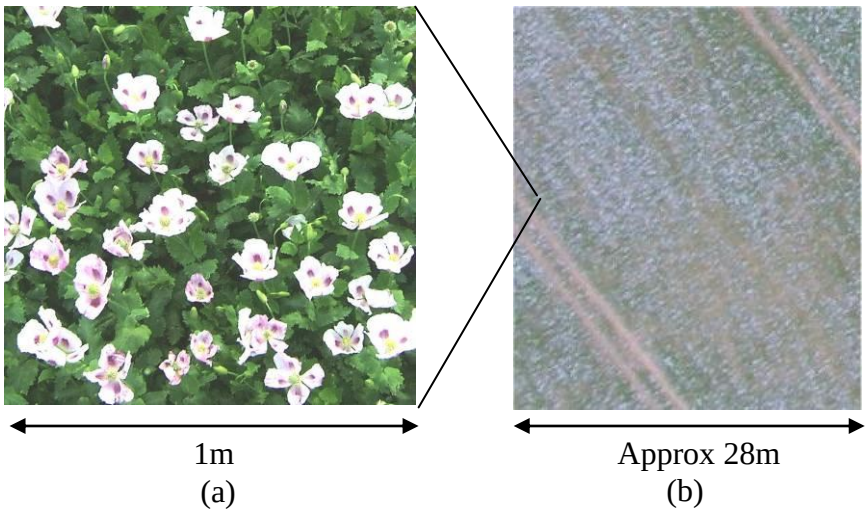

Figure 3-28 - Flowering stage - (a) ground photograph and (b) aerial photograph acquired in Field 34 on 28 Jun 2004 (PDP)

The field was photographed for a third time on 13 Jul 04 when the poppy crop had reached the capsule stage. The ground photograph in Figure 3-29a shows pale green capsules with dark green crowns against darker green leaves and stems. Background brown soil and white stones are also evident in small patches of the sample. In the ADP in Figure 3-29b the contributions from the various components of the green canopy combined with a small proportion of radiant energy from the soil brought about the dark green response seen in the poppy field. The colour of the poppy field at the capsule stage was therefore influenced largely by the various green components of the poppy plants.

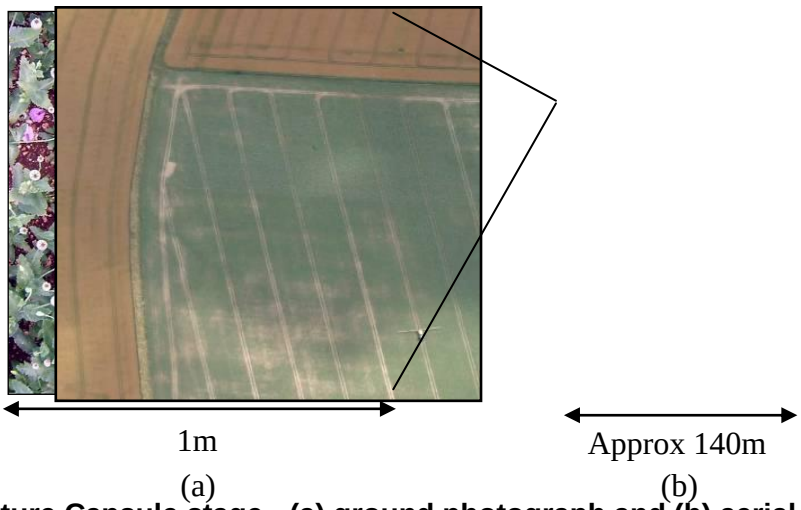

Figure 3-29 - Mature Capsule stage - (a) ground photograph and (b) aerial photograph acquired in Field 34 on 13 Jul 2004 (PDP)

The poppy fields were photographed for a fourth and final time on 08 Aug 04 when the poppy crop was in senescence. The ground photograph in Figure 3-30a shows that the percentage of canopy cover had significantly reduced which thus exposed a large percentage of bare soil and stones. All of the once green leaves had withered and fallen away revealing bare withered brown stems and small brown capsules.

The ADP in Figure 3-30b shows that the colour of the poppy field at senescence was influenced by a combined radiant energy response from the brown plant canopy and the background soil and stones.

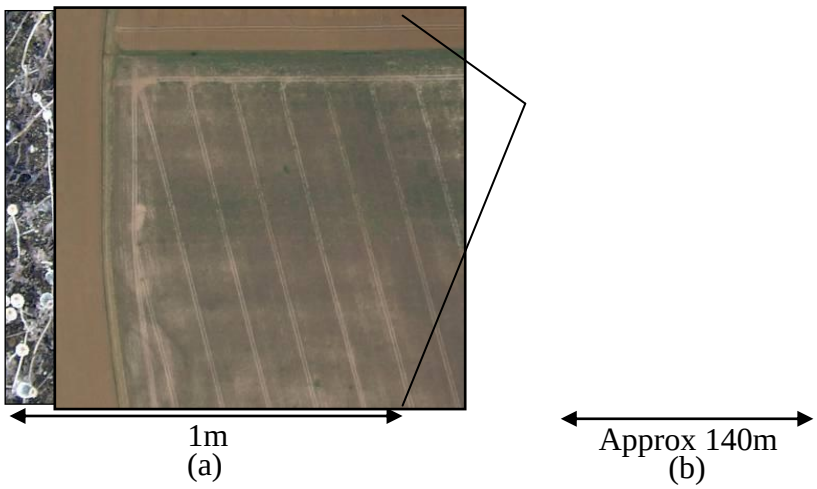

Figure 3-30 - Senescence - (a) ground photograph and (b) aerial photograph acquired in Field 34 on 06 Aug 2004 (PDP)

3.6.2 Local Environmental Factors

This section qualitatively investigates the environmental factors that may influence the spectral-temporal properties of the poppy fields.

Farmers decide when to plant their crops based largely on the prevalent local environmental conditions. In the UK in 2004 the farmer's decision to plant poppy in the month of March was based on the lengthening daylight hours and increasing temperatures warming the soil after a cold winter so that optimal poppy growing conditions could be provided.

Unfortunately, an unexpectedly late frost in southern England in March killed off all of the young, newly emerged and very delicate poppy plants in one exposed field. The farmer subsequently re-planted the field on 23 Apr 04 - a date much later in the growing season than was the norm. This unfortunate event provided an opportunity to investigate how this delayed planting would affect the subsequent poppy plants. The bio-physical characteristics of the poppy plants in the field where planting was delayed were subsequently compared to another field which had survived the frost.

Development was carefully observed in the fields to establish whether later-planted poppies would progress quickly through their growth cycle to catch-up and effectively reach the mature capsule stage at a similar time to the earlier-planted poppies. This was found – growth did eventually synchronise after the later-planted poppies had accelerated through their early growth stages so that by the time the fields were re-visited all of the poppies were in flower at the same time, regardless of planting date.

This subsequent acceleration of growth resulted in shorter, smaller poppy plants with fewer, smaller leaves which resulted in a smaller, less dense and less enclosed canopy. Each plant typically produced just a single flower which resulted in the field undergoing flowering for less time than the earlier-planted poppies because each plant consisted of fewer flowers. Typically, one small capsule per plant was also found.

These qualitative observations are useful in a remote sensing context; they provide evidence that smaller plants may develop with less biomass when poppy is planted later than normal. The spectral signature of a field of later-planted poppies may therefore consist of proportionally more radiant energy recorded from the background bare soil and stones than from the plant foliage itself even when the plants are at a more advanced growth stage than the remote sensing instrument has led the analyst to believe. As a result, care must be taken to ensure that the presence of bare soil in a crop does not influence an analysts decision on crop

type or growth stage reached. Ground data collection should be undertaken to help sort out this uncertainty to ensure that accurate crop identification can be achieved.

As first described in Section 3.4, individual poppy plants may not flower at the same time. As described in the preceding paragraphs, delayed planting may affect the morphology of a poppy plant and cause it to develop a single flower and capsule. Or, the species of poppy itself may determine the number and arrangement of flower petals themselves. Either way, flowering poppies are readily identified on the ADP in Figure 3-28b, particularly when several flowers are present on the same plant.

Another crop with a particularly vibrant petal colour is winter oilseed rape (OSR) which has bright yellow petals when in flower. One study in Poland compared the multi-temporal reflectance characteristics of OSR with wheat and found that the two crops were easily discriminable when the OSR was in flower (Piekarczyk, 2005). The study noted that red reflectance increased rapidly in OSR during flowering, whilst concurrently, reflectance in the red band in the wheat crop decreased steeply and reached lowest values when OSR red reflectance was at its peak (Piekarczyk, 2005).

It is therefore hypothesised that spectral separability between poppy and other crops may also be strongest at flowering. Although this was suggested in the literature it has not been formally quantified, and so this study therefore aims to determine whether this is the case. It is further hypothesised that if this is proven to be correct, the process of correctly discriminating between poppy and other crops could be made much simpler and more accurate than at any other time in the poppy growth cycle if imagery is acquired when poppy fields are in full flower.

To anticipate when flowering may occur, particularly if poppy plants do not come into flower at the same time, a field visit could determine the most likely time that a whole field will come into flower to maximise the chances of a sensor recording the flowering poppy spectral signature. To determine this time, the proportions of hooks, flowers and capsules present in each field could be measured to estimate whether a field is at the beginning, middle or end of flowering to determine when imagery should be acquired. This is simplified in Table 3-4:

Table 3-4 - Flowering maturity, estimated from relative proportions of hooks, flowers and capsules

Hooks	Flowers	Capsules	Flowering Maturity
More	Less	Less	Beginning
Less	More	Less	Middle
Less	Less	More	End

If field visits are impractical, another way that could be used to predict when fields are about to flower is by monitoring the increase in NDVI as photosynthetic activity increases, as discussed in Section 2-3-2 of Chapter 2. Moreover, the PDP successfully demonstrated in their UK poppy field trial work that NDVI profiles acquired from digital aerial photography over successive dates could be used to monitor the photosynthetic activity of the UK poppy fields and determine approximate dates when different growth stages were reached.

Figure 3-31 shows a generalised vegetation NDVI profile from one of the PDP's UK poppy fields. Poppy growth stages have been superimposed onto the profile to indicate the time taken to progress to each successive growth stage and the temporal overlaps between growth stages.

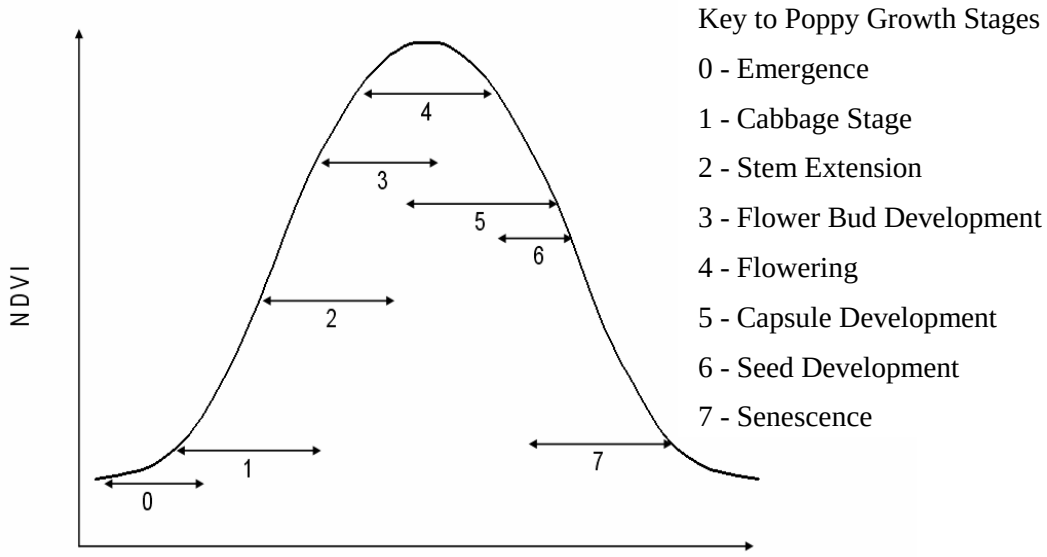

Figure 3-31 - Generalised vegetation NDVI profile through time with approximate timings of poppy growth stages (after PDP, 2004)

3.6.3 Farming Practise

Stand Density

The 2004 UK field trials also provided an opportunity to determine whether planting (stand) density influenced the spectral signature of poppy. Planting was conducted using a tractor-mounted pneumatic seed drill to achieve an optimum planting density of 96 plants per m^2. However, in one small area of Field 34 seeds were accidentally double-drilled. This provided an opportunity to investigate the influence of stand density on the spectral signature of poppy throughout the growth cycle.

In Field 34 at the cabbage stage, crops planted at optimum density were found to have more bare soil exposed than those that were double-drilled. Ground measurements and field photos record this at different locations in the field.

The photographs in Figure 3-32 were taken on 28 Jun 4 at the poppy flowering stage and show that although the plants had reached the same growth stage during image capture, less soil was visible in Figure 3-32b (double-drilled) than in Figure 3-32a (normal planting density) because of the presence of more plants in the double-drilled section of the field. The closely-packed canopies in the double-drilled area therefore hid most of the background bare soil and stones.

(a) (b)

Figure 3-32 – Field 34 on 28 Jun 2004. Poppy flowering (a) normal planting density and (b) high planting density (PDP)

These observations are useful in a remote sensing context because they suggest that the spectral signature of the optimum-drilled field will consist of proportionally more radiant energy from the soil (and therefore consist of a ‘mixed’ spectral signature) than from the double-planted field. This ‘mixed’ spectral signature is expected of the Afghan poppy crops

as poppy is carefully hand sown, thus ensuring each plant has adequate access to light and nutrients. As a consequence, more bare soil is expected to be visible.

Man-made linear features

Across both fields in the UK distinct linear soil tracks (known as tramlines) were evident where the tractor wheels had compacted the soil. Figure 3-33a shows that the light brown soil contrasts clearly with the green foliage and lilac petals.

Figure 3-33 - Influence of linear soil features - tractor tram-lines - on poppy spectral signature in Field 34 (a) ground photography at poppy flowering, (b) ADP at poppy senescence (PDP)

These tracks are also distinct in Figure 3-33b because of their contrasting light brown tone and their linear nature. In Afghanistan, as the poppy crop is hand sown, these tram lines will not be present, but it is expected that other linear soil features such as drainage ditches associated with important cash crops will be clearly visible from satellite imagery regardless of crop maturity. These features may be useful for crop discrimination if their presence could be linked to a unique farming practice associated with a particular type of crop.

3.6.4 Summary

The UK field work results suggest that there may be a proportional relationship between the amount of radiant energy response recorded from the soil and from the poppy canopy. This relationship may be dependent on the growth stage reached, the number of plants (stand density) and farming practices used. Although this relationship may be quantitatively tested using an imaging spectrometer, it is beyond the scope of this research to do so. It is therefore suggested that this work should be conducted in the future.

During the immature growth phases of emergence, leaf production and cabbage stage when biomass is low and the percentage of canopy cover is minimal, remote sensing sensors record

a mixed response of radiant energy from more of the background soil than the plant canopy. As the poppy plants grow and develop, the proportion of spectral reflectance from the background soil diminishes as the plant canopies develop green stems, leaves and buds. By the flowering stage radiant energy from the petals and green foliage contribute most to the overall spectral reflectance of the poppy field. As the poppy capsules reach full maturity and the lower leaves fall away during senescence the percentage of canopy cover significantly reduces. Sensors consequently record radiant energy from more of the dry background soil than the plant canopy.

Poppies which were planted later than normal in the cropping calendar advanced through their growth and development cycle at a greater speed than normal, diverting resources away from vegetative growth into flower and seed development and as a result put up less biomass and canopy cover. This resulted in the prediction that the spectral signature of poppy will be affected most by the soil background during the early and later growth stages. Moreover, analysis of the ADP demonstrated that the process of visually discriminating between poppy and other plants is much easier and more accurate when photography is acquired when a poppy field is in full flower, rather than at any other time in the poppy growth cycle. Together, these two observations led to the prediction that, in remote sensing terms, the best time for poppy identification will be during poppy flowering, when the majority of the radiant energy response recorded from a poppy field will be from the plant canopy itself - when there is less influence from the background soil. Although the Literature Review suggested that this was the case, it has not been quantitatively demonstrated before. This research therefore aims to confirm the optimum time for Afghan poppy identification, based on when spectral separability is highest.

It was recognised that field work should be conducted to determine the approximate dates when poppy fields would reach flowering so that imagery could be acquired at this time to ensure that accurate identification of poppy could take place in Afghanistan.

This qualitative assessment also suggests that an intimate knowledge of the progressive development of the opium poppy plant must be gained for the identification to be reliable using both field work and imagery. This conclusion was also reached by Avery and Berlin who observed that a knowledge of crop growth cycles must be gained when a variety of image dates are used (Avery and Berlin, 1992).

The UK field work was invaluable for gaining an understanding how a poppy plant's biomass content and canopy closure are affected by its age and how the UK farming practices such as planting density and the use of tractors affected the visual appearance of the poppy fields. These qualitative ground and aerial photographic interpretations have been used in this research to make predictions on the degree to which environmental factors and Afghan poppy farming practices influence the spectral signatures of poppies grown in Afghanistan fields, which are subsequently tested in this research.

3.7 Discussion

The successful remote detection of poppy and other crops requires accurate information on both regional cropping calendars (detailing lists of which crops are grown and their planting dates), and an intimate knowledge of the progressive development and growth stages of each crop.

Although spectral discrimination has not yet been tested in this study, several useful predictions have been made about remote sensing at visible wavelengths. For accurate identifications to take place it was demonstrated that specific crops may only be distinguishable from each other in the visible part of the spectrum at particular times in their growth cycles on the ground and from imagery. For example, wheat may be distinguishable from barley during flowering or poppy from wheat and barley when the cereal crops are in senescence.

This suggests a need to acquire imagery a number of times during the cropping cycle to ensure that accurate discrimination can take place. This concurs with a study conducted by Murakami *et al.*, (2001) that as the spectral reflectance characteristics of crops change during their growth season, a multi-temporal approach is required for successful image classifications. This was proposed because "single image dates rarely offer sufficient spectral differentiation between crops for their accurate classification" (Murakami *et al.*, 2001).

This study therefore aims to establish whether there is one single stage in the poppy growth cycle when poppy appears different from other crops, or whether certain combinations of dates during the growing season are promising for improving crop discrimination.

To help assess the acquisition of imagery at optimal times, accurate cropping forecasts are necessary. However, it may never be possible to create accurate regional cropping forecasts because environmental conditions vary significantly from one year to another. Therefore, a

reliable method is required that could be used to help construct a detailed imagery acquisition plan. One possible solution would be to use a time-series of NDVI profiles derived from bands 1 and 2 of MODIS to create cropping forecasts. This would also ensure that imagery acquisition dates coincide with a time in the poppy growth cycle when enough vegetative matter is visible to give the greatest possibility for accurate identification of poppy. Section 4.3.1 describes the methodology developed by the PDP to monitor biomass changes in Afghanistan using MODIS NSVI profiles which was subsequently adopted in this research.

3.8 Chapter Summary

Only a sparse amount of formal documentation exists on the appearance of poppy at each of its growth stages and how farming practises such as thinning, weeding and irrigation could affect the spectral signature of poppy.

This chapter therefore provides the first formal synthesis of the appearance of poppy during its growth cycle from both ground and aerial perspectives.

Visual analysis of the ADP revealed that the UK poppy crop appeared to be more distinct in the visible part of the spectrum at flowering than at any other time in the UK field trials because of the colour contrast between the brightly coloured poppy petals and the green foliage. The Literature Review also suggested that flowering was the best time for discriminating between poppy and other crops, although these studies were only qualitative.

This research therefore formally tests for the first time the hypothesis that spectral separability of poppy is greatest at flowering than at any other time in the growth cycle, using imagery acquired from the IKONOS sensor. The addition of the NIR band is also formally tested to determine whether this extra information makes a useful contribution to the analysis.

This study has consequently:

- Systematically researched, collated, analysed and formally documented the poppy growth cycle with reference to how the bio-physical characteristics of poppy alter as it progress through its growth cycle.
- Formally documented factors which could influence the development of the crop, including terrain, farming practices, climate, pests and disease which each have an influence on the spectral properties of the opium poppy.

- Placed the appearance of poppy at the field level at different growth stages into the context of remote sensing by demonstrating how the changes affect the appearance of UK poppy fields on aerial photography.
- Investigated the links between cropping calendars and environmental factors with reference to determining the optimum times in the poppy growth cycle for accurate discrimination between crops from imagery.
- Revealed from UK field trials how the influence of soil on the appearance of poppy is fundamentally linked to biomass and canopy closure, which in turn are both linked to the health and age of the plant (i.e. the growth stage reached).
- Revealed that the hue of poppy petals also affects the appearance of poppy at the flowering stage at visible wavelengths.
- Revealed that delayed planting caused the UK crop to accelerate through its growth cycle to reach the mature capsule stage in synchronisation with earlier planted poppy. As a consequence the trials revealed that:
    - Smaller plants developed with less biomass. More background soil was visible at a more mature growth stage than expected.
    - The reflective properties of poppy at visible wavelengths could be influenced by its background soil, as had been hypothesised in Chapter 2
    - Accurate ground data collection is important for validation of crop types identified on imagery and aerial photography.

Chapters 4 and 5 now investigate the variability of spectral reflectance of poppy in Afghanistan to determine how factors identified in this chapter (climate, pests, diseases, growth stage and farming practices) and those identified in Chapter 2 (crop bio-physical characteristics, sensor capabilities and remote sensing techniques used to discriminate cover types) have the potential for influencing the accuracy of poppy identification from satellite imagery.

4. Acquisition and Pre-processing of Multi-temporal Datasets

Together, this chapter and Chapter 5 introduce a method developed in this study to meet the overall aim of this research; to investigate the application of remote sensing for discriminating poppy from other land cover types in Afghanistan using spectral signatures obtained from the analysis of multi-spectral imagery.

This chapter begins by describing how large datasets were collected from several study areas in Afghanistan. The locations of all multi-temporal IKONOS images, true-colour Zeiss aerial photography and ground data were selected from a sampling frame created by UNODC to assist in the identification of crops.

Details of the data pre-processing methods used are provided at the end of the chapter and include geo-rectification of IKONOS images and visual photographic interpretation (PI) of both Zeiss photography and modified pan-sharpened IKONOS imagery in locations where UN ground data was insufficient. Details of how representative training and evaluation pixels were selected for each cover type from these training areas are provided in Chapter 5.

4.1 Selection of Suitable Study Areas

Figure 4-1 shows the locations of ten provinces surveyed by UNODC in their 2004 imagery survey (shaded in yellow). Of the ten, only a sample of UNODC's study areas could be used in this study owing to budget and time constraints. These samples were located in three of the ten provinces highlighted.

The three provinces were selected in the anticipation that they were representative of the geographic distribution of poppy cultivation in Afghanistan and because they were reported to have contained the highest levels of opium poppy cultivation in 2003 (UNODC, 2004). Figure 4-2 illustrates these three provinces.

Figure 4-1 - Afghanistan Opium Poppy Cultivation - Source UNODC, 2003

10 x 10 km IKONOS Image Survey Sites

The Literature Review in Chapter 1 described how UNODC used a sampling frame to select fifty-six 10 km by 10 km survey sites within their ten provinces from which IKONOS images and ground data were collected. For this study a sub-sample of these survey sites were selected - four in Helmand in the South of Afghanistan, four in Nangahar to the East and three in Badakshan to the North. Figure 4-2 shows the approximate locations of these eleven sites.

The eleven 10 km x 10 km survey sites located within the three provinces were specifically chosen for this study because they represented a good distribution of growing conditions that reflected the different terrain types and agricultural practices previously described in Chapter 3, so that their effects on the poppy crops could be identified. For example, cropping in Helmand is typically based on a wide strip of high intensity, flat, canal-irrigated land fed from the River Helmand. This is in contrast to the scattered, steep terraced valley slopes of Nangahar and the high altitude, rain-fed areas in Badakshan.

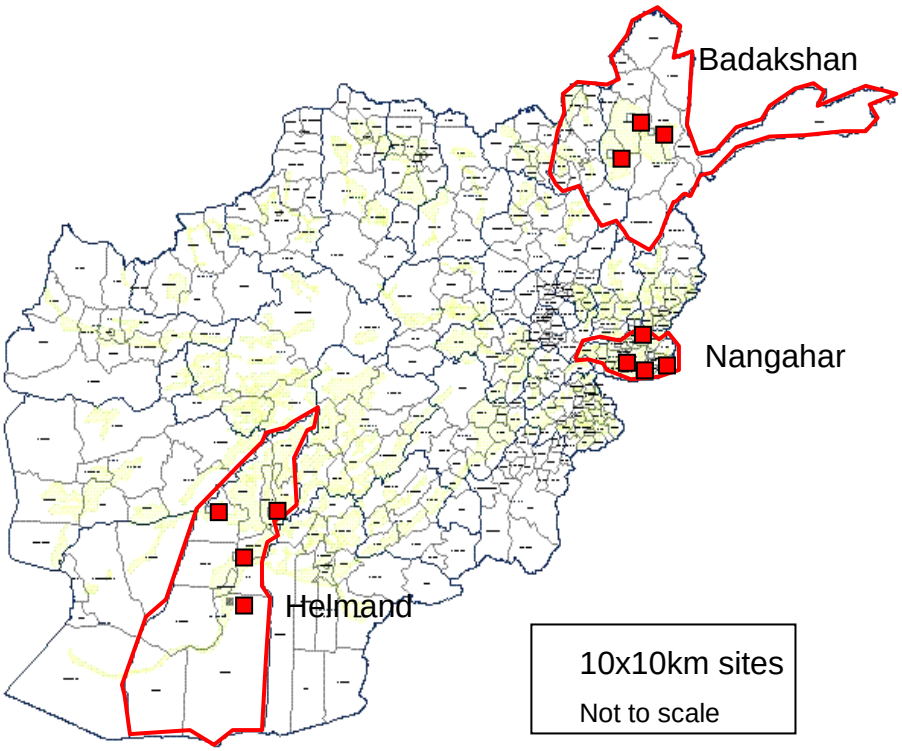

Figure 4-2 - Approximate locations of UK imagery survey sites in Afghanistan

250m x 250m Segment Training Areas

The ground data used in this study (*in-situ* field measurements and ground photos) was kindly provided by UNODC. All ground data was collected by local Afghan surveyors from three randomly selected 250m by 250m segment training areas located within each 10 km by 10 km survey site situated within agricultural areas. In addition, Zeiss photography was also collected over each segment training area. Figure 4-3 shows an example of the locations of three ground data segment training areas in Musa Quala District, Helmand Province, with field boundaries highlighted and overlaid onto one of the IKONOS images used in this research.

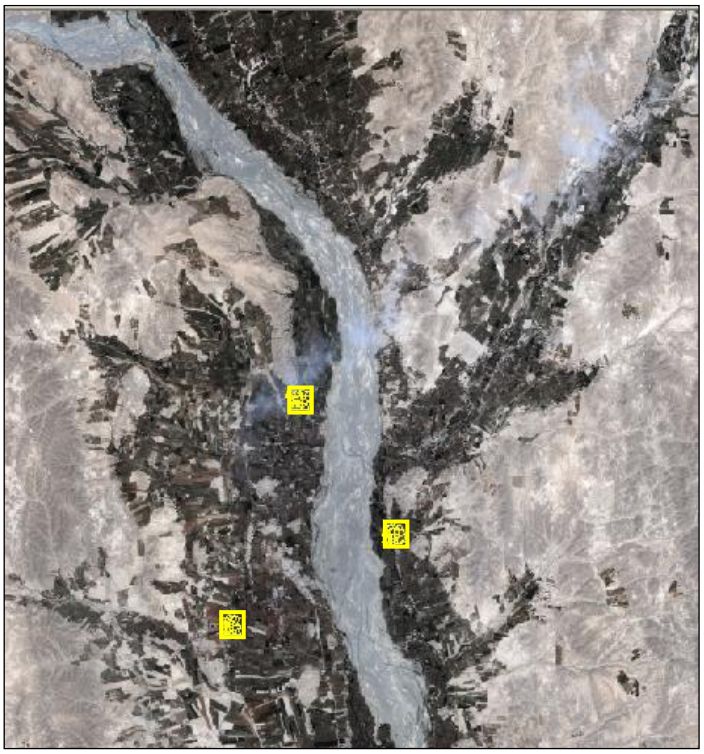

Figure 4-3 - Locations of three 250m x 250m ground data segments with field boundaries overlaid onto a 10 km x 10 km 4m resolution IKONOS image, acquired on 28 Apr 04 in Musa Quala District, Helmand Province. The image is displayed in true colour, i.e. RGB = bands 3, 2 and 1.

4.2 Data Collection Plan

Several consecutive IKONOS images were planned to be acquired over each of the eleven sites during the 2004 and 2005 growing seasons in order to gain an understanding of how poppy reflectance characteristics alter as it matures through the growth cycle. Specifically, a data collection plan was devised that incorporated UNODC's imagery collection plan of pairs of IKONOS images over the eleven sites into a larger research strategy to collect IKONOS images during five major poppy growth stages at each site (as highlighted in Chapter 3), which included; cabbage; stem elongation; flowering; mature capsule and senescence, plus an extra image post-poppy harvest after the crop residue had been removed. A US sponsor agreed to fund and deliver the additional four IKONOS scenes per site.

In addition to the IKONOS imagery and ground data provided by UNODC it was agreed that a UK platform would also collect Zeiss colour aerial photographs over each site at three specific times in the poppy growth cycle.

Time of Image Collection

Research conducted on cropping calendars in Chapter 3 revealed that local environmental conditions and availability of labour influenced when crops were planted. It also revealed that the timing of crop emergence and rate of crop maturation were influenced by the local environmental conditions. As no means existed to forecast meteorological conditions in advance UNODC's anticipated dates for collection of imagery and ground data were based on the previous years cropping calendar (2003) and planting dates for the 2004 growing season. This information was collected by UNODC and reported in their 2003 Annual Poppy Survey and their 2004 Rapid Assessment Survey (UNODC, 2004). This information was also used in this study to forecast collection dates for the US-sponsored IKONOS imagery and UK aerial photography. In order to allow for some advances or delays to crop growth, windows of imaging opportunity were provided to the IKONOS vendors Space Imaging rather than specific dates in the hope that the requested dates would adequately cover the 2004 growth cycle.

2004 IKONOS Imagery

Source: UN – Two IKONOS images/site

The first collection of shared UNODC IKONOS imagery was designed by UNODC to be acquired when the poppy crops were in flower, a time when the colour of the petals was predicted to make Afghan poppy appear different to other crops on imagery (which concurs with the research conducted in the UK poppy fields in Chapter 3). UNODC's second acquisition date was planned to take place after the poppy harvest when the poppy crop had been removed from fields.

Source: US – Four IKONOS images/site

Once UNODC's collection dates had been confirmed the imagery collection plan for the remaining four dates was devised and submitted to Space Imaging, the IKONOS vendors. Two IKONOS images were requested at each site prior to UNODC's poppy flowering image, and two in-between UNODC's flowering and post-harvest images. The first acquisition was planned to coincide with the poppy crop having reached the cabbage stage, which UK field work had demonstrated was the earliest time that poppy

was visible on aerial digital imagery. The next acquisition was planned to coincide with stem-elongation. The third image was to be acquired at the mature capsule stage post-flowering and the fourth image at senescence before the poppy crops were removed from the fields.

Consequently, 2004 IKONOS imagery was requested to begin in Nangahar Province at the end of March 2004 (predicted to be coincident with poppies having reached the cabbage stage) and subsequent collections over the four 10 x 10 km sample sites every ten days thereafter until the opium harvest was complete. The final collection over Nangahar Province was requested to be completed by the beginning of the third week in May 2004.

The request for image collection in Helmand Province followed the same time intervals but commenced and finished ten days later than the Nangahar dates to account for the forecasted later harvesting. In Badakshan Province the first collection was requested to commence on 01 May 2004 with four subsequent collections every ten days thereafter with the final collection anticipated to be completed by 15 July 2004.

2004 Ground Data

UNODC planned to acquire ground data at each segment training area at a time coincident with the acquisition of the first corresponding IKONOS image during poppy flowering. This was to ensure that the crops were still in the ground prior to the poppy harvest to enable the surveyors to identify all of the crops grown in each segment. For each segment surveyors were provided with a 1:1,000 segment map, and, wherever possible, a panchromatic IKONOS image that had been acquired for the 2003 survey to show each field boundary within the 250m by 250m ground segment, and a segment form for data entry.

At each segment surveyors were required to draw the exact shape of each field boundary onto the segment map and allocate each one a unique serial number. On the segment form surveyors were required to record crop type, growth stage, height and uniformity, irrigation practices, the presence of disease and/or drought, evidence of harvesting from previous crops (if applicable) and the presence of other crops being intercropped alongside the main crop (if applicable), for each field. Digital ground

photographs and GPS locations of each field parcel in the segment were also requested from surveyors.

UK Visits to Segment Training Areas

During 2004 it was hoped that field visits would be conducted to at least one segment training area per province to collect photographs and learn at first hand about cropping and agricultural practices in each of the provinces selected. A visit incorporating several sites was planned.

2004 Zeiss Colour Aerial Photography

The UK agreed to share with UNODC Zeiss true-colour aerial photography that would be acquired by its own aircraft for a separate task over the eleven survey sites, in order to assist in cover type identification and to help verify the UN's ground survey data. Photographic collection was requested to take place on three separate occasions during the growth cycle at the cabbage/stem elongation stages, flowering and senescence stages to coincide with the IKONOS acquisitions.

4.2.1 Summary of 2004 Data Collection Plan

Table 4-1 shows the overall data collection plan for 2004. In total it was anticipated that six IKONOS images would be acquired at each of the eleven 10 km by 10 km sites totalling 66 IKONOS images.

Within the eleven sites Zeiss photographs would be acquired on three separate occasions at each of the three 250m by 250m segment training areas (totalling 99 Zeiss photographs).

Data would also be provided from one field survey at each segment training area coincident with UNODC's pre-harvest IKONOS images.

Table 4-1 - 2004 Imagery and Ground Survey Collection Plan

Province	Site (District)	Requested IKONOS acquisitions (per 10km x 10km site)	Requested ZEISS acquisitions (per 250m segment)	Requested Ground Surveys (per 250m segment)
Nangahar	Batikot	6	3 x 3 segments	1 x 3 segments
	Dara-e-Nur	6	3 x 3 segments	1 x 3 segments
	Surkh Rod	6	3 x 3 segments	1 x 3 segments
	Chapahar	6	3 x 3 segments	1 x 3 segments
Helmand	Nad-e-Ali	6	3 x 3 segments	1 x 3 segments
	Garmser	6	3 x 3 segments	1 x 3 segments
	Washir	6	3 x 3 segments	1 x 3 segments
	Musa Qala	6	3 x 3 segments	1 x 3 segments
Badakshan	Faizabad	6	3 x 3 segments	1 x 3 segments
	Jurm	6	3 x 3 segments	1 x 3 segments
	Keshem	6	3 x 3 segments	1 x 3 segments
Total		**66**	**99**	**33**

4.3 Data Acquired - 2004

IKONOS Imagery

One of the key findings of the IKONOS acquisitions was that most of the image acquisition dates had been delayed and some collection windows were shortened, for unknown reasons. As there were no reports of continual dust storms or extensive periods of cloud cover (i.e. covering 1-2 weeks) there should have been sufficient opportunity for collections to occur as requested, as the sensor's temporal resolution is published to be 3-5 days as listed in Table 2-5 in Chapter 2. For example, in Nangahar and Badakshan Provinces collections were approximately four weeks late. In Helmand Province collection began approximately two weeks late and finished in the middle of May two weeks earlier than requested. The reasons for these were not known.

Unfortunately, these delays meant that the earliest time of collection coincided with poppy flowering in all three provinces and not at the earlier growth stages of poppy cabbage and stem elongation as requested. In addition subsequent reporting indicated that the 2004 poppy harvest had started earlier in Helmand and Nangahar Provinces by between one to two weeks in every area (UNODC, 2004) than had been forecasted. This early harvesting was attributed to weather conditions (no further details were provided) and in some cases, farmer's decisions to harvest early to avoid rumoured poppy

eradication activities (UNODC, 2004). All of this resulted in fewer growth stages being captured on imagery.

A second key finding was that delivery of images was neither timely nor consistent. For example, of the images supplied by UNODC, some were received within four weeks of image capture and some were received after twelve weeks. Delivery of US-supplied IKONOS images was similarly inconsistent - some were received after two months and others four to six months after acquisition – particularly in Badakshan Province. The reasons for this varied from higher priority work activities taking precedent and the requirement for permissions to be granted from higher UN and US authorities before images could be released to this study.

Additional key findings include:

- Duplication of the 2004 IKONOS acquisitions over the same sites, (i.e. images collected for the UN on one date was also provided to the US)
- Only partially covered ground segment training areas
- Ground segment training areas which were almost totally obscured by cloud or haze, rendering them unusable.

Consequently, only two images per site were useful for this study captured from two different growth stages in 2004. The exception to this was in Batikot District in Helmand Province where only one image could be used.

In total, only 21 of the 66 images requested could be used (from both UNODC and US sources). Table 4-2 shows this. Numbers underlined in red have been used to indicate sites where collections fell short of the requests.

Table 4-2 - 2004 IKONOS Imagery Collection Received

Province	Site (District)	Requested IKONOS acquisitions	Collected IKONOS	Useable Imagery
Nangahar	Batikot	6	1	1
	Dara-e-Nur	6	**5**	2
	Surkh Rod	6	3	2
	Chapahar	6	**5**	2
Helmand	Nad-e-Ali	6	**5**	2
	Garmser	6	**5**	2
	Washir	6	**6**	2
	Musa Qala	6	2	2
Badakshan	Faizabad	6	**5**	2
	Jurm	6	**5**	2
	Keshem	6	**5**	2
Total		**66**	47	21

Zeiss Aerial Photography

Once photography from the UK's Zeiss survey camera had been captured concerns relating to its release to this study were subsequently raised and several weeks were spent trying to overcome this problem. Eventually, permission was granted but the physical transfer of the Zeiss photography from the point of collection to the UK created an unexpected technical hurdle. In the end authority was granted for the data to be downloaded onto an external hard drive in theatre and self-couriered to the UK - again causing further, unexpected delays.

Disappointingly, only one of the eleven sites was photographed, as shown in Table 4-3, because higher priority tasking took precedence over this study. This photography was captured on two dates in Nad-e-Ali District, Helmand Province approximately six weeks apart from 20,000 feet above ground level, which achieved a 59cm spatial resolution. Numbers underlined in red in the table have been used to indicate sites where collections fell short of the requests.

Table 4-3 – 2004 Zeiss Collection Received

Province	Site (District)	Requested Zeiss acquisitions	Collected Zeiss
Nangahar	Batikot	3 x 3 segments	0
	Dara-e-Nur	3 x 3 segments	0
	Surkh Rod	3 x 3 segments	0
	Chapahar	3 x 3 segments	0
Helmand	Nad-e-Ali	3 x 3 segments	2 x 1
	Garmser	3 x 3 segments	0
	Washir	3 x 3 segments	0
	Musa Qala	3 x 3 segments	0
Badakshan	Faizabad	3 x 3 segments	0
	Jurm	3 x 3 segments	0
	Keshem	3 x 3 segments	0
Total		**99**	2

Ground Data

Although collection of the 2004 UNODC ground data did occur at each of the eleven sites the intention to collect it during the main poppy growing period prior to the poppy harvest was only met in approximately half of the segments (two each in Nangahar and Helmand and one in Badakshan Province). This was again because the harvest took place earlier than had been forecasted. In the remainder of sites data was acquired post-harvest when only residue was visible in the fields – and in some sites this residue was interspersed between summer crops that had just emerged.

Table 4-4 shows the locations of the ground data collected at each 250m by 250m site in 2004. The last column indicates the instances where data was collected prior to the poppy harvest as planned.

Table 4-4 -2004 Ground Survey Date per Segment per District Site

Province	Site (District)	Useable Segment Data	Actual Survey Date	Prior to Poppy Harvest?
Nangahar	Batikot	S1, S2, S3	5-8 Apr 04	Yes
	Dara-e-Nur	C1, S3, S4	1-7 Jun 04	No
	Surkh Rod	C1, S2, S4	9-15 Apr 04	Yes
	Chapahar	S1, S2, S4	19-28 May 04	No
Helmand	Nad-e-Ali	S1, S2, S3	3-4 Apr 04	Yes
	Garmser	C1, S1, S3	12-20 Apr 04	Yes
	Washir	S1, S2, S3	10-12 May 04	No
	Musa Qala	C1,S2, S3	20-21 Apr 04 8 May 04 (C1)	Yes/No
Badakshan	Faizabad	S1, S3, S4	29-30 Jun 04	Yes
	Jurm	S2, S3, S4	10-Jul-04	No
	Keshem	S1, S2, S3	2-4 Jul 04	No

Field Visits

Although field visits were planned to at least one segment per province, security and political implications prevented this. Two social visits were subsequently made to Kabul to meet with UNODC international staff coordinating the surveys to discuss methodology, progress and the realities of field surveying in Afghanistan when poor road surfaces, security constraints and wary farmers were the norm. It was clear, however, that the only viable way to gain an appreciation of the growing conditions and crops being grown in each training area given the security and political constraints imposed was through remotely sensed means, i.e. by acquiring satellite images and aerial photographs.

Although not ideal, regular visits to the commercial poppy fields in the UK also helped in some way towards directly building up a working knowledge of the growth and development cycle of poppy (albeit in the UK). A UK pharmaceuticals agronomist was also available to answer agronomical questions as they arose.

In addition, liaison visits to the UK Foreign and Commonwealth Office (FCO) Drugs and International Crime Department became an excellent opportunity to draw on the extensive experience of the Afghan Drugs Policy and Projects Adviser, whose work is referred to in Chapter 3. The advisor was able to describe his fieldwork experiences in Afghanistan and provide more details on Afghan farming practices. Each visit proved to be invaluable throughout this research.

A site visit to the US Department of Agriculture in Washington DC also provided a useful opportunity to examine individual poppy plants at the early stages of growth collected from a variety of countries. Once again this was not ideal because the plants were out of context but it contributed towards making up for the inability to visit the Afghan poppy fields.

4.3.1 Forecasting Crop Growth Cycles using MODIS Imagery

In view of the poppy harvest having taken place earlier than had been forecasted a more rigorous way had to be determined to predict the rate of crop growth. This was needed for two purposes; to verify the 2004 growth stages and to select images to acquire in 2005 based on more reliable and up to date information. As such, it was subsequently hoped that a technique could be used which was similar to the NDVI profiles generated from digital aerial photography in the PDP's UK field work (described in Chapter 3). The NDVI profiles would be used to predict and monitor the photosynthetic activity of the Afghan crops and determine the general times of crop growth and subsequent poppy harvest.

Security, logistical and cost constraints made it impractical to employ a small aircraft and camera similar to that used in the UK field trials. Instead, efforts were made to utilise a sensor capable of acquiring imagery across a large spread of locations which had a near-daily revisit capability and recorded reflectivity in the NIR and red spectral bands. This was in the hope that NDVI profiles could be generated across Afghanistan so that regional and national cropping activity could be monitored and forecasted. As such, an investigation was initiated into the suitability of using 250m spatial resolution MODIS imagery for crop calendar forecasting.

Concurrently, the PDP were using MODIS imagery to determine its suitability for calculating the total area of agriculture in Afghanistan. The PDP subsequently agreed to provide this study with the tools required to generate averaged MODIS NDVI profiles over segment training areas.

Although the 250m spatial resolution of the MODIS red and NIR bands was insufficient for recording reflectivity from the average 20m by 20m Afghan poppy field it was found that the averaged NDVI value from a 3 x 3 matrix (750m x 750m) centred over

each 250m x 250m segment area was sufficient for indicating the average photosynthetic activity of all crops present in and around each segment training area.

Near-daily MODIS imagery was subsequently downloaded from NASA's online archive and negative NDVI values (which occurred as a result of cloud and haze in the atmosphere) from each dataset were removed using the smoothing algorithm in Erdas Imagine 8.7. An averaged NDVI value for each site was then extracted every three to four days during the 2004 growth cycle using the profiling tool in Erdas Imagine 8.7. This was then plotted onto one graph per segment to create segment NDVI profiles for the 2004 growth season. Profiles from every segment training area in each of the eleven survey sites were subsequently created and updated at regular intervals during the 2004 growth cycle.

A valid secondary objective for this study's MODIS analysis also evolved; by cross-referencing the UN's ground data with the PDP's generalised vegetation NDVI profile (Figure 3-31 in Chapter 3) it was possible to retrospectively confirm the growth stages reached by the crops during each IKONOS image acquisition in the 2004 cycle and verify the growth stage recorded by ground surveyors at each segment training area.

Figure 4-4 shows an example of a MODIS NDVI profile generated from segment S1 in Nade-Ali District, Helmand Province. According to the UN surveyors the fields were visited on 11 April 2004 during poppy flowering. This was confirmed on the segment's NDVI profile which showed that peak NDVI activity took place sometime between 25 March 2004 and 05 May in 2004 (the green line in Figure 4-4), which corresponded to poppy flowering.

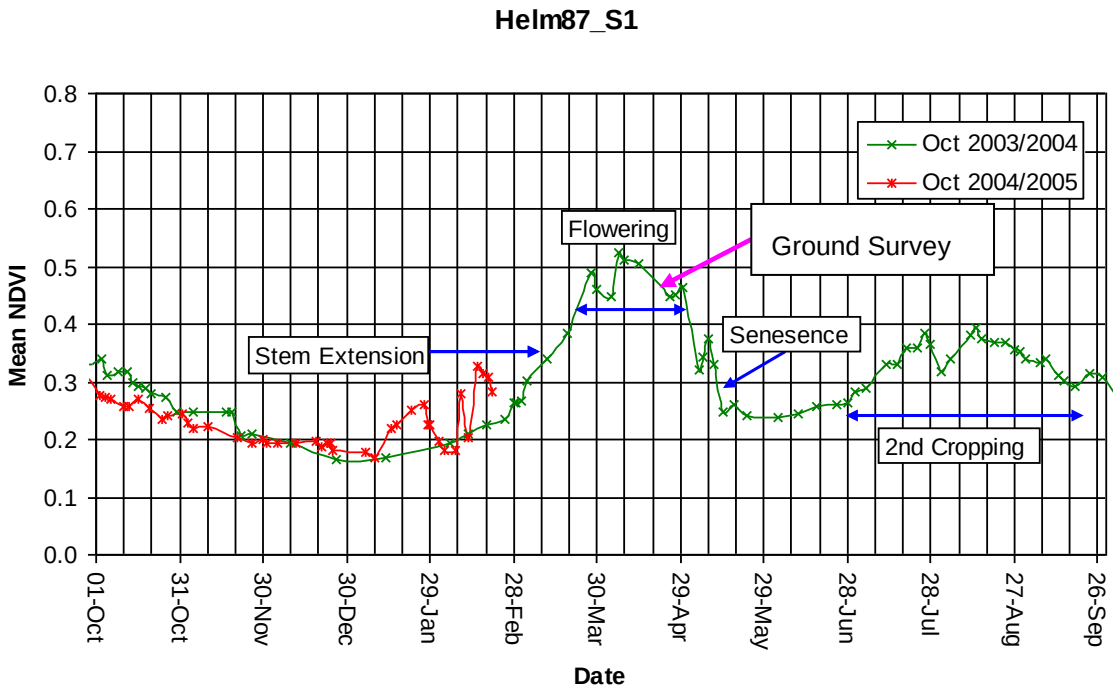

Figure 4-4 – MODIS NDVI profile of Nade-Ali District, Helmand Province. The green line indicates vegetation activity in the 2004 growth cycle; the red line indicates activity at the beginning of the 2005 growth cycle.

After the MODIS profile had been generated from imagery collected at the beginning of the 2005 cycle (the red line in Figure 4-4) it was confirmed that the new cycle had begun approximately at the same time of year as the 2004 cycle. However, the steeper curve and higher mean NDVI values from 20 January 2005 onwards meant that the crops had probably grown at a faster rate than the previous year - or may have resulted from a denser planting scheme being used or because different crops were planted in the fields in 2005 that had different spectral responses to those in 2004.

Of significance was the fact that the profiles could be used to identify the onset of photosynthetic activity at each segment (i.e. the greening up of vegetation) in near-real time. Moreover, the profiles could be used to forecast approximate dates when different growth stages would be reached in each growth cycle. This was invaluable because it meant that imagery collection plans could be submitted to the IKONOS and Zeiss suppliers and updated using current data rather than by relying on the dates of previous year's growth cycles to plan subsequent year's collections. In theory, this meant that image acquisitions could take place at exactly the required growth stages, unlike acquisitions in 2004.

4.4 Data Collection Plan - 2005

In January 2005 the proposed dates for concurrent imagery, aerial photography and ground data collections were submitted using information generated from early 2005 MODIS NDVI profiles from each of the study's segment training areas.

Using Figure 4-4 as an example, crops were forecasted to reach stem extension by the time the 2005 NDVI line had extended to approximately 50% of the predicted maximum NDVI level (50% of maximum biomass), based on the previous year's maximum NDVI value. The flower bud development–early flowering phase was predicted to occur when crops reached approximately 75% of their predicted maximum NDVI level (75% of their maximum biomass). The mid to end flowering stage was forecasted to occur when mean NDVI reached the highest level (100% of maximum biomass).

By using near-real time profiles generated at each segment training area it was possible to assist UNODC with both their imagery collection bid and ground data collection plan and to provide the UK with dates for Zeiss collections. Unfortunately, unlike 2004, the opportunity to acquire IKONOS images from US sources in addition to UNODC's collection of two images per site was not available in 2005. Therefore, only two IKONOS images per site could be used for the 2005 study, the first of each image pair was to be acquired at the flower bud development-early flowering stage (75% of predicted maximum NDVI values to try to capture imagery earlier than the 2004 mid-end flowering) and the second post poppy harvest (after the initial steep decline in NDVI values following the end of flowering).

Acquisition of 2005 ground data was also planned to take place before the poppy harvest at approximately the poppy flowering stage. Collection of 2005 Zeiss photography was again requested to take place three times during the growth cycle. The MODIS profiles were used to determine; when stem extension would occur (at 50% of predicted maximum NDVI level); the flower bud development-early flowering stage (75% of predicted maximum NDVI values) which would be coincident with the first IKONOS image; and post harvest, coincident with the second IKONOS image.

4.4.1 Data Acquired 2005

IKONOS Imagery

Like 2004, actual 2005 IKONOS image collection did not occur within the acquisition windows requested. No reason was given by Space Imaging as to why this occurred. In Nangahar Province collection began later than planned - by three weeks in Dara-e-Nur, Surkh Rod and Batikot Districts and by five weeks in Chapahar District. This delay in Nangahar Province resulted in the first images being acquired at mid-flowering rather than at the flower bud development-early flowering stage as requested. In Helmand Province collection began much earlier than requested, at emergence/stem elongation and not at the flower bud development-early flowering stage. No reason was given by Space Imaging as to why this occurred. In Badakshan Province, collection occurred on time in Faizabad District but was one week late in Keshem District and three weeks late in Jurm District. In all three districts this meant that the first images were acquired at mid-flowering rather than at the flower bud development-early flowering stage as requested. Table 4-5 shows an example of how the first image acquisition dates differed to the acquisition dates requested.

Table 4-5 - 2005 IKONOS Imagery Collection Requested (source: UNODC, 2005) and Received.

Province	Site (District)	Requested 1st Date of Acquisition	Actual Acquisition Date	Growth Stage	Useable Imagery
Nangahar	Batikot	10 Mar 05	31 Mar 05	Mid-Flower	0 Insufficient poppy
	Dara-e-Nur	15 Mar 05	31 Mar 05	Mid-Flower	0 No poppy
	Surkh Rod	10 Mar 05	31 Mar 05	Mid-Flower	0 No poppy
	Chapahar	10 Mar 05	16 Apr 05	Mid-Flower	0 No poppy
Helmand	Nad-e-Ali	15 Mar 05	16 Feb 05	Stem Elongation	2
	Garmser	25 Mar 05	10 Feb 05	Emergence/ Stem Elong	2
	Washir	25 Mar 05	10 Feb 05	Emergence/ Stem Elong	2
	Musa Qala	25 Mar 05	19 Feb 05	Emergence/ Stem Elong	2
Badakshan	Faizabad	07 May 05	11 May 05	Mid-Flower	2
	Jurm	15 May 05	08 Jun 05	Mid-Flower	2
	Keshem	07 May 05	17May05	Mid-Flower	2
Total	22	11			14

Zeiss Aerial Photography

In 2005, two collections of Zeiss photographs were acquired over half of the segment training areas as shown in Table 4-6. In Nangahar Province the first Zeiss photographs were correctly acquired on time at stem elongation/flower bud development in all locations except in Dara-e-Nur District where collection was not achieved at all. The second collection in all but Dara-e-Nur District was acquired at mid-end flowering.

In Nad-e-Ali and Garmser Districts of Helmand Province initial Zeiss photographs were acquired at the requested time but the crops had only reached emergence and not poppy stem elongation as predicted. The second images were acquired at the mid-end of flowering. Photography was not acquired in either Musa Quala or Washir Districts because of higher priority tasking. In Badakshan Province two segment training areas in Faizabad District were captured by the Zeiss camera, both at mid-flowering. Neither of the other districts were photographed.

Table 4-6 – 2005 Zeiss Collection Requested and Received

Province	Site (District)	Requested ZEISS acquisitions	Collected Zeiss
Nangahar	Batikot	3 x 3 segments	6
	Dara-e-Nur	3 x 3 segments	-
	Surkh Rod	3 x 3 segments	6
	Chapahar	3 x 3 segments	6
Helmand	Nad-e-Ali	3 x 3 segments	6
	Garmser	3 x 3 segments	6
	Washir	3 x 3 segments	-
	Musa Qala	3 x 3 segments	-
Badakshan	Faizabad	3 x 3 segments	4
	Jurm	3 x 3 segments	-
	Keshem	3 x 3 segments	-
Total		**99**	**34**

Ground Data

Although security and logistical constraints imposed during the 2005 growth cycle meant that ground surveyors were unable to visit segments in Dara-e-Nur District of Nangahar Province and Musa Quala District of Helmand Province the surveyors were able to visit the remainder of the 11 sites – see Table 4-7. Unlike 2004 when the surveyors found that poppy had already been harvested and removed from fields in half of the segments, this occurred twice in 2005, in Batikot District of Nangahar Province

and Keshem District of Badakshan Province. Logistical constraints were given as the reasons for this (no further details provided).

Table 4-7 - 2005 Ground Survey Date per Segment per District Site

Province	Site (District)	Segment	Actual Survey Date	Prior to Poppy Harvest?
Nangahar	Batikot	S1, S2, S3	20-28 Apr 05	No
	Dara-e-Nur	C1, S3, S4	None	x
	Surkh Rod	C1, S2, S4	10-18 Apr 05	Yes
	Chapahar	S1, S2, S4	3-15 Apr 05	Yes
Helmand	Nad-e-Ali	S1, S2, S3	7-8 Apr 05	Yes
	Garmser	C1, S1, S3	9-10 Apr 05	Yes
	Washir	S1, S2, S3	13-Apr-05	Yes
	Musa Qala	C1,S2, S3	None	x
Badakshan	Faizabad	S1, S3, S4	11-May-05	Yes
	Jurm	S2, S3, S4	25-May-05	Yes
	Keshem	S1, S2, S3	11-Jun-06	No

4.5 Collection Gaps – Revision of Training Sites

After careful cross-checking of all useable 2004 and 2005 IKONOS imagery, Zeiss photography and ground data many data collection gaps were discovered. For example, in Washir District of Helmand Province ground data was not acquired prior to the poppy harvest in 2004 and Zeiss photography was not acquired in either 2004 or 2005.

Similarly, in Dara-e-Nur District of Nangahar Province Zeiss photography was not acquired in either year, the 2004 ground data was acquired after the poppy had been harvested and not acquired at all in 2005. Consequently, this acute lack of ground and Zeiss data made it difficult to discriminate between some of the crops within each segment training area in Dara-e-Nur District. In light of this data inadequacy, it was decided that processing would not continue in this district. However, as some ground and imagery data were of good quality a number were used to supplement a reference database being built up during this study to show the appearance of the crops at different growth stages in Nangahar Province. This database has been included in the manual in Appendix C entitled “Instructions on Field Data Collection in Afghanistan”.

Of the remaining three districts in Nangahar Province detailed cross-referencing of 2005 data revealed that poppy was not grown in many areas in that year (see the last column of Table 4-5). UNODC attributed this to a successful counter-narcotics campaign headed by Afghan President Karzai which made farmers fear very serious retribution if

they were caught growing poppy (UNODC, 2005). Although the lack of poppy fields across Nangahar Province in 2005 meant that there was insufficient data to permit further investigation of the spectral signature of poppy in 2005 it was decided that sufficient data of satisfactory quality existed for processing of the 2004 data to continue in the districts of Batikot, Surkh Rod and Chapahar.

In Badakshan Province ground data was not acquired prior to the poppy harvest in 2004 in either Jurm or Keshem Districts. Some ground data inconsistencies were also found in all three districts in both years. Zeiss photography was not acquired in either year in either Jurm or Keshem District. In view of this lack of adequate ground data and the total absence of Zeiss photography in two of the three districts of Badakshan Province it was decided that there was not enough information available in either year for the crops to be accurately identified. As a consequence, further investigations were not continued in Badakshan Province. The data was consequently forsaken and a substitute province was investigated.

For the substitute to adequately reflect the environmental conditions and agricultural practices of Badakshan Province the agricultural areas in the new province ideally had to be under similarly high altitude and rain-fed conditions to those in Badakshan. Moreover, sufficient image and ground data had to have been collected by UNODC during both 2004 and 2005 in order for the best understanding of the poppy growing conditions to be obtained.

Subsequently, other north-eastern provinces of Afghanistan were investigated and data from Balkh, Khost and Ghor Provinces was examined. Unfortunately, it was discovered that the ground data was inadequate in either or both years, and/or Zeiss photography was not available in either year and/or the IKONOS imagery was obscured by cloud or haze leaving each of the three provinces largely unusable. Other provinces with similar growing conditions to those found in Badakshan were also considered if remote sensing surveys had been conducted by UNODC but were also discarded when it was discovered that there was insufficient image and ground data.

Finally, after extensive examination of the image, ground and air photo archives it was discovered that there was only one other province where sufficiently good quality ground survey, imagery and aerial photographic data had been acquired. Unfortunately,

this data was collected in 2005 only, not both years, and was situated adjacent to the eastern boundary of Helmand Province.

At first Kandahar Province was deemed to be less than ideal because the environmental conditions were similar to those already found in Helmand Province, not the high altitude, rain fed areas of Badakshan. However, it became apparent that Kandahar was the only other province that could be investigated for two reasons; 2005 Zeiss photography existed in three Kandahar districts, and, of the other provinces where remote sensing surveys had been conducted by UNODC, fewer data inadequacies were found. Although its close proximity to Helmand Province meant that environmental conditions would be similar, its lack of large irrigation canals and its greater area given over to fruit and vegetables provided sufficient contrast and justification for poppy cultivation in Kandahar Province to be investigated. As a result, despite no data being available in 2004, Kandahar Province was adopted as the third area of interest. As a consequence, the study of high altitude, rain fed areas was forsaken.

Figure 4-5 shows the location of Kandahar Province, together with the approximate locations of three district study sites in this province. The remaining six other district sites are also indicated, three in Helmand Province and three in Nangahar Province.

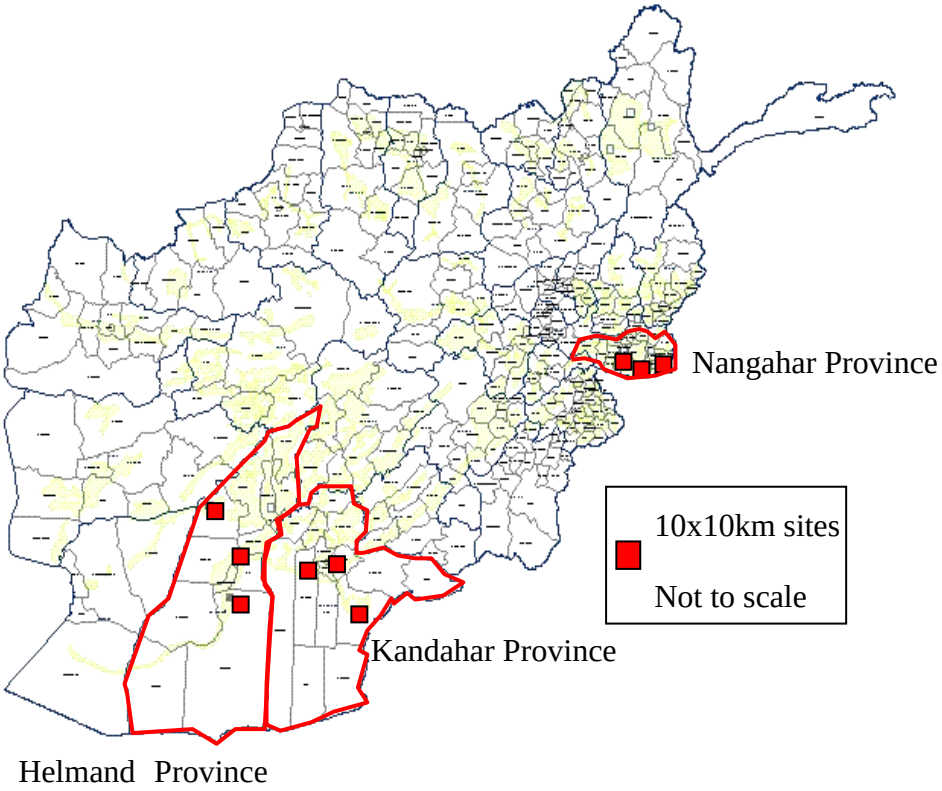

Figure 4-5 – Approximate locations of eventual UK study sites in Afghanistan

Table 4-8 shows a summary of the data collected in Kandahar Province in 2005 which included three IKONOS images, ground survey data from nine segment training areas and six Zeiss photographs.

Table 4-8 – Data collected in Kandahar Province, 2005

Site (District)	IKONOS	Segment Name	Ground Survey Date	Prior to Poppy Harvest?	Zeiss Collections
Daman	26-Mar-05	S2, S3, S4	4-7 Apr 05	Yes	2
Panjawi	26-Mar-05	S1, S2, S4	8-10 Apr 05	Yes	2
Spin Baldak	26-Mar-05	S1, S2, S4	20-Apr-05	Yes	2

4.5.1 Summary of Study Areas

As a consequence of the data collection gaps and inadequacies described, datasets from only nine study sites were used in this research. The fields in the districts of Batikot, Surkh Rod and Chapahar in Nangahar Province; Nad-e-Ali, Garmser and Musa Quala in Helmand Province; and Daman, Panjawi and Spin Baldak in Kandahar Province were subsequently examined. Table 4-9 lists these nine sites and provides the acquisition dates of each of the IKONOS images used in this research per site.

Table 4-9 – IKONOS Images used in 2004 and 2005.

Province	Site (District)	IKONOS 04 #1	IKONOS 04 #2	IKONOS 05 #1	IKONOS 05 #2	IKONOS TOTAL
Nangahar	Batikot	11-Apr-04	x	*	*	**1**
	Surkh Rod	25-Apr-04	17-May-04	*	*	**2**
	Chapahar	11-Apr-04	25-Apr-04	*	*	**2**
Helmand	Nad-e-Ali	25-Apr-04	17-May-04	16-Feb-05	21-Mar-05	**4**
	Garmser	29-Apr-04	17-May-04	10-Feb-05	21-Mar-05	**4**
	Musa Qala	28-Apr-04	20-May-04	19-Feb-05	29-Mar-05	**4**
Kandahar	Daman	*	*	26-Mar-05	x	**1**
	Panjawi	*	*	26-Mar-05	x	**1**
	Spin Baldak	*	*	26-Mar-05	x	**1**
TOTAL		**6**	**5**	**6**	**3**	**20**

x - no image collection
*** - poppy not grown**

4.6 Data Preparation

This next section summarises the pre-processing activities that took place on the ground, image and Zeiss data received. It begins by illustrating a number of common

ground data inconsistencies found, including mis-labelled fields, un-labelled fields and missing field boundaries. It describes how ground photos, IKONOS images and Zeiss photographs were used to correct the errors so that representative pixels from each cover type could be selected. It then describes how pairs of IKONOS images were co-registered to facilitate comparison of different date classifications over the same site.

4.6.1 Identification of Ground Data Errors

Before the datasets could be used the ground data was examined, cross-referenced with imagery/Zeiss photography and then corrected wherever necessary. This cross-referencing was conducted to ensure that sufficient numbers of good quality training and evaluation data could be collected (described in Chapter 5).

Data Capture Pre-harvest

During the course of the examination it was discovered that very few ground data inconsistencies existed in the field data sheets when UN survey data was collected prior to the poppy harvest and/or the ground data had been acquired at/or close to the time when the corresponding IKONOS images were acquired. This concurred with one of the observations made in the literature review outlined in Chapter 1. For example, Figure 4-6 shows one example of field labels overlaid onto imagery acquired during poppy flowering in Nade-Ali District of Helmand Province. Both field boundaries and field labels recorded by UN surveyors were found to be correct - because the image quality was very good and the ground data and imagery were acquired at the same growth stage (poppy flowering) prior to the poppy harvest. The IKONOS image in Figure 4-6 is displayed in true colour, i.e., using a three band combination where RGB = band 3, band 2 and band 1. The spatial resolution of the imagery is 4m. This display is used in subsequent figures.

Figure 4-6 -IKONOS image of Held87 acquired 25 Apr 04 with ground data acquired on 11 Apr 04 overlaid. The image is displayed in true colour, i.e. RGB = bands 3, 2 and 1 at 4m spatial resolution.

In addition, when ground photographs were acquired prior to the poppy harvest in each 250m x 250m segment training area, they proved to be very useful for confirming the crop types recorded by the surveyors. Moreover, the photos were particularly useful when labels had not been assigned to fields or when the crop type was clearly wrong.

Figure 4-7 shows several ground photographs acquired in Surkh Rod District of Nangahar Province. The ground photographs were taken three weeks before IKONOS image capture at a time when the poppy crops were at the mature capsule stage. The photographs showed that while the lower leaves of the poppy crops had begun to senesce some of the onion fields were still in flower. The one alfalfa field appeared to be immature at the time of the ground survey, indicating that this crop had recently been harvested.

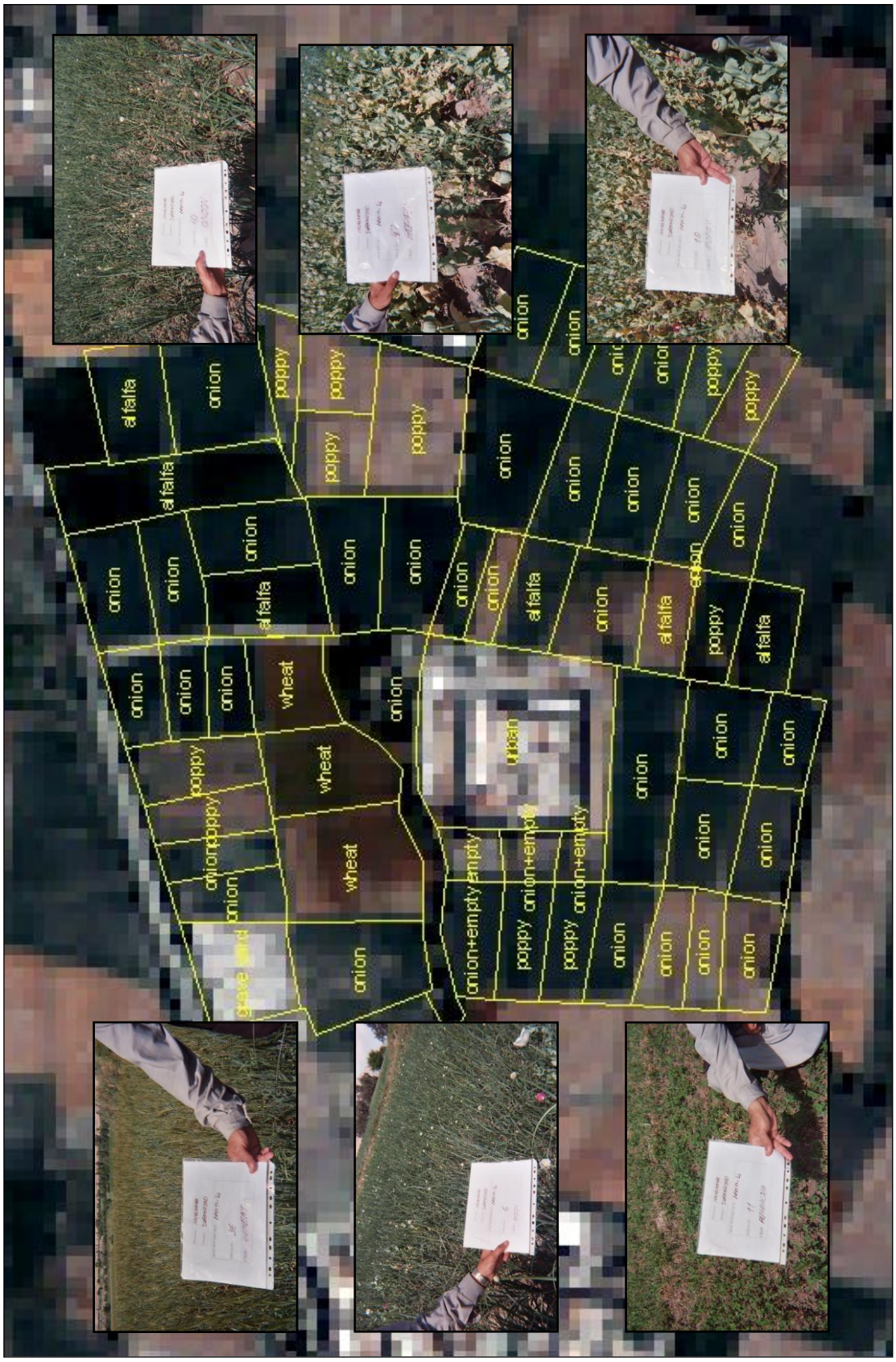

Figure 4-7 - Nan11 S2 IKONOS image acquired on 29 Apr 04 at mid-end flowering with UN ground photographs acquired on 12 Apr 04 overlaid.

Data Capture Post-harvest

When ground survey visits were conducted after the crops had been harvested and sufficient crop residue remained in the fields, surveyors were either able to identify the previous crop or make an educated guess as to what the crops had been. In other cases insufficient residue existed for the crops to be identified because second cropping had already commenced by the time the surveyors visited the fields. Consequently, surveyors either labelled the fields as 'empty', applied guesswork or interviewed farmers so they could assign (sometimes incorrect) field labels.

Figure 4-8 shows examples of crop residue left in fields after the harvest in Dara-e-Nur District, Nangahar Province. Fields were labelled 'wheat' when large numbers of yellow stalks remained or 'empty' if only a few clumps of yellow stalks remained.

The only way that incorrect labels could be identified was if the IKONOS imagery or aerial photography had been acquired prior to harvest and were of sufficient high quality that the crops could be readily identified. If this could not occur the fields were subsequently not used in the training stage of the supervised classification.

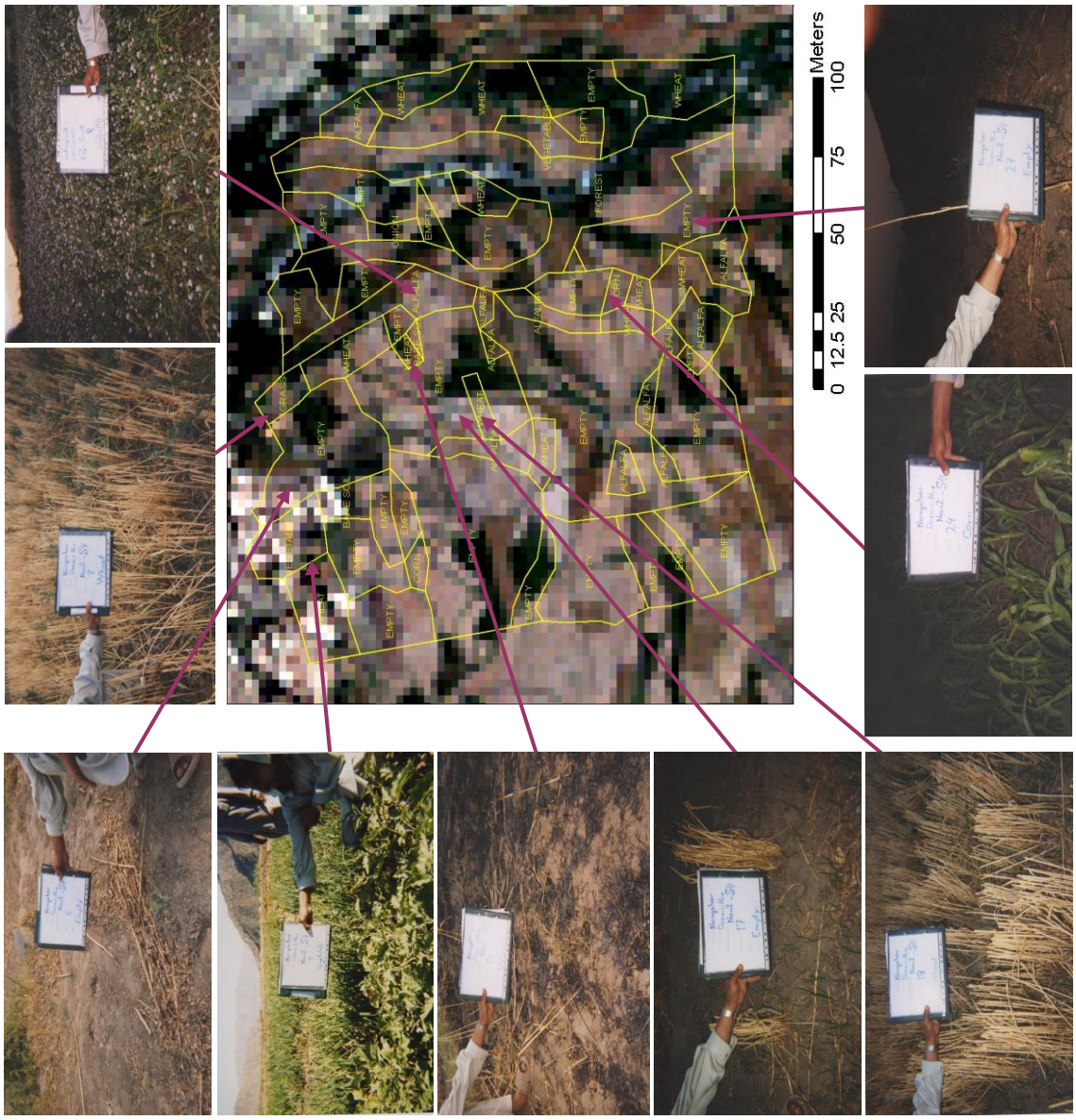

Figure 4-8 - Nan 2_S4 Dara-e-Nur District, Nangahar Province. Ground photographs acquired late in the growth cycle on 07 Jun 04 are overlaid onto an IKONOS image acquired 11 May 04.

Additional Comments on Ground Data Capture

Incorrect field boundaries were found in approximately one quarter of the ground data sheets, and were corrected in all instances using IKONOS as the boundaries were clearly identifiable at all stages in the poppy growth cycle on IKONOS images. Incorrect field boundaries mainly occurred when; security constraints prevented the surveyors from spending sufficient time in the fields which also resulted in some fields

not being labelled at all; farmers had sub-divided or amalgamated fields between ground survey and image capture; or because a careless approach was taken when the boundaries were drawn.

The Joint Research Centre's Monitoring Agriculture with Remote Sensing (MARS) project identified similar errors in their fieldwork when they investigated an operational methodology for carrying out inventories of crop areas with the aid of remote sensing, within selected statistical reporting regions in Europe (Action 1). In particular, the MARS project found incorrect delineation of field parcels with borders between fields being mis-located (Taylor *et al.*, 1997). Problems of mis-classification of cover types were also reported, mainly in non-cropped areas such as fallow and pasture land (Taylor *et al.*, 1997) but overall, the general precision of the ground survey in Action 1 was considered acceptable.

In this research, missing field labels were also found when security constraints prevented the surveyors from conducting a full and detailed assessment or as a result of human error in the data transfer process when the hardcopy data was migrated onto softcopy. Figure 4-9 is an example of segment S4 in Daman District, Kandahar Province and demonstrates the absence of field labels.

Figure 4-9 – IKONOS image from Kand 073_S4, Daman District, Kandahar Province acquired on 26 Mar 05. Field labels are missing from the ground data.

The missing field labels were subsequently discovered and the softcopy corrected after the hardcopy ground data sheets were made available.

Overall, this study found that the ground data collection was generally reliable when the ground surveys took place at or near to the time of image acquisition and both took place prior to the poppy harvest. It also found that errors increased with the time lag between image acquisitions and ground surveys. Errors included missing boundaries, missing labels and incorrect recording of crop type.

The ground photos proved to be an invaluable and additional source of information about how crops appeared at different growth stages, the farming practices used and the condition of the crops.

4.6.2 Development of a UN Field Data Collection Manual

During the course of a visit to UNODC's office in Afghanistan in 2004 and after examination of some of the ground data received it was found that although the surveyors were given verbal instructions on ground surveying techniques by the international staff of UNODC, no formal reference notes were carried into the fields. It was subsequently agreed that the lack of reference material may have contributed to the ground data inconsistencies found. As a result it was established that a manual would be developed during the course of this study to provide the ground surveyors with a standardised set of written instructions on how the:

- Main crops could be recognised in the fields and recorded on the field sheets.
- Growth stage reached by each crop could be recognised and recorded.
- Ground photographs should be acquired.
- Field boundaries should be drawn.

It was hoped that this manual would provide the surveyors with as much assistance as possible to improve the consistency of their ground data collection and documentation. This manual was subsequently developed, agreed and adopted by UNODC international staff and used in the field by UN surveyors from 2005 onwards. This manual entitled "Instructions on Field Data Collection in Afghanistan" has been included in Appendix B.

4.6.3 Identification of Unknown Field Parcels

Using Photographic Interpretation of IKONOS Imagery

In the instances where fields had not been assigned a label because the ground data had been acquired post-harvest, ground photographs were cross-referenced with IKONOS images and crop types were determined through photographic interpretation (PI).

The key recognition elements explored in the fundamentals of photographic interpretation section of Chapter 2 were used to aid the PI. For example, by drawing on experience gained from other segment areas it was possible to determine the identity of the crops in segment S4 of Daman District, Kandahar Province in Figure 4-9. Labels were subsequently assigned to the dark green fields (wheat) and the grey-green fields (mixtures of bare soil and non-agricultural vegetation, i.e. weeds) in Figure 4-10.

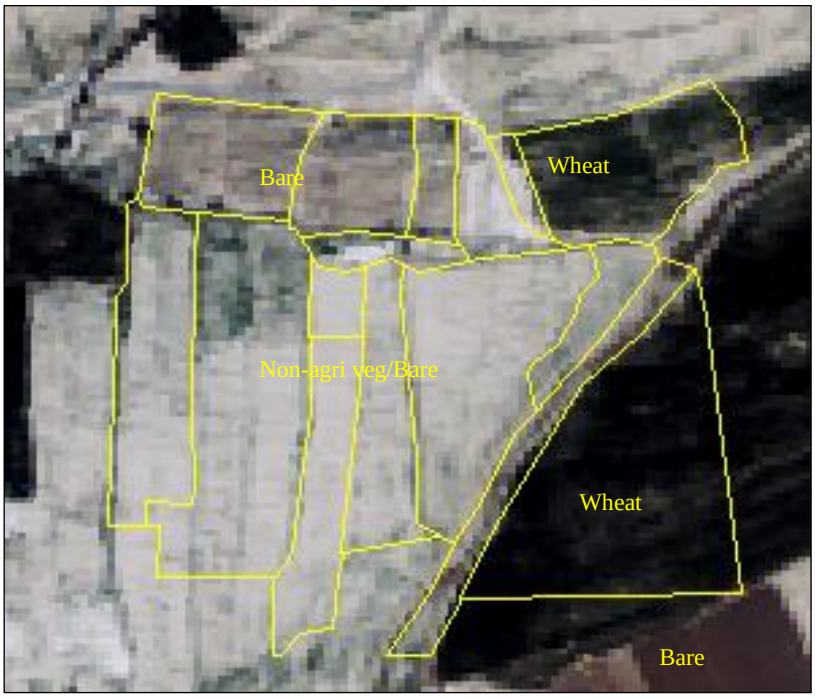

Figure 4-10 - IKONOS image from Kand 073_S4, Daman District, Kandahar Province acquired on 26 Mar 05. Field labels have been photo-interpreted.

Although it was not immediately apparent what the crop type in the dark brown fields were, an examination of a false colour composite (FCC) showing NIR, red and green reflectivity revealed that no crops were present in these fields at the time of imaging because NIR returns were not found on the imagery. These darker brown fields were subsequently identified to be ploughed fields of bare soil that had a higher degree of

moisture content than the paler brown fields, probably as a result of being newly ploughed.

Using Photographic Interpretation of Zeiss Aerial Photography

The Zeiss photography also proved useful for verifying the ground data and for identifying unknown fields. This was because its 60cm spatial resolution allowed examination of different crop textures, brought on by different phenological characteristics and/or farming practices. For example, the Zeiss photography in Figure 4-11 of segment S1 in Nad-e-Ali District, Helmand Province reveals wide cross-field rows of bare soil interspersed with much narrower along-field soil rows. These textures were in direct contrast to the very densely planted wheat fields where along-rows were also visible but to a much smaller extent. The Zeiss photography is displayed in true colour (RGB = 3, 2 and 1) at a resolution of approximately 60cm acquired from 20,000ft. This display is used in subsequent figures.

Figure 4-11 – Held87_S1 Nade-Ali District, Helmand Province. True colour Zeiss photography acquired on 17 Apr 04 from 20,000' at 60cm resolution.

In contrast to the Zeiss photograph the corresponding IKONOS image is shown in Figure 4-12, acquired 8 days later on 25 Apr 04. Along-field rows are not visible in this IKONOS image – and this is due to the poorer resolving power of the IKONOS sensor (4m) rather than the increase in biomass expected after 8 days of growth. The Zeiss

photographs were therefore invaluable in the identification of ground data inconsistencies and for determining unknown field labels.

Figure 4-12 - Held87_S1 Nade-Ali District, Helmand Province IKONOS imagery acquired on 25 Apr 04. True colour photography (3, 2, 1) at 4m resolution

Using the Higher Resolution IKONOS Panchromatic Band

In instances where it was impossible to identify an unknown field parcel from ground photographs or IKONOS imagery and no Zeiss photography had been acquired, pan-sharpening was used to create a high resolution colour image to aid in the PI. This pan-sharpening technique could only be used when panchromatic IKONOS imagery had also requested by UNODC and had been acquired at the same time as the multi-spectral IKONOS bands.

Although the IKONOS panchromatic band covers the same geographical area as the 4m blue, green, red and NIR sensors it does so at a higher spatial resolution (1m) because it is able to collect reflected energy across a wider spectral range than the multi-spectral sensors, from the blue, green, red and across to longer NIR wavelengths. By using the pan-sharpening technique available in the spatial enhancement section of the image interpreter tool in Erdas Imagine version 8.7, the four 4m multi-spectral IKONOS bands were combined with the 1m panchromatic band to create a new higher resolution image. This meant that the spectral integrity of the original multi-spectral data was preserved but additional spatial information from the panchromatic band was added. It therefore allowed for better visualisation and easier interpretation.

A number of different methods and resampling techniques were available in Erdas Imagine 8.7 to enable pan-sharpening. Each were investigated in terms of trade-offs in processing time and results. The three resampling techniques methods investigated were Nearest Neighbour, Bilinear Interpolation and Cubic Interpolation. The quickest resampling method was the Nearest Neighbour which assigned the DN of the closest pixel in the original image to the 'corrected' pixel value in the output image, but which resulted in images with a 'stepped' appearance. The next quickest method was bilinear interpolation which generated images with a smoother appearance than the nearest neighbour. However, based on visual inspection of the output of each resampling technique, the best results were produced from the cubic interpolation method as linear features appeared sharper than in the other two – which was ideal for photo-interpretation. Therefore, the cubic interpolation resampling technique was used in this research.

Figure 4-13 shows an example of a panchromatic image taken from the same segment in Nade-Ali District, Helmand Province previously shown in Figure 4-12.

Figure 4-13 Held87_S1 Nade-Ali District, Helmand Province. 1m resolution Panchromatic IKONOS image, 25 Apr 04

When the corresponding multi-spectral sub-set was merged with this panchromatic image the pan-sharpened image product shown in Figure 4-14a resulted. Whilst the colours of the new pan-sharpened image product remained similar to the original multi-spectral image the addition of textural information permitted more detail to be visible in

the fields. This was particularly noticeable in the poppy fields where, similar to that found in the Zeiss photography, both across- and along- field rows of bare soil were visible.

(a)

(b)

Figure 4-14 - Held87_S1 Nade-Ali District, Helmand Province. (a) Pan-sharpened IKONOS image, 25 Apr 2004 (b) un-sharpened true-colour IKONOS image.

Unfortunately, the large amount of time required to pan-sharpen a whole IKONOS image (upwards of two hours) and the file space required for the new higher resolution

image (upwards of 1.5G) meant that it was only possible to use this method in instances where a large number of crops were unknown in ground segments rather than for every image. In these instances small areas of interest were sub-set from the original multi-spectral and panchromatic images and pan-sharpening then applied so that the file sizes and processing time was reduced.

The pan-sharpening technique was subsequently used to identify unknown field parcels in all areas that had not been captured by Zeiss photography or ground photographs where panchromatic imagery had been acquired and proved to be a very useful tool for verifying the survey data.

4.6.4 Surrogate Ground Data

The previous section has demonstrated how PI of Zeiss and pan-sharpened IKONOS images was used to identify mis-labelled and un-labelled fields in the segment training areas. In addition to this, PI techniques were also used on images and aerial photographs acquired in other areas where ground surveyors had not been tasked. The remote sensing data was therefore used as a surrogate for actual ground data collected in the field.

After ad-hoc cross-checks had been performed by PDP analysts to validate the PI results this study found that Zeiss and modified-pan-sharpened IKONOS images were suitable surrogates for ground data. Chapter 5 explains how this surrogate ground data was used in the areas where ground survey data had not been collected.

4.6.5 IKONOS image-to-image Registration

Prior to conducting the first stage of image classification (training), images were examined for geometric distortions. An initial examination of image pairs revealed horizontal displacements in the range of 10-50m. These displacements were expected due to inherent errors in the standard processing of the images by the vendor Space Imaging and from non-systematic distortions of the individual images. In either case, the distortions were found to preclude the direct overlay of the multi-temporal image datasets, necessary to ensure that classification results could be compared from the same site over sequential image dates.

Unfortunately, the only available mapping of Afghanistan was Russian 1:1,000,000 maps last updated in the 1970's which had very few obvious roads, rivers and towns. It was therefore not possible to rectify both images in each image pair to a map projection (a standard image-to-map rectification), where each pixel in an image is assigned a unique *x, y* coordinate in a map projection (Jensen, 2005). Instead, image-image registration was performed (a translation and rotation alignment process) which ensured that IKONOS image pairs were positioned coincident with respect to one another so that corresponding elements of the same ground area appeared in the same place on the registered images (Jensen, 2005). The first IKONOS image acquired at each site was used as the reference image.

Thirty ground control points (GCPs) were located on each reference image and the same 30 GCPs were then identified on the corresponding image. GCPs were located uniformly throughout each image, usually at the intersections of two well-trodden paths, or at an intersection between a path and bridge, at the corners of buildings, or occasionally on individual trees where no obvious man-made features were to be found. Care was taken to ensure that chosen GCPs locations did not alter position in time (Gibson and Power, 2000). Data were transformed using first-order polynomials and a nearest neighbour resampling algorithm was used to avoid modification of radiometric values. Root mean square (RMS) values associated with each registration were less than one pixel which ensured that pixel grids coincided to within an acceptable level (one 4m IKONOS pixel).

Overall, image registration was successful (to within one pixel) at all sites in Helmand Province because the sites were flat and the sensor look angle for each image was very similar. However, problems were encountered when the geometric corrections were applied to the Nangahar Province images. These problems were due to a combination of different sensor look angles and large height differences occurring across relatively short distances in a few of the agricultural areas located along the bottom of steep river valleys. Both factors contributed to displacement between successive images. As a result ortho-rectification was investigated which would reduce the image displacement but the difficulties in acquiring accurate digital elevation models for all areas at the time meant that the ortho-rectification procedure could not be adopted.

Consequently, it was decided the best way to geo-rectify the Nangahar images was to focus the reference points on the flatter agriculture areas along the river floodplains and on the areas around the 250m segment training areas. This was to ensure that the pixel grids would match in the localised areas where training and evaluation pixels were collected, but at the expense of pixels accurately overlapping in the remaining areas.

4.6.6 Multi-temporal Image Datasets

An investigation into multi-temporal image classification was also to be investigated in this study to identify whether their use increased classification accuracy over successive single date image classifications, as per Objective 4 and reported for example by Turner and Congalton, (1998); and Key *et al.*, (2001). As such, commonly used multi-date image stacks were prepared (Key *et al.*, 2001) prior to the multi-date classifications being performed.

Each pair of registered images acquired at the same site on two dates from the same growth cycle were combined into single 2-date image stacks using the layerstack tool in the utilities menu of Erdas Imagine. This resulted in an 8-band image product (two dates by four bands) for each site during each growth cycle imaged. The image stacks were then classified using the same methods defined for the single-date classifications in Chapter 5.

4.7 Chapter Summary

This section provides a summary of the points raised in this chapter concerning the acquisition of data in an operational theatre.

A large number of good quality consecutive IKONOS images, Zeiss aerial photographs and ground data were collected at different growth stages during the 2003-2004 and 2004-2005 growth cycles in Afghanistan.

Difficulties were encountered in planning, co-ordinating and acquiring ground data, aerial photography and imagery from UN, US and UK sources against specific timetables over the two year period. For example, imagery was collected later than requested in 2004 and earlier than requested in 2005 due to a number of factors including; security and possible weather constraints, competition from higher priority tasking authorities for each asset, internal supplier misunderstandings and technical

problems. Acquisition of IKONOS, Zeiss and ground data in an operational theatre meant that concerns relating to their classification and provision were also encountered. Significant delays were subsequently experienced whilst these issues were discussed. Permissions were finally granted for the Zeiss photography to be used as unclassified material, and both the IKONOS imagery from US sources and UN ground data to be used in this study only. In future studies permissions should be sought well in advance of data collection to prevent further problems and delays.

IKONOS images from both the UN and US in 2004 were delivered late and consequently significantly delayed the start of planned image processing. For example, the 2004 IKONOS imagery provided by UNODC was received between two and four months late and the Badakshan imagery up to six months late. The US imagery was also received up to six months behind schedule in 2004. Again, policies and procedures should be worked out well in advance of data collection taking place to ensure timely delivery of imagery.

Of the 47 IKONOS images received from UN and US sources in 2004; only 21 images were subsequently used. This was because several images were duplications, several were obscured by cloud or haze and two were taken from districts that were subsequently not studied because of lack of ground data.

Higher priority tasking significantly impacted the acquisition of Zeiss photography, particularly in 2004, where only two of the planned 99 photographs were acquired in 2004, and only thirty-four aerial photographs were acquired in 2005.

Approximately two-thirds of the ground data contained little or no error, particularly when the ground surveys had taken place at or near to the time of image acquisitions and both image and ground data capture had taken place prior to the poppy harvest. Representative samples of good, poor and very poor ground data were shown in Figure 4-6 to Figure 4-9. However, the larger the time lag between image acquisitions and ground surveys the greater the number of errors recorded in the form of missing field boundaries, missing labels or incorrect crop type. Inconsistencies in the ground data were removed after careful cross-referencing with corresponding IKONOS imagery, and Zeiss and ground photographs.

By 2005, the collection and receipt of data significantly improved due to continuity, precedent and good working relationships being established.

A novel use of low resolution MODIS NDVI data was formally reported for the first time. By mapping and monitoring average photosynthetic activity in and around each segment training area, the following activities occurred:

- Retrospective identification of 2004 crop growth stages.
- Verification of 2004 growth stages recorded by UN surveyors.
- Identification of 2005 photosynthetic activity onset at each segment in near-real time.
- Forecasting of approximate growth stages in 2005.
- Submission of 2005 image collection plans with predictive updates using current data.

Zeiss photography and modified-pan-sharpened IKONOS images were useful for verifying ground data, identifying crops in unlabelled field parcels and as suitable surrogates for ground data in areas where such data was not acquired.

Horizontal displacements of between ten and fifty metres were found in successive IKONOS image acquisitions. Image-to-image registration of each coincident image pair was performed to reduce these displacements to within one 4m IKONOS pixel.

After careful examination of all available data and after necessary ground data corrections and imagery pre-processing techniques had been applied, Chapter 5 describes the methodology used to select suitable training and evaluation data from fields identified from both the corrected ground survey data and surrogate ground data, as described in this chapter. Datasets from nine districts in Helmand, Nangahar and Kandahar Provinces were used.

5. Selection of Training and Evaluation Pixels

Seven of the ten surveys outlined in the Literature Review in Chapter 1 used digital image classification methods to identify poppy in Thailand, India and Afghanistan. Analysis of these studies identified several remote sensing limitations, some of which were addressed wholly or in part in previous chapters, namely; the determination of an appropriate method to identify the optimum time for image acquisition (Chapter 4); the collection of suitable ground and image data (Chapter 4), and the need for high spatial resolution imagery (i.e. 4m IKONOS) to discern small poppy fields (Chapter 4).

This chapter introduces a method that was developed to overcome another potential limitation of remote sensing surveys which was outlined in Chapter 2 - the introduction of errors in training and evaluation data which could result in misleading classification results. Chapter 2 described how potential error could be minimised in training and evaluation data if they were independent, representative, free from the effects of spatial autocorrelation or spectral mixing and selected using optimum sampling parameters (Congalton, 1991).

Chapter 2 also described the choice of classification approach used in this study, the traditional Maximum Likelihood Classifier (MLC) on practical and logistic grounds, because of the end-user's requirements for easy to use, already available software which did not require an extended training process, and where analyst training could be easily and rapidly transferred to analysts operationally employed in Afghanistan. Moreover, although some of the alternative approaches outlined in Chapter 2 were reported to yield higher accuracies, the choice of the MLC was supported by the fact that it remains an effective method for classifying individual land cover types (Wang et al., 2004).

In keeping with the assumptions of the MLC, the aim of this chapter is to develop a methodology that enabled suitable training data to be selected so that high classification accuracies could be achieved. As such, this chapter describes how independent training and evaluation pixels were selected from pure cover types in sufficient numbers to minimise the impact of any source of bias. The first investigation concentrates on limiting the amount of spatial autocorrelation and the second deals with the identification of mixed pixels. The third section outlines how the training and evaluation data selected in this study were examined for spectral separability.

5.1 Investigation into Spatial Autocorrelation

The methodology employed by UNODC and many others to collect training data makes use of polygons drawn around the boundaries of homogenous cover types to collect all pixels contained within. Chapter 2 argued that whilst this method is simple to use and quick to employ, the collection of groups of contiguous training pixels would not satisfy one of the assumptions of the MLC - that these pixels are independent observations (i.e. non-spatially autocorrelated). The accuracy of the MLC would therefore be affected if non-independent pixels were used because the data values collected would not be truly representative of the cover type being mapped.

The objective of this section, therefore, was to determine the minimum distance required between IKONOS training and evaluation pixels to ensure that the data was free of spatial autocorrelation (i.e. independent; where none of the training and evaluation pixel digital number values (DNs) were influenced by the DN values of other pixels). This examination was conducted using a geo-statistical tool known as a variogram, first described in Chapter 2, to determine how far apart samples need to be spaced to make them spatially independent of one another. This distance is commonly referred to as the range, and is the separation between sample points at which covariance between samples becomes zero. If samples (i.e. 4m IKONOS pixels) are spaced at a distance greater than the range, then adjacent samples are no longer correlated and will be independent. For sample spacing's less than the range, adjacent measurements will be correlated to one another.

The range obtained from the variogram was used to decide upon an appropriate spacing between training and evaluation pixels. Figure 5-1 shows the distance in metres (x axis) against IKONOS pixel proportional semi-variance (y axis) and the range.

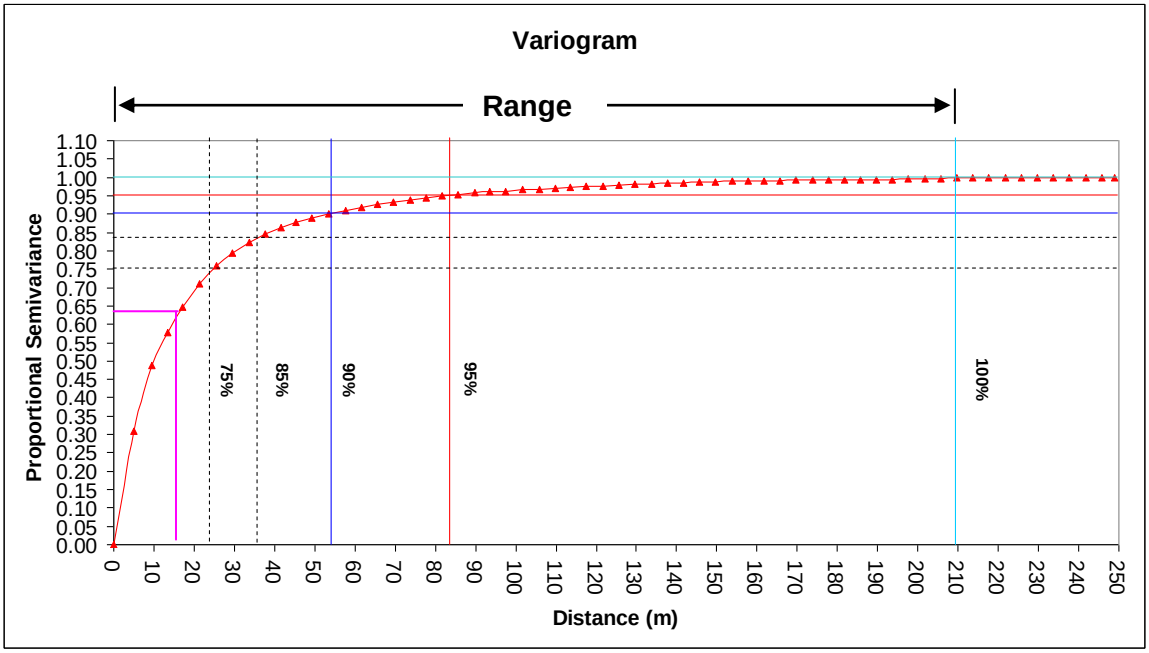

Figure 5-1- Variogram illustrating the effects of spatial autocorrelation on IKONOS pixels, after PDP, 2005. Light blue–100% independence, red–95%, navy blue-90%, black dots, 85% and 75%, pink line 62%.

As anticipated, a positive correlation was found, that as distances between pixels increased, pixel independence also increased. The red curve on the variogram in Figure 5-1 shows this relationship.

At a range of 210m (light blue line) a proportional semi-variance of 100% was found. This meant that a spacing of 210m between IKONOS training pixels would ensure that the training data would be free of spatial autocorrelation. This equated to a sampling rate of 1 pixel in every 52.5 pixels being selected for training.

For this Afghan poppy study, a simple test with this sampling rate revealed that fewer than 25 pixels would be selected to become training or evaluation pixels in each of the 250m x 250m segment training areas identified in Chapter 4. Unfortunately, this rate would result in insufficient numbers of training data being gathered using the universally accepted guidelines set by Richards and Jia (1999), Lillesand and Kiefer (2000), and Swain and Davis (1978), that 40 training pixels per spectral class should be collected (for IKONOS imagery).

Instead a compromise between pixel independence and sample size had to be found. Table 5-1 summarises other sampling rates that could be achieved with different levels of proportional semi-variance, calculated from Figure 5-1.

Table 5-1 – Comparison of Proportional Semi-variance against sampling rate achieved.

Proportional Semi-Variance (%)	Distance Between Pixels (m)	Sampling Rate	No. of samples possible in a 250m^2 segment
100	210	1 in 53	2
95	84	1 in 21	9
90	54	1 in 14	21
85	36	1 in 9	49
75	24	1 in 6	108
62	16	1 in 4	243

In order to achieve a proportional semi-variance of 90% (dark blue lines in Figure 5-1) 1 in 14 pixels would have to be selected. Whilst this was deemed an acceptable level of independence it was found that the maximum number of pixels which could be selected for training or evaluation in a 250m by 250m segment (21) was too few. Similarly, a pixel spacing of 36m (85% proportional semi-variance) still meant that too few pixels would be selected (49).

In order to achieve an acceptable compromise between pixel independence and number of pixels a distance of 24m between pixels was chosen. With 75% proportional semi-variance, up to 108 pixels could be selected – and this sampling rate of one in every six pixels was deemed to be acceptable.

A test was subsequently conducted on a small number of training areas in Helmand Province to determine whether an appropriate number of training pixels would be collected with this sampling rate. To do so, a dot grid matrix was created using Erdas Imagine 8.7's Dot Grid Matrix tool selected from its Frame Sampling menu to create a 250m by 250m grid from which single-point (and relatively) non-spatially autocorrelated training pixels could be selected. Figure 5-2 shows a 250m by 250m subset of an IKONOS image acquired over Segment 2 of the Nad-e-Ali District segment training area in Helmand Province (Held87 S2) acquired on 25 April 2004. Four cover types were recorded by the ground surveyors - poppy, wheat, house and bare soil.

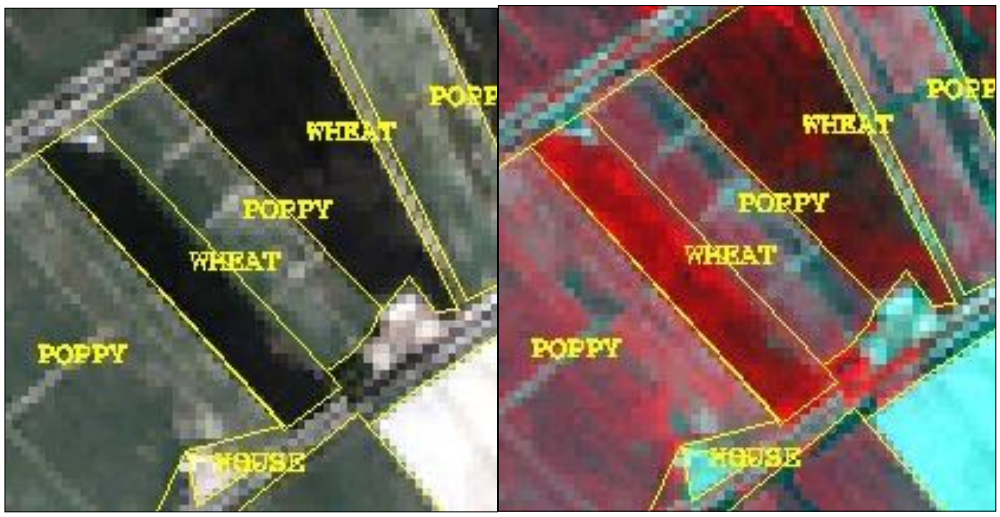

Figure 5-2 - True colour (bands 3, 2,1) and false colour (bands 4, 3, 2) composites of a 4m IKONOS image acquired on 25 Apr 04 showing the 250m x 250m Held87 S2 segment training area.

Figure 5-3 shows the corresponding dot grid created for Held87 S2 overlaid onto the FCC of the area. The grid matrix was used to select one in every sixth pixel (enclosed within white circles) across the entire 250m by 250m segment training area. A spacing of 24m between the centres of each selected pixel was achieved.

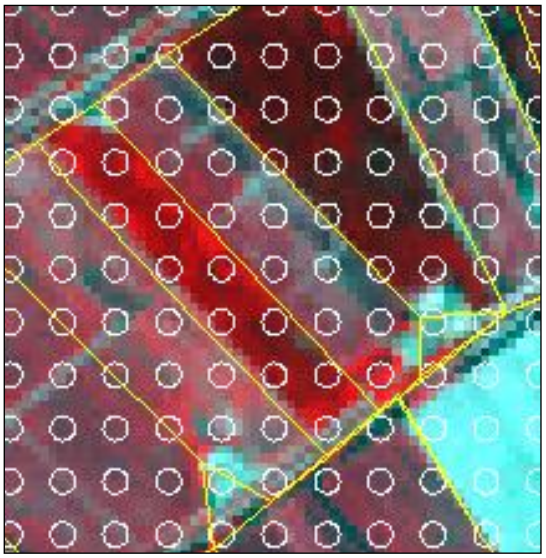

Figure 5-3 – FCC of a 4m IKONOS image of Held87 S2 25 Apr 04 with dot grid overlaid. 1 in 6 pixels selected by the dot grid matrix are enclosed within white circles giving a spacing of 24m between the centres of each selected pixel.

From this dot grid matrix, pixels were then assigned to their respective classes according to the cover types recorded.

Figure 5-4 shows all of the pixels initially selected to represent the poppy class. In this example, boundary pixels between poppy and obvious linear soil bunds had not yet been removed, although these were subsequently removed using the method described in Section 5.2.1.

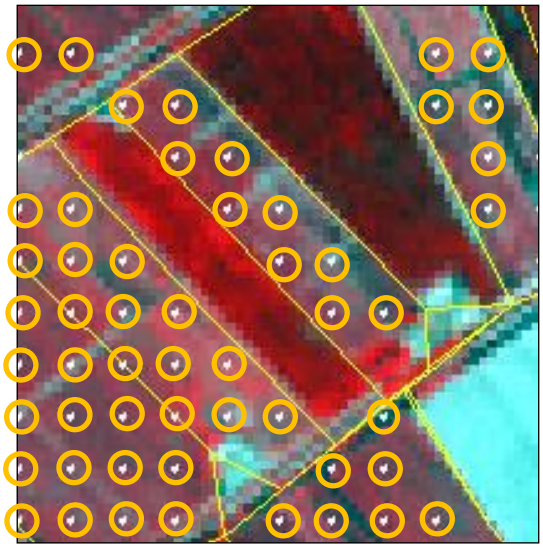

Figure 5-4 – FCC of a 4m IKONOS image of Held87 S2 25 Apr 04 with overlaid training and evaluation poppy pixels spaced 24m apart

Using the selected poppy pixels from Figure 5-4 as an example, each pixel was then assigned to either a poppy training class or an evaluation class, depending on whether it had been allocated an even-number in Erdas Imagine's vector attribute editor (training pixel) or an odd number (evaluation pixel). Once assigned, although a sampling rate of 1 in 6 was used with a distance of 24m spacing between each selected poppy pixel, the selected even numbered pixels in the training file were actually spaced 48m apart, as were evaluation pixels. This meant that a proportional semi-variance of between 85% and 90% was achieved. In total, 24 out of 53 poppy pixels were selected for training as illustrated in Figure 5-5, once boundary pixels had been removed.

It was anticipated that resultant even-numbered pixels (poppy training pixels) would be selected in a regular pattern (i.e. equally distributed in the x and y axes) but this did not occur in the example shown in Figure 5-5, perhaps due to an error in the vector attribute editor.

This process was used for every cover type in Nade-Ali District and then repeated across the two remaining segment training areas. The training pixels from the three segments were then amalgamated into one file for Nad-e-Ali district and the total

numbers of training pixels per cover type were determined to ensure that the minimum number of training pixels had been collected. The process was then repeated for Garmser District of Helmand Province (Held115).

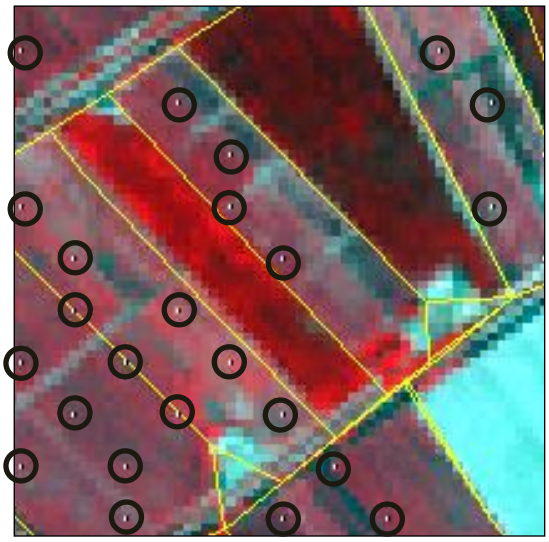

Figure 5-5 - FCC 4m IKONOS sub-set of Held87 S2 25 Apr 04 with poppy evaluation pixels overlaid

Results from Held87 in Table 5-2 show that the minimum number of training pixels (40) was met in all cover types except house and water. This meant that if the training pixels selected in Held87 were used in the MLC a small amount of undesirable classification bias would occur, where the house and water classes would be underestimated whilst poppy, wheat and bare would be overestimated.

Table 5-2 – Number of training pixels collected per cover type in Nade-Ali (Held87) and Garmser (Held115) Districts, Helmand Province.

Dot Grid		District	Date	Poppy	Wheat	Alfalfa	Vine	Bare	House	Water
Size	Selection									
250m	1 in 6	Held87	25-Apr-04	151	135	0	0	54	2	13
250m	1 in 6	Held115		26	59	5	12	75	6	5

Table 5-2 also illustrates the results from Garmser District and shows that the minimum number of training pixels required was not met in the poppy, alfalfa, vineyard, house and water classes.

This second test revealed that too many classes were represented by insufficient numbers of training pixels when the one in six sampling rate was used.

In addition, it was found that in areas strongly affected by drought or disease, where more bare soil was visible than the ailing crops themselves (as identified on ground photography and by PI of Zeiss and modified-pan-sharpened IKONOS imagery) the selection of 'pure' crop pixels was more difficult. This resulted in smaller numbers of training pixels being collected from the crops in these areas than had been selected from the healthy crops in Nade-Ali and Garmser Districts of Helmand Province.

It was subsequently decided that instead of reducing the pixel spacing further, which would increase the effects of spatial autocorrelation, the size of the training areas used to select training pixels should be increased to 1000m x 1000m. This would effectively increase the size of the training samples whilst keeping the effects of spatial autocorrelation to within an acceptable level.

5.2 Revised Experimental Methodology – Training Area Expansion

Figure 5-6 illustrates, using Held87 S2 as an example, the revised size of the segment training areas (1000m by 1000m) expanded from the original 250m x 250m segment area (yellow squares). The white crosses highlight locations of poppy evaluation pixels on imagery dated 17 May 04.

One consequence of this expansion in training area size was the new requirement for additional ground data to be available to assist in training and evaluation pixel selection throughout the 1000m by 1000m areas. This was because the ground data that had been acquired by the UN surveyors now only covered a small part of each new training area. This requirement was met by photo-interpreting (PI) all available modified-pan-sharpened IKONOS images and Zeiss aerial photographs, in addition to the ground data already available within each expanded area. This meant that the photography and imagery were used as surrogates for ground data, as described in Chapter 4.

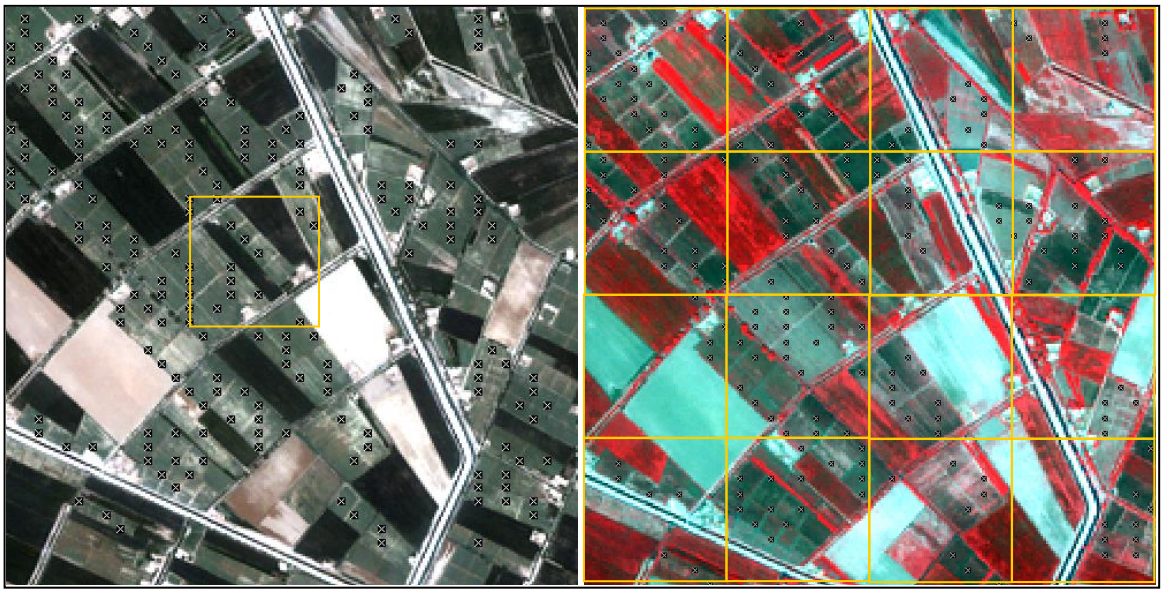

Figure 5-6 – True and False Colour Composites of 17 May 04 IKONOS imagery showing the original Held87 S2 250m by 250m segment training area on true colour imagery (yellow square) - and the expanded 1000m by 1000m training area on false colour imagery.

Once all training and evaluation pixel data had been acquired using the dot grid matrix to select one in six pixels in the newly expanded segment areas, the data was then amalgamated into a Helmand District dataset. The numbers of training pixels were counted and then compared to the previous dot grid iteration in order to determine whether the enlarged training areas enabled sufficient numbers of training and evaluation pixels to be selected.

The results are displayed in Table 5-3 and show that the expansion of the training areas resulted in acceptable numbers of training pixels being selected in Held87 in all but alfalfa and water.

Table 5-3 – Comparison of the number of training pixels selected in Held87 in the new and old training areas

Dot Grid		District	Date	Poppy	Wheat	Alfalfa	Bare	House	Water
Size	Selection								
250m	1 in 6	Held87	25-Apr-04	151	135	0	54	2	13
1000m	1 in 6	Held87	25-Apr-04	375	407	33	225	72	15

5.2.1 Identification and Removal of Mixed Pixels

Sections 5.1 and 5.2 demonstrated how a variogram was used to select training and evaluation data that were independent and free from the effects of spatial

autocorrelation (as far as possible) and were representative of all cover types present in the expanded study areas. This section deals with another factor reported in Chapter 2 which potentially introduces errors in the training and evaluation data – the presence of mixed pixels (Congalton, 1991).

The Literature Review reported several poppy studies where training signatures were derived from heterogeneous mixtures of vegetation (i.e. Chuinsiri *et al.*, 1997; Spot Image, 2000a) and resulted in training classes that were characterised with varying degrees of internal spectral variability. For example, UNODC reported that Afghan poppy crops exhibited a high degree of spectral variability on SPOT 5 imagery due to different growth stages being imaged and different agro-climates and topographic conditions (UNODC, 2005b). This problem resulted in the generation of poor quality training signatures from SPOT 5 data.

In this study the training and evaluation pixels collected for each class using the dot grid matrix were carefully re-examined to ensure that they correctly belonged to the class of interest and contained only data values from single cover types, and not mixtures of different cover types. To do so the training data was overlaid onto two colour composites viewed simultaneously side by side in full resolution windows for each segment training area. Both a true-colour composite using bands 3, 2, 1 (RGB) and a false-colour composite (FCC) using IKONOS bands 4, 3, 2 (RGB) were used.

The yellow dots in Figure 5-7 are taken from an enlargement of Held87 S2 (Nad-e-Ali District, Segment 2) and highlights pixels selected to become either poppy training or evaluation pixels. Two boundary pixels contained within yellow circles are located between a field of poppies (red-pink tones) and a strip of soil running along the side of the field (represented by light-blue tones). These highlighted pixels were subsequently removed from the poppy file so that the accuracy of the subsequent supervised classification would not be influenced by the selection of boundary pixels.

Figure 5-7 - Mixed soil/poppy pixels highlighted in a FCC subset of a 4m IKONOS image from Held87 S2 25 Apr 04

A second example from Held87 S2 highlights mixed pixels on wheat field boundaries in Figure 5-8. Four pixels are enclosed within yellow ovals, sitting on the border between wheat on one side (bright red) and poppy (pink) on the other. As their spectral responses would contain mixtures of both wheat and the adjacent poppy spectral signatures these mixed pixels were subsequently manually removed from the wheat training dataset. On average, between 5 and 10% of pixels were removed in each district.

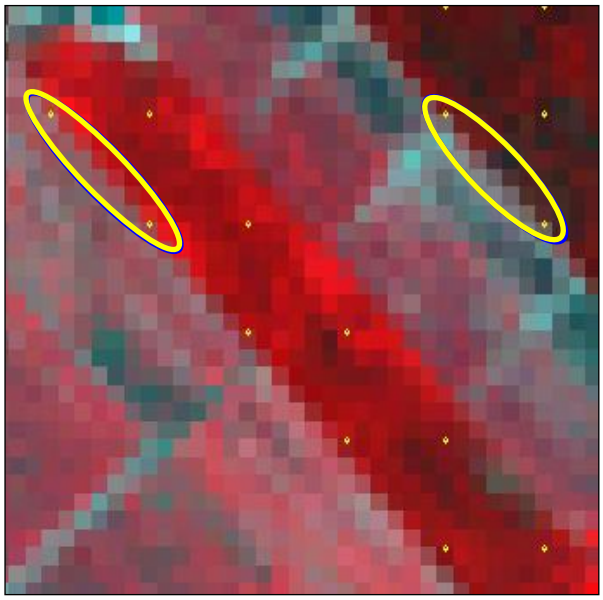

Figure 5-8 - FCC subset of a 4m IKONOS image of Held87 S2 25 Apr 2004. Enlargement on the right shows wheat training pixels identified on the edge of wheat and poppy fields.

Within field variation also existed in fields where very thin cropping existed and so mixed spectral responses from both the bare soil and the crop was found. However, as Section 2.3.1 of Chapter 2 stated, the crop's vegetated surface consisted of all components of the plant including its background soil, and so training pixels were still collected in these areas where within field variation existed.

Histograms were then used to establish whether the class training data in each dataset were spectrally characterised by a Gaussian distribution. Unfortunately, the low numbers of pixels collected (as highlighted in Figure 5-9 of poppy training pixels in Held115 Segment 2) meant that is was difficult to assess whether the training classes were normally distributed, bi-modal or multi-modal. Although this meant cases of bi-modality could not be identified, the removal of all known mixed pixels collected along borders of different cover types minimised the chances of bi-modality.

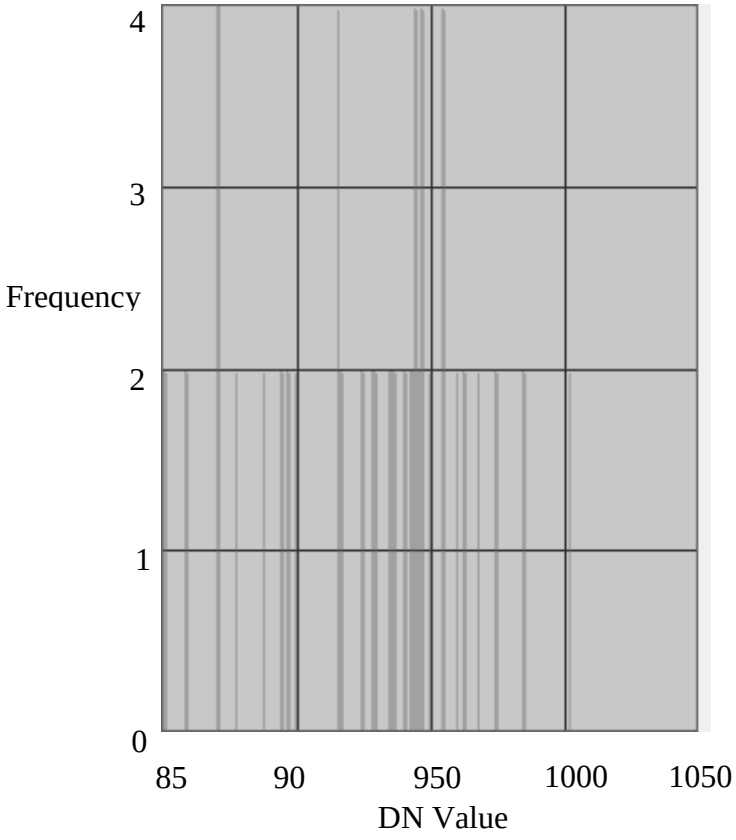

Figure 5-9 - Histogram of Poppy Training Pixels from Held115 S2

Training and evaluation pixels for every cover type in Held87 S2 were examined in this way and then the entire method of collecting, reviewing and refining signatures was repeated for each cover type present in the other two segment training areas in Held 87.

Finally, training pixels from each training area segment in Held87 were subsequently amalgamated to create one training dataset per cover type in Held87.

The above methodology was adopted across segment training areas in every IKONOS image used in this research. Evaluation pixels were also selected in exactly the same way for use in accuracy assessment post-classification. Care was taken to ensure that the locations of training and evaluation pixels were the same on each pair of co-registered images.

On the whole, sufficient numbers of training and evaluation pixels were selected for each cover class across the survey sites in Afghanistan as demonstrated in Table 5-4 from one date per district.

Table 5-4 - Training and Evaluation Pixels per Cover Type per District

	District	Date	Poppy	Wheat	Alfalfa	Trees	Vine	Onions	Bare	House	Non Agri Veg	Water
Training Pixels	Held87	25-Apr-04	445	323	33	0	0	0	160	66	0	10
	Held57	28-Apr-04	617	69	24	54	0	0	363	162	46	0
	Held115	29-Apr-04	104	519	59	19	56	0	229	92	34	29
	Nan25	11-Apr-04	728	57	64	74	0	0	257	74	0	0
	Nan11	25-Apr-04	468	139	67	117	0	188	203	125	0	0
	Nan29	11-Apr-04	416	453	0	135	0	0	303	132	0	0
	Kand73	26-Mar-04	88	482	0	0	0	0	562	0	459	0
	Kand87	26-Mar-05	452	112	0	142	340	0	472	125	93	0

	District	Date	Poppy	Wheat	Alfalfa	Trees	Vine	Onions	Bare	House	Non Agri Veg	Water
Evaluation Pixels	Held87	25-Apr-04	441	329	21	0	0	0	175	67	0	4
	Held57	28-Apr-04	512	102	29	65	0	0	373	139	115	0
	Held115	29-Apr-04	88	521	62	9	42	0	315	27	63	14
	Nan25	11-Apr-04	719	39	56	107	0	0	234	99	0	0
	Nan11	25-Apr-04	506	137	73	118	0	167	227	79	0	0
	Nan29	11-Apr-04	398	430	0	261	0	0	319	31	0	0
	Kand73	26-Mar-04	18	550	249	0	0	0	774	0	249	0
	Kand87	26-Mar-05	523	172	8	25	358	0	568	49	33	0

5.2.2 Summary of Training and Evaluation Data Selection

Section 5-2 showed results of research conducted to improve the selection of training and evaluation data for this Afghan poppy study. Overall, a pragmatic balance between theoretical requirements and field reality was found, guided by a geo-statistical approach. The method proposed to select and review class training and evaluation pixels in each image is as follows:

- Sub-set images into segment training areas and overlay ground data.
- Use variogram to identify an appropriate sampling rate to minimise the potential for spatial autocorrelation.
- Create dot grid matrix with appropriate sampling rate selected.
- Create Areas of Interest (AOIs) to collect individual pixels per cover type.
- Divide pixels into training and evaluation files.
- Visually review class pixels to identify any that did not belong to the cover type of interest and identify locations of possible mixed pixels.
- Remove incorrectly assigned pixels and mixed pixels.
- Amalgamate training pixels from all segments in district.
- Amalgamate evaluation pixels from all segments in district.

5.3 Determining Spectral Separability and Classification Accuracy

5.3.1 Spectral Separability Measures

After all training and evaluation datasets had been created at each site on each image date, graphical and statistical measures were used to examine the training class signatures to investigate their separability with one another at various dates in the growth cycle. The results were used to characterise the spectral signature of poppy and other crops at different growth stages to determine if, when and where the poppy spectral signature contrasts with the signatures of surrounding crops in Afghanistan, as per Objective 2a, and to determine the most appropriate time(s) in the growth cycle for discriminating poppy from other crops (Objective 2b).

Spectral coincident plots and the JM distance statistical measure described in Chapter 2 were used to establish and compare the amount of spectral variability within and between the selected training pixels from different image dates and different locations. These results are presented in Chapters 6 and 7.

5.3.2 Determining Classification Accuracy

Once spectral separability had been quantified at each location from each image date, the signatures generated from each set of training pixels were used to classify their corresponding images using the MLC. Labels were subsequently assigned to all pixels in each image. The MLC was performed on every image using only the training pixels collected from the same image from the same date.

Two different outputs were generated for each image classification. The first was the classified image (a thematic map) where each pixel was assigned a colour label to identify which class it had been assigned to. The second output was in tabular form - the error matrix - which was used to assess the accuracy of the classification by showing the overall classification accuracy and the poppy user's accuracy, as described in Chapter 2.

The Kappa statistic described in Chapter 2 was also used to test whether the classified maps were significantly better than if they had been generated by randomly assigning labels to cover types on the images. Regression analysis was used to establish whether a relationship exists between spectral separability and classification accuracy at any growth stage.

5.3.3 Multi-temporal Classification Accuracy

In many studies classification accuracy was found to increase when multi-temporal imagery was used (e.g. Turner and Congalton, 1998). To determine whether classification accuracy improved when MLCs were performed on the multi-temporal Afghan datasets, as per Objective 4, the image data was sorted to eliminate districts where only single images had been acquired in either growth cycle from the multi-temporal study. The districts of Nan29 in Nangahar Province and Kand73, Kand84 and Kand135 in Kandahar Province were subsequently eliminated from the multi-temporal investigation.

Then, by adding two co-registered images together using the layerstack option in Erdas Imagine 8.7 two-date image stacks were created from pairs of co-registered images acquired over the same area at different times in the growth cycle. Eight band training signatures were then generated from training pixels collected from the fused image pairs – from exactly the same locations as the training pixels collected from the single images.

In total, sixteen single images were used in the multi-temporal classifications from five of the nine districts. Two layerstacks were produced from the images acquired in Held57, Held87 and Held115 over the 2004 and 2005 cycles and one layerstack was produced for Nan11 and Nan 25 from 2004 data.

The results from the multi-temporal classifications were then compared with the original single date classification results. Kappa was used to identify whether any classification accuracy improvements achieved using multi-date image datasets occurred as a result of chance. Single-date and two-date classification results are presented in Chapter 7.

5.3.4 Determining a Link between Separability and Classification Accuracy

A link between high spectral separability and high classification accuracy was not established in the Literature Review. This study therefore formally investigated whether statistical measures of separability can be used to quantify how successfully training classes will be classified in a subsequent classification, by comparing the JM distance measure results to the classification results, as per Objective 3. The results are presented in Chapter 6 and 7.

5.4 Chapter Summary

A method was developed in this chapter to collect samples of training and evaluation pixels on the premise that different Afghan cover types could be separated into sets of spectral classes representative of the cover types being mapped in a form that was suited to the MLC. This method improved upon previous methods outlined in the Literature review by employing a variogram to identify the effects of spatial autocorrelation on IKONOS imagery. A sampling rate of 1 in 6 maintained an appropriate distance between IKONOS training and evaluation pixels so that the effects of spatial autocorrelation were minimal.

By using a dot grid matrix, independent and non-spatially auto-correlated training and evaluation pixels were initially acquired from twenty-seven 250m x 250m segment training areas from Nangahar, Helmand and Kandahar Provinces in Afghanistan. However, the 1 in 6 sampling rate chosen meant that less than the guideline minimum

of 40 training pixels per spectral class were collected in some locations and so the segment training areas were expanded up to 1000m x 1000m.

After mixed pixels had been removed to minimise the impact of any source of bias the training and evaluation pixels were examined using SCPs and the JM distance measure to establish the amount of spectral variability within and between the selected training pixels prior to the MLC being used.

After single date and two-dated MLCs were performed error matrices and Kappa statistics were used to assess the accuracies of the single and multi-temporal classifications. The results from these and from the investigation into the link between spectral separability and classification accuracy are presented in Chapter 6. Chapter 7 presents results from the multi-spectral analysis.

6. Results

The methodology developed in Chapter 4 was designed to collect multi-temporal IKONOS images across the different stages of the poppy growth cycle over nine locations. Chapter 5 described how representative training and evaluation pixels were collected from the images before applying the MLC. The chapter also described the methods used to examine the spectral characteristics of different cover types at each date and how two-dated image layer stacks were prepared prior to performing the MLC.

This chapter begins by summarising what imagery was acquired and at what growth stages. It then draws together the measures of separability described in Chapter 2 and presents the results of the investigations conducted on single date IKONOS data. Spectral Coincidence Plots (SCPs) were used to provide a visual and qualitative display of the spectral characteristics of the training pixels. The Jeffries-Matusita (JM) distance measure was applied to all four IKONOS bands to quantify the degree of separability between cover types to establish how, when and where poppy reflectance spectra contrasted with surrounding crops, in order to achieve Objective 2 of Chapter 1.

The chapter also reviews the two outputs from the image classification, the classified images and the tables used to assess classification accuracy. Kappa is also used to investigate the agreement between the reference and classified data (described in Chapter 2), to establish if the MLC produced significantly more reliable results than if labels were randomly assigned to the cover types on each image. Regression is applied to the results to establish if it is possible to predict classification accuracy from spectral separability, as per Objective 3.

Chapter 7 goes on to present the results from the multi-temporal classification investigation. A full set of results for each site are presented in Appendix D.

6.1 Imagery Acquired

Figure 6-1 illustrates the nine sites surveyed in Helmand, Nangahar and Kandahar Provinces and Table 6-1 lists all of the growth stages imaged at each district site.. In Helmand and Nangahar images were acquired in both 2004 and 2005 coincident with the early growth stages in 2005, and the later stages in 2004. Unfortunately, the 2005 data from Nangahar Province was excluded because very little poppy was grown due to

the success of the Afghan Government's counter-narcotics campaign. In Kandahar Province imagery was only acquired in the 2005 growing season.

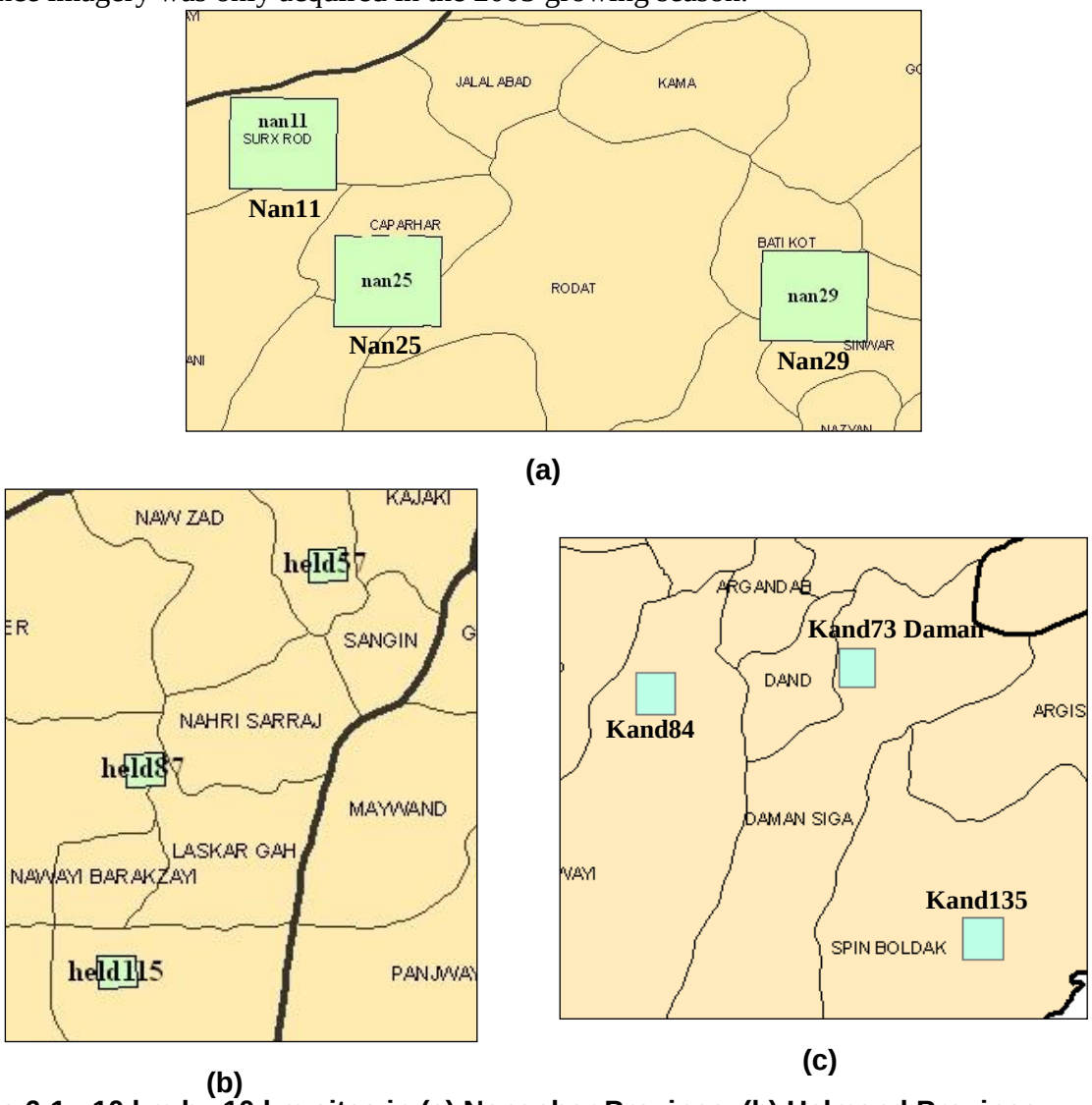

Figure 6-1 - 10 km by 10 km sites in (a) Nangahar Province, (b) Helmand Province and (c) Kandahar Province

Table 6-1 – Growth stages reached at the time of imaging in all locations

Growth Stage Reached	District	Year
Stem Elongation	Held57, Held87, Held115	2005
Stem elongation/beginning of flowering	Kand73, Kand84 and Kand135	2005
Beginning-mid flowering	Held57, Held87, Held115	2005
Mid-end flowering	Held57, Held87, Held115, Nan11, Nan25 and Nan29	2004
End flowering-Mid-Senescence	Held55, Held115, Nan11, Nan25	2004
End-Senescence	Held87	2004

6.2 Spectral Separability

The spectral characteristics of cover types were examined by observing the position of class means and the width of class ranges on SCPs and by determining the statistical JM distance between poppy and other cover types. The results from each method are discussed in turn in Section 6.2.1 and 6.2.2. Finally, a summary of the spectral separability results across all sites is presented in Section 6.2.3.

6.2.1 Visual Analysis – SCPs

More growth stages were captured on imagery during the 2004 and 2005 cycles in Nade-Ali District of Helmand Province than any other location. Therefore, for simplicity, results common to each site are discussed and illustrated using SCPs from Nade-Ali District (UN code Held87) in growth stage order from stem elongation to senescence. SCPs for the remaining eight sites can be found in Appendix C.

2005 Stem Elongation (Held55, Held87 and Held115 only)

The graph in Figure 6-2 shows the NDVI profiles created from MODIS imagery acquired over segment S1 in Nade-Ali District in 2004 and 2005. The approximate growth stages reached by the crops at the time of image acquisition were calculated from these profiles and summarised in Table 6-2.

During 2005 in Held87, Held57 (Musa Qala District) and Held115 (Garmser District) poppy fields were grown alongside wheat and alfalfa fields, against a background of bare soil and houses. In some areas there were also weeds (Held57 and Held115), water irrigation channels (Held87 and Held115) vine crops (Held115) and trees (Held57).

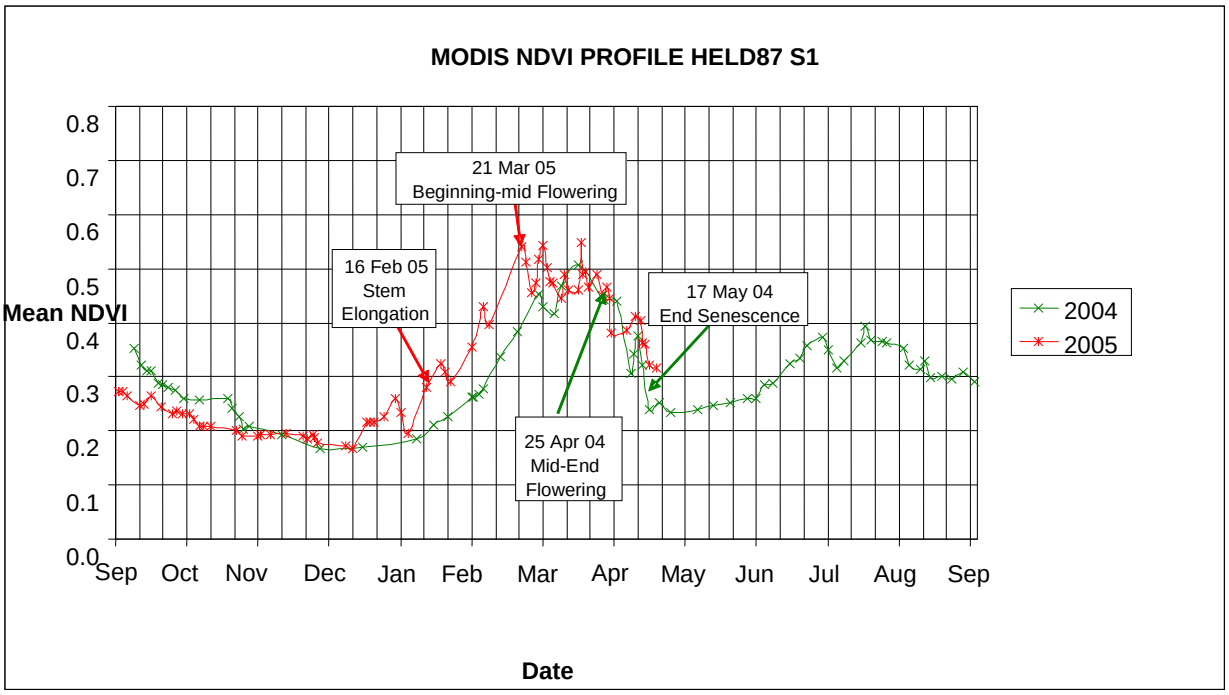

Figure 6-2 - MODIS NDVI Profile for Held87 indicating the dates and approximate growth stages reached by the crops at the time of imaging

Table 6-2 - Growth stages reached at the time of image acquisitions in Held87

Image Date	Growth Stage Reached	SCP
16 Feb 05	Stem Elongation	Figure 6-3
21 Mar 05	Beginning-mid Flowering	Figure 6-4
25 Apr 04	Mid-end of Flowering	Figure 6-5
17 May 04	End-Senescence	Figure 6-6

Figure 6-3 shows the SCP created from training signatures collected using imagery acquired during stem elongation from Held87 on 16 Feb 05. The mean value for poppy training signatures (red triangle) is shown in all four IKONOS bands, together with the means of wheat, alfalfa, bare soil and house.

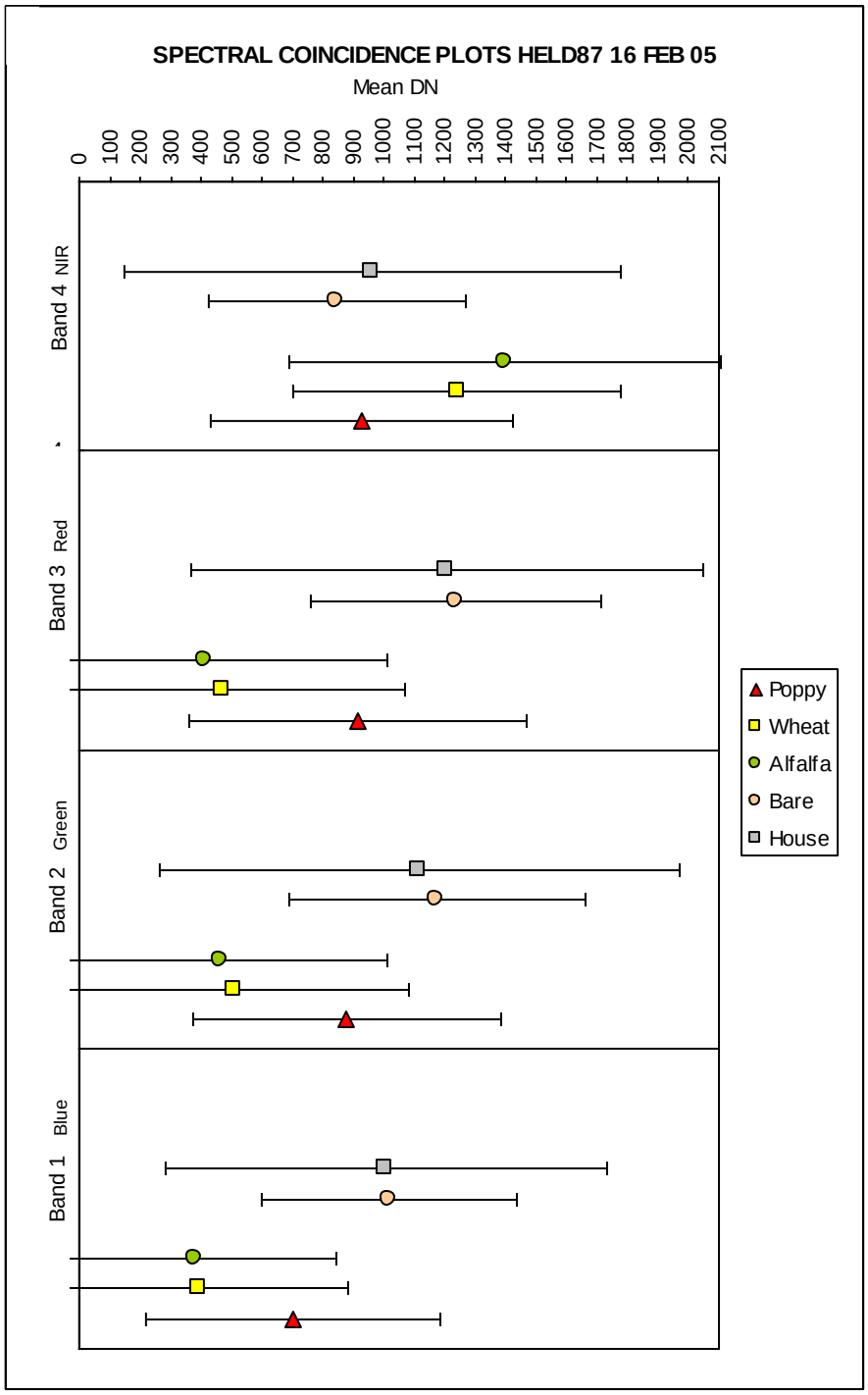

Figure 6-3 - Spectral Coincidence Plot from IKONOS imagery, Held87 on 16 Feb 05 at Stem Elongation (Band 1-blue, band 2–green, band 3–red and band 4–NIR). Class ranges indicated by⊢⊣

Figure 6-3 shows that poppy class means were different from all other class means in the visible bands at stem elongation. This was also the case in Held57 and Held115 at emergence/stem elongation. Overall, the closest class means to poppy were house and wheat in the visible bands. In the NIR band (band 4) in Held87 bare and house class

means were situated very close to the poppy class mean. In all three locations the poppy means were higher than the other vegetative class means (wheat and alfalfa) across the three visible bands.

Figure 6-3 also illustrates broad class ranges at stem elongation. For example, in Held87 the poppy class ranges extended from very low DN values to over 2100. In Held57 class ranges were even broader - particularly in band 1 at emergence-stem elongation.

In Held87 class ranges overlapped in all bands. In Held57 and Held115 the same was found at the early growth stages (see Appendix C-12 and Appendix C-16 respectively). The overlapping class ranges indicated that large amounts of in-class variability existed at stem elongation. For example, in Held87 the upper and lower limits of poppy overlapped at least half of every other class range in the visible bands, particularly across the upper limits of wheat and alfalfa, and the lower limits of bare and house. As a result, very poor statistical separability was expected between poppy and all other classes at stem elongation because of the overlap. Consequently, it was likely to cause errors in the subsequent classifications and lead to poor classification accuracies at stem elongation.

2005 Stem Elongation/Beginning of Flowering (Kand73, Kand84 and Kand135 only)

In Kandahar Province, poppy was grown alongside wheat, weeds and bare soil (Kand73-Daman District; Kand84 - Panjawi District; and Kand135 Spin Baldak District). Alfalfa, vine crops, trees and houses were also present in Kand84 and vegetables and houses were found alongside poppy in Kand135.

Imagery was only acquired at stem elongation/beginning of flowering in Kandahar Province. SCPs at Appendix C-18, C-19 and C-20 showed that class means were well separated in the visible bands in Kand73 and Kand135 (but very poorly separated in Kand84, where poppy class means were overlapped by wheat and alfalfa). In all three locations weeds had higher class means than all other vegetation in the visible bands.

Class ranges at all three sites were broad and overlapping in all four IKONOS bands, indicating poor class separability and wide in-class variability. Accordingly, very poor statistical separability between poppy and all other classes, and low overall classification accuracies were expected.

2005 Beginning-mid Flowering (Held55, Held87 and Held115 only)

Figure 6-4 illustrates the SCP produced from training pixels collected from imagery acquired in Held87 on 21 Mar 05 at the beginning/mid-flowering. By comparing the SCPs created at stem elongation with the beginning-mid flowering from all three districts in Helmand, class means appeared to have moved closer together by the later growth stage.

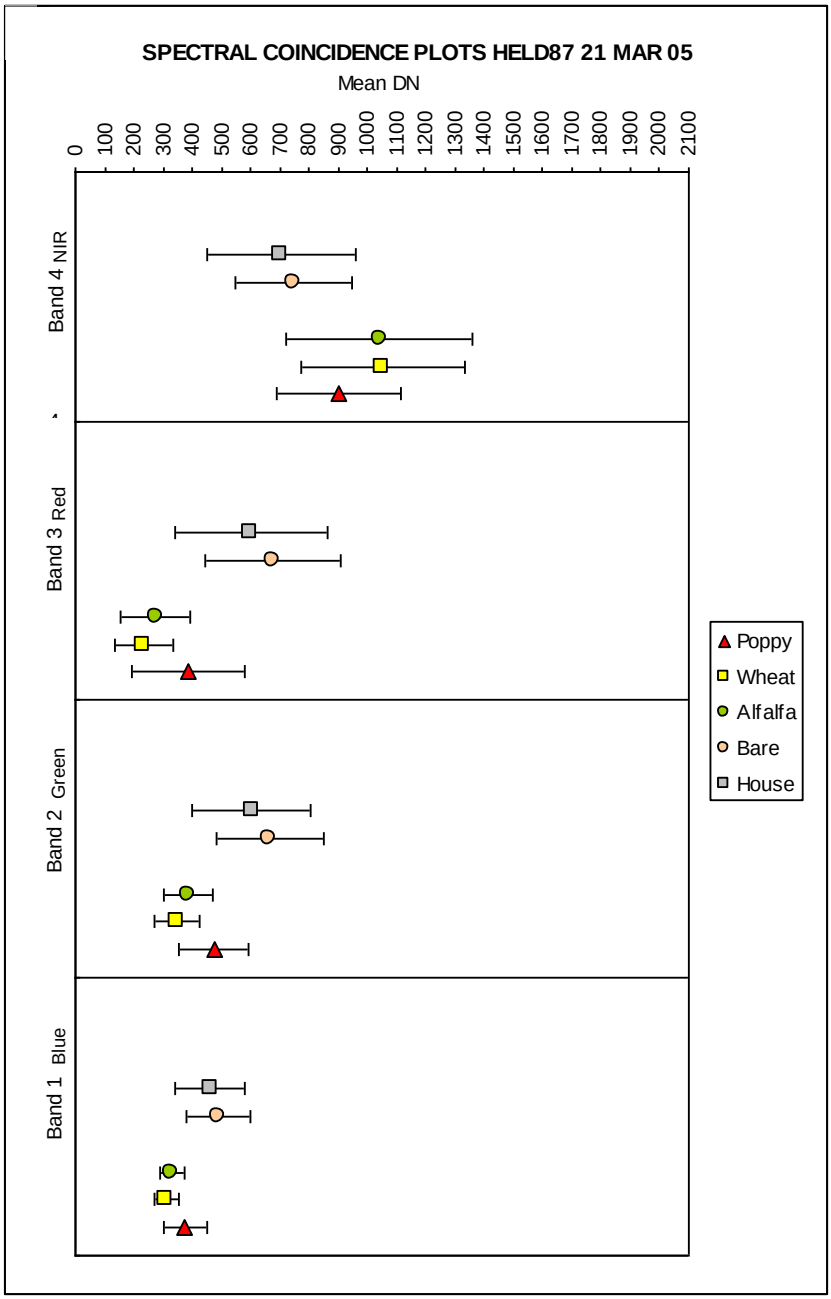

Figure 6-4- Spectral Coincidence Plot Held 87 on 21 Mar 05 at Beginning-mid Flowering, blue (Band 1), green (Band 2), red (Band 3), NIR (Band 4) displayed using 2 Standard Deviations. Class ranges are indicated by ⊢⊣

In addition, by beginning/mid-flowering in two of the three sites (Held57 and Held87), the wide and overlapping class ranges evident at stem elongation (Figure 6-3) had substantially narrowed. This meant that the reflectance characteristics of the cover types at these two sites had become internally more homogeneous as the crops matured towards beginning/mid-flowering. Therefore, statistical separability between classes was expected to improve between stem elongation and flowering, resulting in fewer classification errors.

2004 Mid-end Flowering (Held57, Held87, Held115, Nan11, Nan25 and Nan29)

Imagery was captured at mid-end flowering in all districts of Helmand and Nangahar Province in 2004. In Nangahar Province poppy was grown alongside wheat, trees, bare soil and houses in all three districts (Nan11-Surkh Rod District; Nan25-Chapahar District; and Nan29-Batikot District). Alfalfa was also grown in Nan11 and Nan25 and onions in Nan11.

Figure 6-5 shows the SCP created from training pixels collected from imagery acquired on 25 Apr 04 from Held87 at mid-end flowering. It shows that poppy class means were separated from every class in the three visible IKONOS bands except water. Poppy class means were also separable in Held57, Held115 (although vineyard overlapped poppy), Nan11, Nan25 and Nan29.

In all Helmand and Nangahar districts except Held115 class ranges were narrow in all bands at mid-end flowering. Figure 6-5 illustrates the narrow ranges found in Held87, particularly in bands 1-3 in the vegetative classes. In some locations poppy class ranges were totally separable from other classes. Figure 6-5 shows that the wheat class in Held87 is separable from poppy in the visible bands, and bare and house are separable from poppy in bands 2 and 3. In band 4 all classes overlapped poppy except water.

As a consequence of the lack of overlap between poppy and all other class means (except water) and the narrow and barely overlapping class ranges in the visible bands, statistical separability and classification accuracies were expected to be higher than found at either stem elongation or the beginning to mid-flowering in the 2005 season.

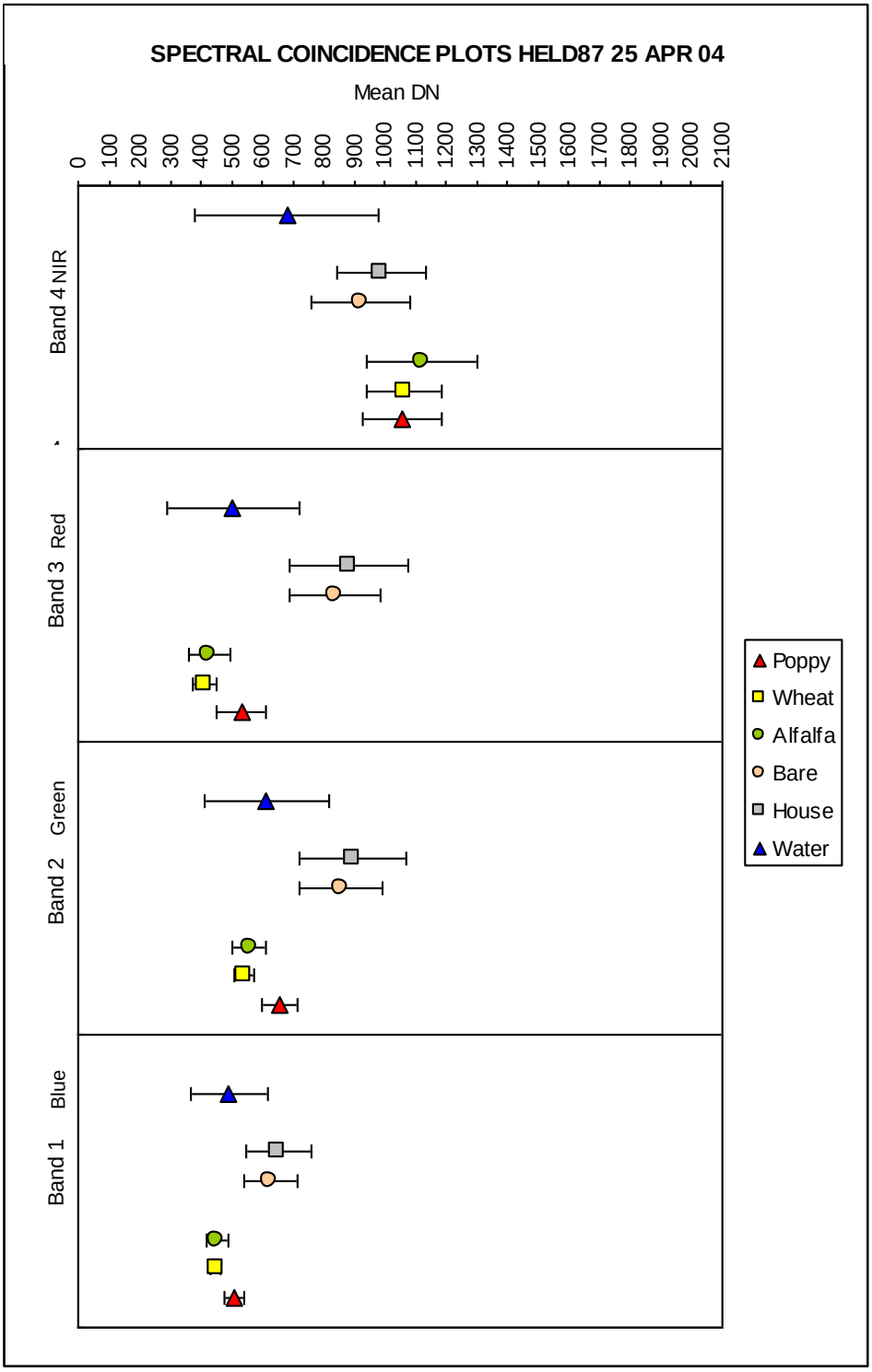

Figure 6-5 - Spectral Coincidence Plot Held 87 on 25 Apr 04 at Mid-end of Flowering (Band 1-blue, band 2–green, band 3–red and band 4–NIR). Class ranges indicated by ⊢⊣

2004 End flowering-Mid-Senescence (Held55, Held115, Nan11, Nan25)

By mid-senescence in 2004 class ranges appeared narrower than 2005 results. Overlap between the classes was more visible during senescence than seen at flowering in 2005.

Class means also appeared to overlap in some instances, indicating the potential that classes were not as internally homogenous or as separable as at mid-flowering. Accordingly, statistical separability was expected to be lower than had been found at flowering in 2005 which would result in poor classification accuracies.

2004 End-Senescence (Held87)

The SCP created in Figure 6-6 from imagery acquired at end-senescence in Held87 is typical of the general pattern found at senescence in all six Helmand and Nangahar sites.

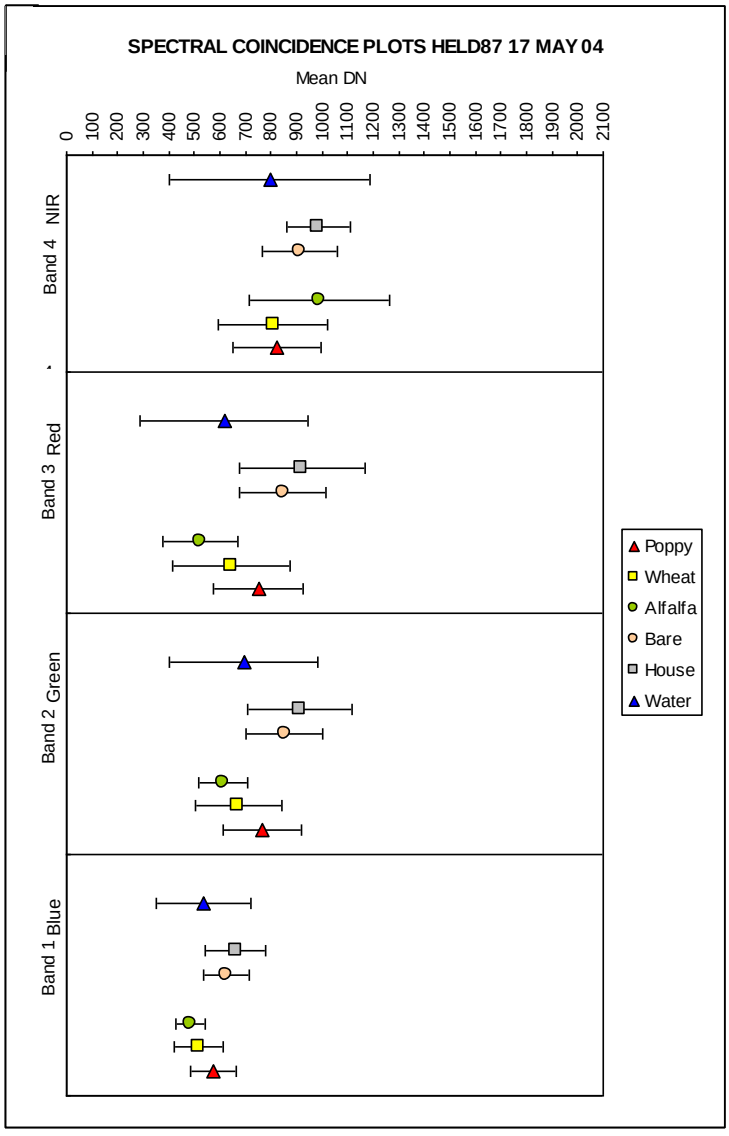

Figure 6-6- Spectral Coincidence Plot Held 87 on 17 May 04 at end of Senescence (Band 1-blue, band 2–green, band 3–red and band 4-NIR band). Class ranges indicated by ⊢⊣

By end-senescence class means moved slightly further apart and class ranges lengthened. As a consequence, more overlap between poppy and other classes was visible at end-senescence than at flowering. Accordingly, statistical separability was expected to decline by end-senescence and result in poor classification accuracies.

Summary of Class Separability by SCP's

The SCPs provided a visual display of the spectral characteristics of the training pixels. In the cases studied the range of spectral responses for each class and the amount of spectral overlap varied according to growth stage. Class ranges were broader at the early growth stages of emergence/stem elongation than at any other time, particularly at flowering, indicating high degrees of internal class variability at the early growth stages. Similarly, class overlap was more pronounced at emergence/stem elongation than at flowering, and provided an indication that classification accuracy would be reduced at the early growth stages.

As predicted in Chapter 3, separability appeared to be higher at flowering than at any other growth stage, corroborated by narrower class ranges and fewer cases of spectral overlap in the nine sites. As a result, higher classification accuracies were expected at flowering.

Section 6.2.2 examines the statistical separability between classes at each growth stage to quantify the degree of separation between poppy and other cover types using the JM distance measure as already discussed.

6.2.2 Statistical Analysis – JM Distance

Separability from Poppy

The JM distance statistical measure was applied to all IKONOS bands to find an average JM distance between poppy and all other cover types. By using the breakpoint indicators of separability outlined in Table 2-2 of Chapter 2, good separation was identified when JM distance values lay between 1378 and 1414, poor separation between 1000 and 1378 and very poor separation between 0 and 1000. These ranges helped to quantify the degree of separation or overlap between poppy and other cover types. This information was used to determine the most appropriate time in the growth cycle for discriminating poppy, as per Objective 2 and provide an indication of the probability of correct classification. The JM distance measure was also used to

determine which cover type was most often confused with poppy at each growth stage to identify the classes most likely to cause spectral confusion in the classification process.

Table 6-3 summarises the general statistical separability results for the nine sites investigated, ranked from highest to lowest. Growth stages are indicated by asterix's set within yellow boxes.

Table 6-3 - Summary of average JM distance between poppy and other classes in nine selected sites across Afghanistan in 2004 and 2005

District	Date	Emergence	Stem Elongation	Beginning Flowering	Mid Flowering	End Flowering	Beginning Senescence	Mid Senescence	End Senescence	Average JM Distance
Held 87	25-Apr-04				*					**1395**
Nan 25	11-Apr-04				*					**1378**
Nan 11	25-Apr-04					*				**1313**
Nan 29	11-Apr-04				*					**1278**
Held 57	28-Apr-04					*				**1251**
Nan 25	25-Apr-04					*				**1246**
Held 87	21-Mar-05			*						**1225**
Held 115	21-Mar-05			*						**1171**
Kand 84	26-Mar-05		*							**1150**
Held 115	29-Apr-04				*					**1144**
Held 57	29-Mar-05				*					**1138**
Kand 135	26-Mar-05		*							**1107**
Held115	10-Feb-05	*								**1097**
Held 115	17-May-04						*			**1096**
Kand 73	26-Mar-05		*							**1089**
Held 57	20-May-04							*		**1077**
Nan 11	17-May-04							*		**1047**
Held 87	17-May-04								*	**1017**
Held 57	19-Feb-05	*								**974**
Held 87	16-Feb-05		*							**831**

As expected after the analysis of the SCPs in Section 6.2.1, the poorest statistical separability between poppy and other classes occurred when images were acquired during the earliest stages of emergence-stem elongation and stem elongation, as shown at the bottom of Table 6-3. Poorest separability was found in Held87 from imagery

acquired on 16 Feb 05 at stem elongation (JM distance of 831, indicating very poor separability) and Held57 at emergence-stem elongation (JM distance of 974, very poor separability). This concurs with the results from analysis of the SCPs from the other Helmand and Kandahar districts, where poor separability was characterised by very wide class ranges - indicating the existence of large amounts of in-class variability in all classes, large amounts of overlap between all cover types – indicating inseparable classes and class means that were reasonably far apart.

The highest JM distance results were found at mid-end flowering in Held87 (JM distance of 1395) and Nan25 (JM distance of 1378), which confirmed that spectrally separation was good at this growth stage.

Table 6-4 presents a ranked summary of the average JM distance results showing when cover types were most and least separable.

Table 6-4 –Poppy Separability Ranking - results by growth stage

Separability Rank	Growth Stage Reached
1	Mid-end Flowering
2	End-Flowering-Beginning Senescence
3	Beginning-mid Flowering
4	Stem Elongation
5	Mid-end Senescence
6	Emergence-Stem Elongation

Spectral Confusion

The JM distance measure was also used to determine which cover type was most often confused with poppy at each growth stage to identify which class was most likely to cause spectral confusion in the classification process.

The JM distance results between poppy and each cover type are summarised in Table 6-5, colour-coded to indicate the separability between poppy and other cover types at each growth stage, as per the breakpoints defined in Table 2-2 of Chapter 2. The green shading indicates where separability from poppy was good, yellow indicates poor

separability and red indicates very poor separability. The percentage figures at the bottom of the table could be used operationally to provide a quick indication of how well poppy may be distinguished from other cover types in a subsequent digital classification.

By looking at the proportion of green shading compared with yellow and red in each column it was possible to identify which cover type was most often well separated from poppy. Results are listed by cover type.

Table 6-5 - JM distance between poppy and other cover types

Growth Stage	Location	Wheat	Alfalfa	Trees	Weeds	Vine	Onion	Bare	House	Water
Emerg-Stem elongation	Held57									
	Held115									
	Held87									
	Kand84									
	Kand73									
	Kand135									
Beg-mid flow	Held87									
	Held57									
	Held115									
Mid-end flow	Nan25									
	Held87									
	Held115									
End flow-beg Senescence	Nan11									
	Held57									
Beg-mid Senescence	Held115									
	Nan25									
Mid Sen	Held57									
Mid-end Sen	Nan11									
End Sen	Held87									
% figures indicate how often a cover type was separable from poppy, divided into good, poor and v poor separability categories		15.8	**5.9**	**18.18**	**0**	**0**	**0**	**44.4**	22.2	22.0
		31.6	**88.2**	**81.8**	**54.54**	**75.0**	**100**	**27.8**	55.6	80.0
		52.6	**5.9**	**0**	**45.45**	**25**	**0**	**27.8**	22.2	0

Key to Separability		Good		Poor		V Poor

Bare

Bare soil was more often separated from poppy than any other cover type (44% of the time). For example, bare was well-separated from poppy at; emergence-stem elongation in each of the Kandahar district sites; at mid-end flowering in Nan25, Held87 and Held115; and at both end flowering-beginning senescence and mid-senescence in

Held57. These good separability results indicated that bare had the highest possibility of being correctly classified in the subsequent MLC than any other cover type.

Conversely, bare was very poorly separated from poppy in all of the Helmand sites at emergence-stem elongation, at beginning-mid senescence in Held115 and at end senescence in Held87.

House

Separability of poppy from house was similar to the bare results –very poor at emergence-stem elongation in all of the Helmand districts and good at mid-end flowering in Nan25, Held87 and Held115. In the remainder of locations separability was poor. Discrimination of poppy from house was therefore best only within a narrow window of opportunity –mid-end flowering.

The JM distance measure confirmed bare and house were the most inconsistently separated cover types from poppy across the growth cycle.

Wheat

Wheat was the least separable cover type from poppy (the highest proportion of red shading in Table 6-5), particularly at emergence-stem elongation across Kandahar Province, in two of the three Helmand districts (Held57 and Held115) and at end flowering-beginning senescence in Nan11 and Held57. In Held87 and Nan25 separability between poppy and wheat was good at mid-end flowering.

Discrimination of poppy from wheat was therefore best only within a narrow window of opportunity - mid-end flowering. Consequently, classification accuracy was expected to be lower at both the early growth stages and end flowering-beginning senescence than at mid-end flowering.

Alfalfa

Alfalfa was consistently poorly separated from poppy at every growth stage in every location, with only two exceptions (Held115 at beginning-mid-flowering in 2005 (very poor) and in Nan11 at end-flowering-beginning of senescence (good). In the SCP of Nan11 poppy class ranges were completely separable from alfalfa in the visible bands at this time. Consequently, alfalfa user's accuracies were expected to be low in every location at all growth stages except in Nan11 at end-flowering-beginning of senescence.

Weeds

Separation between weeds and poppy ranged from very poor to poor although there were too few cases to identify the existence of temporal or spatial patterns.

Vineyard

Similarly, vineyard was only identified on three image dates in Held115 and one occasion in Kand84. At these sites separation of poppy from vineyard was consistently poor at every growth stage except mid-end flowering where it was very poor.

Onions

For the one site where onions were recorded (Nan11) separation from poppy was poor at end flowering-beginning senescence and at mid-end senescence. There were too few cases to identify the existence of temporal or spatial patterns.

Trees

Separability between poppy and trees was consistently poor with two exceptions, end flowering-beginning senescence (Nan11) and at beginning-mid senescence (Held115) where separability was good.

Water

Water was recorded only once at three sites (Nan25, Held57 and Held115) and on two occasions in Held87. In each instance separation from poppy was poor except in Nan25 at mid-end flowering where it was good.

Summary of Individual Cover Type Spectral Variability

Spectral separability between poppy and other cover types varied according to the cover type and growth stage. Bare was consistently more separable from poppy across the growth cycle than any other cover type. Wheat was the least separable cover type, particularly at emergence-stem elongation and end-flowering-beginning senescence.

Additional observations are required in order to determine when poppy can be discriminated from onions, water, vineyard and weeds. The lack of additional data meant it was difficult to determine whether the results were one-off incidents or valuable and significant observations.

6.2.3 Summary of Spectral Separation

Consistent with expectations from visual interpretation of ADP over UK poppy fields (Chapter 3) spectral separability was found to vary according to the growth stage at the time of imaging. Overall spectral separability was poorest at emergence-stem elongation (for example, in Held57 and Held87) and greatest at mid-end flowering (Held87 and Nan25) in the nine cases studied.

The best time to spectrally separate poppy from other cover types was found to be mid-end of flowering, closely followed by end-flowering - beginning of senescence. The worst time was at emergence-stem-elongation.

6.3 Classification

Classifications were performed for all single date images using the MLC. The images were classified into classes using spectral information derived from representative datasets from each image and used in their corresponding image classifications. Appendix D presents the results of each 10 km by 10 km image classification.

Qualitative visual checks were conducted to assess the results of the classifications, by comparing the classified images to the original and focusing on the nature, magnitude and location of classification errors. For example, Figure 6-7 shows a classification of Nan25 using imagery dated 11 Apr 04 (mid-end flowering). The approximate locations of the original three 250m by 250m ground data segments have been overlaid. An enlargement of Segment 4 in Nan25 is also included below the classified image.

Poppy is shown to be the predominant crop (red shading) with some wheat (yellow) and occasional areas of individual trees (dark green). The overlapping spectral values of trees, wheat and alfalfa in the SCP were evidenced by the results of this classification, particularly in the enlargement of S4, as very small pockets of wheat and alfalfa were not located inside field boundaries as expected but interspersed around the trees.

The predominant non-crop cover types were bare soil and house, although the house class appears to surround all areas of bare soil in the classified image subset. This was largely due to houses and bare soil having overlapping spectral signatures, as identified in the corresponding SCP.

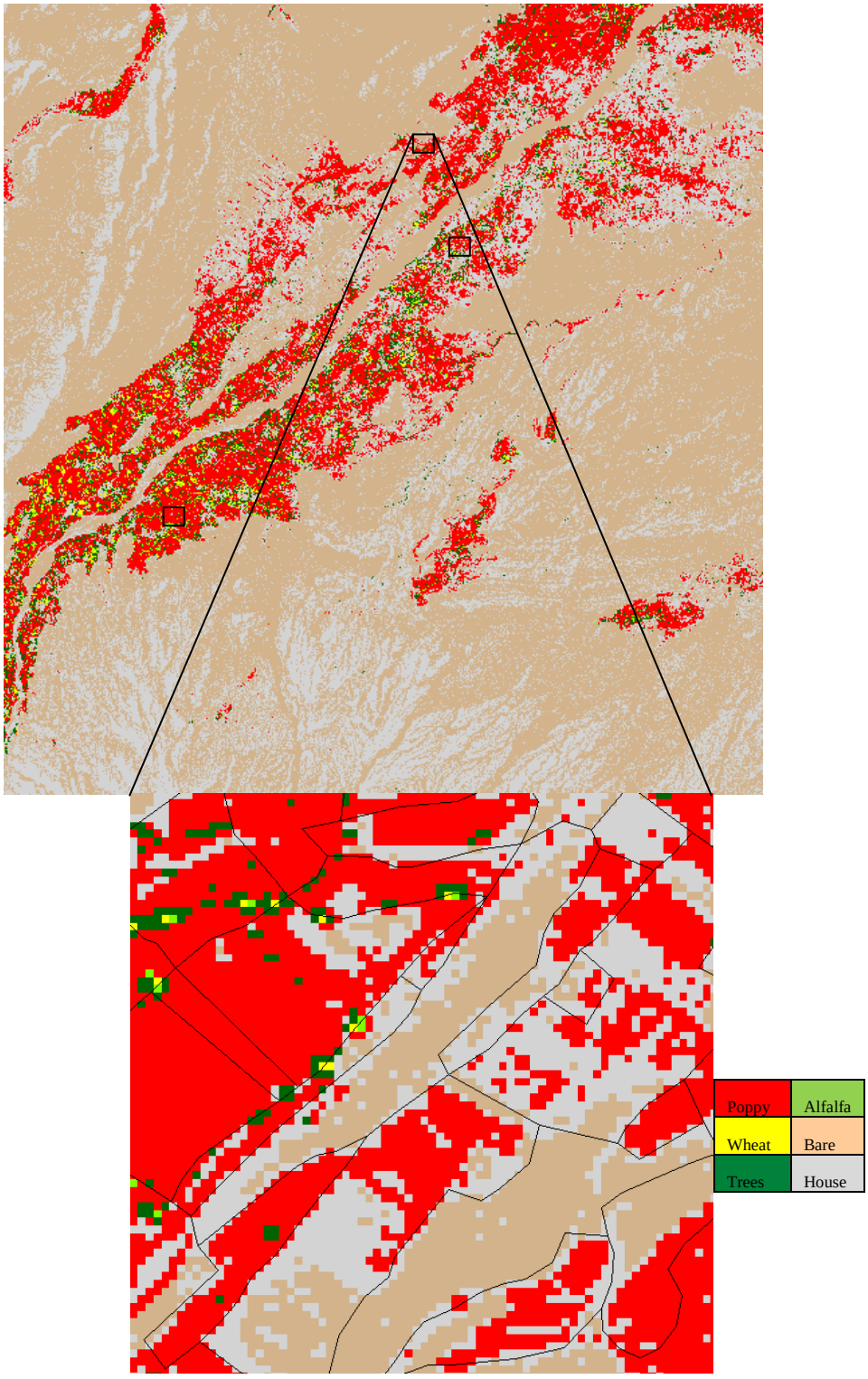

Figure 6-7 - Supervised Classification of Nan25 from imagery dated 11 Apr 04 at mid-end flowering. Segment S1 enlargement is below the main image.

Large areas of misclassification of houses in the barren desert area to the south of the image can be seen, largely due to house building materials being made of stones, rocks and soil with similarly bright reflectance values. Overall, however, the MLC appears to have produced a useful map product. Figure 6-8 shows the classification result from the

next image acquired in Nan25 on 25 Apr 04 at end flowering-beginning of senescence with the S4 subset enlarged below. The subset from the 11 Apr 04 classification has been added for comparison on the left.

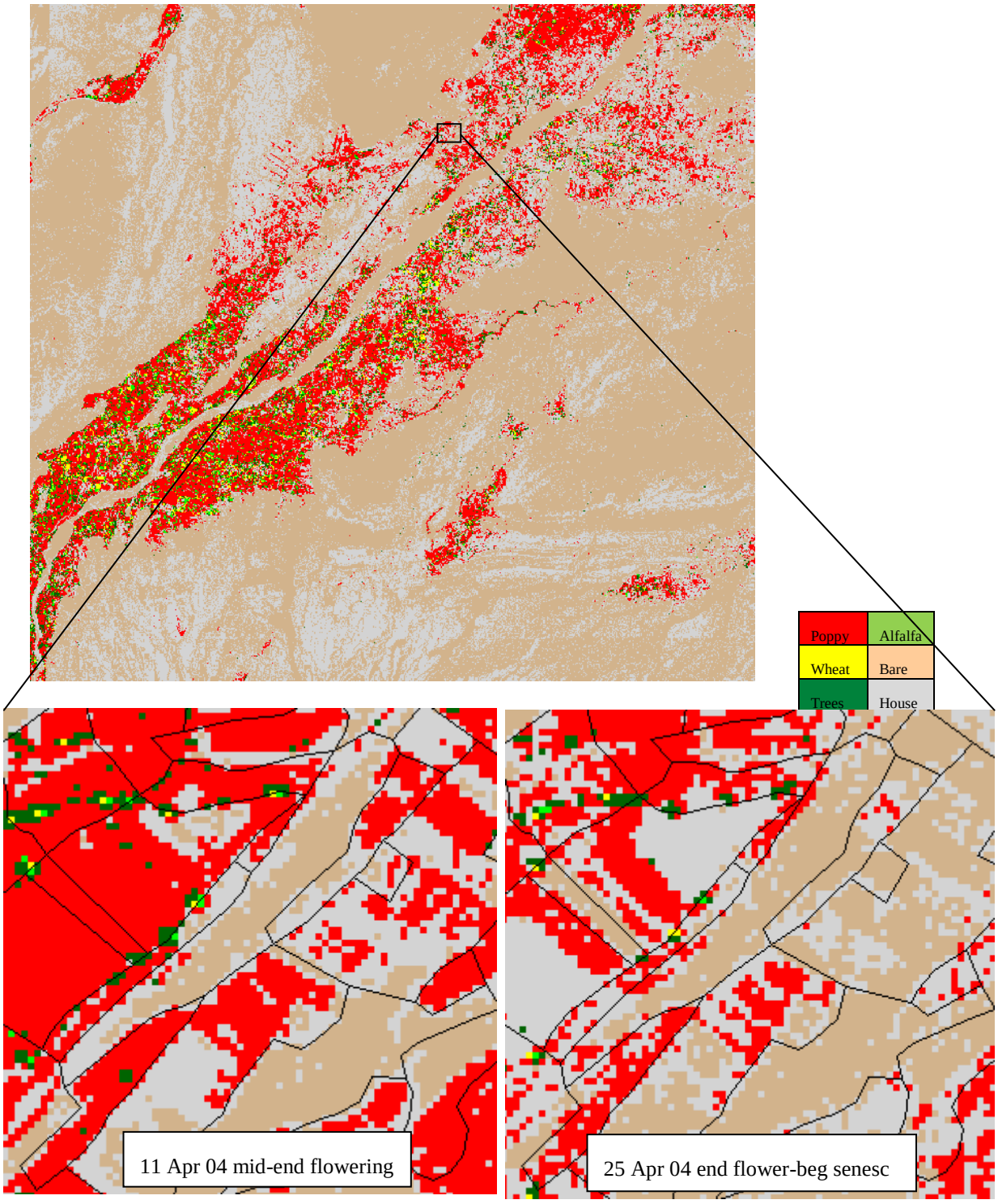

Figure 6-8 - Supervised Classification of Nan25 from imagery dated 25 Apr 04 at end-flowering - beginning senescence with S4 subsets included below

In the S4 subset of the 25 Apr 04 classification, approximately 1/3 of the poppy crop had been removed from the fields by the end of flowering – beginning of senescence and replaced by houses - as had some of the trees. This was clearly not the case, but an example of an increase in spectral confusion between poppy and all other cover types evidenced in the average JM distance decrease from 1378 (good separability) to 1246 (poor separability) by 25 Apr 04, leading to misclassification of cover types.

Overall, the above examples demonstrate the findings of the classifications from all 5 Nangahar and Helmand study sites where images were acquired from flowering through to senescence; that more confusion and visual errors were found on classifications of images acquired towards the end of the cropping cycle than from those acquired during flowering. Conversely, visual analysis of 05 Helmand imagery revealed more confusion and misclassifications at the early growth stages than at flowering.

Although Chapter 3 described the importance of determining how well a classification identified individual classes, classification accuracy could not be quantified from a visual inspection of the output classified images. Instead error matrices were used to calculate and present overall, producers and poppy users accuracy, from each MLC performed. For ease, error matrices are presented in Section 6.3.1 from sites where the highest and lowest overall classification accuracies were found in Nangahar Province, in Nan25 and Nan29. Error matrices from the remainder of sites are presented in Appendix E.

6.3.1 Classification Accuracy

A table summarising overall classification accuracy results from every location is presented in Section 6.3.2. Kappa statistics are used to test the accuracy of each classification minus chance agreement, grouped into three categories (strong, moderate and poor agreement between reference and classified data), as per the categorisation in Section 2.8.2. A graph is used to compare overall accuracy against the average separability results first presented in Section 6.2.2. Regression analysis was used to establish whether a relationship exists at any growth stage between spectral separability and classification accuracy, as per Objective 3 in Chapter 1.

A table summarising poppy users accuracy and Kappa statistics is displayed for each location in Section 6.3.4 with a graph showing poppy users accuracy against the average separability results (from Section 6.2.2). Regression results are also presented.

This chapter presents results from single date classifications only, per province and in growth stage order. Results from two-dated classifications are presented in Chapter 7 and are used to determine whether the multi-temporal classifications improved accuracy over single date classifications, as per Objective 4 in Chapter 1.

Error Matrices

Table 6-6 displays the error matrix associated with the classified image in Figure 6-7 from Nan25 at mid-end of flowering in 2004 - the district and date where the highest overall classification accuracy was achieved by the MLC compared to all other classification results. At 89.79% this surpasses the commonly used benchmark of 85% (Foody, 2002) and indicates that overall, the classification was successful – as judged from the output classified map in Figure 6-7.

Table 6-6 - Error matrix for Nan25 11 Apr 04 – Mid-end Flowering

		Reference Evaluation Data											
		Poppy	Wheat	Alfalfa	Trees	Bare	House	Row Total	Reference Totals	Classified Totals	Number Correct	Producers Accuracy	Users Accuracy
Classification Data	Poppy	**707**	3	4	10	1	3	728	719	728	707	98.33%	97.12%
	Wheat	0	**31**	4	22	0	0	57	39	57	31	79.49%	54.39%
	Alfalfa	1	3	**46**	14	0	0	64	56	64	46	82.14%	71.88%
	Trees	9	2	2	**61**	0	0	74	107	74	61	57.01%	82.43%
	Bare	0	0	0	0	**221**	36	257	234	257	221	94.44%	85.99%
	House	2	0	0	0	12	**60**	74	99	74	60	60.61%	81.08%
	Col Tot	**719**	**39**	**56**	**107**	**234**	**99**	**1254**	**1254**	**1254**	**1126**		

Overall Classification Accuracy: 89.79%
Kappa: 83.42%

The columns in the table correspond to errors of omission, where pixels were not correctly identified by the classifier. For example, out of 719 poppy training pixels 9 were misclassified as trees, 2 as house and 1 as alfalfa. This small number of misclassified pixels resulted in a very high poppy producers accuracy of 98.33%. However, only 57.01% of the tree training pixels were correctly classified, principally because 22 tree pixels were misclassified as wheat, 14 as alfalfa and 10 as poppy.

The error matrix in Table 6-7 presents the classification accuracy results from Nan29 from imagery acquired at mid-end flowering (like Nan25, the previous example). Similar to Nan25, Nan29 poppy producer's accuracy was very high (91.96%) indicating

that only a small number of poppy training pixels were misclassified as wheat (29) and house (3).

Table 6-7 - Error matrix for Nan29 11 Apr 04 – Mid-end Flowering

		Reference Evaluation Data										
		Poppy	Wheat	Trees	Bare	House	Row Total	Reference Totals	Classified Totals	Number Correct	Producers Accuracy	Users Accuracy
Classification	**Poppy**	**366**	22	21	7	0	416	398	416	366	91.96%	87.98%
	Wheat	29	**266**	110	48	0	453	430	453	266	61.86%	58.72%
	Trees	0	52	**58**	24	1	135	261	135	58	22.22%	42.96%
	Bare	0	58	49	**190**	6	303	319	303	190	59.56%	62.71%
	House	3	32	23	50	**24**	132	31	132	24	77.42%	18.18%
	Col Total	398	430	261	319	31	**1439**	1439	1439	904		

Overall Classification Accuracy: 62.82%
Kappa: 51.1%

However, this example shows that the classification was not as successful as found in Nan25 (62.82% overall classification accuracy). The main reason for this was because of a large amount of spectral confusion between trees and all other classes, (also found in Nan25, but to a lesser degree). For example, out of 261 tree pixels 110 were mis-classified as wheat, 49 as bare, 23 as house and 21 as poppy, leading to a tree producer's accuracy of just 22.22%. Unfortunately, it was not possible to identify whether the misclassification of tree, wheat and bare pixels was consistent over time in this district as a second image was not acquired in 2004 and no images were acquired in 2005.

The next section places the overall accuracy results from Nan25 and Nan29 into context with all classification accuracy results collected from each site on each image date. Results are discussed by province, beginning with Nangahar.

6.3.2 Overall Classification Accuracy

Nangahar Province (2004)

Overall classification accuracy results from Nangahar Province are presented alongside JM distance results in Table 6-8 in overall classification accuracy order. Consistent with the highest spectral separability results in Nangahar Province the highest overall classification accuracies were achieved during mid-end flowering in Nan25, and at end flowering-beginning senescence in Nan11. After this time spectral separability decreased as the crops progressed further through to end-senescence, and similarly,

overall classification accuracy also decreased. Lowest overall classification accuracy was found in Nan29 at mid-flowering, mainly due to incorrectly classified wheat, trees and bare soil. The error matrices showed that poppy producers accuracies also declined from mid-end flowering to senescence.

A high Kappa value (83.42%) for Nan25 at mid-end flowering shows that there was strong agreement between reference and classification data. Consequently, the resultant thematic classified image from imagery acquired at 11 Apr 2004 in Nan25 (Figure 6-7) represents the most reliable information. The lowest Kappa value of 51.10% associated with Nan29 at mid-flowering reveals that this classification was the least reliable of all Nangahar results.

Table 6-8 - Summary of Overall Classification Accuracy and corresponding average JM Distance in Nangahar Province during the 2004 growth cycle.

District	Date	Emergence	Stem Elongation	Beginning Flowering	Mid Flowering	End Flowering	Beginning Senescence	Mid Senescence	End Senescence	Average JM Distance	% Overall Classification Accuracy	% Kappa Coefficient
Nan 25	11-Apr-04				*					1378	89.79	83.42
Nan 11	25-Apr-04					*				1313	83.09	78.55
Nan 25	25-Apr-04						*			1246	79.11	68.02
Nan 11	17-May-04							*		1047	67.10	58.13
Nan 29	11-Apr-04				*					1278	62.82	51.10

The graph in Figure 6-9 compares overall classification accuracy with spectral separability in Nangahar Province (2004) in growth stage order and shows that as spectral separability decreased, so did classification accuracy.

When the two variables were plotted on a scatter plot a positive linear association was found (Figure 6-10). The strength of the association was tested using the regression equation. With an r^2 value of 0.421, a weak linear association was found, where 42.10% of the variability in classification accuracy can be explained by variation in spectral separability.

Figure 6-9 % Overall Classification Accuracy and corresponding average JM Distance in Nangahar Province during the 2004 growth cycle

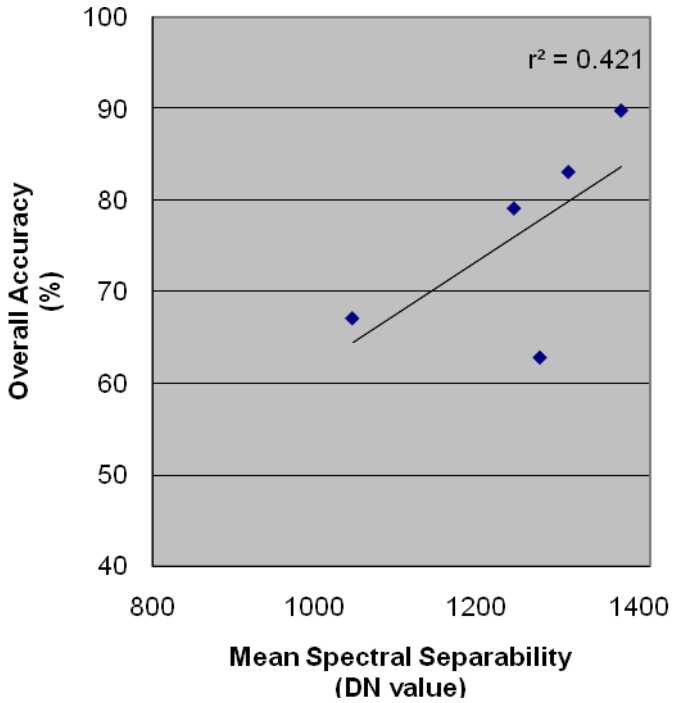

Figure 6-10 – Regression Analysis: Spectral Separability and % Overall Classification Accuracy for Nangahar Province, 2004

Helmand Province (2005)

Overall classification accuracy results from Helmand Province in 2005 are presented alongside JM distance results in Table 6-9, in overall classification accuracy order. Appendix C, pages C8-9, C12-13, C16-17 and Appendix E contains spectral separability and classification results for Helmand Province in 2005.

Consistent with the lowest spectral separability results found in Helmand Province in 2005 the lowest overall classification accuracies were achieved at emergence-stem elongation in both Held115 and Held57. The error matrix for Held115 showed that a high amount of misclassification occurred, mainly due to wheat pixels being misclassified as poppy (184 from a total of 538 wheat pixels), bare (67) and house (64). Surveyors reported disease which affected both poppy and wheat in this district which may account for the poor poppy producer's accuracy of just 63.33%.

Overall, 05 Helmand results were lower than 04 Nangahar and Helmand results because the crops were less mature. Therefore, the spectral responses of the fields were influenced more by the colour of the bare soil than the plant themselves, hence the poor spectral separability and low classification results.

As the crops progressed to beginning-mid flowering, overall classification accuracy and spectral separability increased. Producers accuracies also improved between emergence-stem elongation to beginning-mid flowering. The highest overall classification accuracy results were achieved at beginning-mid flowering in Held87, and at mid-flowering in Held57. Kappa values for all classifications from images acquired at or after stem elongation ranged from 47.67-62.82% which showed that the classifications represented moderate agreement between the reference and classified data.

Kappa results showed poor agreement between reference and classification data in Held115 and Held57 at emergence-stem elongation and confirm that these classifications were least reliable of all 2005 Helmand Province classifications.

Table 6-9 - Summary of Overall Classification Accuracy and corresponding Kappa coefficient in Helmand Province during the 2005 growth cycle

District	Date	Emergence	Stem Elongation	Beginning Flowering	Mid Flowering	End Flowering	Beginning Senescence	Mid Senescence	End Senescence	Average JM Distance	% Overall Classification Accuracy	% Kappa Coefficient
Held 87	21-Mar-05			*						1225	73.23	62.65
Held 57	29-Mar-05				*					1138	72.08	62.83
Held 115	21-Mar-05			*						1171	61.67	47.67
Held 87	16-Feb-05		*							831	60.94	48.28
Held 57	19-Feb-05	*								974	46.70	35.18
Held115	10-Feb-05	*								1097	42.46	32.30

Figure 6-11 compares overall separability and accuracy results for Helmand Province from the early growth stages in 2005, listed in growth stage order. Similar to Nangahar Province, a link between spectral separability and classification accuracy in Helmand Province in 2005 can be seen.

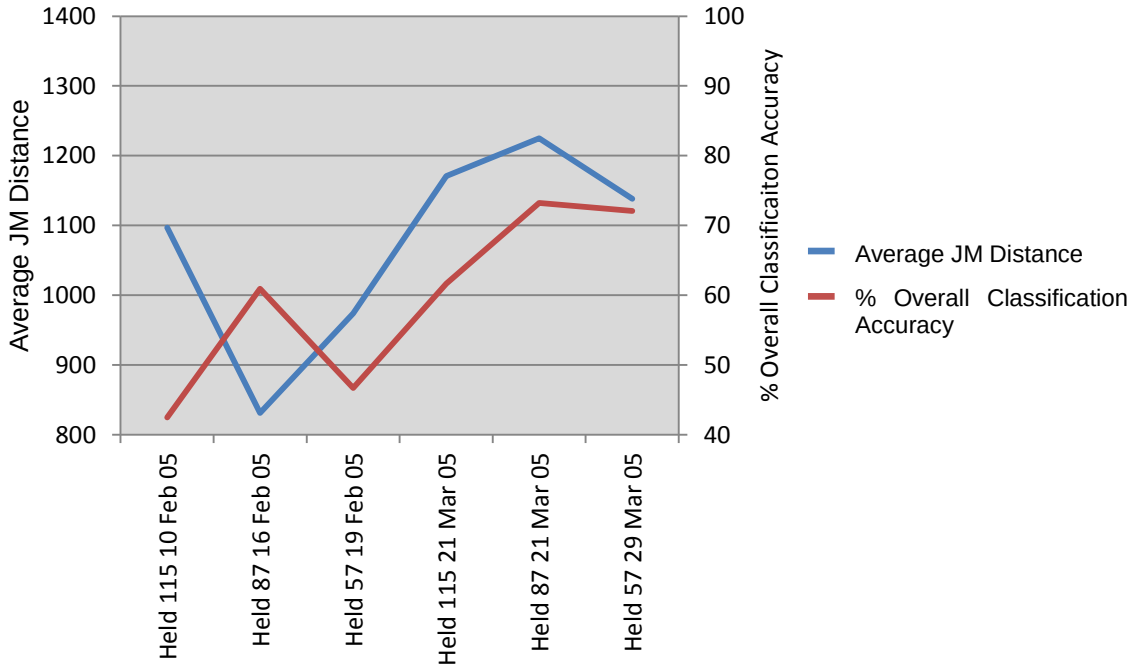

Figure 6-11- % Overall Classification Accuracy and corresponding average JM Distance in Helmand Province during the 2005 growth cycle

However, when the results were entered onto a scatter plot a very weak linear correlation was found between classification accuracy and spectral separability. The r^2 figure of 0.153 in Figure 6-12 indicated that only 15.3% of the variation in classification

accuracy can be explained by the variation in spectral separability. The two variables were therefore not linked at the early growth stages in Helmand Province in 2005.

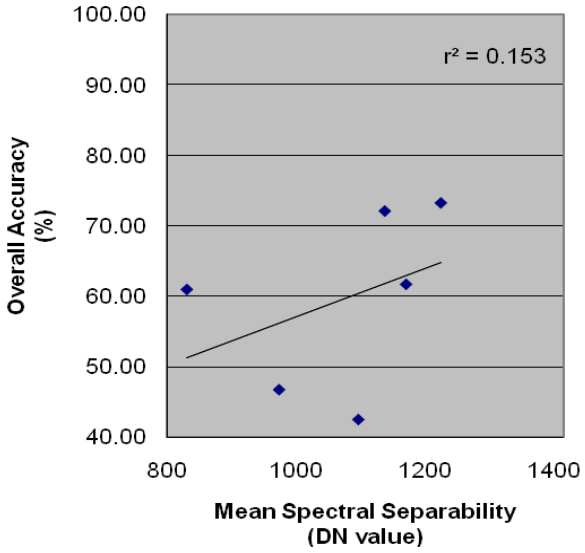

Figure 6-12 - Regression Analysis: Weak positive relationship between Spectral Separability and % overall Classification Accuracy in Helmand Province, 2005

Helmand Province (2004)

Table 6-10 presents the overall classification accuracy results from Helmand Province (2004) in overall classification accuracy order. All Helmand 04 error matrices can be viewed in Appendix E. The table shows overall classification accuracy was highest at flowering and progressively decreased thereafter. Similarly, high spectral separability at flowering decreased as the crops progressed through to end-senescence.

The error matrix for Held57 from 20 May 2004 imagery in Appendix E showed that poppy producers accuracy was just 63.21%, mainly because 95 of the 617 poppy pixels had been misclassified as wheat and 77 as house. Conversely, poppy producers accuracy in Held87 at mid-end flowering was considerably higher, at 97.96%, where only 4 poppy training pixels were misclassified as house, 4 as water and 1 as wheat.

Of note were the relatively similar overall accuracy results and Kappa coefficients between mid-end flowering and end-senescence in the middle of Table 6-10. In particular, the classification accuracy for Held115 at mid-end flowering was much lower than found at Held87 at a similar growth stage. Similarly, poppy producers accuracy was also low in Held115 at mid-end flowering, where 12 poppy training pixels were misclassified as vineyard, 6 as weeds and 1 as wheat. Given that the total number

of poppy training pixels was only 88, these misclassifications made a significant contribution to the low poppy producers accuracy results.

Table 6-10- Summary of Overall Classification Accuracy and corresponding Kappa coefficient in Helmand Province during the 2004 growth cycle

District	Date	Emergence	Stem Elongation	Beginning Flowering	Mid Flowering	End Flowering	Beginning Senescence	Mid Senescence	End Senescence	Average JM Distance	% Overall Classification Accuracy	% Kappa Coefficient
Held 87	25-Apr-04				*					1395	90.94	86.82
Held 57	28-Apr-04					*				1251	77.68	69.21
Held 87	17-May-04								*	1017	**74.73**	**64.97**
Held 115	17-May-04						*			1096	74.50	64.74
Held 115	29-Apr-04				*					1144	74.23	64.27
Held 57	20-May-04							*		1077	**67.64**	**56.15**

The high Kappa value for Held87 at mid-end flowering showed that this classification was the most reliable. Moderate agreement between reference and classification data was found in all other classifications.

When overall classification accuracy and spectral separability results were plotted onto a scatter plot in growth stage order (Figure 6-13) a strong positive linear association was found in the 2004 Helmand data.

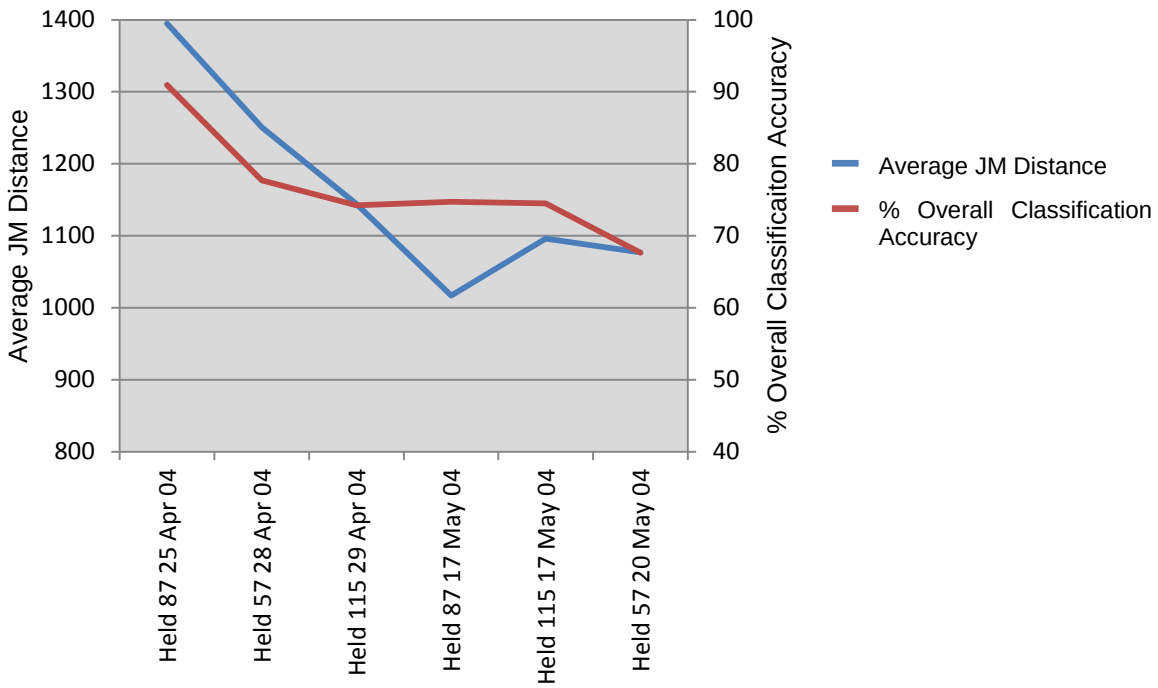

Figure 6-13 - % Overall Classification Accuracy and corresponding average JM Distance in Helmand Province during the 2004 growth cycle

The high r^2 value of 0.758 (Figure 6-14) confirmed a strong positive correlation, that high spectral separability in the 2004 Helmand data was linked to high overall classification accuracy. This r^2 value was much higher than had been seen in any of the previous datasets.

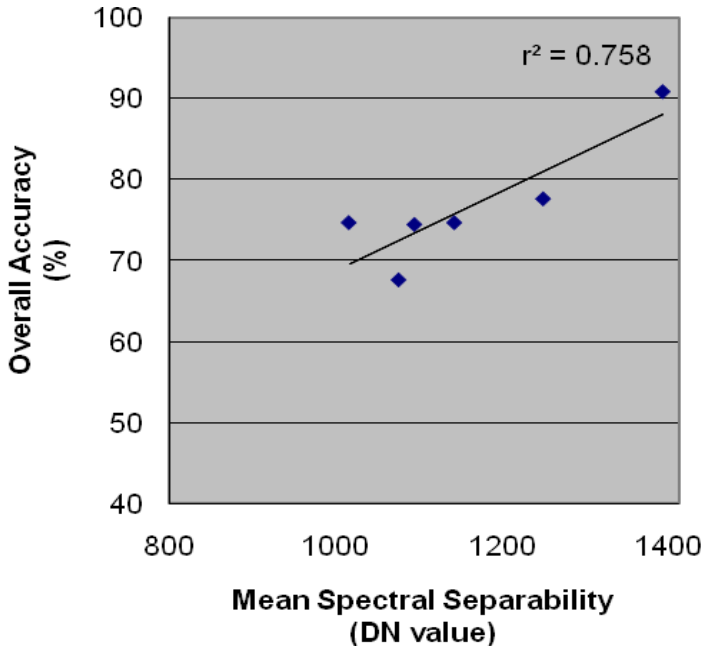

Figure 6-14- Regression Analysis: Strong positive relationship between Spectral Separability and % Overall Classification Accuracy in Helmand Province, 2004

Kandahar Province (2005)

The three Kandahar Province classified images can be viewed in Appendix D. Table 6-11 presents the overall classification accuracy and separability results from these classifications in classification accuracy order from stem elongation (no other images were available for comparison). Spectral separability results can be viewed in full in Appendix C, pages C-18 to 20. Error matrixes can be viewed in Appendix E.

District	Date	Emergence	Stem Elongation	Beginning Flowering	Mid Flowering	End Flowering	Beginning Senescence	Mid Senescence	End Senescence	Average JM Distance	% Overall Classification Accuracy	% Kappa Coefficient
Kand135	26-Mar-05		*							1107	83.63	71.83
Kand73	26-Mar-05		*							1085	77.69	67.07
Kand84	26-Mar-05		*							1150	72.58	64.92

Table 6-11 - Summary of average JM Distance, overall Classification Accuracy and Kappa coefficient in Kandahar Province during the 2005 growth cycle

Whilst the table shows uniform poor spectral separability in all three districts at stem elongation, overall classification accuracy results were, on average, higher than had been found from imagery acquired at a similar time in Helmand Province (2005).

The error matrices for Kand73 and Kand135 (see Appendix E) showed very low poppy producers accuracies of 27.78% and 39.69% respectively. In both sites these poor results were due to more wheat pixels being misclassified as poppy than the number of correctly classified poppy pixels.

As only three sets of data (overall classification accuracy and JM distance results) existed from the three images acquired in Kandahar Province it was deemed that no conclusions could be drawn from such a small dataset. Therefore, regression analysis was not performed on Kandahar data.

Summary

The single date overall classification accuracy results were consistent across Helmand and Nangahar Provinces. In 2005 overall classification accuracies were lowest at emergence-stem elongation but had improved by flowering. In 2004 highest overall classification accuracies were found at flowering but had lowered by the end of senescence. In Kandahar Province classification accuracies at stem elongation were higher than had been found in Helmand Province at emergence-stem elongation.

The results also showed that poppy producers accuracies improved from emergence-stem elongation through to flowering in 2005, and declined between mid-end flowering to senescence in 2004.

6.3.3 Significance of Single Image Classifications

Kappa results across all sites at every growth stage are summarised in column l of Table 6-12.

Table 6-12 – Results of Kappa Analysis – Test of Significance for Individual Image Classifications

District (a)	Date (b)	Emergence (c)	Stem Elongation (d)	Beginning Flowering (e)	Mid Flowering (f)	End Flowering (g)	Beginning Senescence (h)	Mid Senescence (i)	End Senescence (j)	% Overall Single Date Classification Accuracy (k)	% Kappa Coefficient – Single Date (l)	% Z Statistic (m)	Result[a] (n)
Nan 25	11-Apr-04				*					89.79	83.42	7.35	S[b]
Nan 25	25-Apr-04					*				79.11	68.02		
Nan 11	25-Apr-04					*				83.09	78.55	9.78	S[b]
Nan 11	17-May-04							*		67.10	58.13		
Nan 29	11-Apr-04				*					62.82	51.10		
Held 87	25-Apr-04				*					90.94	86.82	9.93	S[b]
Held 87	17-May-04								*	74.73	64.80		
Held 87	16-Feb-05		*							60.94	48.28	5.34	S[b]
Held 87	21-Mar-05			*						73.23	62.65		
Held 57	28-Apr-04					*				77.68	69.21	5.96	S[b]
Held 57	20-May-04							*		67.64	56.15		
Held 57	19-Feb-05	*								46.70	35.18	11.36	S[b]
Held 57	29-Mar-05				*					72.08	62.83		
Held 115	29-Apr-04				*					74.23	64.27	-0.20	NS[b]
Held 115	17-May-04						*			74.50	64.74		
Held115	10-Feb-05	*								42.46	32.30	6.16	S[b]
Held 115	21-Mar-05			*						61.67	47.67		
Kand 84	26-Mar-05		*							72.58	64.92		
Kand 73	26-Mar-05		*							77.69	67.07		
Kand 135	26-Mar-05		*							83.63	71.83		

[a]At the 99% confidence level

[b]S – significant, NS – not significant

Strong Agreement (80% +)
Moderate Agreement (40-80%)
Poor Agreement (less than 40%)

The table shows high Kappa values (Kappa coefficient greater than 80%) for Nan25 and Held87 images acquired at mid-end flowering. These results were shaded in green in column l and indicate that these classifications were the most reliable. Moderate agreement (40-80%) was found in twelve of the classifications. Poor agreement (less than 40%) was found in two classifications from Held57 and Held115 in 2005 (shaded in red) when imagery was acquired at emergence-stem elongation. These last results indicate that classifications of imagery acquired at the immature growth stages were the least reliable.

Delta Kappa and Z Statistic

In the cases where two images had been acquired at the same site at different growth stages (in all sites except in Kandahar Province and Nan29), Delta Kappa and the Z statistic were used to determine whether each classification produced a significantly different result. The Z statistic results are presented in column m of Table 6-12 and prove that the classification accuracy results were significantly different in all of the eight cases investigated, with the exception of Held115 in 2004. In this case no significant increase in overall classification accuracy was found between images acquired at mid-end flowering and beginning-mid senescence.

Summary

In the instances where moderate-high Kappa values were found and where significantly different results were found between images acquired from the same growth cycle, Kappa analysis validated the conclusions reached, that classification accuracies were highest during flowering and lowest at emergence-stem elongation.

6.3.4 Poppy Users Accuracy

In addition to determining poppy producers and overall classification accuracy trends Chapter 2 described the importance of identifying how well a classification identifies individual classes. The key indicator of classification accuracy was therefore determined by how well each output thematic map represented the real poppy on the ground. This section therefore presents poppy users accuracy results per province.

Nangahar Province (2004)

Poppy user's accuracies in Nangahar Province ranged from 72.92% (in Nan11 at mid-end senescence) to 97.12% (in Nan25 at mid-end flowering). Relative to all other cover types poppy user's accuracies were consistently placed in the top three highest user's accuracies, indicating that the classifications represented the real poppy on the ground well, as assessed in Figure 6-7. Coincident with the decline in both spectral separability and overall classification accuracy from mid-end flowering until mid-end senescence in Nangahar Province, poppy user's accuracies also declined during this time. Average JM distance and poppy user's accuracy results are displayed in Table 6-13 and Figure 6-15.

Table 6-13 – Average JM Distance and Single Date % Poppy Users Accuracy Results, Nangahar Province, 2004

District	Date	Emergence	Stem Elongation	Beginning Flowering	Mid Flowering	End Flowering	Beginning Senescence	Mid Senescence	End Senescence	Average JM Distance	Single Date % Poppy User's Accuracy
Nan 25	11-Apr-04				*					1378	97.12
Nan 25	25-Apr-04						*			1246	94.84
Nan 11	25-Apr-04					*				1313	94.23
Nan 29	11-Apr-04				*					1278	87.98
Nan 11	17-May-04							*		1047	72.92

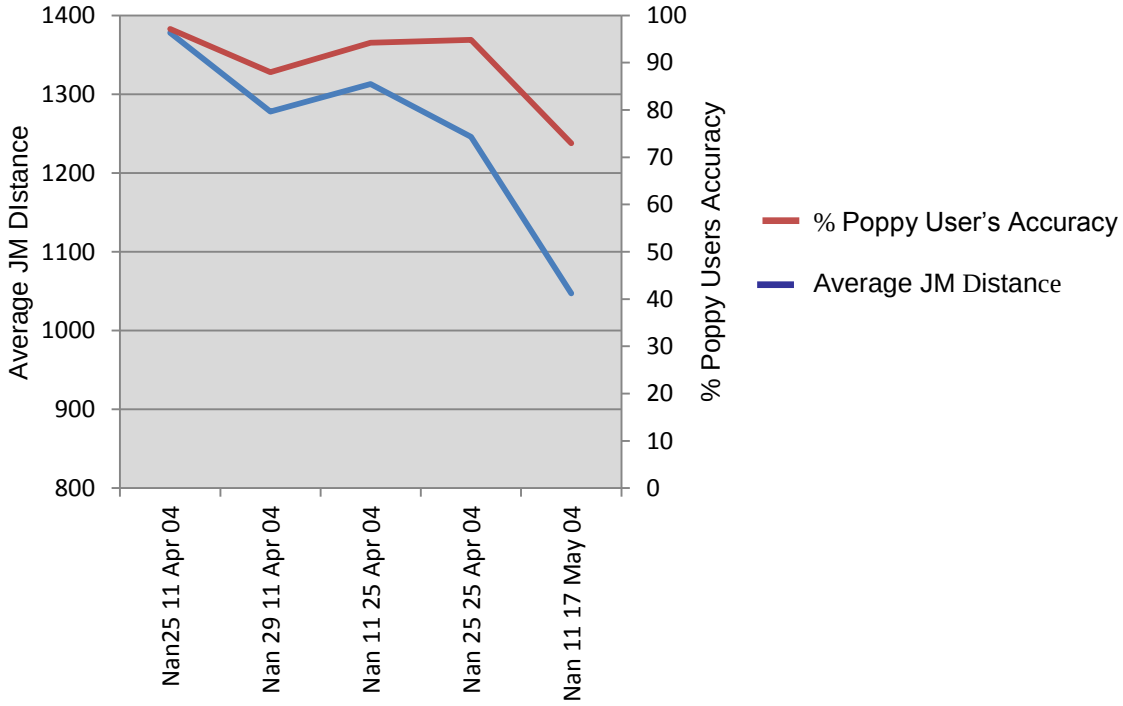

Figure 6-15 – Single Date % Poppy Users Accuracy Results and Spectral Separability results, Nangahar Province, 2004

The scatter plot in Figure 6-16 shows a high r^2 value of 0.87 indicating a strong positive correlation, that spectral separability and poppy user's accuracy results from Nangahar Province dataset are linked.

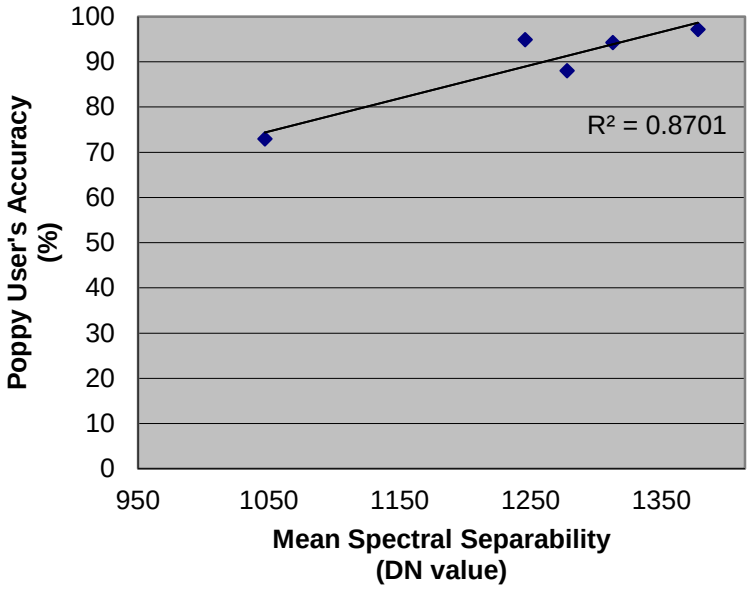

Figure 6-16 - Regression Analysis: Spectral Separability and % Poppy Users Accuracy for Nangahar Province, 2004

Helmand Province (2005)

Table 6-14 and Figure 6-17 show the results of JM distance and poppy users accuracy in the cases studied in Helmand Province in 2005. Figure 6-17 shows a general rise in spectral separability and classification accuracy from emergence to flowering. Of note are the very low poppy users accuracies found at the earliest growth stages of emergence-stem elongation (47.69% and 8.37%) and stem elongation (32.30%).

Table 6-14 – Average JM Distance and Single Date % Poppy Users Accuracy Results, Helmand Province, 2005

District	Date	Emergence	Stem Elongation	Beginning Flowering	Mid Flowering	End Flowering	Beginning Senescence	Mid Senescence	End Senescence	Average JM Distance	Single Date % Poppy User's Accuracy
Held 57	29-Mar-05				*					1138	63.36
Held 115	21-Mar-05			*						1171	59.38
Held 87	21-Mar-05			*						1225	48.11
Held 57	19-Feb-05	*								974	47.69
Held 87	16-Feb-05		*							831	32.30
Held115	10-Feb-05	*								1097	8.37

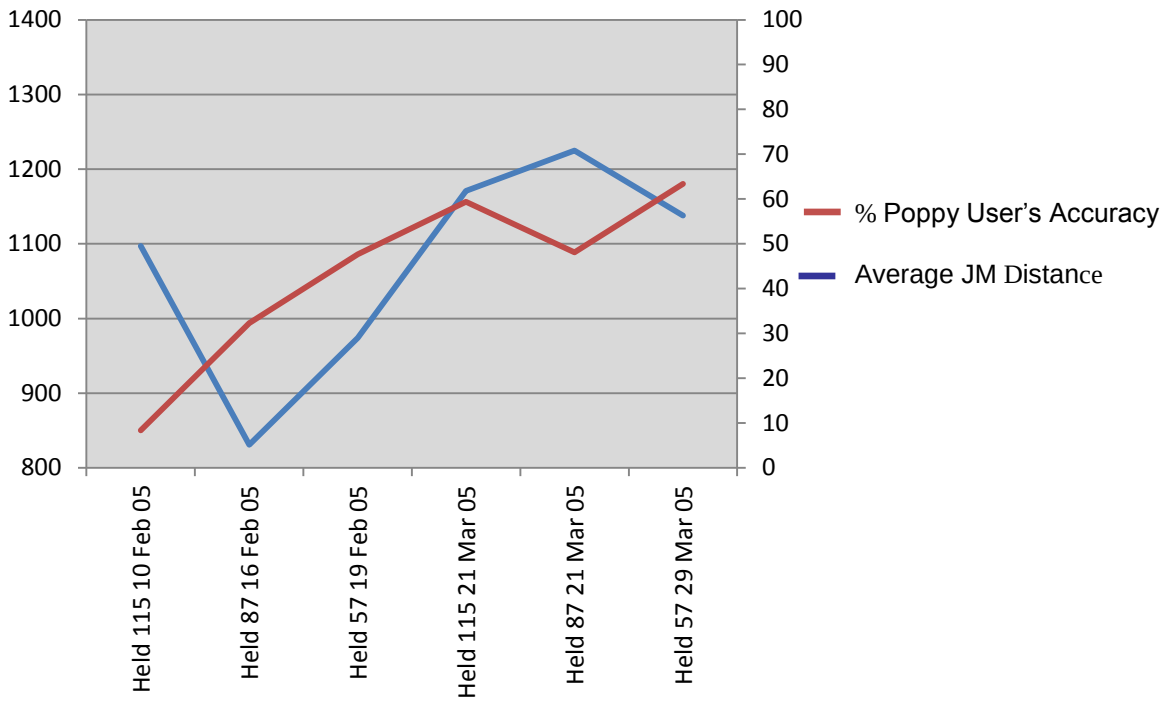

Figure 6-17 – Average JM Distance and Single Date % Poppy User's Accuracy Results, Helmand Province, 2005

However, the r^2 value of 0.115 (Figure 6-18) shows no relationship between spectral separability and poppy user's accuracy at the early growth stages in 2005 in Helmand Province.

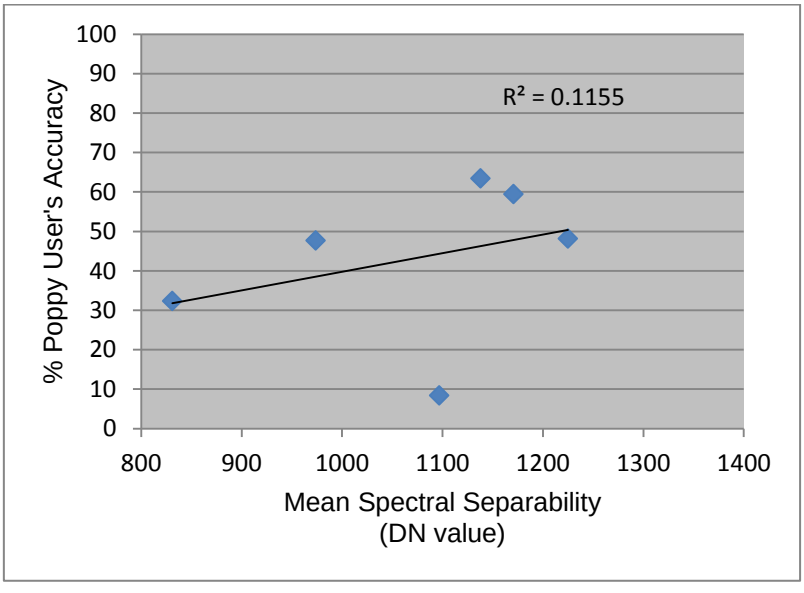

Figure 6-18 – Regression Analysis: Spectral Separability and % Poppy User's Accuracy for Helmand Province, 2005

Helmand Province (2004)

Table 6-15 and Figure 6-19 show poppy users accuracy results from 2004 in Helmand Province.

Table 6-15 – Single Date % Poppy User's Accuracy Results, Helmand Province, 2004

District	Date	Emergence	Stem Elongation	Beginning Flowering	Mid Flowering	End Flowering	Beginning Senescence	Mid Senescence	End Senescence	Average JM Distance	Single Date % Poppy User's Accuracy
Held 87	25-Apr-04				*					1395	97.08
Held 57	28-Apr-04					*				1251	96.09
Held 57	20-May-04							*		1077	89.86
Held 87	17-May-04								*	1017	89.60
Held 115	29-Apr-04				*					1144	66.35
Held 115	17-May-04						*			1096	44.35

Poppy user's accuracies range from 44.35% (Held115 at beginning-mid senescence) to 97.08% (Held87 at mid-end flowering).

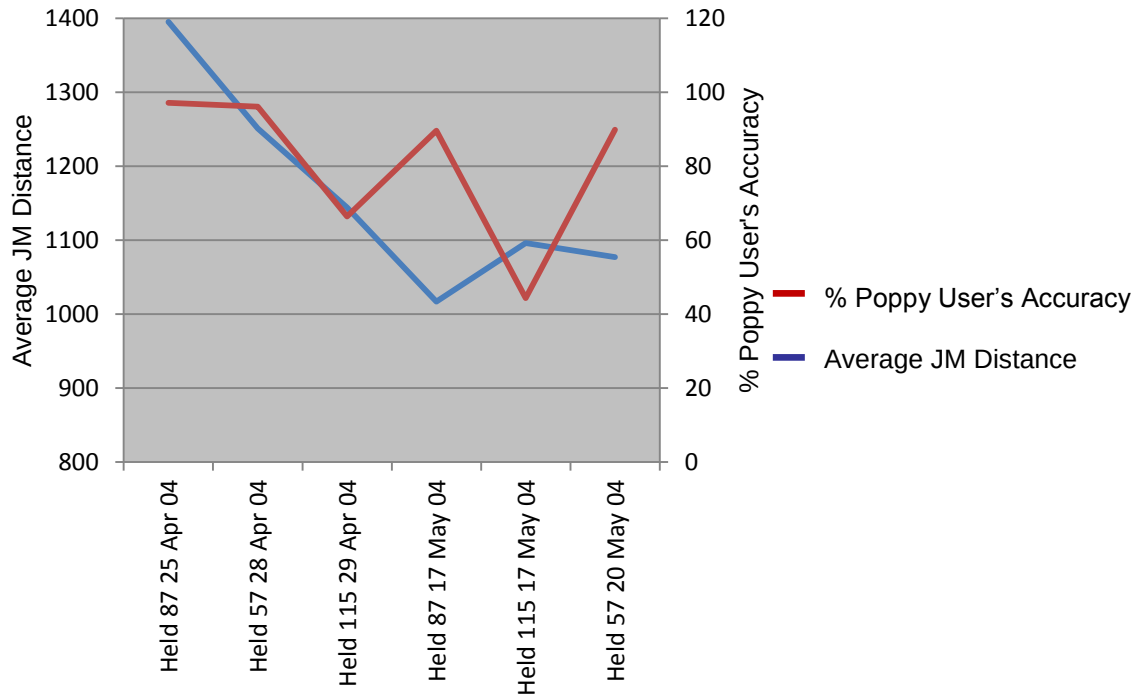

Figure 6-19– Single Date % Poppy User's Accuracy Results, Helmand Province, 2004

Like Nangahar Province, relative to users accuracies of all other cover types, poppy users accuracies were consistently placed in the top three highest accuracies, indicating that the classifications represented the real poppy on the ground well. The only exception to this was in Held115, where the error matrix revealed weeds, wheat, alfalfa and vineyard pixels were misclassified as poppy. This may have been due to disease reported by UN surveyors in this district (no further details given).

Overall, the results show that poppy user's accuracies decreased between mid-end flowering and end-senescence.

The r^2 value of 0.159 in Figure 6-20 shows that there was no linear relationship between spectral separability and poppy users accuracy in Helmand Province in 2004.

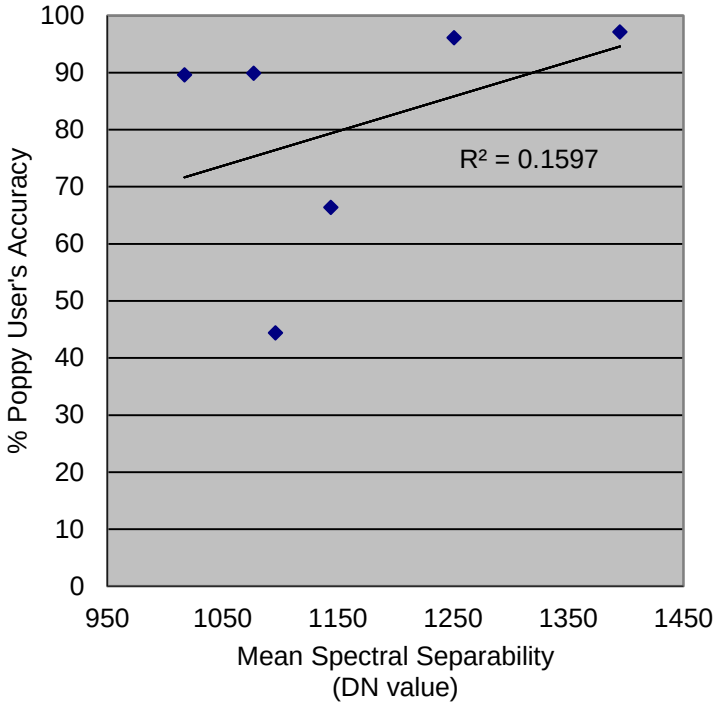

Figure 6-20 – Regression Analysis: Spectral Separability and % Poppy User's Accuracy for Helmand Province, 2004

Kandahar Province (2005)

Table 6-16 shows the poppy user's accuracy results from the three districts examined in Kandahar Province. It shows that whilst spectral separability results were relatively similar to results from Helmand Province at similar growth stages, poppy user's

accuracies were much higher than two of the Helmand Province sites at the earliest growth stages. Classification errors were predominantly between poppy and wheat, with wheat being misclassified as poppy.

Table 6-16 – Single Date % Poppy User's Accuracy Results Kandahar Province, 2005

District	Date	Emergence	Stem Elongation	Beginning Flowering	Mid Flowering	End Flowering	Beginning Senescence	Mid Senescence	End Senescence	Average JM Distance	Single Date % Poppy User's Accuracy
Kand84	26-Mar-05		*							1150	82.96
Kand135	26-Mar-05		*							1107	61.25
Kand73	26-Mar-05		*							1089	5.68

No conclusions could be drawn from the small dataset available from the three images acquired in Kandahar Province in 2005 (poppy user's accuracy and JM distance results).

Poppy Users Accuracy Summary

Both poppy users accuracies and JM distances increased between emergence and flowering in Helmand Province in 2005 and decreased between flowering and senescence in Helmand and Nangahar Provinces in 2004. However, unlike overall classification accuracy results from Nangahar and Helmand Provinces, no strong statistical relationship was found between spectral separability and poppy users accuracy. Kandahar Province results were the exception although the sample size was too small. Poppy users accuracy was therefore not related to spectral separability results or growth stage.

The next section investigates whether a relationship exists between spectral separability and classification accuracy, as per Objective 3.

6.4 Relationship between Spectral Separability and Classification Accuracy

Kappa and regression analysis revealed that the reliability of the overall classification accuracy results and the strength of the association between overall classification accuracy and spectral separability varied according to growth stage reached.

Conclusions are drawn from growth stages within the same cropping cycle, i.e. early growth stages to beginning of flowering in 2005 (Helmand and Kandahar Provinces) and mid-flowering to senescence in 2004 (Helmand and Nangahar Provinces).

End-Flowering to beginning of Senescence, 2004

Highest separability was achieved at mid-end flowering in 2004 (Nan25 and Held87) followed closely by end flowering-beginning senescence (Nan11, Held57 and Nan25), coincident with highest overall classification accuracies (see Table 6-17). Highest 2004 Kappa values were also found at these growth stages. Results from Nan29 at mid-flowering and Held115 at mid-end flowering were not included in this summary because either the Kappa co-efficient (Nan29) or the average JM distance (Held115) were low, making these two sites a-typical of the general findings at these growth stages.

Table 6-17 – Spectral Separability and Classification Accuracy at Mid-flowering-Beginning Senescence in Helmand and Nangahar Provinces, 2004

District	Date	Emergence	Stem Elongation	Beginning Flowering	Mid Flowering	End Flowering	Beginning Senescence	Mid Senescence	End Senescence	Average JM Distance	% Overall Single Date Classification Accuracy	% Kappa Coefficient – Single Date
Held 87	25-Apr-04				*					**1395**	**90.94**	86.82
Nan 25	11-Apr-04				*					**1378**	**89.79**	83.42
Nan 11	25-Apr-04					*				**1313**	**83.09**	78.55
Nan 25	25-Apr-04					*				**1246**	**79.11**	68.02
Held 57	28-Apr-04					*				**1251**	**77.68**	69.21
Held 115	*29-Apr-04*				*					***1144***	***74.23***	*64.27*
Nan 29	*11-Apr-04*				*					***1278***	***62.82***	*51.10*

Regression analysis (Figure 6-21) of the five images with the highest 2004 results reveals a very positive linear association at mid-flowering to beginning of senescence (r^2 value of 0.983), indicating that spectral separability and overall classification accuracy are related at these growth stages. Therefore, spectral separability can be used to predict overall classification accuracy at mid-flowering to beginning of senescence.

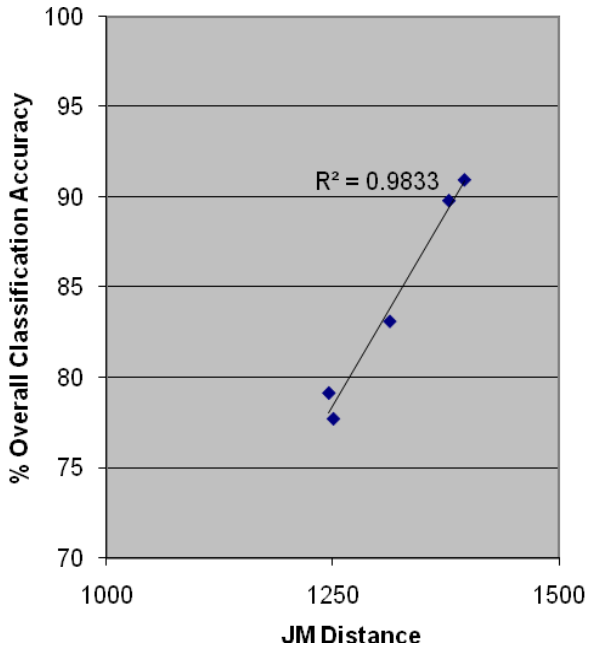

Figure 6-21 - Relationship between Spectral Separability and % Overall Classification Accuracy at Mid flowering–Beginning Senescence in Nangahar and Helmand Provinces, 2004

Beginning-End Senescence, 2004

At the latter stages of the 2004 growth cycle, spectral separability, overall classification accuracy and Kappa values were lower (Table 6-18). Accordingly, regression analysis (Figure 6-22) of the four images with the lowest 2004 results reveals no linear relationship at beginning-end senescence (r^2 value of 0.01), indicating that spectral separability and overall classification accuracy were not linearly related at these growth stages.

Table 6-18 – Spectral Separability and Classification Accuracy at Beginning Senescence-End Senescence in Nangahar and Helmand Provinces, 2004

District	Date	Emergence	Stem Elongation	Beginning Flowering	Mid Flowering	End Flowering	Beginning Senescence	Mid Senescence	End Senescence	Average JM Distance	% Overall Single Date Classification Accuracy	% Kappa Coefficient – Single Date
Held 115	17-May-04						*			**1096**	**74.5**	64.74
Held 57	20-May-04							*		**1077**	**67.6**	56.15
Nan 11	17-May-04							*		**1047**	**67.1**	58.13
Held 87	17-May-04								*	**1017**	**74.7**	64.97

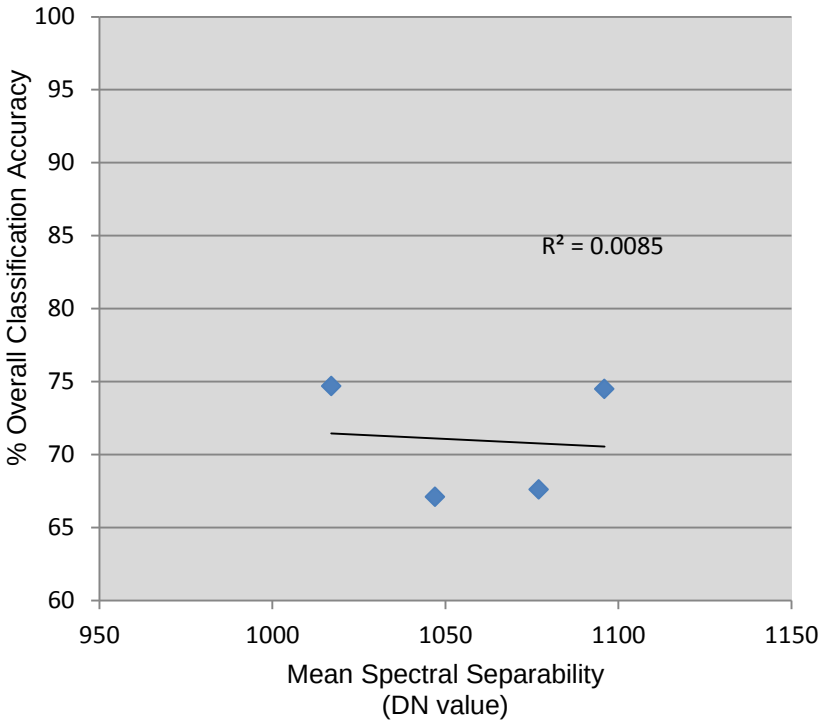

Figure 6-22 - Relationship between Spectral Separability and % Overall Classification Accuracy at Beginning-End Senescence in Nangahar and Helmand Provinces, 2004

Stem Elongation – Mid-Flowering, 2005

In 2005 lowest separability and overall classification accuracy results were achieved at emergence-stem elongation. The Kappa coefficients confirmed that results from Held57 and Held115 were the least reliable. Regression analysis of all other 2005 classification and separability data in Figure 6-23 shows a very weak positive relationship between stem elongation and mid-flowering with an r^2 value of 0.28.

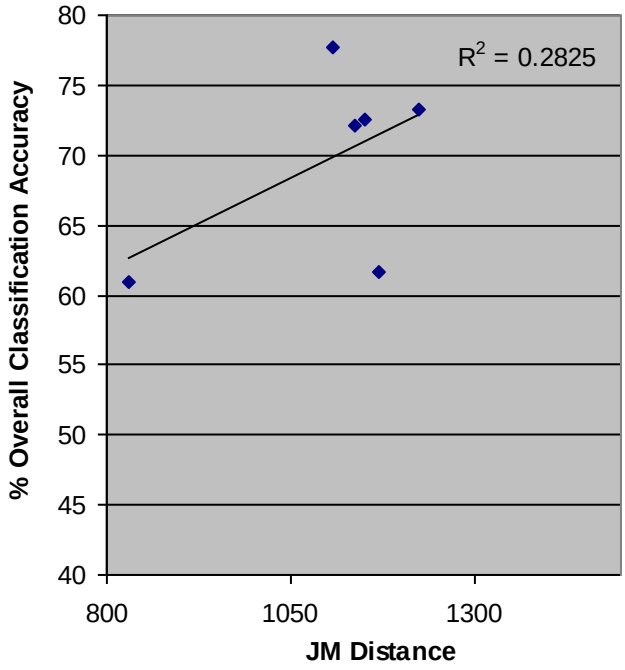

Figure 6-23 - Relationship between JM Distance and % Overall Classification Accuracy at Stem Elongation-Mid Flowering in Helmand and Kandahar Provinces, 2005

6.4.1 Chapter Summary

Temporal and Spatial Variability

As per Objective 3, and consistent with both the predictions made from visual interpretation of aerial photography in Chapter 3 and with separability conclusions drawn in Section 6.2.3, the results confirmed that spectral separability and overall classification accuracy was related to growth stage; that the highest overall classification accuracies were found during flowering and the lowest were found at emergence-stem elongation. This relationship was also quantified through statistical testing of the data, which confirmed that overall classification accuracy can be predicted from spectral separability at flowering. In addition, the results revealed that spectral separability and classification accuracy were spatially consistent across each Province, that spectral separability and overall classification accuracy improved with crop maturity until flowering, and after flowering spectral separability and overall classification accuracy decreased.

The next chapter (Chapter 7) presents results from the multi-temporal investigations to determine whether a multi-temporal classification approach improves classification accuracy, relative to those performed on single image dates, as per Objective 4.

Chapter 8 discusses the causes behind the patterns observed, based on the general spectral characteristics of vegetation and bare soils previously outlined in Chapter 2 and their consequences on classification accuracy, as per Objective 1.

7. Multi-temporal Results

The previous chapter presented spectral separability and classification accuracy results from single images acquired across the nine sites investigated, in order to determine the relationship between single date classification accuracy and spectral separability.

This chapter presents results obtained with more dimensions added to the MLC clustering process by using two-dated image classifications to establish whether multi-temporal image classifications are more accurate than single-date classifications, as per Objective 4. The two-date classifications were generated using two steps; combining pairs of images into a single two-date stack using the layerstack option in Erdas Imagine 8.7 and classifying the image stacks using the same method used in the single-date classifications (the MLC). Unfortunately, image pairs were not available for Nan25 in Nangahar Province or the three sites in Kandahar Province so results only focus on two districts in Nangahar and three in Helmand Provinces.

The same measures used in the single date results have been repeated to determine the accuracy of the two-dated classifications. Visual analysis of two-date classifications *versus* the corresponding single classifications was conducted first, before standard error matrices were used to calculate overall, user's and producer's accuracies for the two-date classifications. Kappa statistics were also used to determine whether the two-dated classification method was more reliable and produced significantly improved classification accuracies then single image classifications alone.

7.1 Visual Analysis

For simplicity, multi-temporal results are illustrated from one district only, from Held115 in 2005. All other two-date classifications have been included in Appendix D.

The example in Figure 7-1 illustrates (a) the 10km x 10 km two-date 05 classification of Held115 05 and location of Segment 3, (b) an enlargement of Segment 3 from the two-date 05 classification. For comparison, the results of the single image classifications have been included as enlargements of S3 in (c) dated 10 Feb 05 and (d) dated 21 Mar 05.

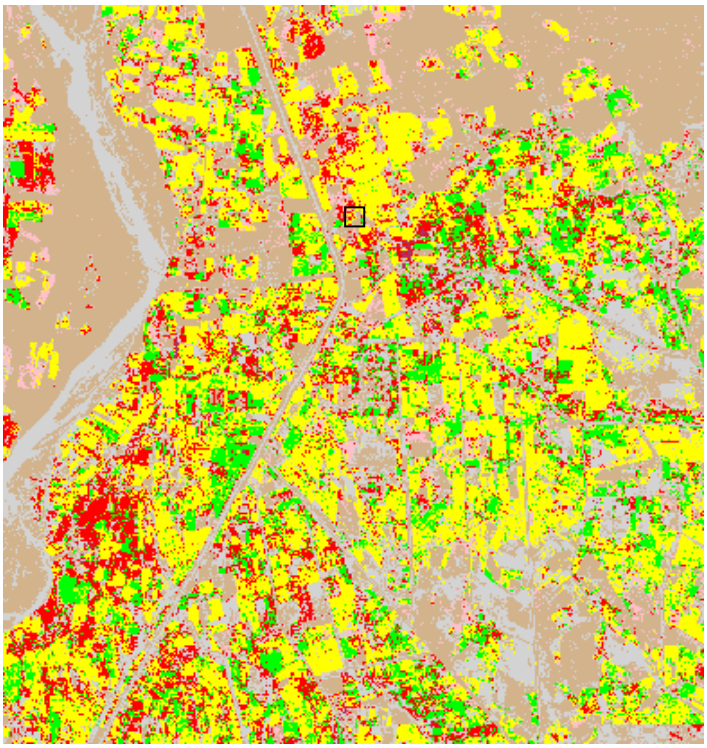

(a) Held115 10 Feb 05 and 21 Mar 05

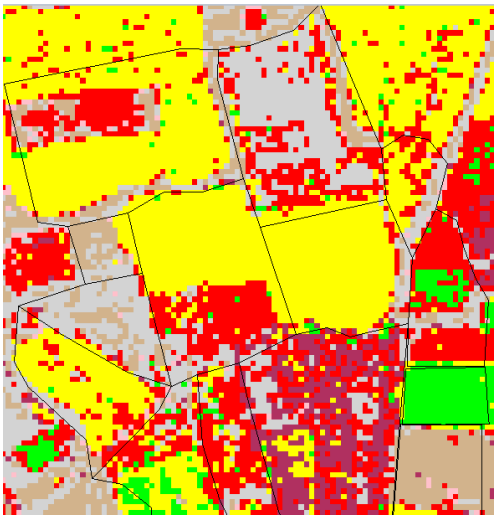

(b) Held115 **S3** 10 Feb 05 and 21 Mar 05

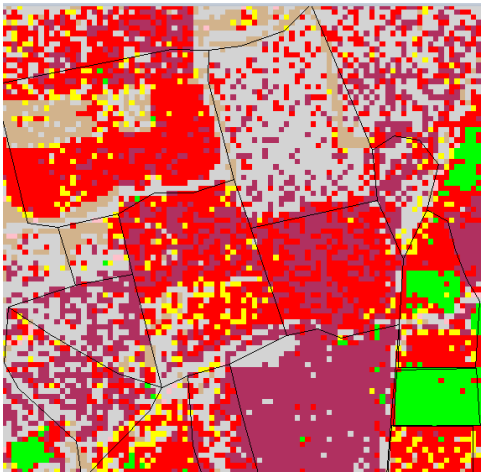

(c) Held115 **S3** 10 Feb 05

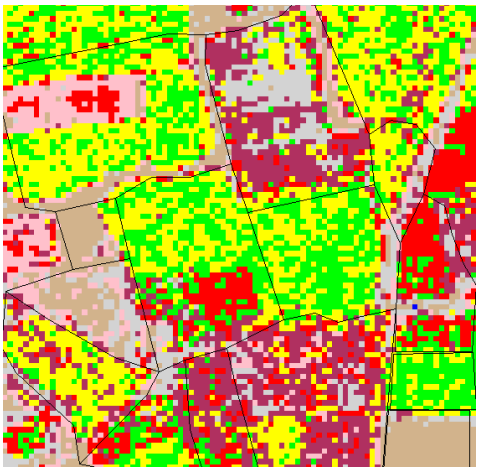

(d) Held115 **S3** 21 Mar 05

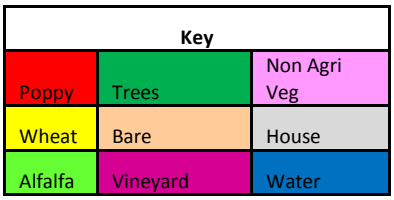

Figure 7-1 - Multi-temporal classification of (a) Held115 05 with S3 location; (b) Held115 S3 05 classification, (c) Held115 S3 10 Feb 05 and (d) Held115 S3 21 Mar 05

The two-date classification in (a) shows that wheat and bare are the predominant cover types and appear to have been classified well, with smaller amounts of alfalfa and poppy present in the surrounding fields. Spectral confusion has occurred however, as houses are found in the

river channel at the left of the image. Spectral confusion was also evident in the Feb 05 classification (at stem-elongation) as water in the channel was incorrectly surrounded by houses but surrounded by bare in the later Mar 05 image (at beginning-mid flowering).

The SCP's from these image dates reveal broad and overlapping class ranges for all cover types which explains the spectral confusion evident on all three classified images.

The enlargement of the two-date classification of Segment 3 in (b), clearly demonstrates an improvement in classification of cover types in the two-date classification. For example, wheat appears to have been classified consistently well, but with some isolated misclassified poppy pixels present within the wheat fields. However, very little wheat was identified in the Feb 05 imagery at stem elongation, mainly as vineyards (incorrectly) appeared to be the predominant crop, particularly in the large field at the bottom of the enlargement and in some of the fields that the two-date classification identified to be wheat.

By beginning-mid flowering, spectral confusion was still evident in the wheat fields, particularly between wheat and alfalfa – and this was evidenced on the SCP's, where large overlap existed between these two cover types. However, both wheat and alfalfa appear to have been classified well in the two-date image.

Overall, the above example demonstrates the findings of the majority of multi-temporal classifications, that visually, they were more accurate than their corresponding single image classifications. However, the example also demonstrates how difficult it was to determine classification accuracy based on visual analysis alone, hence error matrices were used to quantify classification accuracy.

7.2 Overall Multi-temporal Classification Accuracy

The overall multi-temporal classification accuracy results for each two-dated classification are presented in column l of Table 7-1. For comparison, overall accuracy results from the original single date classifications have been included in column k of the results table. Column m shows the resultant percentage change in classification accuracy between the single- and two- date classifications.

Nangahar Province (2004)

Table 7-1 shows that two-date image classifications increased overall classification accuracy against single date classifications for all instances in Nangahar Province. For example, in Nan11 a higher overall classification accuracy of 86.0% was achieved using the two-dated

image (end-flowering/beginning senescence image fused with the mid-end senescence image) showing an improved accuracy of between 2.1% and 18.9% over the single date image classifications. Similarly, the two-date classifications also increased accuracy by 2.47% and 13.15% in Nan25.

Table 7-1 - Mean Spectral Separability and Overall Classification Accuracy - Multi-Temporal Classification

District	Date	Emergence	Stem Elongation	Beginning Flowering	Mid Flowering	End Flowering	Beginning Senescence	Mid Senescence	End Senescence	% Overall Single Date Classification Accuracy	% Overall Multi-Temporal Classification Accuracy	% Improvement in Overall Classification Accuracy
(a)	(b)	(c)	(d)	(e)	(f)	(g)	(h)	(i)	(j)	(k)	(l)	(m)
Nan 11	25-Apr-04					*				**83.09**	**86.00**	2.91
Nan 11	17-May-04							*		**67.10**		18.9
Nan 25	11-Apr-04				*					**83.42**	**92.26**	2.47
Nan 25	25-Apr-04					*				**79.11**		13.15
Held 57	28-Apr-04					*				**77.68**	**88.24**	10.56
Held 57	20-May-04							*		**67.64**		20.6
Held 57	19-Feb-05	*								**46.70**	**82.92**	36.22
Held 57	29-Mar-05				*					**72.08**		10.84
Held 87	25-Apr-04				*					**90.94**	**83.51**	**-7.43**
Held 87	17-May-04								*	**74.73**		8.78
Held 87	16-Feb-05		*							**60.94**	**81.5**	20.56
Held 87	21-Mar-05			*						**73.23**		8.27
Held 115	29-Apr-04				*					**74.23**	**87.12**	**12.89**
Held 115	17-May-04						*			**74.50**		**12.62**
Held 115	10-Feb-05	*								**42.46**	**82.72**	40.26
Held 115	21-Mar-05			*						**61.67**		21.05

Helmand Province (2004 and 2005)

Similar results were also found in Helmand Province during both 2004 and 2005 where two-date image classifications increased classification accuracy over single date classifications in all but one instance. Greatest improvements were consistently found when the image pairs were acquired at the early and later growth stages (i.e. emergence-stem elongation and senescence).

The one exception where a two-date classification didn't achieve a higher accuracy than a single image date was from imagery acquired in Held87 during 2004 at mid-end flowering. This high exception may have occurred because the Held 87 image acquisition coincided well

with peak poppy flowering (i.e. peak reflectivity). However, this cannot be proved as no concurrent and in situ reflectivity measurements were taken from the poppy crop.

Judging by the MODIS profile generated from the Held87 S1 segment (previously shown in Figure 4-4 of Chapter 4), the 25 Apr 04 acquisition occurred at the end of a three week period of high vegetation activity, indicating that a 3 week lead-in window of acquisition opportunity may exist for optimum single data classification accuracy.

7.2.1 Summary

The two-date classifications achieved higher overall accuracies than the corresponding single image classifications with one exception. The magnitude of improvements ranged from minor enhancements (minimum 2.47%) to larger increases (maximum 40.26%). The largest improvements coincide with the early and later growth stages. Only minor improvements were observed during flowering. Both the reliability and significance of these results are tested in the next section using Kappa statistics.

7.2.2 Kappa Statistic

Kappa analysis conducted on the multi-temporal datasets provided an additional measure of accuracy for multi-temporal classifications (less chance agreement) to determine the reliability of the results. The combined results from Kappa analysis are expressed as percentages in column l of Table 7-2. The single data Kappa statistic results are included in column k for comparison. Column m shows the resulting percentage change.

As established in the previous chapter (Section 6.3.3) two single date classifications showed strong agreement between the reference and evaluation data (Kappa co-efficient above 80%, shaded green in column k), indicating reliable results. Here four two-date classifications from 2004 also produced reliable results between mid-end flowering and senescence in Nan25 and Nan11, Held57 and Held115. The remainder from the 2005 emergence-flowering classifications showed moderate agreement between reference and classification data. Therefore, two-dated classifications were proved to be more reliable.

Similar to the improvements found in two-date overall classification accuracy, the magnitude of improvements of the Kappa coefficients over single date accuracies varied according to the growth stage. Small improvements were established at mid-end flowering (ranging from 7.45-22.85%) and larger improvements when images were acquired at emergence-stem elongation (ranging from 33.22-50.42%).

District	Date	Emergence	Stem Elongation	Beginning Flowering	Mid Flowering	End Flowering	Beginning Senescence	Mid Senescence	End Senescence	Single Date % Kappa Coefficient	Multi-Date % Kappa Coefficient	% Improvement in Kappa
(a)	(b)	(c)	(d)	(e)	(f)	(g)	(h)	(i)	(j)	(k)	l)	(m)
Nan 25	11-Apr-04				*					**83.42**	**87.54**	8.84
Nan 25	25-Apr-04					*				**68.02**		24.24
Nan 11	25-Apr-04					*				**78.55**	**82.17**	7.45
Nan 11	17-May-04							*		**58.13**		27.87
Held 87	25-Apr-04				*					**86.82**	**76.35**	-3.31
Held 87	17-May-04								*	**64.97**		18.54
Held 87	16-Feb-05		*							**48.28**	**73.61**	33.22
Held 87	21-Mar-05			*						**62.65**		18.85
Held 57	28-Apr-04					*				**69.21**	**83.19**	19.03
Held 57	20-May-04							*		**56.15**		32.09
Held 57	19-Feb-05	*								**35.18**	**76.34**	47.64
Held 57	29-Mar-05				*					**62.83**		19.99
Held 115	29-Apr-04				*					**64.27**	**81.89**	22.85
Held 115	17-May-04						*			**64.74**		22.38
Held115	10-Feb-05	*								**32.30**	**74.59**	50.42
Held 115	21-Mar-05			*						**47.67**		35.05

Strong Agreement (80% +)
Moderate Agreement (40-80%)
Poor Agreement (less than 40%)

Table 7-2 -– Results of Kappa Analysis – Test of Significance for Individual Error Matrices from Single and Multi-date Image Classifications

Overall, the Kappa coefficients indicated that the two-date classifications were more reliable than fifteen of the sixteen single date results. Again, the exception to this was Held87 (2004) at mid-end flowering, which achieved the highest single-date classification accuracy.

Delta Kappa

Delta Kappa (normally distributed as Z) was used to determine the significance of the two-date classifications, i.e. whether the increases in accuracy of two-date results were significant. To do this, the results from the best single-date classification accuracy per site at each growth cycle were compared with the corresponding multi-temporal results. The choice was based on the assumption that future poppy surveys may be limited to using single date imagery. Therefore, single images should be acquired at the best growth stage for optimum

classification results. Consequently, the Z statistic was calculated using a single date with the highest Kappa coefficient from each image pair (column k in Table 7-3) and compared with the corresponding multi-temporal image Kappa coefficient (column l). The Z statistic is presented in column m and the significance in column n.

Table 7-3 shows that in five of the eight multi-temporal datasets the two-date classifications resulted in significantly higher accuracies than single date classifications (shaded in green) - Held87 (2005), Held57 (both years) and Held115 (both years). Of the remaining three results, two-date classifications from both districts in Nangahar Province resulted in insignificant increases in classification accuracy; one from Nan25 (2004) where mid-end flowering and end flowering-beginning senescence images were fused together; the other in Nan11 (2004) at end flowering-beginning senescence and mid-end-senescence.

Table 7-3 – Results of Kappa Analysis for Comparison between Single versus Multi-temporal classifications

District	Date	Emergence	Stem Elongation	Beginning Flowering	Mid Flowering	End Flowering	Beginning Senescence	Mid Senescence	End Senescence	Single Date % Kappa Coefficient	Multi-date % Kappa Coefficient	Z Statistic	Result
(a)	(b)	(c)	(d)	(e)	(f)	(g)	(h)	(i)	(j)	(k)	(l)	(m)	(n)
Nan 25	11-Apr-04				*					83.42	**87.54**	2.34	**NS***
Nan 25	25-Apr-04					*				68.02			
Nan 11	25-Apr-04					*				78.55	**82.17**	2.05	**NS***
Nan 11	17-May-04							*		58.13			
Held 87	25-Apr-04				*					86.82	**76.35**	-5.35	**S****
Held 87	17-May-04								*	64.97			
Held 87	16-Feb-05		*							48.28	**82.17**	4.25	**S***
Held 87	21-Mar-05			*						62.65			
Held 57	28-Apr-04					*				69.21	**83.19**	7.29	**S***
Held 57	20-May-04							*		56.15			
Held 57	19-Feb-05	*								35.18	**76.34**	5.80	**S***
Held 57	29-Mar-05				*					62.83			
Held 115	29-Apr-04				*					64.27	**81.89**	8.11	**S***
Held 115	17-May-04						*			64.84			
Held115	10-Feb-05	*								32.30	**74.59**	10.66	**S***
Held 115	21-Mar-05			*						47.67			

*S - Significant at 0.1 level, NS – Not Significant

** - The two-date image classification was worse than the single image date classification.

The spectral coincidence plots for both locations only showed small increases in variance for each crop between the first and second images. It is possible the single images used in these two-date classifications were not collected far enough apart in the growth cycles for sufficient bio-physical changes to engender noteworthy changes to spectral characteristics. As a result, in these instances, two-dated classifications were not significantly different from the best single image classifications. The third exception was Held87 (2004) at mid-end flowering, where the Z statistic of -5.35 confirmed that the multi-temporal result was significantly less accurate than the single-date result. Therefore, there was no additional value in Held87 by classifying two images acquired at mid-end flowering and end-senescence.

In each of the five cases where the two-date results were significantly higher than the single-date accuracies, the single date % Kappa coefficients (column k) were lower than 70%. This percentage appears to be an important threshold for determining whether a second image (two-date classification) is required to improve upon the accuracy of a single date classification. For example, should the first image produce a Kappa coefficient of less than 70% a second image is required to improve the classification result.

7.3 Multi-temporal Poppy User's Accuracy

Also investigated was the effect of using two-date classifications on poppy user's accuracies. For comparison the results are presented in column l of Table 7-4, adjacent to single date poppy user's accuracies (column k).

Nangahar Province

Across Nangahar Province two-date image classifications increased poppy user's accuracy over single date classifications. The largest improvement over single date accuracy was at mid-end senescence in Nan11 (21.69%).

Helmand Province

Similarly, poppy user's accuracies using two-date image classifications also improved in 10 of the 12 images from Helmand Province. Again, the magnitude of improvements ranged from very minor increases to large enhancements dependant on the growth stage. The smallest changes were linked to flowering, where accuracy increased by just 0.67% in Held57 (2004) at end flowering-beginning senescence, 1.89% in Held87 (2005) at beginning-mid flowering and by 7.72% in Held115 (2004) at mid-end flowering.

The largest improvements over single classifications were found at emergence-mid flowering in Held57 (26.25%) and Held115 (24.96%).

Two-date poppy user's accuracy results were poorer than single date results in Held87 (-0.5%) in 2004 where the highest single-date classification accuracy was achieved at mid-end flowering and in Held115 (-26.05%) in 2005 at beginning-mid flowering. The latter anomaly was due to disease affecting both poppy and wheat which is discussed further in Chapter 8.

Table 7-4– Poppy User's Accuracy Results after Multi-temporal Classification

District	Date	Emergence	Stem Elongation	Beginning Flowering	Mid Flowering	End Flowering	Beginning Senescence	Mid Senescence	End Senescence	Single data % Poppy User's Accuracy	Multi-Temporal % Poppy User's Accuracy	% Improvement in poppy user's accuracy
(a)	(b)	(c)	(d)	(e)	(f)	(g)	(h)	(i)	(j)	(k)	(l)	(m)
Nan 11	25-Apr-04					*				94.23	94.61	**0.38**
Nan 11	17-May-04							*		72.92		**21.69**
Nan 25	11-Apr-04				*					97.12	97.35	**0.23**
Nan 25	25-Apr-04					*				94.84		**2.51**
Held 57	28-Apr-04					*				96.09	96.76	**0.67**
Held 57	20-May-04							*		89.86		**6.90**
Held 57	19-Feb-05	*								47.69	73.94	**26.25**
Held 57	29-Mar-05				*					63.36		**10.58**
Held 87	25-Apr-04				*					97.08	96.58	**-0.50**
Held 87	17-May-04								*	89.60		**6.98**
Held 87	16-Feb-05		*							32.30	50.00	**17.70**
Held 87	21-Mar-05			*						48.11		**1.89**
Held 115	29-Apr-04				*					66.35	74.07	**7.72**
Held 115	17-May-04						*			44.35		**29.72**
Held 115	10-Feb-05	*								8.37	33.33	**24.96**
Held 115	21-Mar-05			*						59.38		**-26.05**

7.3.1 Poppy User's Accuracy Summary

Significantly, the two-date classifications improved poppy user's accuracies in six out of the eight datasets studied, similar to that achieved with overall classification accuracy. Again, the magnitude of improvements over single date accuracies varied according to the growth stage at the time of imaging, from minor enhancements at flowering to larger increases at the earliest growth stages.

7.4 Chapter Summary

When pairs of images acquired at different growth stages over the same areas were fused, class training signatures were characterised by eight bands of spectral data rather than the standard four. This meant that more dimensions were added to the clustering process.

Two-dated classifications were statistically proven to achieve significantly higher overall classification accuracies than the single-date classifications in the majority of cases, when images in each pair were acquired at growth stages where the crops had sufficiently different spectral characteristics. In these instances the magnitude of improvement varied according to the stage of maturity at the time of imaging. Statistically, the most significant improvements coincided with the early stages of emergence-stem elongation. Insignificant increases were found when pairs of images were acquired close together, for example between mid-flowering and beginning of senescence.

In the cases where single images achieved similar or more accurate results than their corresponding multi-temporal classifications, the single-date images were acquired at either mid-end flowering (Nan25 and Held87) or end flowering-beginning senescence (Nan11). In these instances their Kappa coefficients were greater than 70%. This discovery of the 70% Kappa coefficient threshold is useful for future poppy surveys as it proves that a second image can improve the accuracy of poppy identification if a poorly timed single image is collected (i.e. not during peak photosynthetic activity). Moreover, when weather constraints and direct competition from other image users means that optimum single date collections may not be achieved, it proves that the additional cost and processing time for pairs of images outweighs the risks of poor identification accuracy from a single image acquisition at emergence or end of senescence. For mission planning purposes therefore, the default aspiration should be to acquire two images at different growth stages to increase the chances of poppy identification success.

The next chapter draws together all results from this study, summarises what factors influenced data collection, how image processing activities were influenced by the choice of classification technique and the causes and consequences of spectral separability on classification accuracy.

8. Summary and Discussion

This chapter summarises the key elements from each chapter in order to draw out the main findings of this study. Section 8.1 investigates how factors relating to the application of remote sensing for poppy identification (identified in the Literature Review in Chapter 1 and further investigated in Chapters 2 and 3), influenced data collection.

Section 8.2 discusses the factors which influenced image processing, including how the choice of classification technique was influenced by end-user requirements and how the performance of the Maximum Likelihood Classification (MLC) was improved through the collection of independent and non-spatially auto-correlated data. It begins with a short summary of the limitations of the image registration process.

Section 8.3 discusses the potential factors thought to influence the spectral separability of the poppy crop and their consequences on classification accuracy.

8.1 Factors Influencing Data Collection

This section discusses the factors which influenced data collection, including the reliance on UN, US and UK assets to provide ground, aerial and satellite data, the use of MODIS NDVI data to predict suitable times for image acquisition and the presence of ground data errors caused by human error, in part due to Afghanistan's hostile and difficult terrain.

8.1.1 Site Selection

An experiment was set up in Chapters 4 and 5 to collect multi-temporal datasets at eleven sites across all poppy growth stages and over two different growth cycles. The eleven sites were distributed across three different geographical regions in Afghanistan where the highest opium poppy cultivation was recorded in 2003. It was anticipated the eleven sites would be representative of the breadth of poppy growing conditions in Afghanistan covering all major environmental conditions and agricultural practices.

Unfortunately, not all of the images were acquired at the requested growth stages. This made it difficult to distinguish between the geographical and temporal influences on spectral separability.

Initially, Badakshan Province was selected in the north because poppy is rain-fed and grown at high altitudes, in contrast to the flat irrigated poppy cultivation areas of Helmand Province

to the south and the high altitude cultivation areas of Nangahar Province in the east. Although multi-temporal datasets were requested across the 2004 and 2005 growth cycles only partial collection took place in Badakshan. Consequently, the province was discarded and replaced with Kandahar, the only other dataset available due to the reliance on UNODC and UK data sources, unavoidably narrowing the scope of this research to irrigated areas.

In Nangahar Province multi-temporal ground and imagery datasets were collected in both years as requested but gaps in the data led to one district having to be discounted. Additionally, the threat of an Afghan Government backed eradication program meant few farmers planted poppy in 2005 leaving data from the 2004 Nangahar season as the only viable source. Lastly, the 2004 image data was collected four weeks later than requested and resulted in no data from the early growth stages (emergence and stem elongation). It was therefore only possible to investigate and comment on temporal patterns from two mid-late growth stages in Nangahar Province over just one season, once again limiting the scope of this study.

The third province chosen for investigation was Helmand, situated in the south where the climate is warm and dry and the flat cropped lowlands are irrigated by a series of well-connected irrigation canals and ditches. As requested, multi-temporal datasets were collected in 2004 and 2005 but gaps meant that the investigation was limited to three sites. In some instances poppy was not grown in the same fields over both years but this research assumed that the crops would look the same at similar growth stages regardless of year because similar poppy farming practices and environmental conditions were found throughout. This meant it was possible to compare imagery collected from the mid-late growth stages in 2004 and from early to mid-cycle growth stages in 2005 to identify the relationships between spectral separability, classification accuracy and growth stages across both seasons.

In Kandahar Province, selected to replace Badakshan, there is a greater reliance on horticulture and vegetables despite its close geographic proximity to Helmand and similar environmental conditions. Originally the data was only intended to supplement Helmand, but despite the similar environmental conditions the differences in farming practices meant the types of crops were more diverse. Therefore, Kandahar data was used in conjunction with Helmand and Nangahar so temporal and spatial patterns could be investigated. Unfortunately, image data was collected only once in Kandahar Province in the 2005 growth cycle. This limited the scope of this study to a single examination of geographical variability across

Kandahar districts at stem elongation because the poppy growth cycle could not be monitored over successive dates.

Overall this meant that the investigation could only compare the following useful and meaningful results:

- Three sites from one province (Helmand) across two growth cycles, to examine temporal and geographical consistency.
- Six sites from two provinces (Helmand and Kandahar) across one growth cycle (at early-mid growth stages) to examine geographical consistency.
- Six sites from two provinces (Helmand and Nangahar) across one growth cycle (at mid-late growth stages) to examine geographical and temporal consistency.

8.1.2 Image Collection

Poppy identification using remote sensing requires good quality, high resolution images to be acquired during temporal windows to ensure the best opportunity for poppy discrimination. Therefore, this study sought to establish the feasibility of using high resolution multi-spectral and multi-temporal IKONOS image classifications for monitoring crops in near-real time over hostile terrain.

Chapter 4 described how the collection of IKONOS images was difficult to achieve within specific time lines designed to coincide with the key poppy growth stages, despite best efforts by the vendors. Furthermore, the experiences of this study showed that even when finances and working practice agreements were in place with third parties and the IKONOS vendors, not enough influence could be exerted over collection to ensure complete datasets within the specified image acquisition periods. Additionally, weather constraints and direct competition for imagery with other commercial requests hindered the collection of requested datasets, resulting in slippage and/or amalgamated or cancelled collection times. This, as already explained, meant that imagery was not acquired during the early growth stages in the 2004 season and acquired earlier than requested in 2005.

Highly flexible IKONOS acquisitions are important to allow for local climatic variations but experience has shown that it was not possible to alter collection dates once submitted to Space Imaging without considerable additional costs, which were prohibitive. The only way to overcome this was to lengthen the collection windows to account for potential delays or advances in the growth cycle but even this solution was sometimes unsatisfactory.

One image collection constraint imposed by Space Imaging was that image bids were to be submitted four months in advance. In Nangahar and Helmand Provinces this meant collection plans had to be submitted in December, before MODIS NDVI profiles could be used to detect increases in biomass activity. Fortunately, UNODC's long-standing working relationship with Space Imaging meant that concessions were made in the 2005 bid, and collection requests were accepted at the end of January, approximately two months prior to poppy flowering and after the greening up of vegetation was identified on the NDVI profiles. In future, the four month lead-in period between collection bid and acquisition will continue to severely impede poppy surveys using IKONOS imagery if improved working agreements are not in place. This project has proved that once increased photosynthetic activity has been identified on MODIS imagery, orders placed with image providers two months prior to anticipated collection dates is operationally achievable.

8.1.3 Ground Data Acquisition

This study has shown that field visits to specific sites to map and measure surface materials is a vital and integral component in a remote sensing study. Ground data collection implies that cover types have been accurately identified, growth stages correctly recognised and the information precisely recorded (Schowengerdt, 1996). Careful examination and cross-referencing of the hard and soft copy ground data with IKONOS imagery and Zeiss photography was essential to establish the implied quality of UNODC's ground survey work.

The careful examination shows that precision was sometimes not achieved due to time lapses between ground data collection and image acquisition, security constraints and human error. For example, Section 4.6.1 of Chapter 4 demonstrated that surveys should be conducted at or close to the time of image acquisitions, as close to poppy flowering as possible but prior to the poppy harvest to minimise the potential for inaccurate identification of cover types or missing field boundaries and crop labels. In some locations security incidents prevented ground data collection altogether and so surrogate ground data had to be used, which was cross-checked by PDP staff to minimise the chance for error.

8.1.4 Surrogate Ground Data

Initial processing of image data revealed that each segment training area had to be enlarged to enable the acquisition of sufficient numbers of training pixels. This study reported in Section

4.6 of Chapter 4 that pan-sharpened IKONOS images and Zeiss aerial photography were suitable surrogates for ground data when insufficient ground data exists.

8.1.5 Predicting Data Acquisition Times

The Literature Review revealed that past poppy surveys relied on recommendations from other poppy studies, local knowledge and previous cropping calendars to guide and inform image acquisition. Formally reported for the first time in Section 4.3.1, this study demonstrated how MODIS NDVI data can be used to map and monitor average photosynthetic activity in localised areas to forecast and plan image acquisition windows to coincide with suitable growth stages when poppy can be discriminated from other cover types.

8.1.6 Summary

This section discussed how the scope of this study was unavoidably narrowed because of partial image and ground data collections, despite careful planning using NDVI data and the use of surrogate data when necessary. Nonetheless, sufficient data existed for temporal and spatial investigations to take place.

8.2 Factors Influencing Image Processing

This section discusses how image processing activities were influenced by the choice of classification technique, which in turn was influenced by end-user requirements. It begins with a short summary of the limitations of the image registration process.

8.2.1 Image Registration

Even though the MODIS imagery and Zeiss photography were rectified at source by the data providers the feasibility of using multi-source and multi-temporal image and photographic data was limited because the MODIS imagery and Zeiss photography failed to adequately overlay onto the IKONOS imagery. As a result, the MODIS and Zeiss data were treated as independent sources.

Similarly, horizontal displacements between successive IKONOS images were identified and had to be corrected to ensure the locations of the pixels selected for training and evaluation data at each site coincided exactly with the pixels from the reference IKONOS images. Geo-registration successfully removed horizontal displacements in all Helmand and Nangahar

images (to within one 4m IKONOS pixel) after the technique was modified for Nangahar to enable pixel grids to match in the locality of the training areas only. If the registration process had not been successful the accuracy of the image classifications would have been significantly reduced.

8.2.2 Choice of Classifier

Chapter 2 described many different classification approaches with potential to produce accurate results. However the choice of approach was influenced mainly by user requirements listed in Section 2.6.3 of Chapter 2; that the software should already be available, easy to use, should not require significant amounts of user training and be simple enough to be used by analysts inexperienced in the use of digital image classification; the type of data available (IKONOS images) and the wide regard held for the MLC in the remote sensing community.

Methods were developed on the basic premise that the performance of the MLC relies on user-defined training classes that characterise the natural surfaces they are to represent. In keeping with the assumptions of the MLC in Chapter 2, Chapters 4 and 5 described optimum sampling parameters used to select independent and representative training and evaluation pixels that were free from the effects of spatial autocorrelation and spectral mixing, as recommended by Congalton, (1991).

Accordingly, although it was not possible to alter the sampling parameters used by UNODC to select image acquisition sites and segment training areas, it was possible to determine the numbers and locations of each training and evaluation pixel collected. Representative numbers of pixels were collected for each class based on the proportion of each cover type present in the 1 km x 1 km segment training areas to reduce the possibility of bias in the classification process. As the traditional method used by UNODC to collect groups of contiguous pixels within field boundaries violates the independent sample requirement of the MLC, a dot grid was used to collect 1 in every 6 pixels, creating 24m spacing between pixels. This achieved a sampling rate trade-off between spatial auto-correlation and a practical number of training data. When these selected pixels were then divided into training and evaluation data, where even numbered pixels became training data and odd numbered became evaluation data, it meant the pixels were 48m apart. Therefore, less than 15% of the DN value of each training and evaluation pixel data was either related to, or dependent on the reflectance measured from its neighbouring pixel which was deemed acceptable.

The Jeffries-Matusita distance (JM distance) was described in Section 2.7.2 of Chapter 2 as a valid means of measuring the distance between two classes in a given set of spectral bands to determine if training classes are separable and non-overlapping. Spectral Coincidence Plots (SCPs) were used to determine whether classes were spectrally separable, provide a visual display of class separability at different locations on different dates and to help qualitatively appraise the amount of internal spectral variability present in each class. On the whole well-separated classes were identified when the means of the classes were not clustered together on the SCPs, the class ranges were small and the amount of overlap between the classes was minimal.

8.2.3 Use of Multi-temporal Imagery

The use of multi-temporal data was one recommendation made in the Literature Review, either to improve the chances of obtaining cloud-free data (Chuinsiri *et al.*, 1987) or to monitor temporal changes (Prapinmongkolkarn *et al.*, 1980 and UNODC, 2005b).

Although other remote sensing literature report increases in classification accuracy when multi-temporal images are used, none of the poppy studies reviewed had investigated this recommendation. As such, quantitative knowledge and rigorous and quantifiable evidence of the accuracy of poppy identification from multi-temporal image classifications was deemed necessary to advance the current body of scientific knowledge on the remote sensing of poppy.

Accordingly, although imagery was only collected at two growth stages per site per growing season in the majority of cases, this was sufficient to enable two-date classifications to be performed. Similar to results from other multi-date classifications, (e.g. Turner and Congalton, 1998) two-dated image classifications were found to significantly improve classification accuracy relative to the accuracy of single dates in the majority of cases studied. However, single image classifications may be advantageous if budgets and time are not constrained, and neither weather nor other tasking prevents collection.

It is argued that the increases in classification accuracy evident in the majority of multi-temporal classifications performed in this study are sufficient to justify additional time and expense, particularly when higher tasking authorities and weather constraints meant that guaranteed single date acquisitions within the requested collection windows were too difficult to achieve. Providing that the image collections are spread across the cycle and that time and

budgets are not too constrained, doubling the cost of imagery to achieve a 13-40% rise in classification accuracy makes multi-temporal classifications a more favourable option.

This study therefore highlights the dilemma faced in remote sensing crop surveys of whether to use single or multiple acquisition dates. The cheapest and quickest option would be to use one image date per site for crop identification, which this study demonstrated provided high classification accuracies when imagery was collected at mid-end flowering and end flowering-beginning of senescence - if imagery collections within these narrow windows could be guaranteed. However, it was demonstrated that these are very difficult to achieve and cannot be guaranteed and so multi-temporal classifications are recommended for future poppy surveys.

8.3 Causes of Spectral Variability and their Consequences

This section discusses the factors which potentially influenced the spectral reflectance characteristics of Afghan poppy and considers their effect on classification accuracy. It draws on all the investigations conducted during the research phase of this study by cross-referencing the ground data and photographs at each growth stage (Chapter 3), the general spectral characteristics of vegetation (Chapter 2) and ancillary data collected during field visits.

8.3.1 Crop Maturity

Crop maturity was found to be a significant influence on spectral separability because different proportions of bare soil and vegetative surfaces were exposed to the IKONOS sensor at different stages in the growth cycle.

Reflectance from mixed pixels at different stages during crop life cycles was not measured in this study so neither their magnitude of influence nor their dominance over other identified influences was determined. It is therefore proposed that at the immature growth stages of emergence and stem elongation the radiance recorded by the IKONOS sensor from each 4m parcel in all autumn-planted fields contained higher proportions of radiance reflected from the exposed bare soil than from the crop canopies. As a result, wide, overlapping poppy, wheat and alfalfa class ranges were evident on SCPs with resultant low classification accuracy at stem elongation in both Helmand and Kandahar Provinces. Consequently, poppy was consistently less well identified at emergence and stem elongation than at any other growth stage.

Chapter 2 described that as crops develop more leaf layers and expand their green canopies the brightness values of pixels represent the bulk properties of the vegetation rather than the light-toned background bare soil. Moreover, Chapter 2 described how the spectral responses of each crop becomes increasingly distinctive as the internal structures change and different quantities of moisture and incoming visible light are absorbed during pigment development. The general MODIS NDVI profiles presented in Chapter 6 revealed that photosynthetic activity was at its highest level at flowering when most biomass was present. Consequently, the results in Chapter 6 showed that class ranges narrowed and overlapped less by flowering, making the poppy signature more separable at the mid-end of poppy flowering than at any other time. The result was that poppy was consistently identified with the highest accuracies during flowering in Nangahar and Helmand Provinces than at any other time in the growth cycle.

At flowering, it is proposed that the hue of the poppy petals also contributes to the mixed energy returns, as reported in the UK poppy fields. Spectral separability and classification accuracies were found to be lower before and after poppy flowering when the poppy fields were less uniform in texture and tone than the surrounding fields of densely planted wheat and alfalfa. The colour of poppy petals therefore contrasted directly with wheat and other crops at flowering, which lead to poppy being consistently identified with the highest accuracies during flowering.

As each species went into senescence, the amount and effectiveness of chlorophyll deteriorated and the crops withered. Ground photos presented in Chapter 3 showed that bare soil was gradually exposed. It is likely that mixed energy returns from the decaying vegetation and exposed soil reduced spectral separability and classification accuracy, as evident with widened class ranges and increased overlap. This was evident in all of the Helmand and Nangahar sites.

8.3.2 Farming Practice

Farming practices were also found to influence spectral variability. Poppy farming practices were described in Chapter 3 and subsequently verified by Zeiss photography in Chapter 4.

As the different crops increased in biomass, different planting densities and weeding patterns tailored to individual crop species became more apparent. Even though different crops experienced the same local environmental conditions and developed at similar rates, different proportions of soil became hidden under the crop canopies depending on the farming

practices. Therefore, the spectral characteristics of the different mixtures of bare soil and immature crops started to differ after emergence-stem elongation according to crop species as different proportions of soil and crop signatures were recorded by the sensor. For example, Chapter 3 described how poppy farming practices differed to other crops, explaining how poppy is planted in rows, weeded and thinned-out to 15 plants per square metre to ensure the strongest, healthiest poppy plants survive without having to compete for light, water or nutrients. As a result, poppy fields are relatively heterogeneous before and after maximum biomass is reached because proportionally more bare soil is exposed to the sensor between the linear poppy rows before and after flowering (maximum biomass) than from the surrounding more densely planted fields of wheat or alfalfa.

One other outcome of the presence of mixed, lighter-toned bare soil and vegetation pixels was their contribution to the positioning of class means in the visible bands on the SCPs. For example, in Held87, Nan25, Nan11 and Nan29 poppy class means were higher than the relative positions of the alfalfa and wheat at most growth stages. However, wherever weeds and vineyard were present in the segment training areas (Held115, Held57, Kand73, Kand84 and Kand135) class means were relatively higher than those of poppy. This was because vineyards are characterised by rows of vines in-between wide soil aisles (different to the much narrower soil rows found between rows of poppy), so mixed vine and soil energy returns were recorded. Mixed pixels were also found where weeds grew across large areas of bare soil between crops in the different fields and along the sides of tracks and canals, resulting in weed class means being higher than those of poppy in the majority of instances.

At sites where mixed cropping took place, and where poppy was occasionally planted between rows of vineyards, higher numbers of mixed pixels were found, resulting in poppy and vine class means positioned very close to one another at mid-end flowering on the SCPs. As a consequence, wherever more spectral mixing occurred, spectral confusion was higher and so lower classification accuracies were achieved.

Bare soil and house classes consistently had the broadest class ranges across every growth stage and at every site because of the combined spectral responses from bare soil, weeds and rock that made up the bare soil class and the different spectral responses from tracks, houses, roofs, cars and household equipment found in the house class. At flowering when the ranges of the vegetative classes were narrow and less overlap between the extremes of the bare and house ranges was evident, spectral separability and classification accuracies were highest.

8.3.3 Disease and Drought

In UNODC's 2004 Annual Opium Report, 24% of farmers reported their poppy fields were damaged by disease and 8% reported their poppy crops were damaged as a result of either disease or drought (UNODC, 2004). The types and symptoms of the fungal and bacterial diseases recorded by the surveyors were described in Table 3-2 in Chapter 3 and included Blight, Mosaic, Powdery Mildew, Fusarium Wilt and an unknown fungal parasite.

In the ground notes from Held115 in both 2004 and 2005 UN surveyors reported that a well-established disease had caused several of the poppy and wheat fields to wither and die (no further details were provided). In 2005, in ground photographs taken three weeks after images had been acquired, several patches of withered and yellowed wheat and isolated patches of bare soil were visible. At this particular site, widened class ranges, low spectral separability and lower than expected classification accuracies between emergence-stem elongation and beginning-mid flowering were reported (see Chapter 6).

Although there was no direct proof of cause and effect, it is possible that these atypical results were due to either insufficient water or because of diseases reported by UN surveyors, making the range of in-band reflectance of all cover types in Held115 very variable.

One other atypical consequence of the disease reported in Held115 was that the mean brightness values of the wheat crop at emergence/stem elongation were higher than the poppy means in the visible bands. This was because mixed contributions were recorded from bare soil and wheat, raising the mean reflectivity of the crop in the field. However, by beginning-mid flowering in 2005, the wheat means had fallen back to below those of poppy, perhaps because the diseased wheat crop was able to put up more biomass during its greening up phase, hiding more bare soil.

8.3.4 Number of Different Varieties of Crops Grown

At flowering where only three or four cover types existed in a site (Held87 and Nan25) the position of class means and the narrow, non-overlapping class ranges on SCPs indicated well separated classes. Here, classification accuracies were also high. In other sites at flowering where additional vegetation classes were grown alongside poppy such as onions, vines and weeds, there was spectral confusion. Within-class variability in these additional cover types was often much greater than for poppy, where broader, overlapping class ranges resulted in lower separability and classification accuracies.

8.3.5 Chapter Summary

This chapter has documented how the reliance on UN, US and UK assets, the use of MODIS data and the presence of ground data errors influenced data collection. The chapter also discussed how image processing activities were influenced by the choice of classification technique, which in turn was influenced by end-user requirements. The potential influences on spectral separability and classification accuracy through time were also examined, including crop maturity, farming practice, drought and diseases.

It is proposed that all of the fundamental image processing methods described in Chapter 2 which were further developed in Chapters 4 and 5 could be used by non-specialists to integrate satellite imagery, aerial photography and ground data in order to successfully identify poppy in Afghanistan, after gaining initial training in remote sensing techniques and experience of the crops.

Chapter 9 presents the conclusions of this study with reference to the objectives listed in Chapter 1. It also discusses the study limitations and makes recommendations for future studies.

9. Conclusions, Limitations and Recommendations

The purpose of this thesis was to investigate the application of remote sensing to discriminate poppy from other land cover types in Afghanistan using spectral signatures obtained from the analysis of multi-spectral imagery. The consistency of discrimination through time and for different geographical regions was of particular interest and formed part of a broader program intended to improve upon the accuracy of poppy area estimation in Afghanistan.

Arguing that the study would require quantitative knowledge on the spectral-temporal properties of poppy to contribute towards improving the remote detection of Afghan poppy, the research aim was underpinned by the following four study objectives:

1. Identify factors that may influence the spectral properties of the opium poppy crop and investigate their influence with respect to accuracy of identification using multi-spectral image analysis.
2. Investigate the spectral separability of cover types to determine:
    a. The presence or otherwise of a stable spectral signature of poppy that contrasts with the signatures of surrounding crops in Afghanistan.
    b. The most appropriate time(s) in the growth cycle for discriminating poppy from other crops.
3. Quantify the relationship between spectral separability and classification accuracy.
4. Investigate whether a single or multi-date classification approach improves classification accuracy.

The general conclusions are listed according to the study objectives.

9.1 Objective 1

Identify the factors that may influence the spectral properties of the opium poppy crop and investigate their influence with respect to accuracy of identification using multi-spectral image analysis.

The spectral reflectance properties of poppy are determined by how its vegetative surface (leaves, stems, capsules, petals, canopy shadows and soil background) interacts with electro-magnetic energy, which in turn is influenced by environmental stress, a sensor's spatial and spectral resolution, viewing geometry and atmospheric conditions amongst others.

Three of the most significant factors found to influence the reflectance properties of poppy were the age of the plant, which directly influenced how much reflectivity was recorded from the plant's vegetated surface and the underlying background soil, specific poppy farming practices and environmental stresses such as drought and disease. Although these factors were not measured directly, their consequences on classification accuracy were evident.

Soil influences were greatest (as measured by broad and overlapping poppy class ranges on Spectral Coincidence Plots (SCPs)) when crops were immature, coincidental with thinning and weeding (unique poppy farming practices) so pixels predominantly represented soil brightness values rather than poppy. As a consequence, classification accuracies were consistently lower at the earlier growth stages because of this mixed pixel effect.

The influence of soil was least evident when poppy and other crop types reached maximum biomass, and resulted in classification accuracies that were consistently higher at flowering than at any other growth stage. Concurrently, the spectral response of poppy fields at flowering was also influenced by the hue of poppy petals, which also made the spectral characteristics more distinct.

As all crops entered into senescence the soil's influence on poppy spectral properties was found to gradually increase, (shown by broadening class ranges and greater overlap on SCPs compared to flowering) as chlorophyll production deteriorated and crops began to yellow and wither. As a consequence, classification accuracies were consistently found to decrease between flowering and end senescence across all sites.

When the symptoms of drought or disease were well established in a field these also contributed to the overall spectral appearance of the crops. For example, in both 2004 and 2005, patches of decaying and/or dead poppy and wheat were reported in segment training areas. As a result, classification accuracies were atypically lower than found elsewhere at similar times.

9.2 Objective 2

Investigate the spectral separability of cover types to determine the presence or otherwise of a stable spectral signature of poppy that contrasts with the signatures of surrounding crops in Afghanistan and the most appropriate time/s in the growth cycle for discriminating poppy from other crops.

This study confirmed that the matter of a stable poppy spectral signature is much more complex than previously thought. Poppy has a unique spectral signature which contrasts with other cover types at flowering. At all other times in its growth cycle its signature is not separable.

Average spectral separability varied according to crop growth stage at the time of imaging - it was lowest at emergence-stem elongation and highest at flowering, after which it declined. Similarly, separability between poppy and individual cover types also varied according to the growth stage. Bare was consistently found to be the most separable cover type from poppy across the growth cycle at all sites, followed by house, water and trees. Wheat was least separable from poppy, particularly at emergence-stem elongation and end flowering-beginning of senescence.

The most appropriate time for discriminating poppy from other crops was at poppy flowering when spectral separability was highest, supported by high JM distance results, minimal spectral overlap between poppy and other vegetative classes and the lowest in-class spectral variability. This was due to high crop biomass masking the background soil, minimising its influence on the poppy spectral signature. Separability was next best at senescence but very poor at stem elongation.

The feasibility of identifying poppy earlier in the growth cycle prior to flowering was also examined in order to provide maximum planning and execution time to assist with Government-led eradication initiatives (as proposed in Section 1.3.1). The three Kandahar Province datasets proved that poppy could be identified at stem elongation with a good degree of accuracy, but the results were less promising in Helmand Province at a similar growth stage. More case studies are therefore necessary to provide a convincing and statistically more robust result.

9.3 Objective 3

Quantify the relationship between spectral separability and classification accuracy.

A relationship between spectral separability and classification accuracy exists although the reliability of results and the strength of the association varied according to growth stage.

Highest spectral separability was achieved at mid-end flowering followed closely by end flowering-beginning senescence. Similarly, highest overall classification accuracies, and poppy producers and users accuracies were also found at these growth stages. Moreover, accuracy measures indicated a very positive linear association between overall classification accuracy and spectral separability at mid-flowering to beginning of senescence, which suggested that spectral separability and overall classification accuracy were related at this growth stage. Therefore, spectral separability measures can be used to predict overall classification accuracy at mid-flowering to beginning of senescence.

Towards the latter stages of the poppy growth cycle, spectral separability and overall classification accuracy decreased. However, the reliability of the classification results also decreased after flowering and regression revealed that no relationship existed between spectral separability and classification accuracy during senescence.

Overall, lowest separability and overall classification accuracy results were found at emergence-stem elongation. Classification reliability was also lowest at this time.

Results were consistent across the three provinces investigated. Although the growing conditions in Nangahar Province (steep sided, high-altitude terraced slopes with well-drained fertile river valleys) differed to those found in the fertile, flat and irrigated fields in Helmand and Kandahar Provinces, the geography of the sites did not appear to have any impact on either separability of the poppy crops or classification accuracy.

9.4 Objective 4

Investigate whether a single or multi-date approach improves classification accuracy.

This research demonstrates the success and potential operational use of multi-temporal image classifications. Two-dated classifications significantly improved classification accuracy relative to that performed on single dates in the majority of cases. Improvements varied according to crop growth stage at the time of image acquisition. Smallest improvements were found when two-date classification accuracies were compared to single-date results from

images acquired at mid-end flowering. Largest improvements were found when the classifications were compared to single results from emergence-stem elongation.

No improvements were found over single image classification results in cases where the Kappa coefficient of one of the images in the pair was above 70%. Therefore, a single date Kappa coefficient threshold of 70% was proposed to determine whether a second image should be acquired as part of a two-dated classification approach, to improve upon the existing single image classification results. However, user's should be aware that image vendors may charge supplements in addition to the extra image costs because of the short-notice given and the additional work required within their own scheduling constraints.

9.5 Limitations

The scope of this research was limited by data gaps, collection constraints and security constraints. Although IKONOS bids were submitted within the 4 month time-frame specified by Space Imaging, imagery was not collected as requested over the original eleven sites across the three provinces and over two growth cycles. Gaps in ground data collection and significant imagery and aerial photography gaps meant that Badakshan data was disregarded and new sites had to be found. Unfortunately, as the data that underpinned this study was already being acquired for UN, US and UK operational surveys it was not possible to request additional datasets from the already stretched resources. Kandahar Province was chosen as an alternative because 2005 data was available but this meant that poppy growing in rain-fed areas was not investigated. Whilst this research was still able to look at a variety of sites it was not able to prove the temporal consistency of results in Nangahar and Kandahar Provinces.

With limited availability of IKONOS images in 2005, and too few poppy fields in Nangahar Province in 2005 to warrant investigation, the numbers of growth stages investigated were limited and so direct comparisons of growth stage could not be made.

To compound these difficulties, security restrictions also limited the scope of this study. For example, ground data collection by UN surveyors was prohibited in some areas because of the direct security threat which meant aerial photographs and pan-sharpened imagery had to be used as surrogates for ground data. Additionally, the security threat to UK personnel prevented in-field experience being gained in Afghan field surveys, thus limiting first-hand experience to UK-based poppy fields.

Security measures imposed by US and UK authorities also limited the scope of this study. For example, US photo-interpretation methods were not made available for comparison with UN techniques and analysis because of security measures imposed by US authorities. In addition, security constraints imposed by UK authorities delayed the release of Zeiss photography for several weeks after each data capture event and so caused unexpected delays.

9.6 Recommendations for Future Work

Several of the Thai poppy surveys reviewed in Chapter 1 underestimated the absolute requirement for timely and accurate ground data to help identify training signatures, identify the links between visible crop biophysical parameters and their spectral signatures and to help in the assessment of the accuracy of the supervised classifications. As a result, few described how they collected their ground data, what they collected, how accurate it was and how it was used - other than as a check on the analysis performed. In this study, whilst it was possible to identify and correct mistakes in the UN's ground data, it was not possible to provide a full assessment of the survey because of political sensitivities. If it were possible in future, a full, accurate and formal critique should be published.

More cases from the same sites across a wider range of growth stages would have enabled more robust multi-temporal analysis. For example, more cases around flowering would have helped determine whether imagery acquired slightly earlier in Nan11 and Held57 at mid- or mid-end flowering could improve the results already achieved at end flowering-beginning senescence in these locations, to match the existing higher accuracy results from Nan25, Nan29 and Held87 at mid-end flowering.

Cases across northern rainfed areas were needed (as originally planned) to identify whether different environmental conditions affected the spatial and temporal consistency of the spectral signature of poppy. In future, impact statements highlighting the importance of the data should be sufficiently strongly worded to ensure the collection of imagery and aerial photography collection. In addition, sufficient security measures should be in place to enable the collection of ground data. If these statements and measures are in place it is recommended that rain-fed poppy cultivation is examined.

This research only investigated the cover types already recorded in the ground data. Other cover types may have been present on the imagery but not identified in the ground survey – such as some of the vegetation species listed in Chapter 3. If these cover types are identified in subsequent surveys sufficient numbers of training and evaluation pixels would be needed

for each class. It is recommended that future work is conducted to investigate the optimum size of segment training areas so that 40+ pixels can be collected from every cover type to avoid subsequent classification bias. Whilst more and larger ground segment training areas are recommended for future surveys across a wider range of growth stages and growing conditions this additional work would have to be balanced with the extra costs and the additional security implications for surveyors.

This research only investigated the potential influence of crop maturity, farming practices and environmental stresses on the spectral signature of poppy. It is recommended that future studies investigate these factors with *in situ* readings of the crop to determine their magnitude of influence and their dominance over other identified factors.

Although accurate spatial registration was performed in Helmand Province it is recommended that future surveys use ortho-rectification procedures for areas of significant topography when digital elevation data becomes available to ensure that the pixel grids match across the entirety of each image scene.

This research investigated the use of a traditional pixel-based classifier to identify poppy fields in Afghanistan. It did not determine whether different classification methods would provide better discrimination. Further work could investigate which of three different classification methods provides the best discrimination, pixel-based, object-based or a hybrid of these methods, with the highest classification accuracy. In particular, it is recommended that textual classifiers are investigated to determine whether the introduction of an added textural dimension can bring about higher classification accuracies. Moreover, the security measures imposed by US authorities made it impossible to report on the techniques used by the US to identify poppy. If it had been possible, further work would include a comparison of the accuracy achieved through US photo-interpretation of classified images against digital classifications of the same images.

In the multi-temporal investigation the limited availability of IKONOS images meant that it was not possible to determine whether layer-stacking more than two images, or layer-stacking two images where neither is acquired at flowering, would achieve improvements to classification accuracies. Although using a three-dated classification approach may result in a slightly improved classification result it is not clear whether the extra cost and time required to process the images would be cost-effective. It is therefore recommended that further work investigates a two-date classification using images acquired at stem elongation and the

beginning of senescence. This would determine whether this would bring about an improvement in classification accuracy or whether the existing accuracies are already the highest achievable.

9.7 Summary of Key Points

This study has advanced the current body of scientific knowledge in relation to multispectral and multi-temporal remote sensing and its implication for monitoring and mapping opium poppy in Afghanistan, through the following:

- Using a systematic and in-depth multi-scale, multi-spectral and multi-temporal approach this study tests how applied remote sensing principles work within specific operational constraints and a complex security situation. The study was conducted in an operational context to evaluate the techniques developed under conditions representative of future operational missions. Cross-referencing of different data sources ensured a more detailed and improved understanding was gained from robust and consistent interpretation.
- This is the first scientific approach to mapping poppy that improves quantitative knowledge of the spectral-temporal properties of the crop and provides rigorous and quantifiable evidence of the accuracy of poppy identification from remote sensing.
- This is the first synthesis of ground photographs, aerial photographs and satellite images which documents the growth and development stages of the opium-producing poppy, and the diversity of growing conditions and agricultural practices in Afghanistan.
- Documenting for the first time a novel use of low resolution MODIS data to plan the acquisition of high resolution IKONOS data.
- Improving the pragmatic selection of training and evaluation pixels as a trade-off between ideal theoretical requirements and what is actually possible. The dot grid matrix proved excellent for collecting non-contiguous and non-spatially auto-correlated training and evaluation pixels in keeping with the assumptions of the MLC. Selection of one in every six pixels reduced the effects of spatial autocorrelation by over 85% when compared to the traditional collection of groups of contiguous pixels.
- Establishing for the first time (for poppy discrimination) the link that separability can be used to predict overall classification accuracy. Although previous work

hypothesised that flowering was the best time to identify poppy, none conducted quantitative analysis to prove it.

- Deriving a useful method to quantitatively determine when two images are needed to achieve the desired classification accuracy (by proposing a 70% Kappa coefficient threshold).
- Establishing that Zeiss aerial photography and pan-sharpened IKONOS images are suitable surrogates for ground data.
- Illustrating that IKONOS imagery can provide details of the spectral reflectance characteristics of the Afghan opium poppy, beyond that which has been reported in the literature on work conducted in India, Thailand and Afghanistan using either digital image classifications or photo-interpretation methods to identify poppy. Its relatively low cost, frequent revisit capability, wide footprint and high spatial resolution made IKONOS imagery ideal for poppy identification in Afghanistan. Other satellites worth considering are; GEOEYE-1 capable of imaging at 1.65m, WorldView-2 with its 1.8m resolution in 8 spectral bands (blue, green, red, red-edge, NIR, coastal, yellow and NIR-2) and a panchromatic band at 0.46m; Quickbird with its 2.4m multi-spectral resolution and the RapidEye's satellites with sensors capable of collecting data at 6.5m resolution in the blue, green, red, red-edge and NIR.

Overall this study has developed an improved technique to identify opium poppy using remote sensing suitable for use by personnel with limited training. It uses currently available and cost-effective technology to quantify the classification accuracy required to underpin future Government counter-narcotic activity.

References

Afghanistan Information Service (2006). Afghan's Economy (Accessed June 2006). http://www.afghanistans.com

Agrawal, S; Joshi, P.K; Shukla, Y; and Roy, P.S (2003) SPOT Vegetation multi-temporal data for classifying vegetation in south central Asia. *Current Science*, Vol. 84, No. 11, 10 June 2003

American Society for Photogrammetry and Remote Sensing (1997) Manual of Photographic Interpretation, second Edition. Published by ASPRS, Maryland, USA.

Anderson, J. R, Hardy, E.E, Roach, J.T, Wither, R.E (1976). A land use and land cover classification system for use with Remote Sensor data. Geological Survey Professional Paper 964, US Government Printing Office, Washington, 1976.

Avery, T.E; Berlin, G.L. (1992) Fundamentals of Remote Sensing and Airphoto Interpretation. Fifth Edition, 1992. Editor R McConnin, Macmillan Publishing Company

Barrett, E. C and Curtis, L. F (1999). Environmental Remote Sensing. 4th Edition, Stanley Thornes (Publishers) Ltd, UK.

Bascle, L., Font, F. (1994) Illysys V2: A Solution dedicated to the monitoring of illicit crops. Spot Image, France. (Accessed June 2006).

www.gisdevelopment.net/aars/acrs/2004/b6_image/acrs2004_b6003.acrs2004-b6003.asp

Bruzzone, L; Conese, G; Maselli, F and Roli, F (1997) Multisource classification of complex rural areas by statistical and neural-network approaches. *American Society for Photogrammetry and Remote Sensing*. Vol. 63, No. 5, May 1997, pp. 523-533.

Bundela, D. S (2004) Influence of digital elevation models derived from remote sensing on spatio-temporal modelling of hydrologic and erosion processes. Cranfield University PhD Thesis.

Burrough, P. A and McDonnell, R. A (2000). Principles of Geographical Information Systems, Butler & Tanner Ltd, UK.

Campell, J.B (1981) Spatial correlation effects upon accuracy of supervised classification of land cover. *International Journal of Photogrammetric Engineering and Remote Sensing*, vol 47, no. 3, 355-363.

Campbell, J.B (2006) Introduction to Remote Sensing. 4th Edition, Taylor & Francis, Oxon.

Carpenter, G. A; Gopal, S; Macomber, S; Martens, S; and Woodcock, C. E. (1999). A neural-network method for efficient vegetation mapping. *Remote Sensing of the Environment*, 70, pp. 138-152.

Carvalho, L. M. T; Clevers, J. G. P. W; Skidmore, A. K; de Jong, S. M (2004). *International Journal of Applied Earth Observation and Geoinformation*, 5 (2004) pp. 173-186.

Chamnivikaipong, P. (1992) Utilisation de l'imagerie SPOT: des images pour la surveillance et l'amenagement des zones productrices d'opium. Annexes, Universite Paric VI, Paris, France.

Chuinsiri, S., Blasco, F., Bellan, M. F., Kergoat, L. (1997). A poppy survey using high resolution remote sensing data. *International Journal of Remote Sensing, 18*(2), 393-407.

Chung, B (1990). Effects of plant population density and rectangularity on the growth and yield of poppies. The Journal of Agricultural Science, 115, pp 239-245

CIA World Factbook (2006) Afghanistan. (Accessed February 2006). http://www.cia.gov/cia/publications/factbook/geos/af.htm

Cochran, J.G (1977), Sampling techniques. Wiley.

Congalton, R.G (1991) A review of Assessing the Accuracy of Classifications of Remotely Sensed Data. *Remote Sensing of the Environment*, 37:35-46.

Congalton, R.G (1996) Accuracy Assessment. A critical component of land cover mapping. Gap Analysis. ISBN-1-57085 *ASPRS*. pp. 119-131.

Congalton, R.G (1999) Assessing the Accuracy of Remotely Sensed Data: Principles and Practice. Lewis Publications.

Cruchant, H. (1990), Essai d'amelioration du traitement et de l'interpretation des images spatiales, 2 vol., Universite Toulouse III, Toulouse, France.

Curran, P (1985) Principles of Remote Sensing. Longman Scientific and Technical.

Definiens Imaging (2004), eCognition Professional Users Guide. Germany.

Dekeyne, C. H. (1988), Survey of Narcotics Plantations using SPOT data. First report, sponsored by France/Asian Institute of Technology (ONCB), Bangkok, Thailand.

Delenne, C; Durrien, S; Rabatel, G; Deshayer, M; Bailly, J. S; Lelong, C; Couteran, P

(2008) Textural approaches for vineyard detection and characterization using very high spatial resolution remote sensing data. *International Journal of Remote Sensing*, Vol. 29, No. 4, 20 Feb 08 pp. 1153-1167.

Dennis, J., Diab, A, Trutmann, P (2002). Afghanistan Seed and Crop Improvement Situation Assessment Apr-May 2002. The Planning of Emergency Seed. Remote Sensing for the Inventory and Monitoring of Agricultural Land Booklet.

Dikshit, D (1996) Textural classification for ecological research using ATM images. *International Journal of Remote Sensing*, Vol. 17. pp. 887-915.

Dixon, B and Candale, N (2008) Multispectral landuse classification using neural networks and support vector machines: one or the other, or both? *International Journal of Remote Sensing*, Vol. 29, No. 4, 20 Feb 08 pp. 1185-1206

Farrell, G and Thorne, J (2005). Where have all the flowers gone? Evaluation of the Taliban crackdown against opium cultivation in Afghanistan. *International Journal of Drug Policy, 16 (2),* pp. 81-91.

Fitzgerald, R. W and Lees, B. G. (1994) Assessment of the classification accuracy of multisource remote sensing data. *Remote Sensing of the Environment*, 47, pp. 362-368.

Foody, G. M. (2002) Status of land cover classification accuracy assessment. *Remote Sensing of Environment* 80 185-201.

Food and Agriculture Organization of the United Nations on behalf of the United Nations International Drug Control Programme (1997) Evaluation of Commercially Remotely Sensed Data for the Assessment of Illicit Narcotics Crops: A Desk Study. www.fao.org/sd/EIdirect/EIre0021.htm.

Food and Agriculture Organization/World Food Program (2004) Crop and food supply assessment mission to Afghanistan, 8 September 2004. Rome. www.fao.org/giews/

Frank, T. and Tweddale, S (2006). The effect of spatial resolution on measurement of vegetation cover in three Mojave Desert shrub communities. Journal of Arid Environments 2006, 67, 88-99.

Friedl, M. A and Brodley, C. E (1997). Decision tree classification of land cover from remotely sensed data. *Remote Sensing of the Environment*, 61, pp. 399-409.

Galtier, B., Chamnivikaipong, P., Guerre, L.F., and Tasanapak, T. (1990) Survey of the opium growing areas using SPOT imagery, phases II. Final report sponsored by France/Asian Institute of Technology (ONCB), Bangkok, Thailand.

George State University (accessed 2010). Diagram of Chlorophyll in Leaves: http://hyperphysics.phy-astr.gsu.edu/hbase/biology/chlorleaf.html

Gibson, P. J and Power, C. H (2000). Introductory Remote Sensing. Digital Image Processing and Applications. Taylor & Francis, New York.

Hammond, T.O and Verbyla, D.L (1996). Optimistic bias in classification accuracy assessment. *International Journal of Remote Sensing, 1996, vol. 17, no. 6, 1261-1266.*

Herold, M; Gardner, M. E; Roberts; Dar. A (2003). Spectral resolution requirements for mapping urban areas. I*EEE Transaction on geoscience and remote sensing*, vol. 41, no. 9, Sep 2003.

Holland, P. (2006) Afghanistan: Counter Narcotics" conference. (Accessed 2006). http://www.marshallcenter.org/site-graphic/lang-en/page-mc-index-1/xdocs/conf/2006-conferences/static/xdocs/conf/2005-conferences/0601/pres-holland-en.pdf

Home Office (2003) Drugs related crime http://homeoffice.gov.uk/crime-victims/reducing-crime/drug-related-crime (Accessed 2003).

ICARDA (2002a) Afghanistan seed and crop improvement situation assessment, 2002. (Accessed 2006). www.icarda.org/Afghanistan/NA/Agriculture_Su.htm.

ICARDA (2002b) Needs Assessment on Soil and Water in Afghanistan, 2002b. www.icarda.cgiar.org/afghanistan/PDF/NA_SoilWater.pdf

ICARDA (2002c) www.icarda.cgiar.org/oldsite/news/afghanistan/rebuildingafghanistan.htm

The Indian Express (2000). Now satellites spill the beans about poppy plants. http//:www.expressindia.com/ie/daily/2000415/ina15056.html

Jensen, J. R (2000) Remote Sensing of the Environment. An Earth Resource Perspective. Prentice-Hall, pp1-28, 119-136, 333-378, 471-479.

Jensen, J. R (2005) Introductory Digital Image Processing. Third Edition. Prentice-Hall, USA.

Jensen, J. R (2007) Remote Sensing of the Environment. Second Edition. An Earth Resource Perspective. Prentice-Hall, USA.

Joint Research Centre, Europe
http://marswiki.jrc.ec.europa.eu/wikicap/index.php/Resampling_techniques_in_image_processing (accessed 2010)

Key, T; Warner, T.A; McGraww, J. B; Fajvan, M. A (2001). A comparison of multispectral and multitemporal information in high spatial resolution imagery for classification of individual tree species in a temperate hardwood forest. *Remote Sensing of the Environment*, Vol. 75, Issue, 1, pp. 100-112, Jan 2001.

Kiefer and Chipman (2004). Remote sensing and image interpretation, 5th Edition, Wiley, US.

Labovitz, **M. L and Masouka, E.J** (1984). The influence of autocorrelation in signature extraction – an example from a geobotanical investigation of Cotter Basin, Montana. *International Journal of Remote Sensing*, 1366-5901, vol. 15, Issue 2, 1984, pages 315-332.

Lee, K.; Tao, G and Mora, N. J. (2001) The War on Drugs Enlists Spatial Technology. (Accessed 2006) www.geoplace.com/gw/2001/0601/0601gtk.asp

Lillesand, T.M and Kiefer, R. W (1987) Remote Sensing and Image Interpretation, Edition 2. Wiley and Sons, New York

Lillesand, T.M and Kiefer, R. W (2000) Remote Sensing and Image Interpretation, Edition 4. Wiley and Sons, New York

Lobo, A; Chic, O; Casterad, A (1996). Classification of Mediterranean crops with multi-sensor data: Per pixel versus per-object statistics and image segmentation. *International Journal of Remote Sensing*, Vol.17, No. 12 pp. 2385-2400

Lu, D and Weng, Q (2007). A survey of image classification methods and techniques for improving classification performance. *International Journal of Remote Sensing*, Vol. 28, No. 5, 10 March 2007, pp. 823-870.

Mansfield, D (2001a) An analysis of Licit Opium Poppy Cultivation: India & Turkey. A report for DICD. Annex B pp 1-8.

Mansfield, D (2001b). The economic superiority of illicit drug production: Myth and reality. Opium poppy cultivation in Afghanistan. Report for the International Conference on the role of alternative developments in drug control and development cooperation, Germany, 2002.

Mather, P.I (2004) Compute processing of remotely-sensed images: An introduction. Wiley.

Ministry of Defence (2006) John Reid: British task force has a vital job to do in southern Afghanistan. (Accessed: 26 January 2006). http://www.mod.uk/DefenceInternet/DefenceNews/MilitaryOperations/JohnReidbritishTaskForceHasAVitalJobToDoInSouthernAfghanistan.htm

Moore, D.S and McCabe, G. P (1998). Introduction to the practice of statistics. Third Edition, W. H. Freeman and Company, New York, 1998.

Murakami, T; Owaga, S; Ishitsuka, N; Kumagai, K and Saito, G (2001). Crop discrimination with multi-temporal SPOT/HRV data in the Saga Plains, Japan. *International Journal of Remote Sensing*, Vol. 22, No. 7, 1335-1348.

Myanmar Embassy (2003) Myanmar-US Combined Team Conducts Ninth Opium Yield Survey towards Eradication of Narcotics Drugs. (Accessed 21 Jun 2006). www.mewashingtondc.com/ 9_Opium_Yield_Survey2003March.htm.

NASA (date unknown). Goddard Earth Sciences Distributed Active Archive Center http://daac.gsfc.nasa.gov/about.shtml

Opioids (date unknown).(Accessed 2006) http://opioids.com/jh/index.html

Pal, M and Mather, P (2003). An assessment of the effectiveness of decision-tree methods for ecological cover classification. *Remote Sensing of the Environment* 86, pp. 554-565.

Piekatczyk, J (2005). Discrimination between fallow and arable fields by multi-temporal reflectance measurements. *Proceedings of the 4th EARSeL Workshop on Imaging Spectroscopy*. New quality in environmental studies. EARSeL and Warsaw University, Warsaw, 2005.

Poppies (2001). An introduction to the Opium Poppy. (Accessed January 2006).http://www.poppies.org/2001/07/13/an-introduction-to-the-opium-poppy/

Poth, A; Klaus, D; Vos, M and Stein, G (2001). Optimization at multi-spectral kand cover classification with fuzzy clustering and the kohonen feature map. *International Journal of Remote Sensing*, 2001, vol. 22, no. 8, 1423-1439.

Prapinmongkolkarn, P. Thisayakozn, C., and Kattiyakulwanich, N. (1980) Remote Sensing applications to land cover classification in northern Thailand. *Proceedings of International Symposium on Remote Sensing of Environment*, 1 Apr 1980, San Jose, USA (Ann Arbor: Environment Research Institute of Michigan, 1273-1283.

http://www.publications.parliament.uk/pa/cm200203/cmhansrd/vo031106/text/31106w07.htm

Rammell (2003). House of Commons written answer for 8 Dec 2003. www.publications.parliament.uk/pn/cm200304/cmhansard/vo031208/test/31208wll.htm

RAMP (2006) Rebuilding Agricultural Markets Program. (Accessed 02 September 2006) http://www.ramp-af.com/index.html. Ministry of Agriculture and Animal Husbandry, Kart-e-Sakhi, Kabul, Afghanistan.

Richards, J. A; Jia, X (1999). Remote sensing and digital analysis: An introduction, Third, Revised and Enlarged Edition, Springer-Verlag, pp 1-37, 75-110, 181-221.

Rogan, J; Franklin, J; Roberts, D (2002). A comparison of methods for monitoring multi-temporal vegetation change using Landsat TM imagery. *Remote Sensing of the Environment* 80 (2002) 143-156. Elsevier.

Sabins, F. F (2000). Remote Sensing. Principles and Interpretation. Third Edition. Freeman and Company, USA.

Sader, A. S (1991). Remote sensing of illicit narcotics crops from aircraft and commercial satellite platforms. 24th *International Symposium on Remote Sensing of the Environment*, Rio De Janeiro, Brazil, 27-31 May, 1991.

Sarin, R. (2000) Now satellites spill the beans about poppy plants. *The Indian Express*, 15/4/2000. (Accessed 21 June 2006). ww.expressindia.com/ie/daily/20000415/ina15056.html

Schowengert, R. A (1996). On the estimation of spatial and spectral mixing with classifier likelihood functions. *Pattern Recognition Letters* 17, pp. 1379-1387.

Schowengert, R. A (2007). Remote Sensing. Models and methods for image processing. Third Edition, Elsevier, USA.

Sharif, H. E. M. (2002) Afghan interim Deputy Prime Minister speaking at an ICAR meeting, 9-16 May 2002.

Simmons, S.R., Oelke, E.A., Anderson, P. M. (1995) Growth and Development Guide for Spring Wheat. University of Minnesota. www.extension.umn.edu/distribution.cropsystems/DC2547.html#growth. Accessed 18 Aug 06.

Skidmore (2002) Environmental Modelling with GIS and Remote Sensing. Taylor & Francis

Sloane, P. (2001) Food Security for Afghanistan. Revised version. International Conference on Analytical Foundations for Assistance to Afghanistan. UNDP/The World Bank, Islamabad, 5-6 June 2001.

SPOT Image (2000a) Mapping and surveillance of illicit crop-growing www.spotimage.fr

SPOT Image (2000b) http://www.spotimage.fr/html/_167_194_201_738_.php

Srinivas, P., Das, B.K., Saibaba, J., Krishnan, R. (2004) Application of Distance Based Vegetation Index for Agricultural Crops Discrimination. *ISPRS* Conference Paper. www.isprs.org/istanbul2004/comm7/papers/215.pdf. (Accessed 2006).

Swain P. H and Davis S.M (1978) Remote Sensing: Quantitative Approach. Chapter 5 Hoffer, R.M Biological and Physical Considerations in applying Computer-aided Analysis Techniques to Remotely Sensed Data. Editors Swain and Davis, pp. 396 McGraw Hill.

Takeuchi, W and Yasuouka, Y (2004). Development of normalised vegetation, soil and water indices derived from satellite remotely sensed data. 25th *ACRS*, 2004, Chang Mai, Thailand.

Taylor, J. C, Sannier, C, Delince, J and Gallego, F. J (1997) **Regional Crop Inventories in Europe Assisted By Remote Sensing: 1988 – 1993.** Synthesis Report of the MARS Project – Action 1. Joint Research Centre, Ispra, ECSC-EC-EAEC Brussels and Luxembourg.

Taylor, J. C. (2001) Application of the Kappa statistic in Remote Sensing. MSc lecture handout, Cranfield University, Silsoe

Taylor, J. C. (2004) Afghan opium surveys 2004, Poppy Detection Project, Cranfield University.

Travis, A (2001). Experts back startling heroin claims. The Guardian, 31 Oct 01.

Turner, M. D and Congalton, R. G (1998). Classification of multi-temporal SPOT-XS satellite data for mapping rice fields on a west African floodplain. *International Journal of Remote Sensing*, 1998, Vol. 19, No. 1, pp. 21-41.

Uhl, V.W. (2003). Afghanistan overview of groundwater resources and challenges. Uhl, Baron, Rana Associates, Inc. Washington Crossing, PA, USA.

UK Government, '1998-2008: Tackling Drugs Together to Build a Better Britain'. Leaflet.

United Kingdom Parliament (2003). Secretary of State for the Home Office address to the United Kingdom Parliament on 6 Nov 2003. House of Commons Hansard Written Answers for 6 Nov 2003 (pt 7). (Accessed 2006).

UNEP – ITC (2005) Remotely Sensed Image Classification. UNEP-ITC RS/GIS for Monitoring and Assessment of Iraqui Marshland, 6-10 Feb 2005

United Nations Information Service (2002) 27 August 2002 Opium production in Myanmar declines. (Accessed 21 Jun2 2006). www.unis.unvienna.org/unis/pressrels/2002/nar760.html

UNODC (2004) Afghanistan Opium Survey, 2004, UNODC. Vienna.

UNODC (2005a) World Drugs Report, Vol1: Analysis, p. 123.

UNODC (2005b) Afghanistan Opium Survey, 2005. UNODC, Vienna.

USGS (date unknown). (Accessed 23 June 2006) .http://landsat7.usgs.gov/resources/remote_sensing/remote_sensing_applications.php

Van Neil, T. G and McVicar, T R (2004). Determining temporal windows for crop discrimination with remote sensing: A case study in south-eastern Australia. *Computers and Electronics in Agriculture*. 45, pp. 91-108.

Wang, L; Sousa, W. P; Gong, P (2004). Integration of object-based and pixel based classification for mapping mangroves with IKONOS imagery. *International Journal of Remote Sensing*, Vol. 25, No. 24, pp. 5655-5668.

Wikipedia (accessed 2010)

www. Wikipedia.org/wiki/image: Afghanistan_opium_poppy_cultivation.PNG

Wulder, M and Boots, B (1998). Local spatial auto-correlation characteristics of remotely sensed imagery assessed with the Getis statistic. *International Journal of Remote Sensing*, 1998, Vol. 19, no. 11, pp. 2223-2231.

Yasini, M,(2003) Director-General of the Counter Narcotics Directorate, National Security Council, 30 Jan 2003.

Yahoo News http://news.yahoo.com/s/afp/20061202/wl_sthasia_afp/usafghanistandrugs

Appendix A Technical Details

Cover Sheet

Appendix A Technical Details

In multispectral spatial resolution order:

GEOEYE-1 – (**1.65m** resolution). GeoEye-1 (formed through ORBIMAGE and Space Imaging) was launched in 2008 into a sun-synchronous orbit. It orbits at an altitude of 681 km and can collect 700,000 square km per day (panchromatic) and up to 350,000 square km per day of pan-sharpened multispectral area. It has a panchromatic band with a spatial resolution of 41cm).

QUICKBIRD – (**2.4m** resolution). The Quickbird satellite was launched in 2001 by DigitalGlobe in a sun-synchronous orbit at an altitude of 450 km.

IKONOS – (**4m** resolution). The IKONOS satellite was launched in September 1999. It orbits at an altitude of 681 km and revisits every 2.9 days at 1m resolution (panchromatic sensor).

SPOT – *Satellite Pour l'Observation de la Terre* is a series of French commercial earth observation satellites. Each SPOT orbit is polar, sun-synchronous and phased and can fly over any point of the earth during a 26 day cycle. The average revisit interval over a 26-day orbital cycle is 2-3 days, depending on latitude.

SPOT 5 – (**10m** resolution). SPOT 5 was launched May 2002. A High Resolution Stereoscopic (HRS) imaging instrument simultaneously acquires stereo pairs across a 120 km swath in panchromatic mode with a spatial resolution of 10m (along-track sampling of 5m) and a telescopic viewing angle of +/- 20 degrees.

SPOT 1 – (**20m** resolution). SPOT 1 was launched Feb 1996. Each SPOT payload comprises two identical optical imaging instruments, two tape recorders for image data and a payload telemetry package for image transmission to ground receiving stations

SPOT HRV – (**20m** resolution). SPOT High Resolution Visible (HRV) was launched in Jan 1990 on Spot 2. It offerered an oblique viewing capability, the viewing angle being adjustable through +/- 27 degrees relative to the vertical. The ground stations can steer each instrument's strip selection mirror remotely to view regions of interest not vertically below the instrument.

IRS-1D USSS-III – (**23.5m** resolution). IRS-1D carries a combination of three cameras i) a Panchromatic camera with a spatial resolution of 5.8m, ii) Linear Imaging Self

Scanner (LISS-III) operating in 3 spectral bands of 23.5m in the visible and NIR and 70.5m in SWIR bands, and iii) a Wide Field Sensor (WIFS) with a ground resolution of 188m.

LANDSAT – The LANDSAT Program is a series of Earth-observing satellite missions jointly managed by NASA and the US Geological Survey. Landsat 4 was launched in a polar, sun-synchronous orbit in 1982 and carried TM and MSS sensors. It was decommissioned in 2001. It had repeat coverage every 16 days.

LANDSAT TM – (**30m** resolution). LANDSAT Thematic Mapper was designed to achieve a higher image resolution, sharper spectral separation, improved geometric fidelity and greater radiometric accuracy and resolution that the previous MSS sensor.

DMC – (**32m** resolution). The Disaster Monitoring Constellation was designed and built in the UK. The constellation consists of five satellites, independently owned and controlled by five different nations (Algeria, China, Nigeria, Turkey and the UK). All satellites have been equally spaced around a sun-synchronous orbit to provide daily imaging capability.

LANDSAT MSS – (**80m** resolution). The LANDSAT Multispectral Scanner (MSS) sensors were line scanning devises observing the Earth. The first five Landsats carried the MSS sensor. Landsat 3 carried an MSS sensor with an additional thermal band.

MODIS – (**250m** resolution). The Moderate Resolution Imaging Spectroradiometer was launched onboard the Terra (EOS AM) in 1999 and Acqua (EOS PM) in 2002 by NASA. Terra's orbit around the Earth is timed so that it passes from north to south across the equator in the morning, while Aqua passes south to north over the equator in the afternoon. Terra MODIS and Aqua MODIS can image the entire Earth every 1-2 days.

Sensors	Electromagnetic Spectrum	Pixel Size	Spectral Bands (μm)	Image Swath	Absolute Locational Accuracy	Quantisation
GEOEYE-1	Band 1: Blue Band 2: Green Band 3: Red Band 4: NIR Panchromatic	1.65m 1.65m 1.65m 1.65m 0.41m	0.45-0.51 0.51-0.58 0.65-0.69 0.78-0.92 0.46-0.80	300 km x 50 km (large area) 100 km x 100 km (cell size) 224 km x 28 km (stereo)		

QUICKBIRD	Band 1: Blue Band 2: Green Band 3: Red Band 4: NIR Panchromatic	2.4m 2.4m 2.4m 2.4m 61cm	0.45-0.52 0.52-0.60 0.63-0.69 0.76-0.90 0.45-0.90	16.5 km x 16.5 km (single area) and 16.5 km-115 km (strip)		
IKONOS	Band 1: Blue Band 2: Green Band 3: Red Band 4: NIR Panchromatic	4m 4m 4m 4m 4m	0.45-0.52 0.52-0.60 0.63-0.69 0.76-0.90 0.45-0.90	10 km x 10 km	2m horizontally/ 3m vertically with ground control	11 bits
SPOT 5	2 x Panchromatic B1: green B2: red B3: NIR B4: SWIR	2.5m and 5m 10m 10m 10m 20m	0.48-0.71 0.50-0.59 0.61-0.68 0.78-0.89 1.58-1.75	60 km x 60 km to 80 km	10m (HRS) 30m (HRG)	8 bits
SPOT 1	Panchromatic B1: green B2: red B3:NIR	10m 20m 20m 20m	0.50-0.73 0.50-0.59 0.61-0.68 0.78-0.89	60 km x 60 km to 80 km	350m	8 bits
SPOT HRV	Panchromatic B1: green B2: red B3:NIR	10m 20m 20m 20m	0.50-0.73 0.50-0.59 0.61-0.68 0.78-0.89	60 km x 60 km to 80 km	350m	8 bits
IRS-1D USSS-III	Band1: Green Band 2: Red Band 3: NIR Band 4: MIR	23.5m 23.5m 23.5m 70.5m	0.52-0.59 0.62-0.68 0.77-0.86 1.55-1.7	127-141 km		
LANDSAT TM	Band 1: Blue Band 2: Green Band 3: Red Band 4: NIR Band 5: MIR Band 6: Thermal Band 7: LWIR	30m 30m 30m 30m 30m 120m 30m	0.45-0.52 0.52-0.60 0.63-0.69 0.76-09.0 1.55-1.75 10.4-12.5 2.08-2.35	185 km		8 bits
DMC	Band 2: Green Band 1: Red Band 0: NIR	32m 32m 32m	0.52-0.60 0.63-0.69 0.77-0.90	600 x 600 km		

LANDSAT MSS	Band 1: Green Band 2: Red Band 3: NIR Band 4: NIR Band 5: Thermal	80m 80m 80m 80m 237m	0.50-0.60 0.60-0.70 0.70-0.80 0.80-1.1 10.41-12.6	185 km		8 bits
MODIS	Band 1: red Band 2: NIR Bands 3-7 Bands 8-36	250m 250m 500m 1000m	0.62-0.67 0.841-0.876 0.459-2.155 0.405-14.385	2330 km (cross-track) 10 km (along track at nadir)	Not Known	12 bits

www.modis.gsfc.nasa.gov

www.dmci.com

www.landsat.gsfc.nasa.gov

www.spotimage.fr

Appendix B UN Ground Survey Instructions

Cover Sheet

Ground Data Collection

Instructions for Surveyors

A. L. Bennington MSc

CRANFIELD CENTRE FOR
GEOGRAPHICAL INFORMATION MANAGEMENT

Ground Data Collection Instructions for Surveyors

A. L. Bennington MSc

Poppy Detection Project

Cranfield Centre for Geographical Information Management
Cranfield University
Silsoe
Bedford MK45 4DT
UK
Tl +44 (0) 1525 863064
Fx +44 (0) 1525 863099

Feb 2005

Contents

Summary of methodology for collecting ground segment data 4

Purpose 4

Scope 4

Preparation – documents and instruments 5

Locating the segment using GPS, Orientation Map and Segment Map 6

Orientation in the field 7

Taking Photographs 8

Instructions for data collection when denied access to segments 8

Data Recording 9

Segment Form 9

Instructions on completing the Segment Form 10

Segment Map 12

Segment Info Sheet 13

Instructions on Photographic Collection 14

Annex A 17

Photo Guide to the Major Crops Grown in Afghanistan 17

Annex B 24

Names and Codes for different Land Cover Types 24

Summary of methodology for collecting ground segment data

Purpose

The purpose of this manual is to provide assistance to United Nations Office on Drugs and Crime (UNODC) field surveyors for the collection of consistently accurate and timely field data on the main crop types present in selected sites in Afghanistan.

Scope

This document summarises the methodology used for conducting ground data collection in the field, providing detailed guidelines and instructions for surveyors. It also offers a crop identification guide covering the key growth stages of the most common crops found in Afghanistan (at Annex A).

Preparation – documents and instruments

The following documents should be used by each surveyor:

- **Orientation Map** showing the location of the segment and its position next to surrounding villages, to assist the planning of a suitable route to the segment
- **Segment Map**: 1:1,000 of the 250m segment
- **Segment Form** for data entry
- **Segment Info Sheet** for recording locations of photographs taken by the surveyor

The following equipment should be carried by each surveyor:

- **Clipboard** on which survey documents are fixed in order to be used in the field
- Hand-held **GPS unit** to both assist in the approach to the segment and record the central location of each field
- **Digital Camera** with **Memory Stick** for taking photographs of crops in the segment
- **Permanent marker pens** for recording individual field boundaries
- **Pens/Pencils** for data entry on the Segment Form
- **Ruler/Tape Measure** for measuring the height of crops in the segment

Locating the segment using GPS, Orientation Map and Segment Map

Prior to departure, the **Orientation Map** (Figure 1) should be used by surveyors to prepare their itinerary and the route to be taken to the segment. The route should be loaded into the **GPS unit**, by entering in the geo-coordinates of the start location and all major road intersects along the route in the correct order, so that the GPS will guide surveyors from one point to the next.

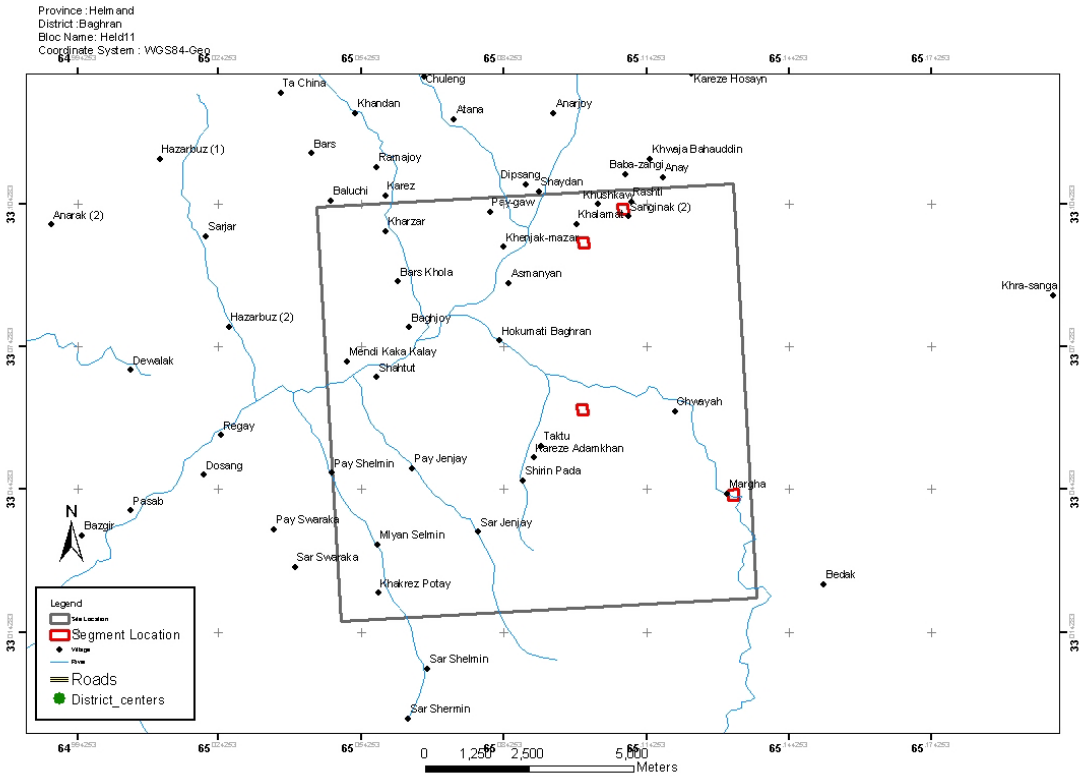

Figure 1 - An example of an Orientation Map

Orientation in the field

The **Segment Map** should be used on the approach to the segment to locate its exact position, by comparing the general shape and positions of the fields to those on the **Segment Map** (see **Error! Reference source not found.**) and for orientation whilst in the segment.

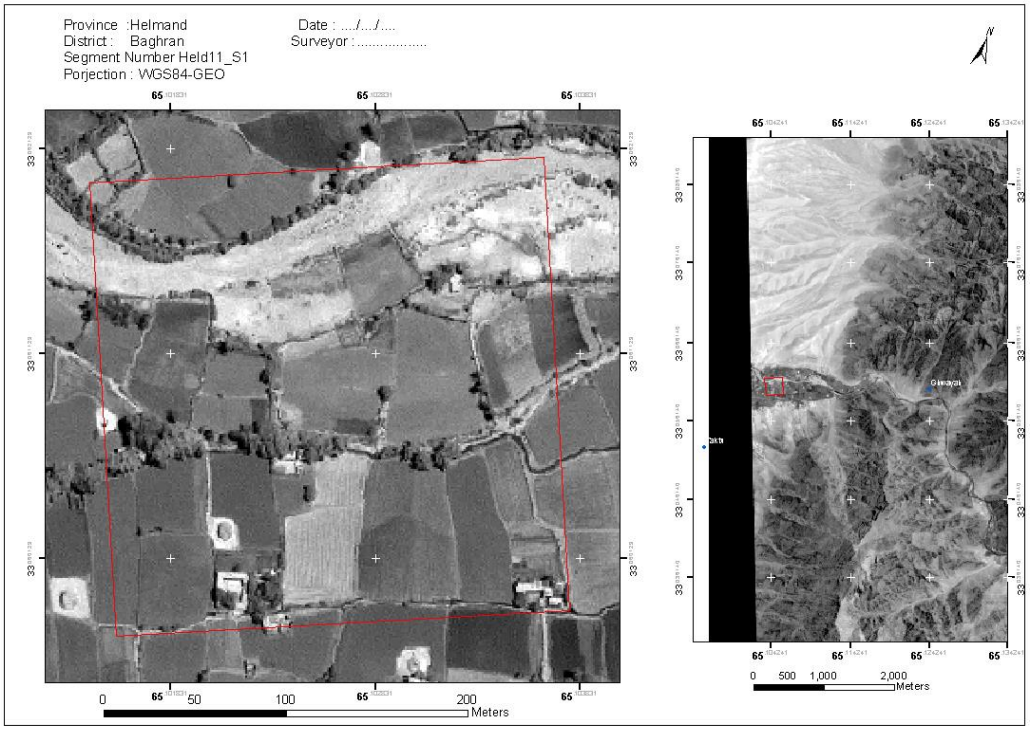

Figure 2 – An example of a Segment Map

At the segment surveyors should orientate the Segment Map to the ground by comparing the map to the immediate landmarks, i.e. tracks, roads, canal, buildings and trees. If the Segment Map is old, surveyors must be aware that changes to the landscape may have occurred since the Segment Map was produced, taking into account any field boundaries that may have been altered or trees and hedges that have been removed.

Surveyors should then familiarise themselves with the field parcels, by walking to suitable vantage points so that each field contained within the Segment Map can be identified.

Surveyors should then plan a suitable route within the segment that will ensure that each field is visited, allocated with a unique serial number (i.e. 1, 2, 3 etc.) and a selected number of fields

photographed. The required information about each field should then be recorded on the **Segment Form**.

Surveyors must not damage any crops in the segments. If asked, surveyors should explain their purpose for being there and present UNODC identity documents if requested to do so.

Taking Photographs

Photographs are to be taken to provide a visual record of each of the various crops present in different fields in the segment. Surveyors are to select suitable fields to photograph. Correct sequential documentation of the photographs is essential on both the **Segment Form** and the **Segment Info Sheet** to enable correct archiving.

Instructions for data collection when denied access to segments

Some difficulties may arise making it impossible to record any data, take photographs or even go to the segment. In these instances, surveyors should adapt their itineraries by removing themselves from danger whilst quickly making observations about the segment that can be recorded onto the **Segment Form** once away from the area.

Data Recording

Segment Form

The following information should be recorded onto the **Segment Form** (see **Error! Reference source not found.**). For ease of reference, these have been enclosed in a red box in Fig. 3 to show where the information should be written.

- Map Reference
- Date
- Surveyor name
- Province
- District
- Village
- Village code

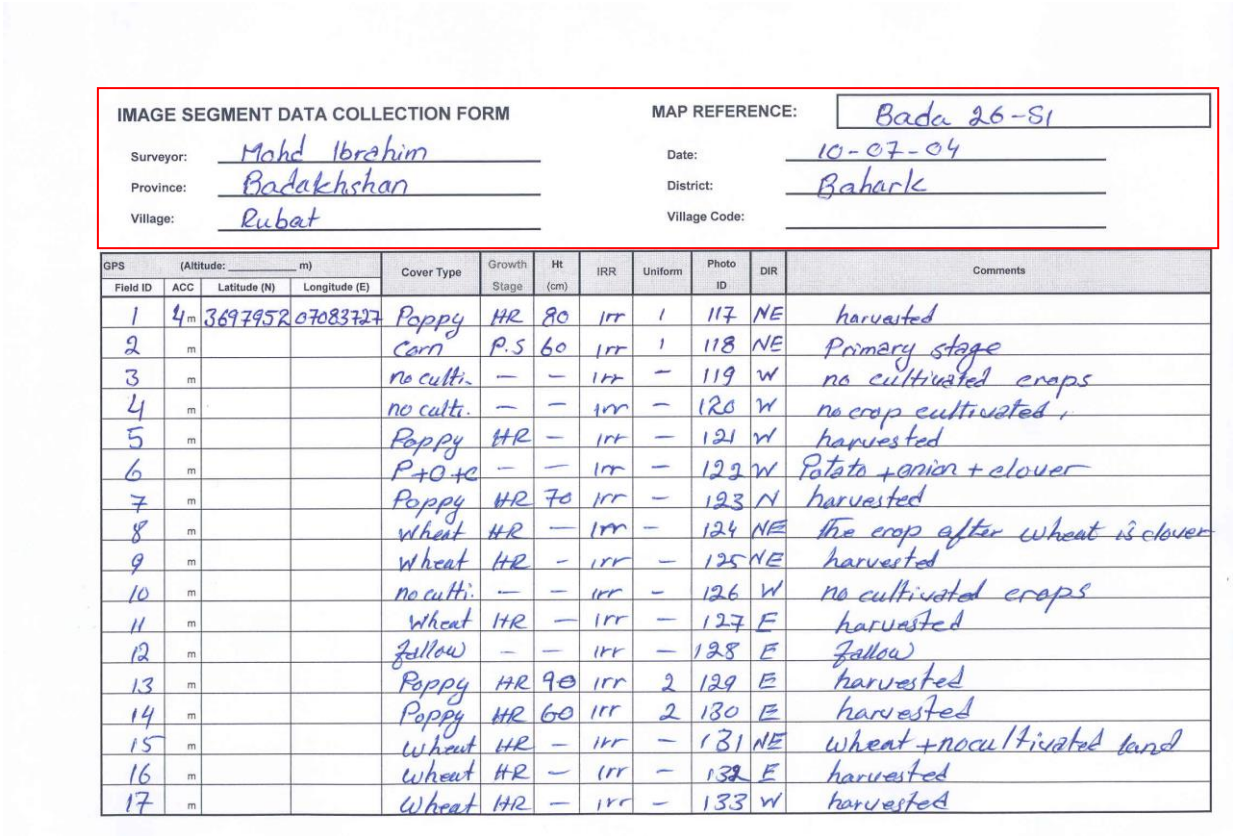

IMAGE SEGMENT DATA COLLECTION FORM

MAP REFERENCE: Bada 26-S1

Surveyor: Mohd Ibrahim

Date: 10-07-04

Province: Badakhshan

District: Baharlc

Village: Rubat

Village Code:

GPS Field ID	ACC	(Altitude: ____ m) Latitude (N)	Longitude (E)	Cover Type	Growth Stage	Ht (cm)	IRR	Uniform	Photo ID	DIR	Comments
1	4m	3697952	07083727	Poppy	HR	80	Irr	1	117	NE	harvested
2	m			Corn	P.S	60	Irr	1	118	NE	Primary stage
3	m			no culti.	—	—	Irr	—	119	W	no cultivated crops
4	m			no culti.	—	—	Irr	—	120	W	no crop cultivated,
5	m			Poppy	HR	—	Irr	—	121	W	harvested
6	m			P+O+C	—	—	Irr	—	122	W	Potato + onion + clover
7	m			Poppy	HR	70	Irr	—	123	N	harvested
8	m			Wheat	HR	—	Irr	—	124	NE	The crop after wheat is clover
9	m			Wheat	HR	-	Irr	—	125	NE	harvested
10	m			no culti.	—	—	Irr	—	126	W	no cultivated crops
11	m			Wheat	HR	—	Irr	—	127	E	harvested
12	m			fallow	—	—	Irr	—	128	E	fallow
13	m			Poppy	HR	90	Irr	2	129	E	harvested
14	m			Poppy	HR	60	Irr	2	130	E	harvested
15	m			Wheat	HR	-	Irr	—	131	NE	wheat + no cultivated land
16	m			Wheat	HR	—	Irr	—	132	E	harvested
17	m			Wheat	HR	—	Irr	—	133	W	harvested

Figure 3 – Example of a Segment Form

Instructions on completing the Segment Form

Field ID: At individual fields surveyors should record the unique field identification number (Field ID) allocated to the field by the surveyor.

Latitude, Longitude and Accuracy (ACC): For the first field entered at the top of each Segment Form **only**, surveyors should remain still to use the **GPS unit** to determine the geo-coordinates (Latitude (N)) and (Longitude (E)) of their position in that field and the accuracy (ACC) of the GPS, and subsequently record the position and accuracy onto the Segment Form.

Cover Type: Surveyors should use the **Land Cover Photo Guide** (at Annex A of these instructions) to identify the predominant land cover type in each field. For ease, shortened names for each land cover type should be entered onto the Segment Form, taken from Column C (Code) of the **Names and Codes** table at **Annex B.**

In cases where 2 crops are being grown (see **Error! Reference source not found.**) both crops must be reported on the Segment Form – the major crop under **cover type** and the secondary crop in the **comments** section.

Figure 4 - Example of 2 crops grown in the same field (wheat and alfalfa)

Crop Growth Stage: The growth stage reached by each crop in each field must also be entered using the **Land Cover Photo Guide** for reference (at Annex A of these instructions). The following table (Table 1) summarises the names surveyors must use to describe the major growth stages of the predominant cover types.

Table 1 - Names to be used to describe the growth stages of the predominant cover types

	Growth Stage Reached by Crop				
Cover Type	**1**	**2**	**3**	**4**	**5**
Poppy	Emergence	Cabbage	Stem elongation	Flowering	Senescence
Wheat	Emergence	Vegetative growth	Stem elongation	Flowering	Senescence
Barley	Emergence	Vegetative growth	Stem elongation	Flowering	Senescence
Corn	Emergence	Vegetative growth	Stem elongation	Flowering	Senescence

Crop Height: The **ruler/tape measure** should be used to measure the average height of the crop in each field by measuring the height from the soil to the highest point on the crop.

Crop Uniformity: Surveyors should look at the crop as a whole across the entire field and record whether on average the crop looks **uniform** (same growth stage, height and healthiness), or **not uniform**.

Irrigation (IRR): Surveyors should record whether each field receives water through **irrigation** (irrigation channels are present), **snow melt** or **rain-fed**.by asking the farmers if necessary.

Comments: Surveyors should note (if applicable)**:**

- **Other crops** being grown in the same field.
- Whether **drought** or **disease** (name the disease if possible) has affected the crops
- Evidence of **crops** grown in **previous growth cycles** in the same year (if applicable)
- Evidence of **harvesting** (if applicable)
- Unusual climate i.e. much **warmer/colder/wetter/dryer** than normal

Photograph Identification Number (Photo ID) and Direction (Dir): Surveyors should use the **Instructions on Photographic Collection** section of these instructions for the methodology to be used to acquire photographs of land cover types in specific fields. When the photograph has been acquired, the photo ID should be recorded and the direction that the photograph was taken from and the direction that the camera was facing (i.e. North – South (N-S)).

Segment Map

With a **marker pen** surveyors should draw the exact shape of each field boundary within the segment, onto the Segment Map as shown in **Error! Reference source not found.** below:

Figure 5 – Drawing field boundaries on the Segment Map with boundary alterations in dotted lines

Surveyors should remember that field boundaries may have changed from those visible on Segment Map and must be amended to reflect the changes in a different colour or line style (i.e. dotted lines). For example, field boundaries may have:

- Been divided by the farmer into smaller fields and now contain more than one crop
- Been made larger by farmers removing the original field boundary completely
- Been altered with construction of new buildings, roads or tracks.

Segment Info Sheet

Correct sequential documentation of the photographs is essential on both the **Segment Info Sheet** and the **Segment Form** to enable correct archiving.

On the **Segment Info Sheet** (**Error! Reference source not found.**) surveyors should ensure that the writing of the **segment number**, **field number**, **crop type** and photograph identification number (**Photo ID**) are clearly visible and large enough to fill each box provided.

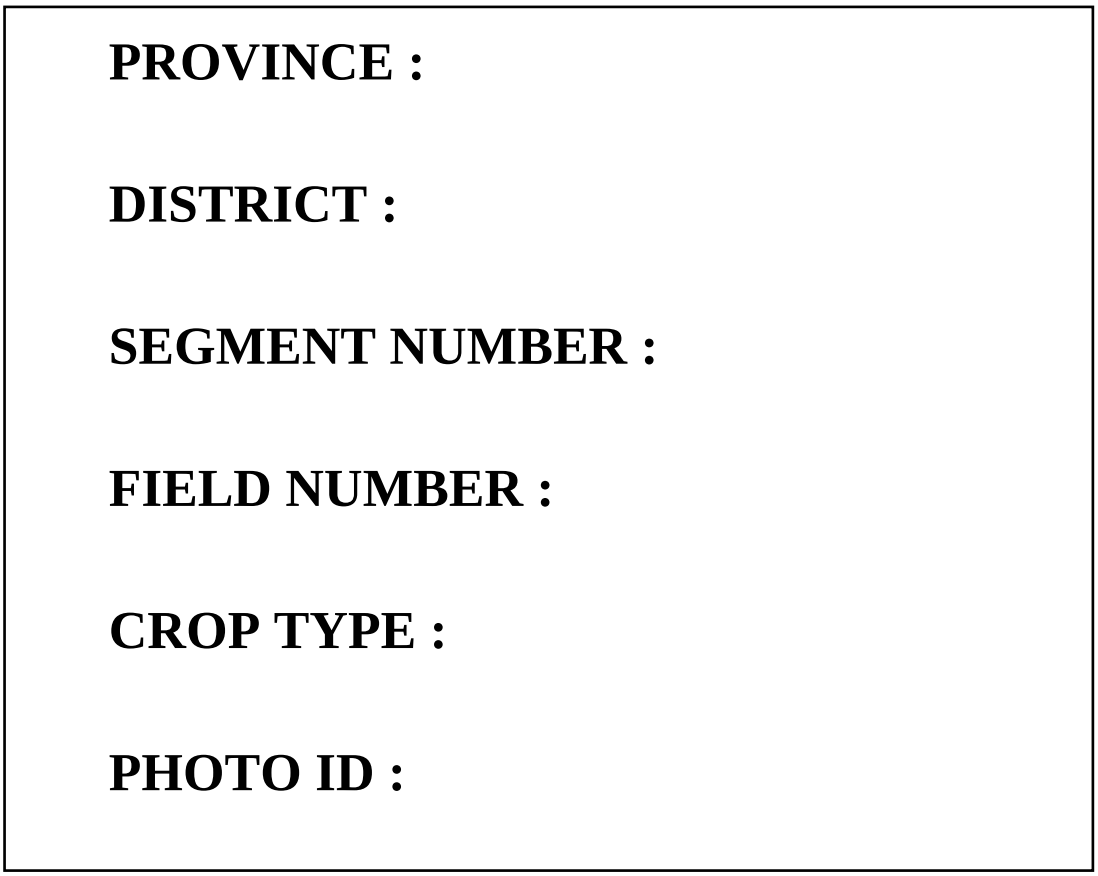

Figure 6 - Data recording on the Segment Info Sheet

On the **Segment Form** surveyors should ensure that the **Photo ID** and direction (**DIR**) that the photograph was obtained are entered.

Instructions on Photographic Collection

The **digital camera** should be used to acquire photographs at each segment. By using the **Memory Stick** up to 50 photographs can be digitally stored. When the memory stick is full, (or when advised to do so by the Provincial Coordinator) surveyors should return back to the UNODC Regional Office to download the photographs with the help of the Provincial Coordinator.

The following steps should be followed:

- Surveyors must select between 5 and 6 suitable fields to be photographed.
- Ideally, the following fields should be photographed:
    - 2-3 Poppy fields
    - 1 Wheat Field
    - 1-2 other crop types
- The direction from the photographer to the centre of the field must be determined using the **GPS** and recorded onto the **Segment Form**
- A second surveyor should stand with his back towards the centre of the field with the **Segment Info Sheet** securely fixed onto a **clipboard** facing up towards the photographer
- The photographer should aim the camera towards the centre of the field ensuring that:
    - The **Segment Info Sheet** is clearly visible and readable in the foreground and does not obscure the view of the crop in the field and does not take up more than ¼ of the photo frame
    - The horizon is visible at the upper edge of the photo frame
    - The entire photo frame contains the crop of interest
    - The photographer does not move when taking the photograph (see **Error! Reference source not found.**)
    - The photographer is not facing directly into sun when taking the photograph (see **Error! Reference source not found.**)
    - Photographer's equipment, fingers and clothes are not obscuring the camera when the photograph is acquired (see **Error! Reference source not found.**)

One example of a good photograph is shown in **Error! Reference source not found.** below where the crop and horizon are clearly visible in the photograph and the words on the **Segment Info Sheet** are very easy to read.

Figure 7 - An example of a good photograph where the words on the Segment Info Sheet are clearly visible in the frame, as are the crop and the horizon

The following photographs (Figures 8, 9 and 10) show examples of poor photographs which should be avoided if possible:

Figure 8 - A poor photograph where the writing on the Segment Info Sheet cannot be read because the photographer did not hold the camera steady when taking the photograph

Figure 9 - A poor quality photograph taken facing into the sun

Figure 10 - A bad photograph where the photographer's finger has been placed over the camera lens

Annex A

Land Cover Photo Guide of the Major Crops Grown in Afghanistan

Crop	Figure
• Poppy	11 - 13
• Wheat	14 - 16
• Barley	17 - 19
• Corn (Maize)	20 - 21
• Onion	22
• Courgette	23
• Watermelon	24
• Alfalfa	25
• Vineyard	26

(a) (b) (c)

Figure 11 - Poppy at (a) emergence, (b) and (c) at the cabbage stage (PDP)

(a) (b) (c)

Figure 12 - Poppy at (a) stem elongation and flower bud development (b) hook stage and (c) at flowering (PDP)

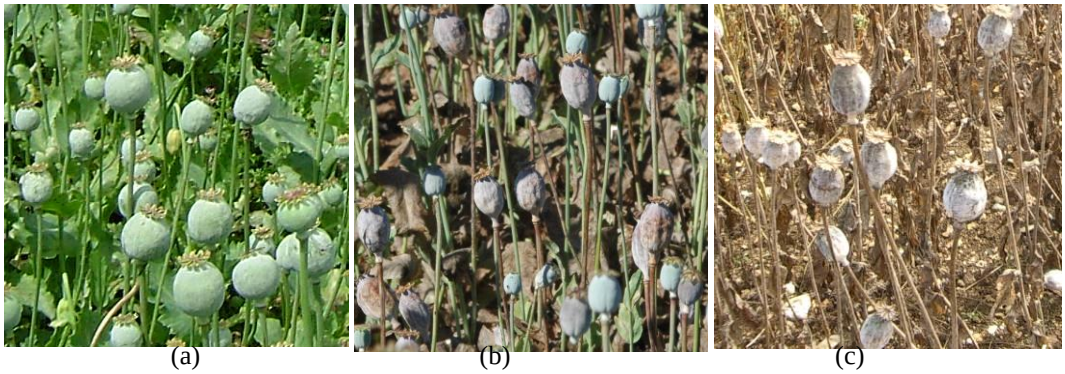

(a) (b) (c)

Figure 13 - Poppy at (a) Maturing capsule, (b) start of Senescence, and (c) end of senescence (PDP)

(a) (b)

Figure 14 - Wheat at (a) emergence and leaf production (b)

(a) (b) (c)

Figure 15 – Wheat - stem elongation (a) heading (b) anthesis (c)

Figure 16 – Wheat at senescence

(a) (b)

Figure 17 - Barley (a) tillering (b) stem elongation

Figure 18 - Barley at flowering

Figure 19 - Barley at senescence

(a) (b) (c)

Figure 20 - Maize (a) emergence (b) leaf production (c) stem extension

(a) (b)

Figure 21 - Maize at (a) flowering and (b) at senescence

Figure 22 – Mature onion

Figure 23 – Watermelon at an early growth stage

Figure 24 – Courgette at flowering

Figure 25 – Mature alfalfa

Figure 25 – Vineyard

Annex B

Names and Codes for different Land Cover Types

Land Cover	Name	Code
(a)	(b)	(c)
Other Crops	Poppy	Pop
Cereal Crops	Wheat	Wh
	Corn/Maize	Corn
	Barley	Bar
Forage Crops	Alfalfa	Alf
Vegetables	Onion	On
	Okra	Ok
	Peas	Peas
	Carrots	Ca
	Tomatoes	Tom
Bare ground and rock	Bare land (for new crops)	Bare (crop)
	Bare land (not for crops)	Bare
Fruit	Watermelons	Melon
Trees and vines	Fruit	Fruit
	Nut	Nut
	Olive	Olive
	Vineyards	Vine
Other	Trees	Tree
Man-made	Buildings	Build
	Graveyard	Grave
	Vehicle track	V track
	Dirt track	D track
	River	River
	Stream	Stream
	Canal	Canal
	Irrigation Ditch	Ditch

Appendix C Spectral Separability Data

Cover Sheet

Appendix D Supervised Classifications

Cover Sheet

Nan25 11 Apr 04

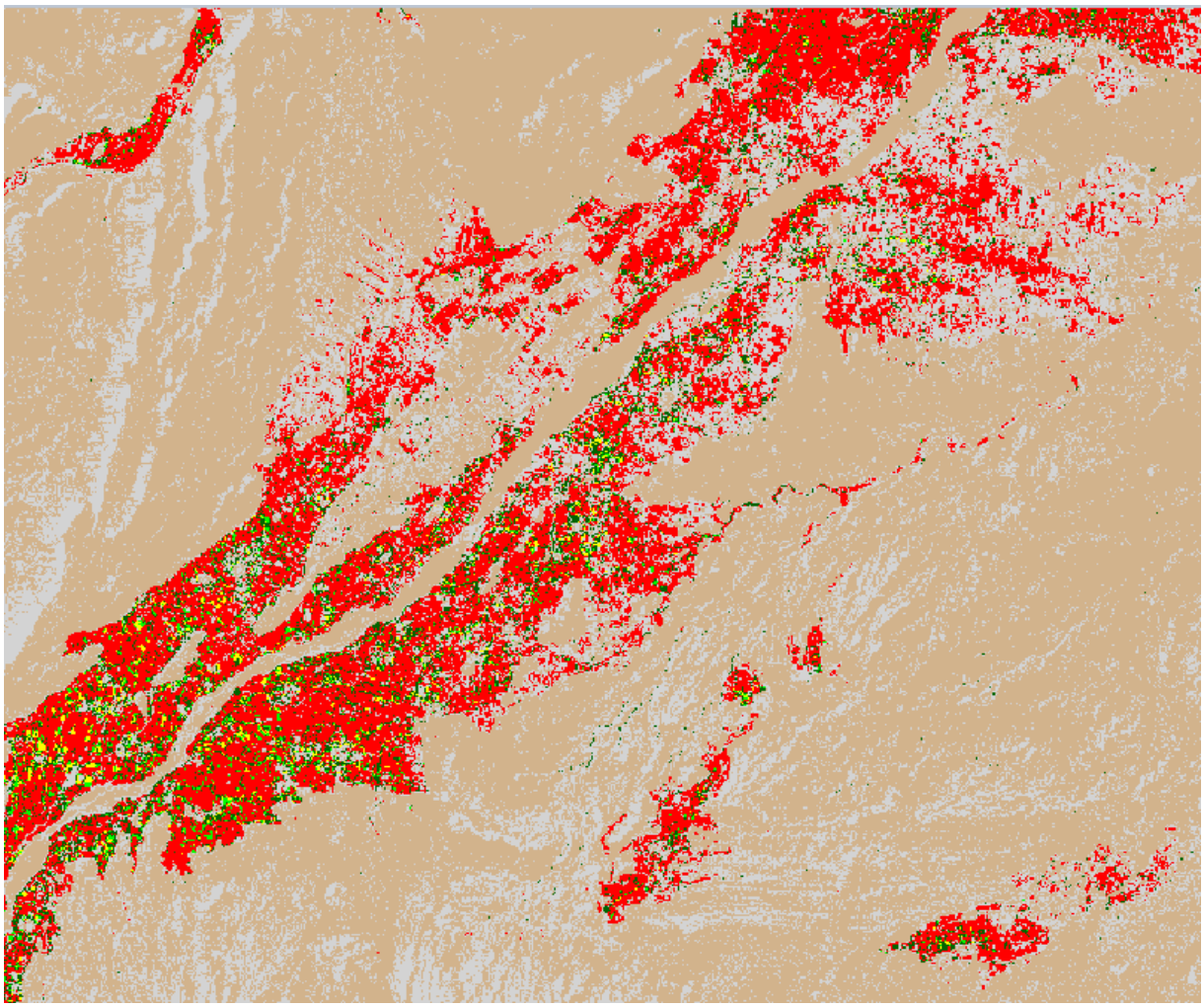

Key
Poppy
Wheat
Alfalfa
Trees
Bare
House

Nan25 25 Apr 04

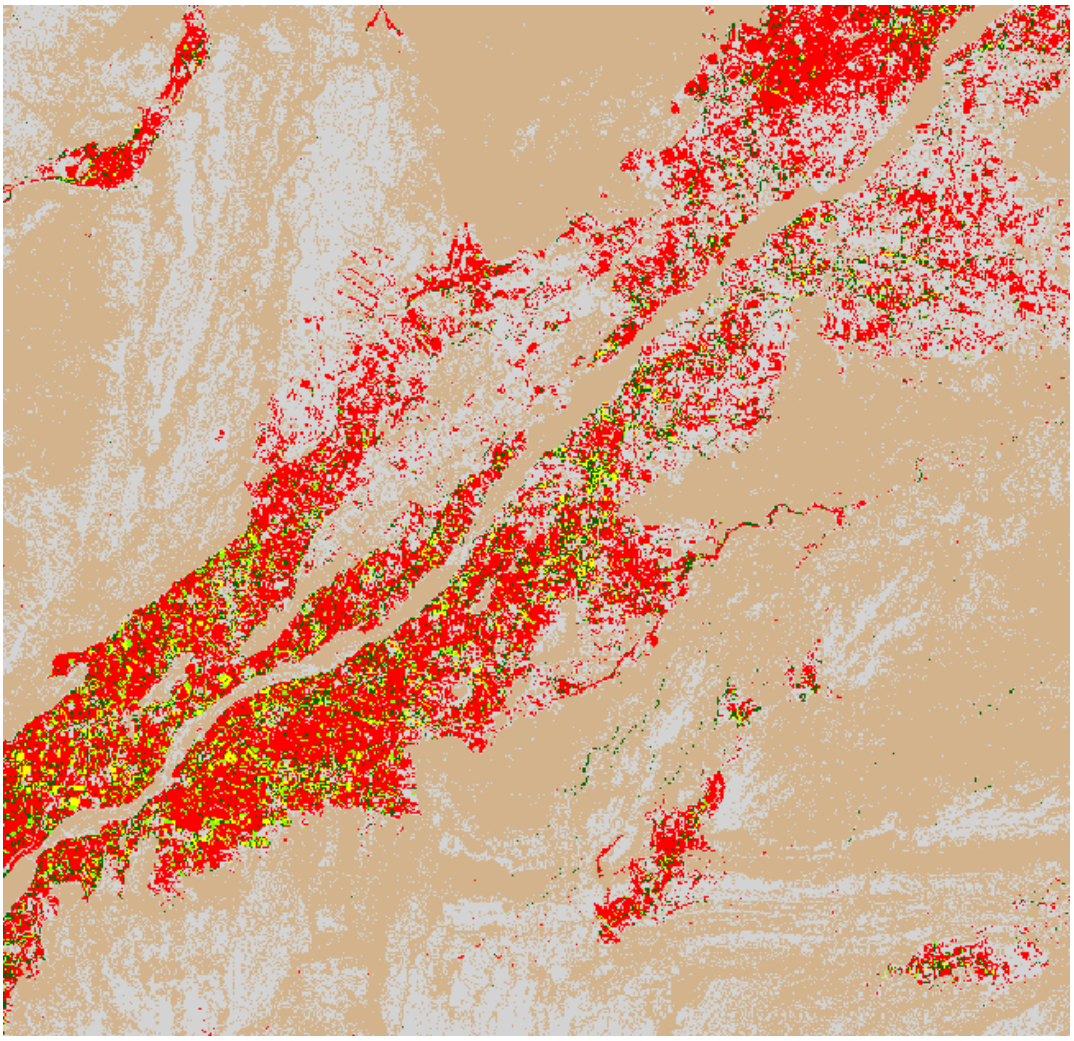

Key
Poppy
Wheat
Alfalfa
Trees
Bare
House

Nan11 25 Apr 04

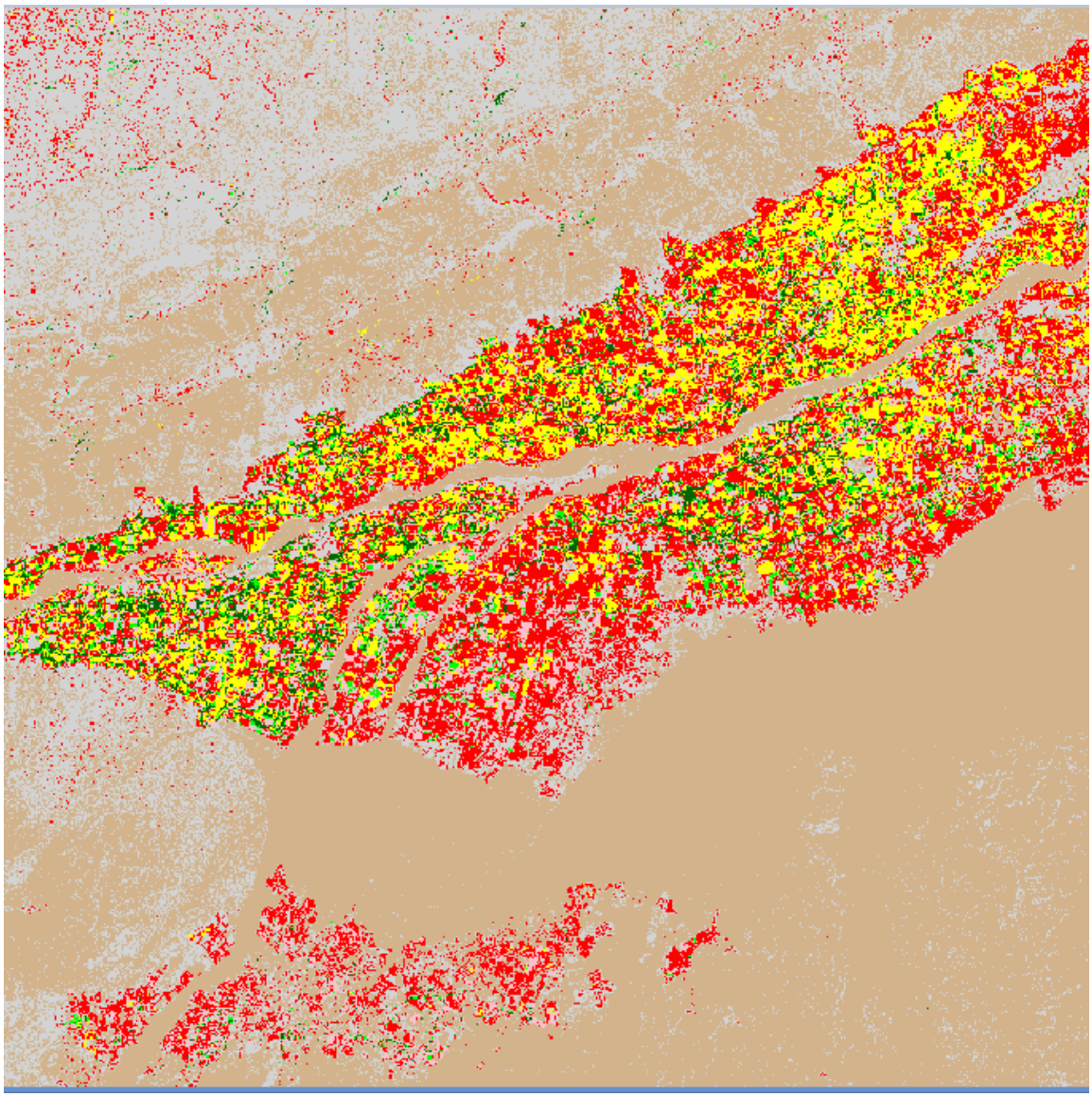

Key
Poppy
Wheat
Alfalfa
Trees
Bare
Onions
House

Nan11 17 May 04

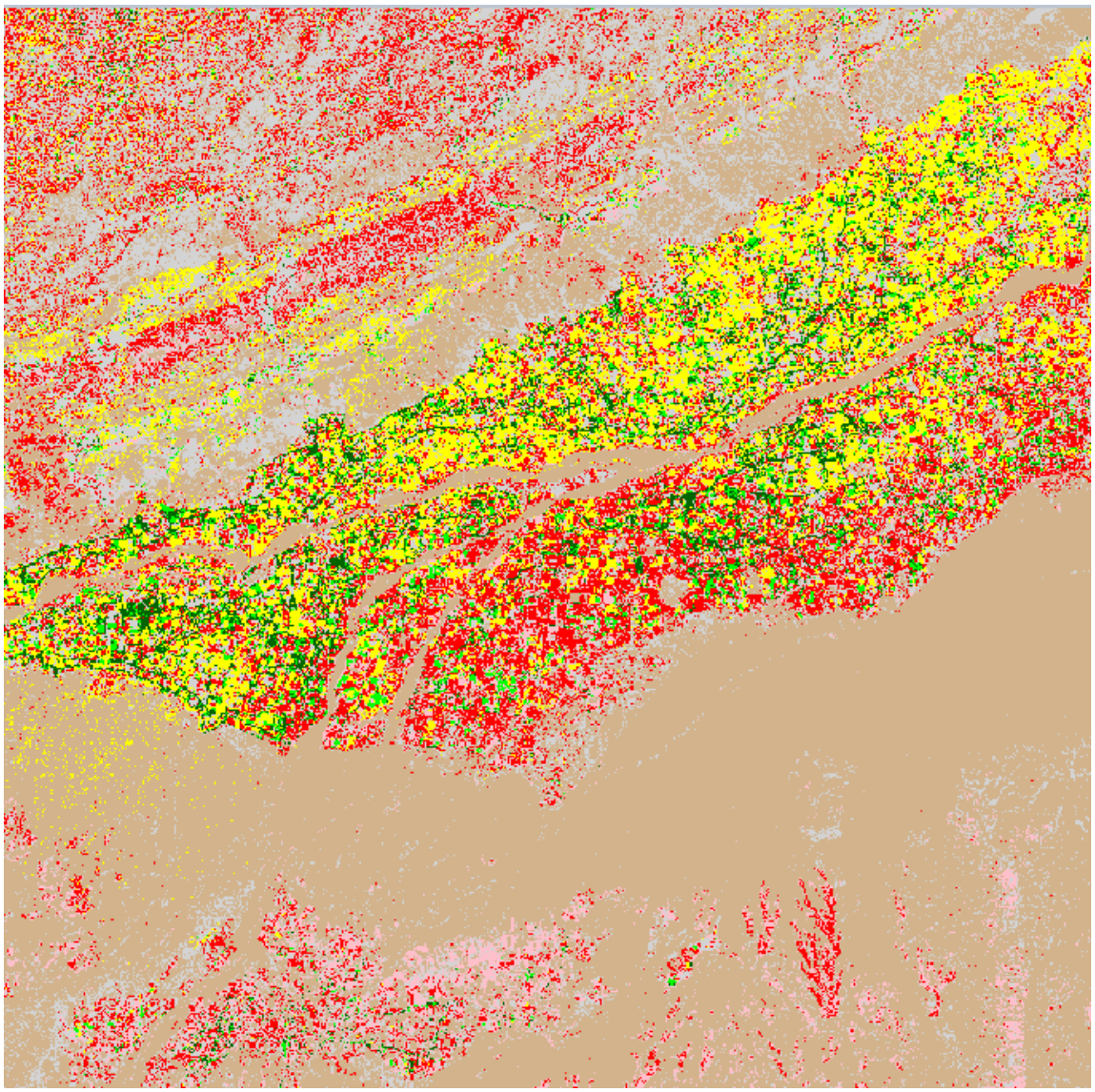

Key
Poppy
Wheat
Alfalfa
Trees
Bare
Onions
House

Nan29 11 Apr 10

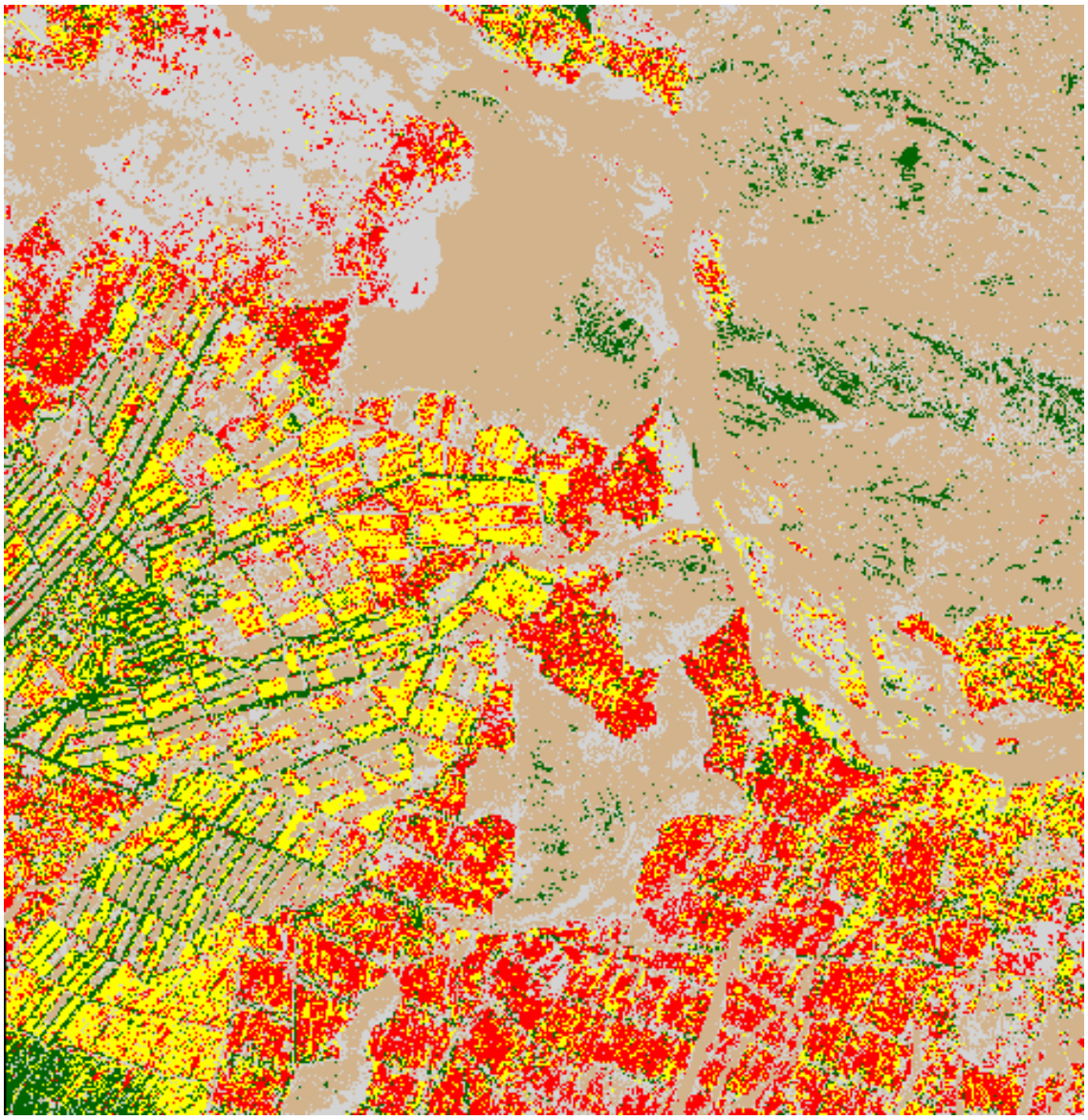

Key
Poppy
Wheat
Trees
Bare
House

Held87 25 Apr 04

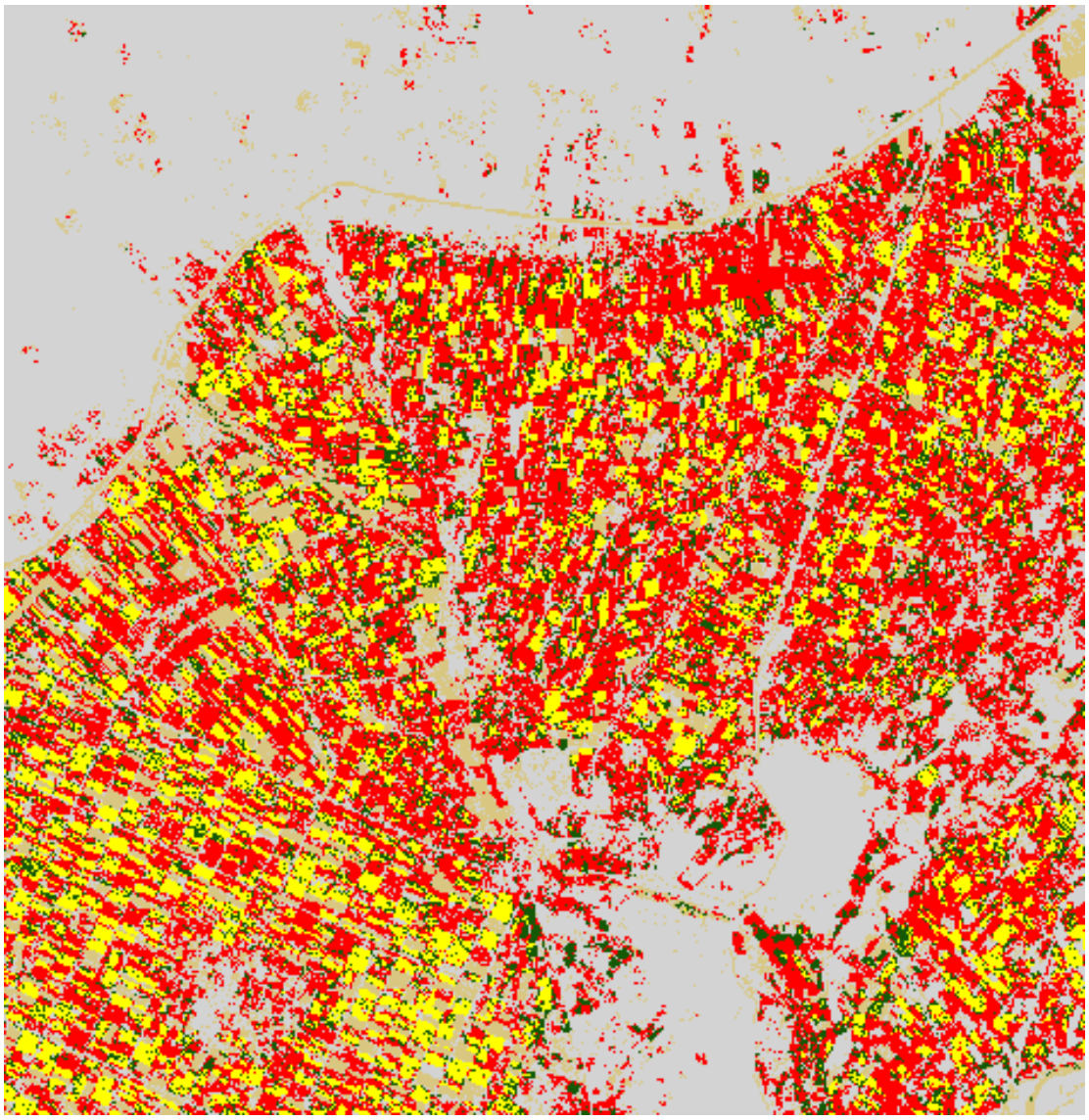

Key
Poppy
Wheat
Trees
Bare
House
Water

Held87 17 May 04

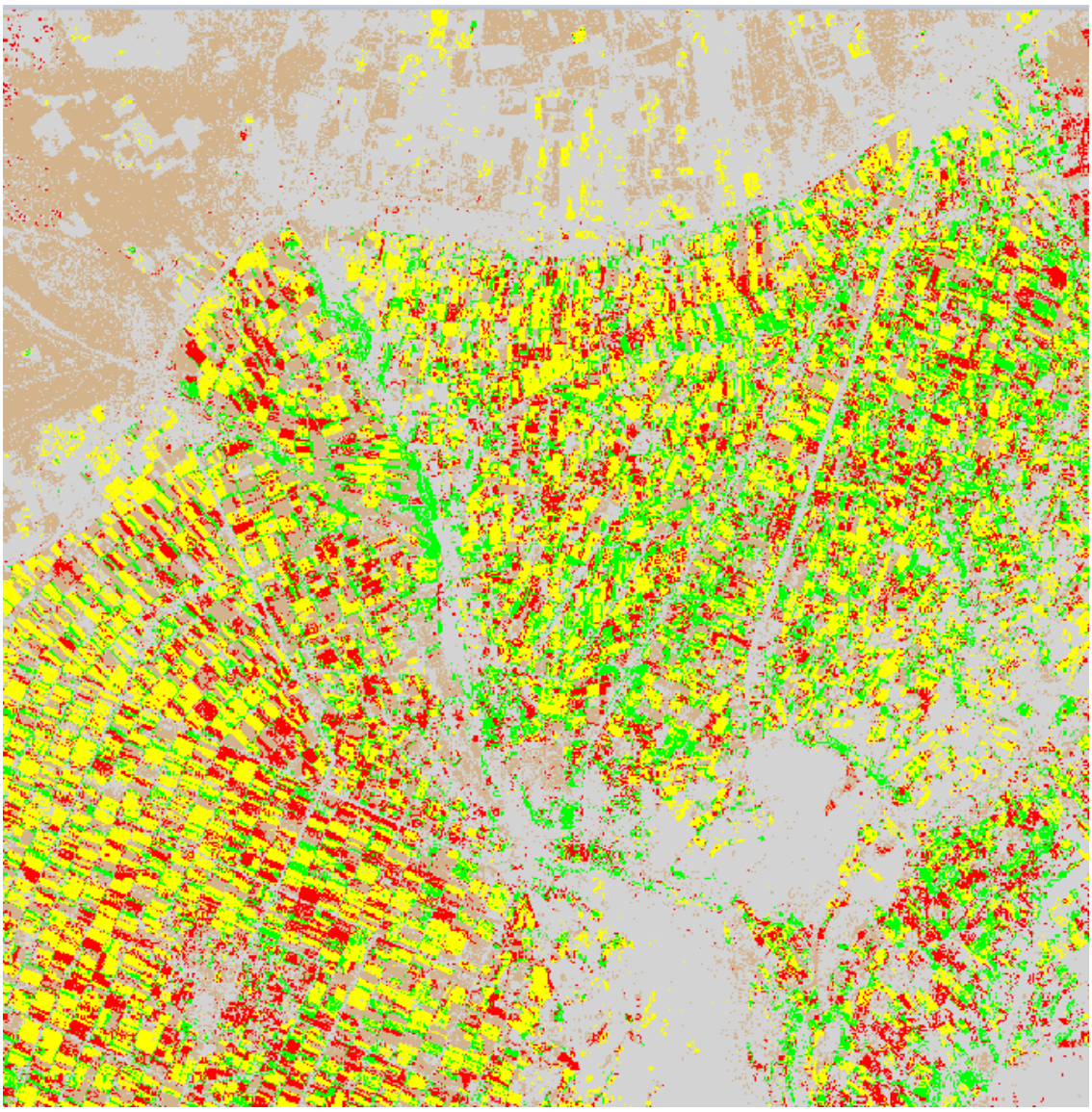

Key
Poppy
Wheat
Trees
Bare
House
Water

Held87 16 Feb 05

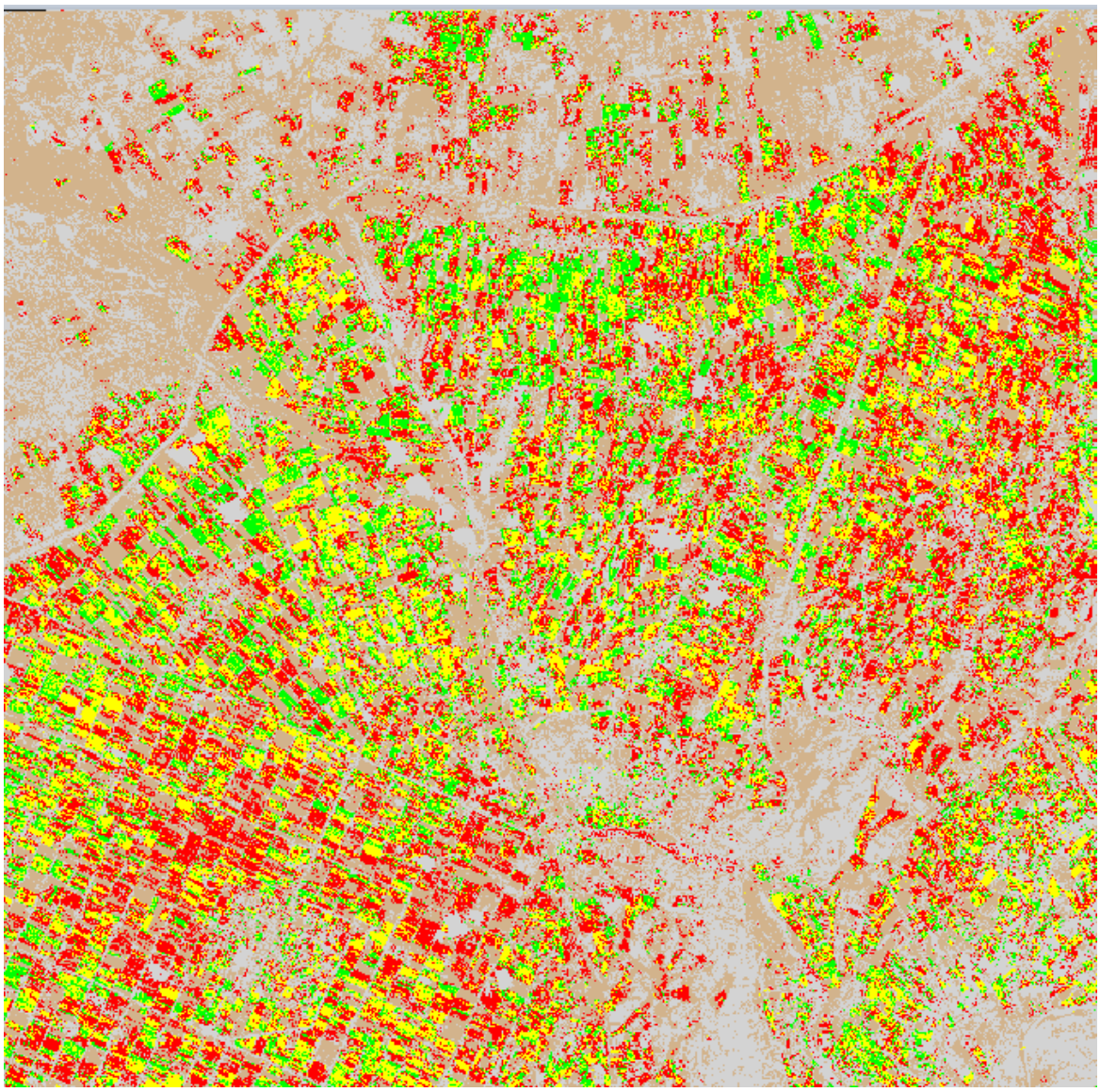

Key
Poppy
Wheat
Alfalfa
Bare
House
Water

Held87 21 Mar 05

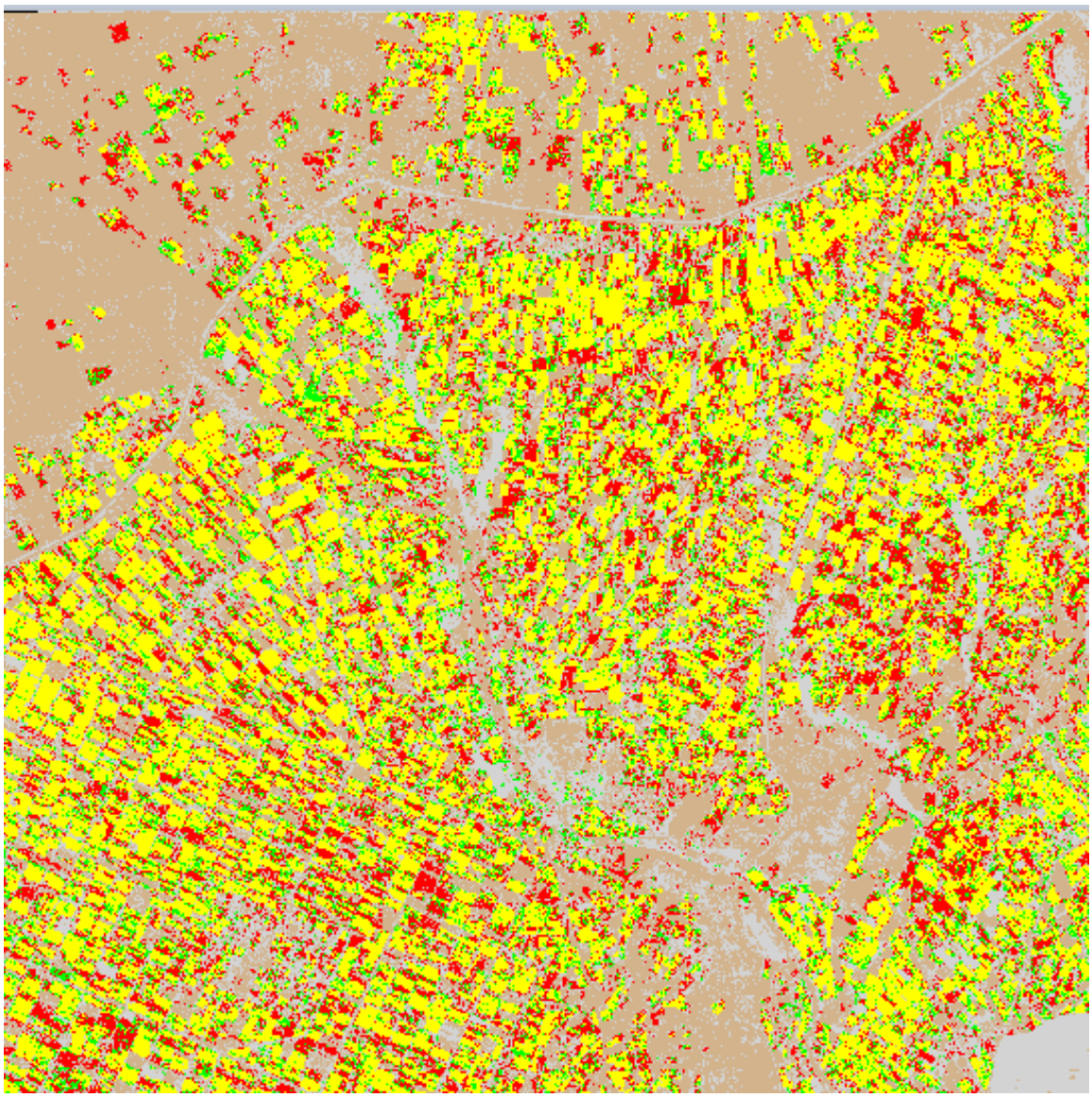

Key
Poppy
Wheat
Alfalfa
Bare
House
Water

Held57 28 Apr 04

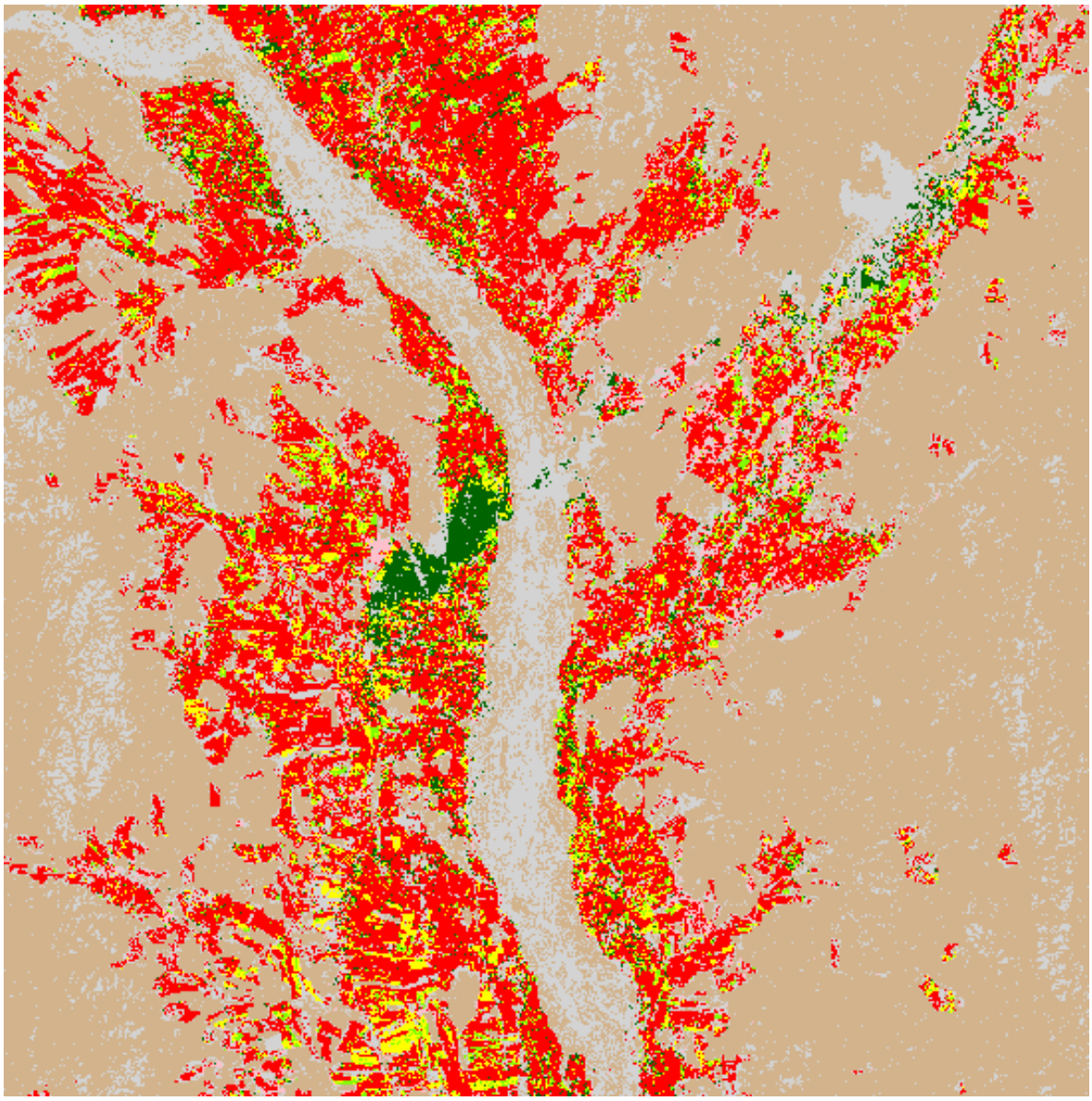

Key
Poppy
Wheat
Alfalfa
Trees
Bare
Non Agri Veg
House

Held57 20 May 04

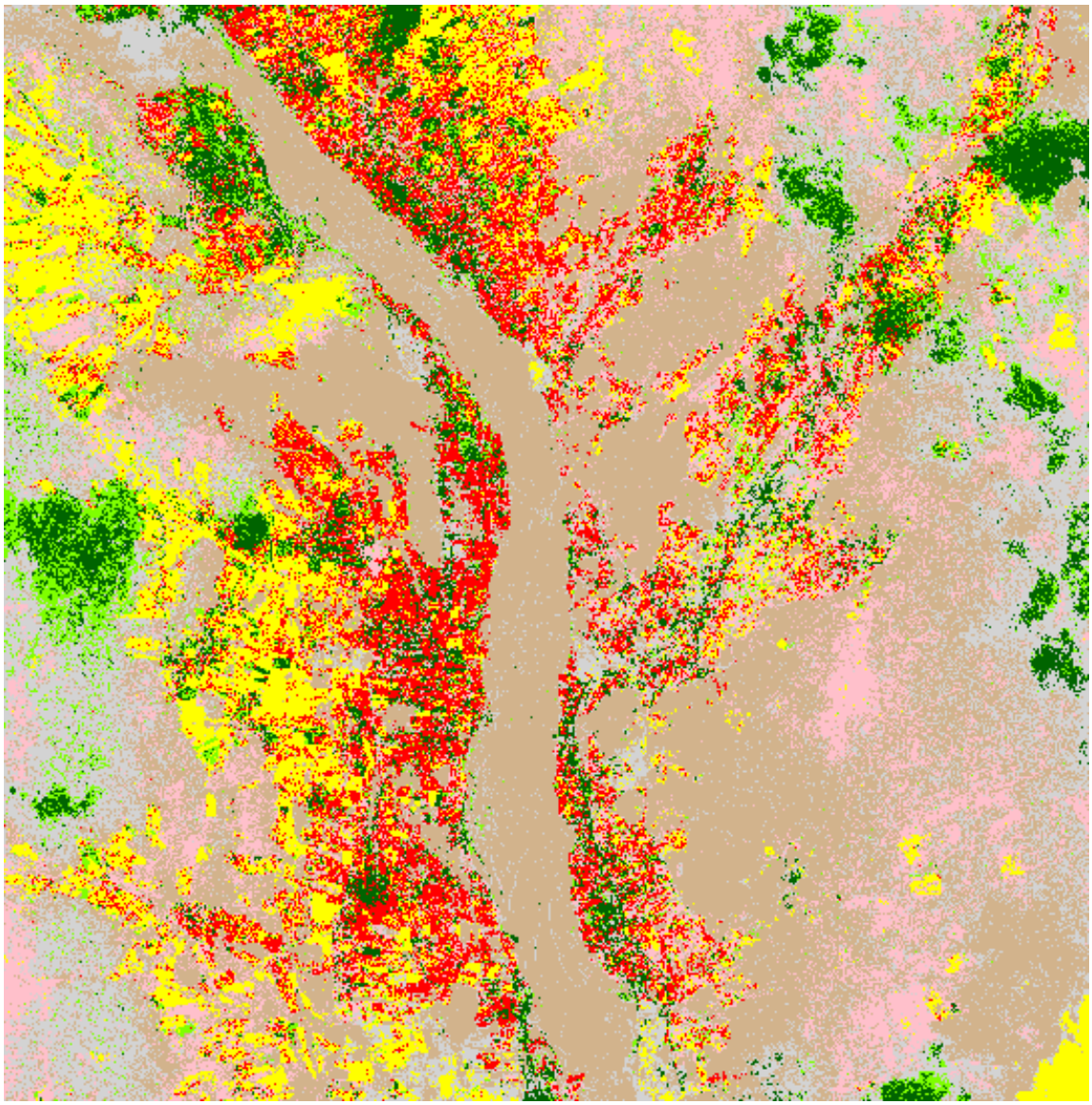

Key
Poppy
Wheat
Alfalfa
Trees
Bare
Non Agri Veg
House

Held57 19 Feb 05

Key
Poppy
Wheat
Alfalfa
Trees
Bare
Non Agri Veg
House

Held 57 29 Mar 05

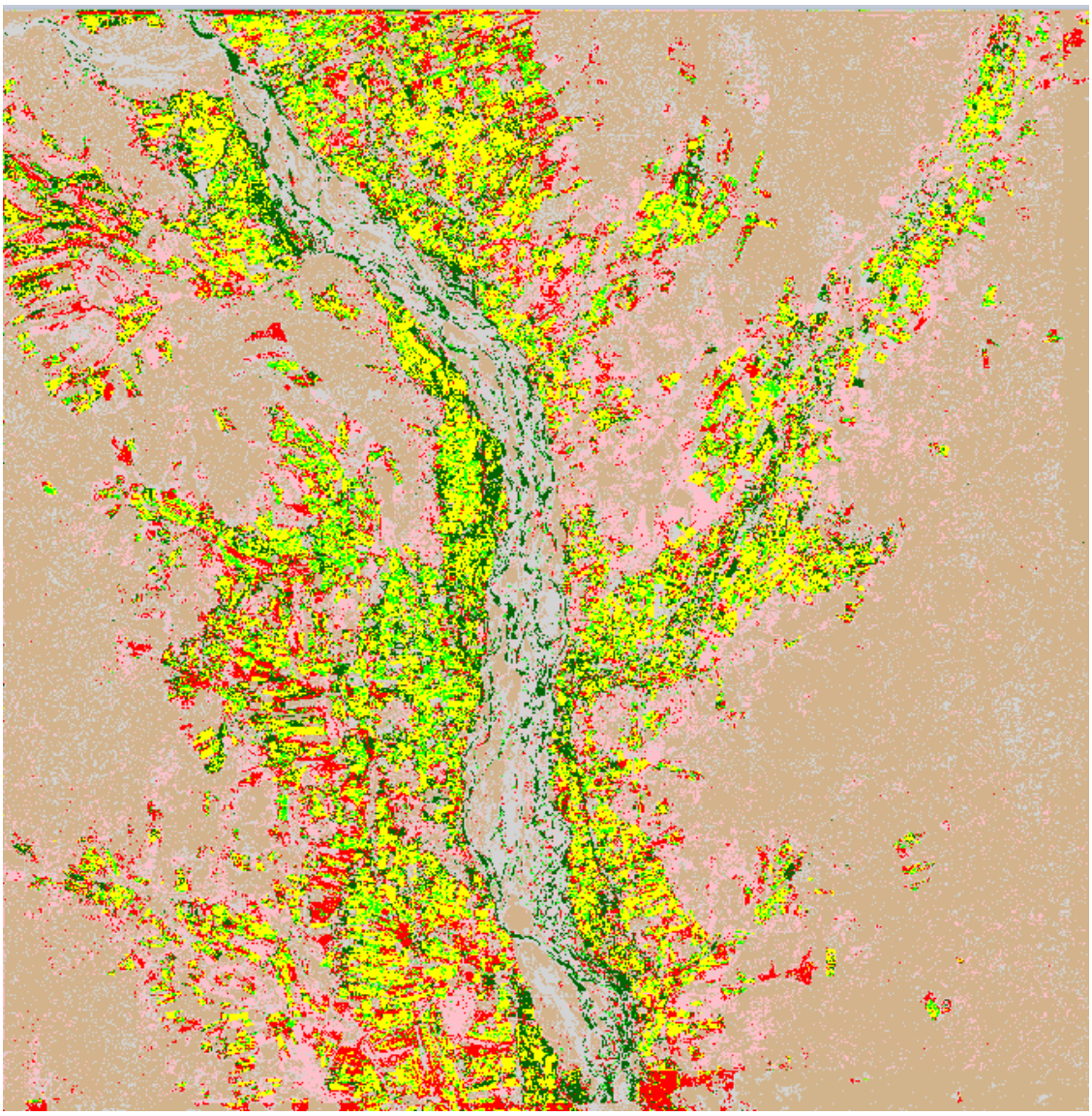

Key
Poppy
Wheat
Alfalfa
Trees
Bare
Non Agri Veg
House

Held115 29 Apr 04

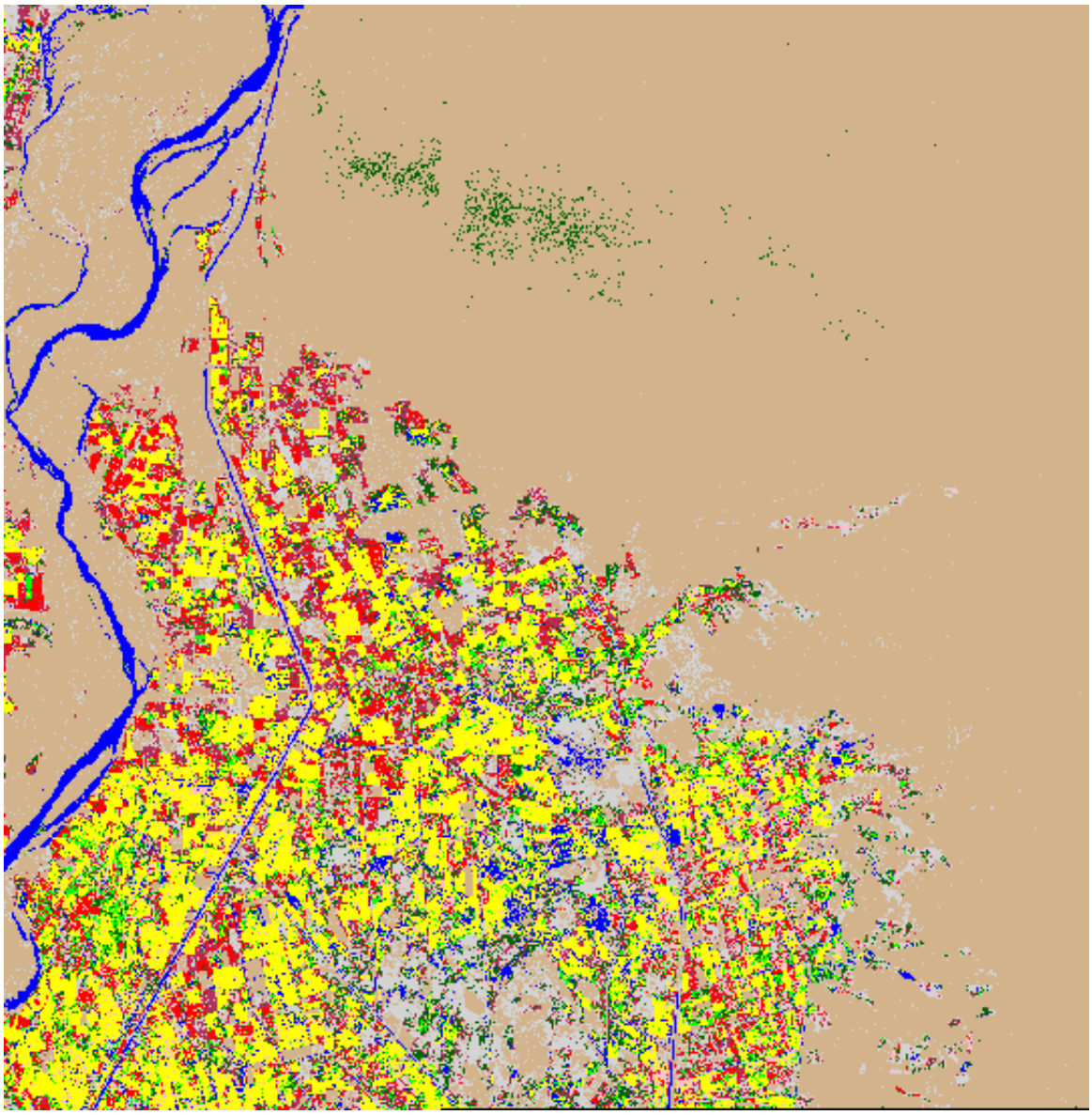

Key
Poppy
Wheat
Alfalfa
Trees
Bare
Vineyard
Non Agri Veg
House
Water

Held115 17 May 04

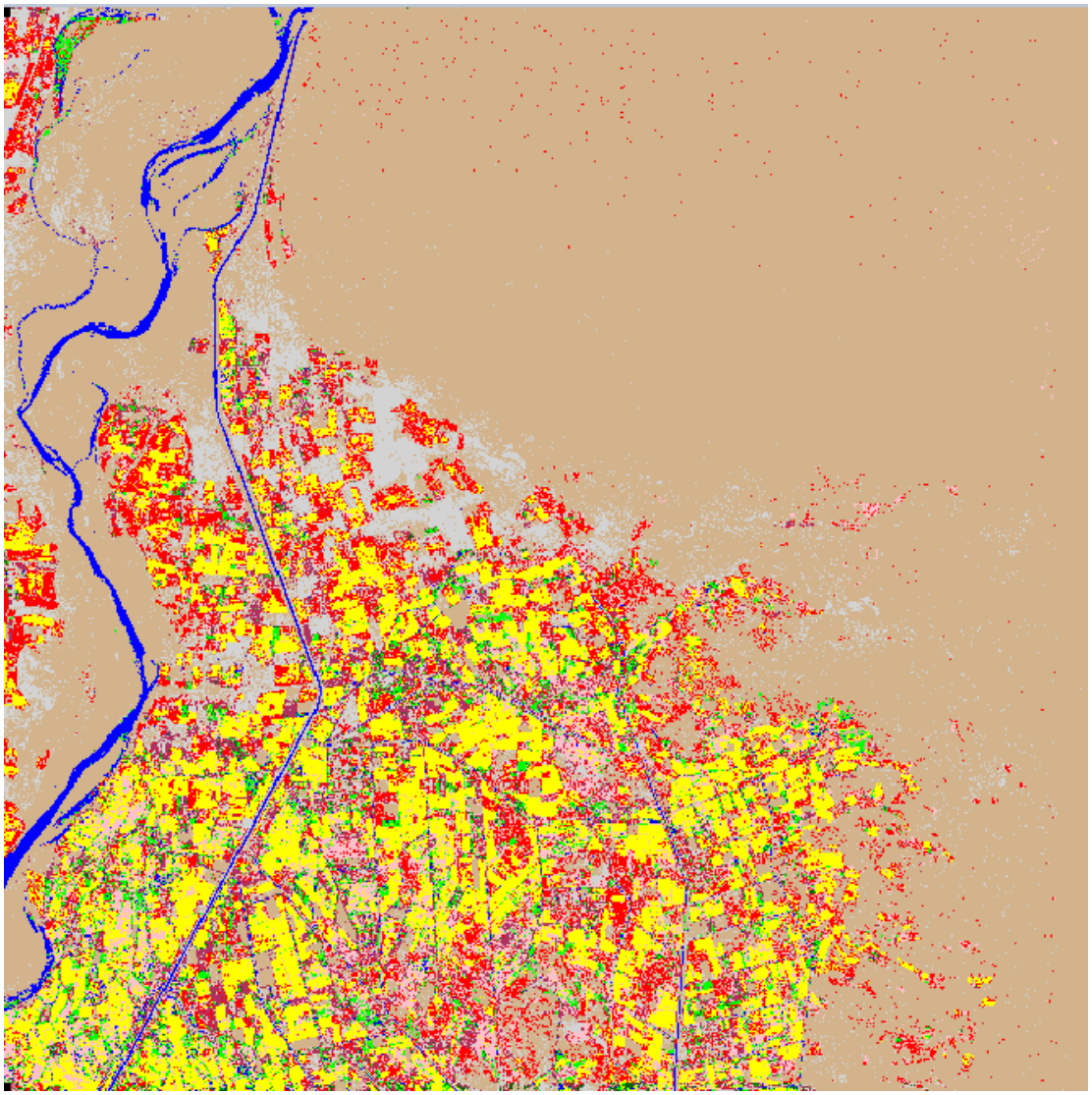

Key
Poppy
Wheat
Alfalfa
Trees
Bare
Vineyard
Non Agri Veg
House
Water

Held115 10 Feb 05

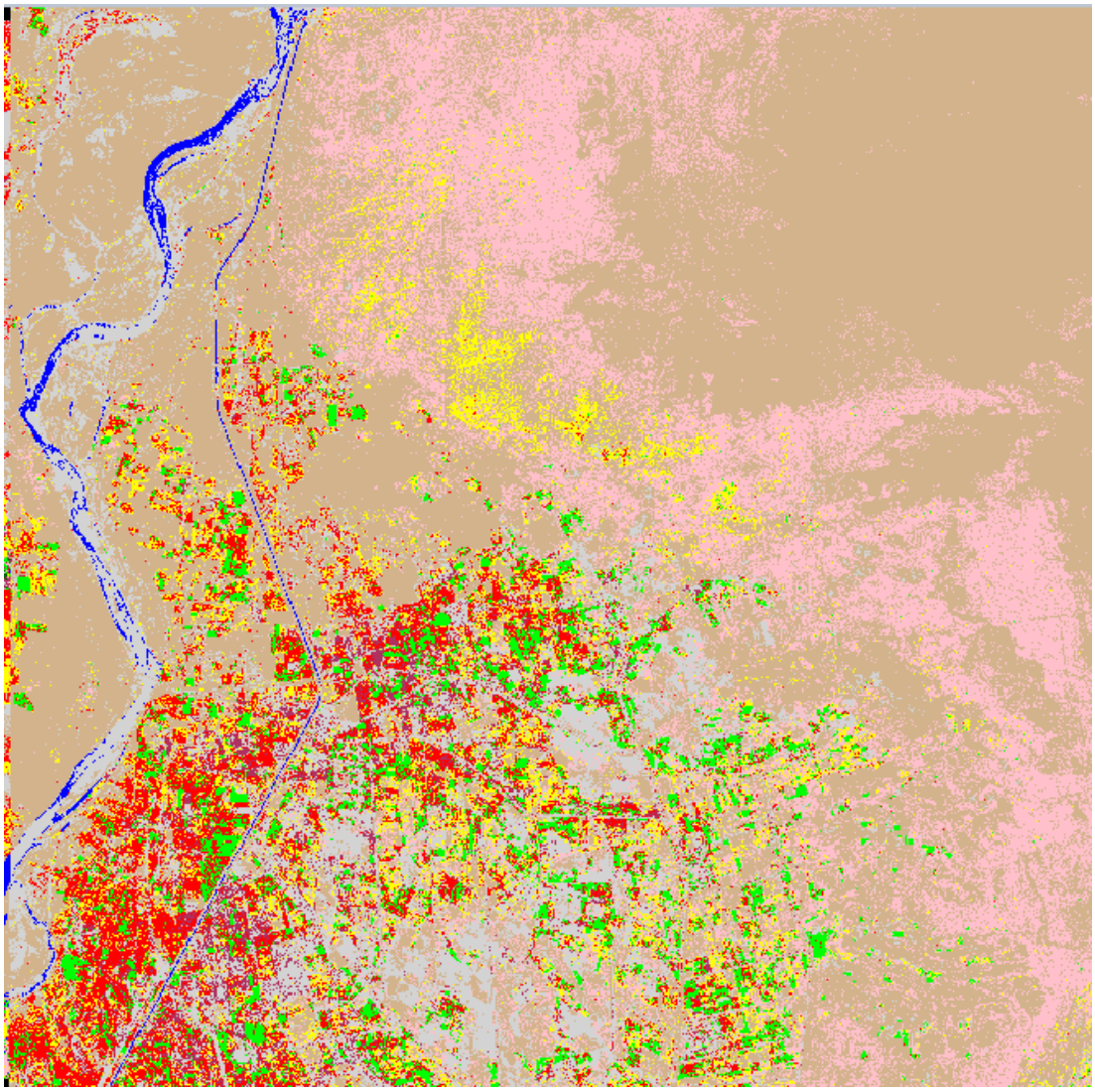

Key
Poppy
Wheat
Alfalfa
Trees
Bare
Vineyard
Non Agri Veg
House
Water

Held115 21 Mar 05

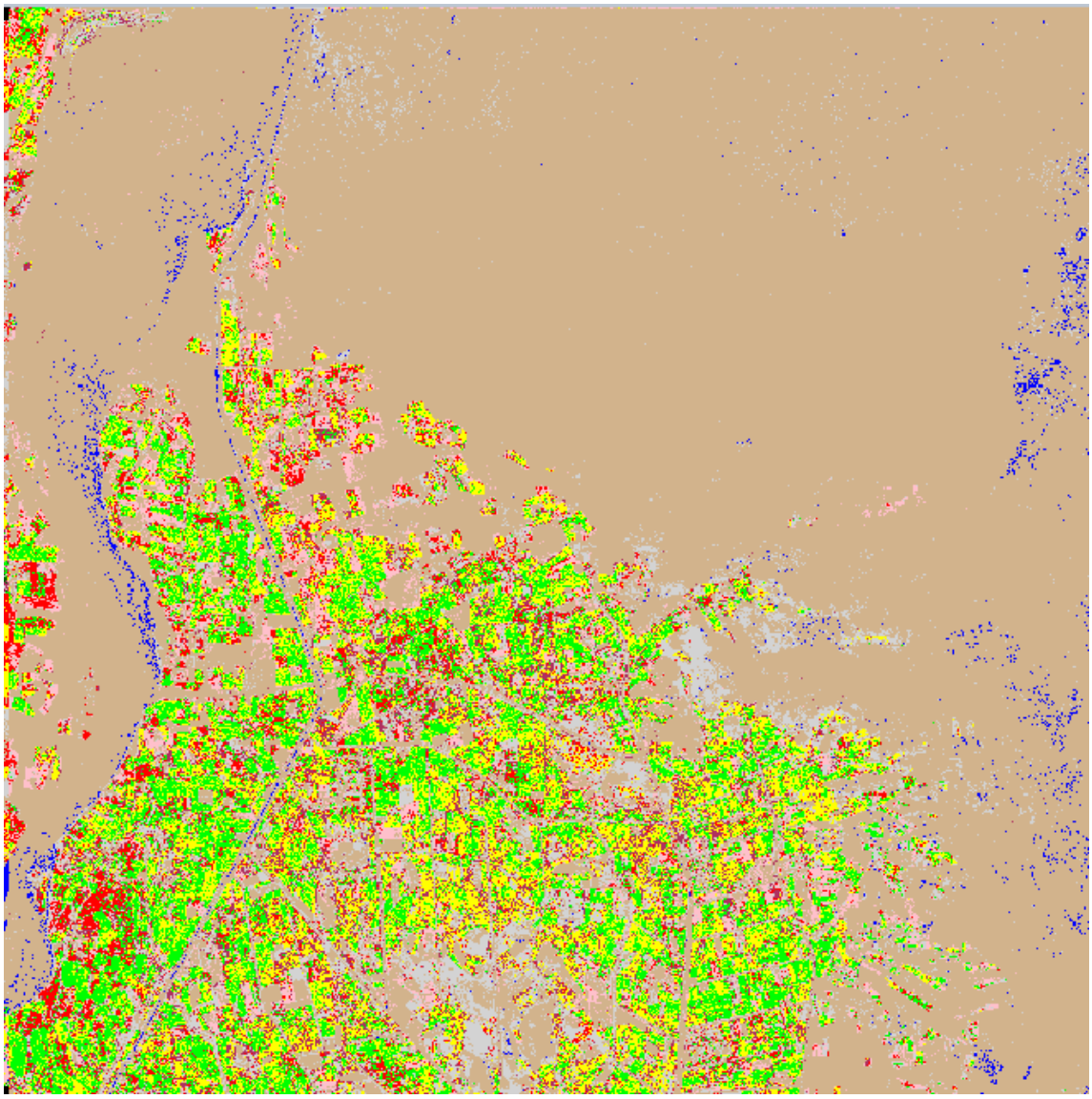

Key
Poppy
Wheat
Alfalfa
Trees
Bare
Vineyard
Non Agri Veg
House
Water

Kand73 26 Mar 05

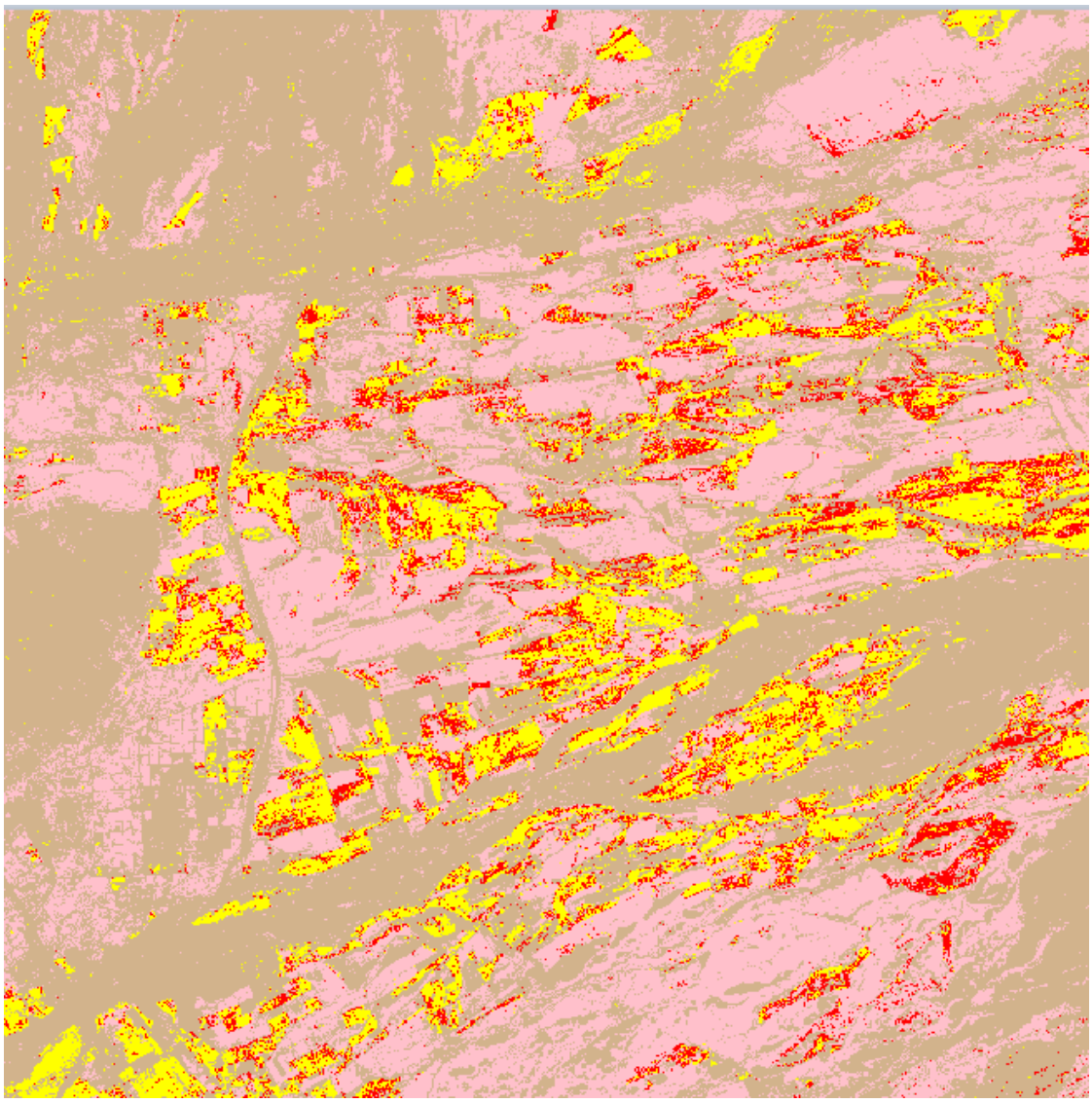

Key
Poppy
Wheat
Non Agri Veg
Bare

Kand84 26 Mar 05

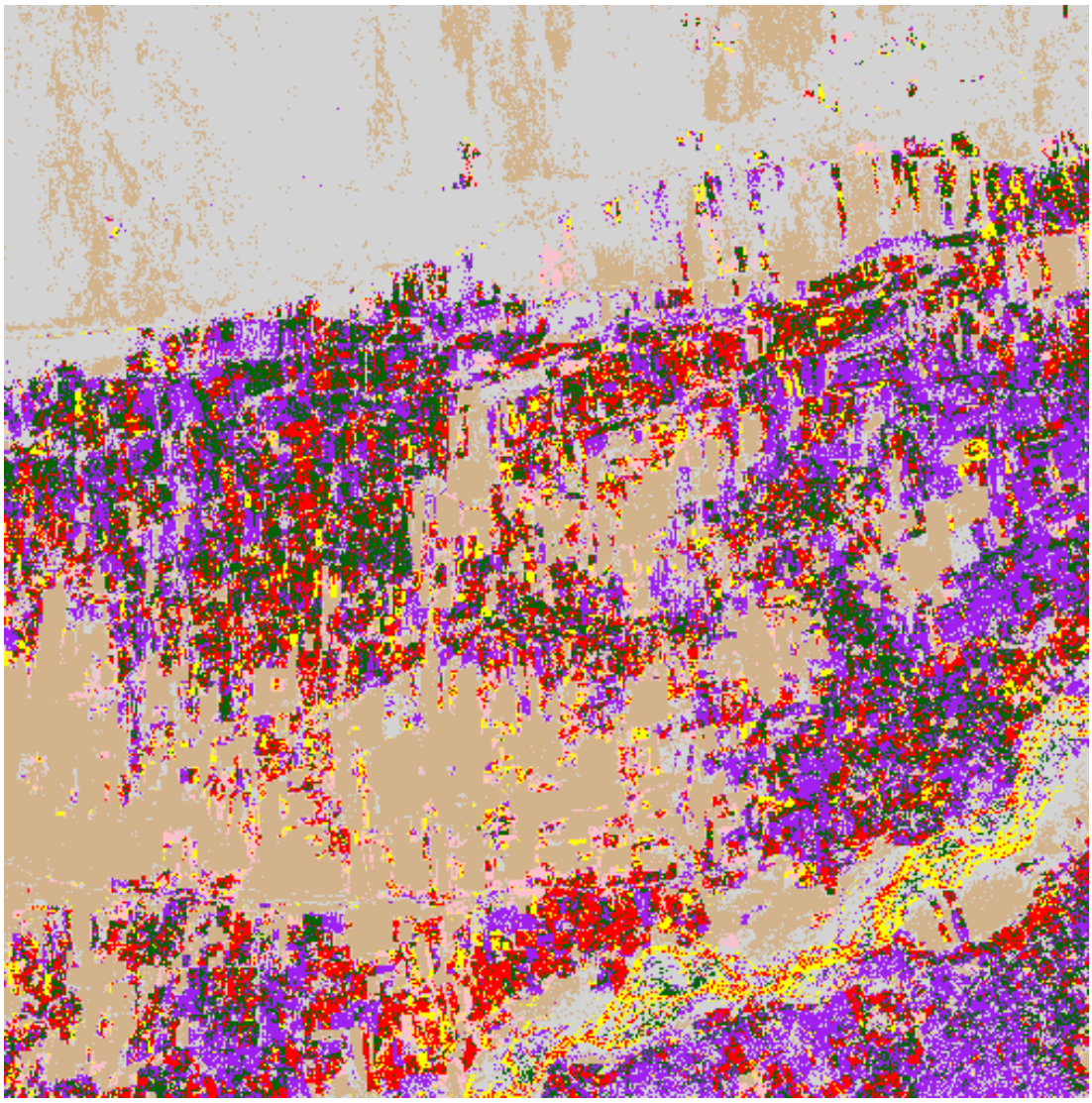

Key
Poppy
Wheat
Alfalfa
Trees
Bare
Vineyard
Non Agri Veg
House

Kand135 26 Mar 05

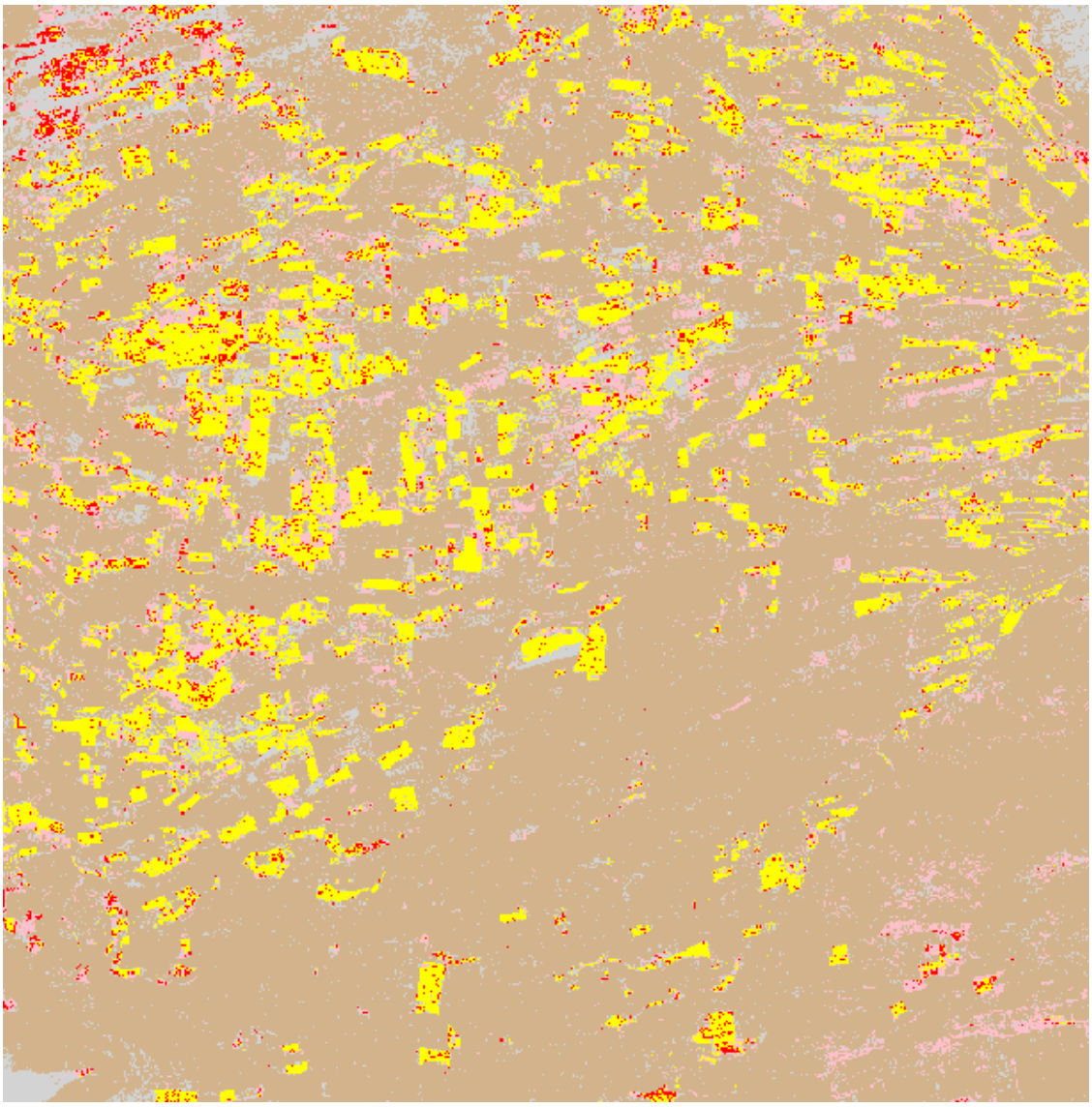

Key
Poppy
Wheat
Bare
Non Agri Veg
House

Nan25 Two-date Classification - 11 Apr 04 and 25 Apr 04

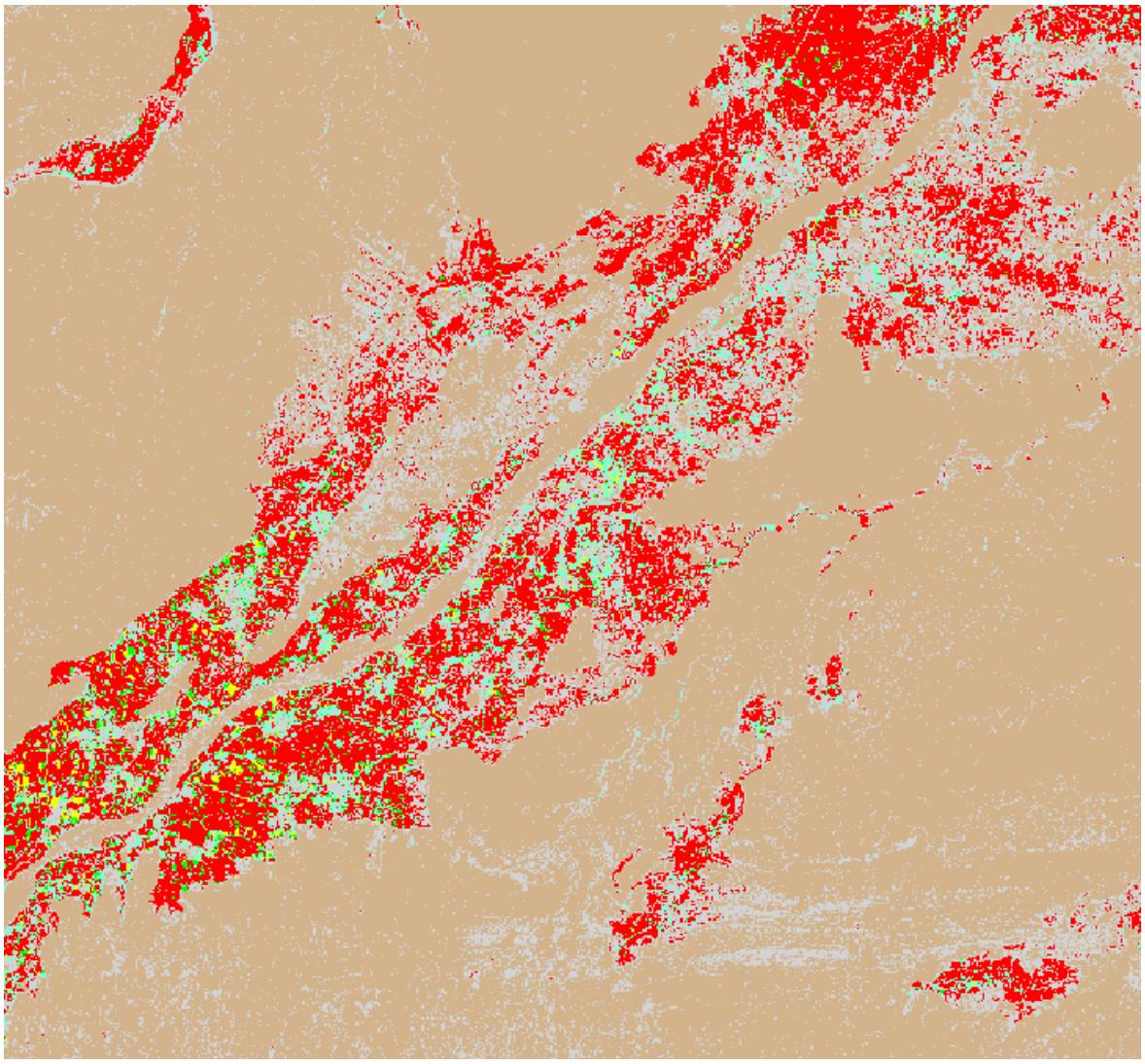

Key
Poppy
Wheat
Alfalfa
Trees
Bare
House

Nan11 Two-date Classification - 25 Apr 04 and 17 May 04

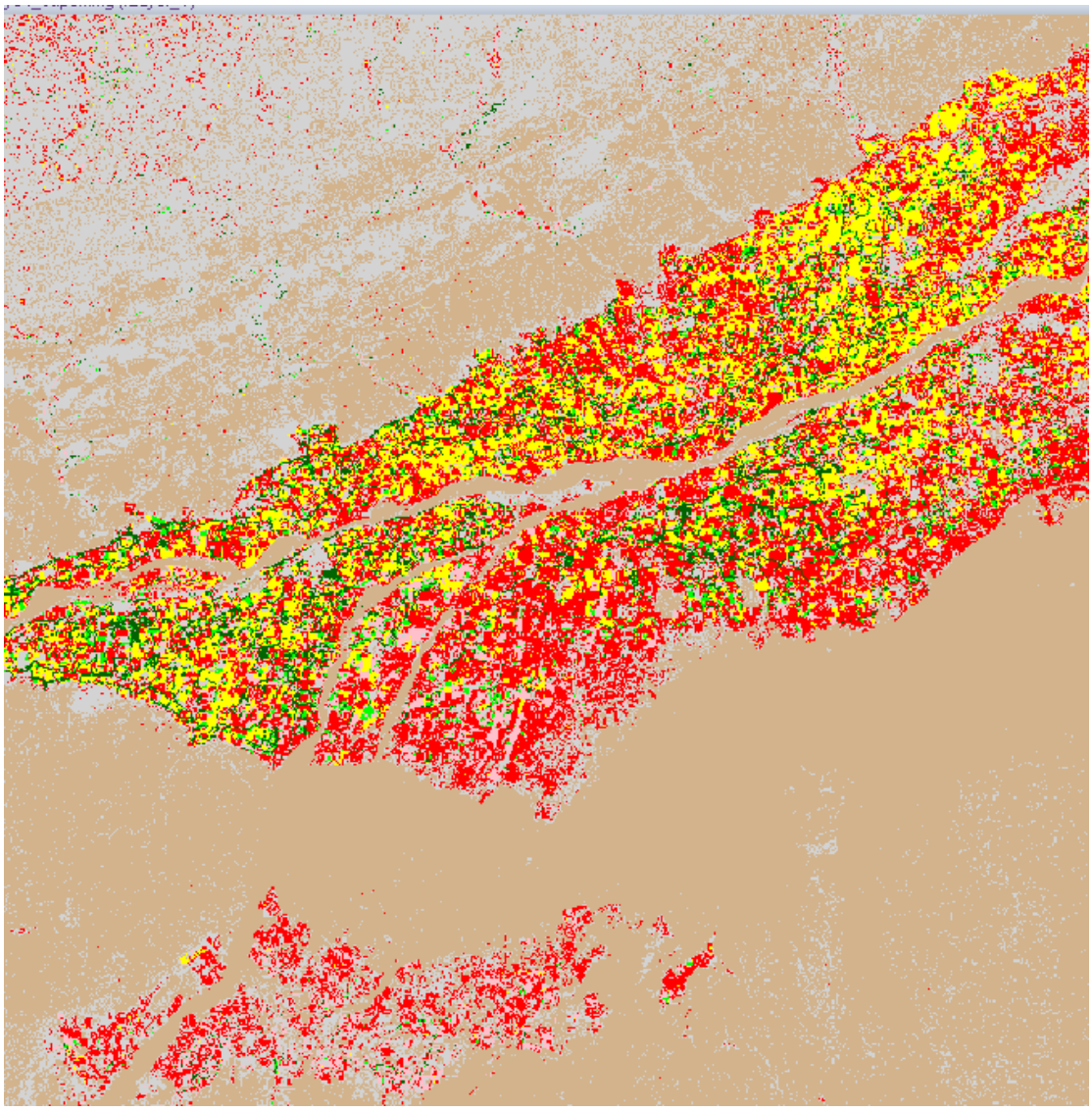

Key
Poppy
Wheat
Alfalfa
Trees
Bare
Onions
House

Held87 Two-date Classification - 25 Apr and 17 May 04

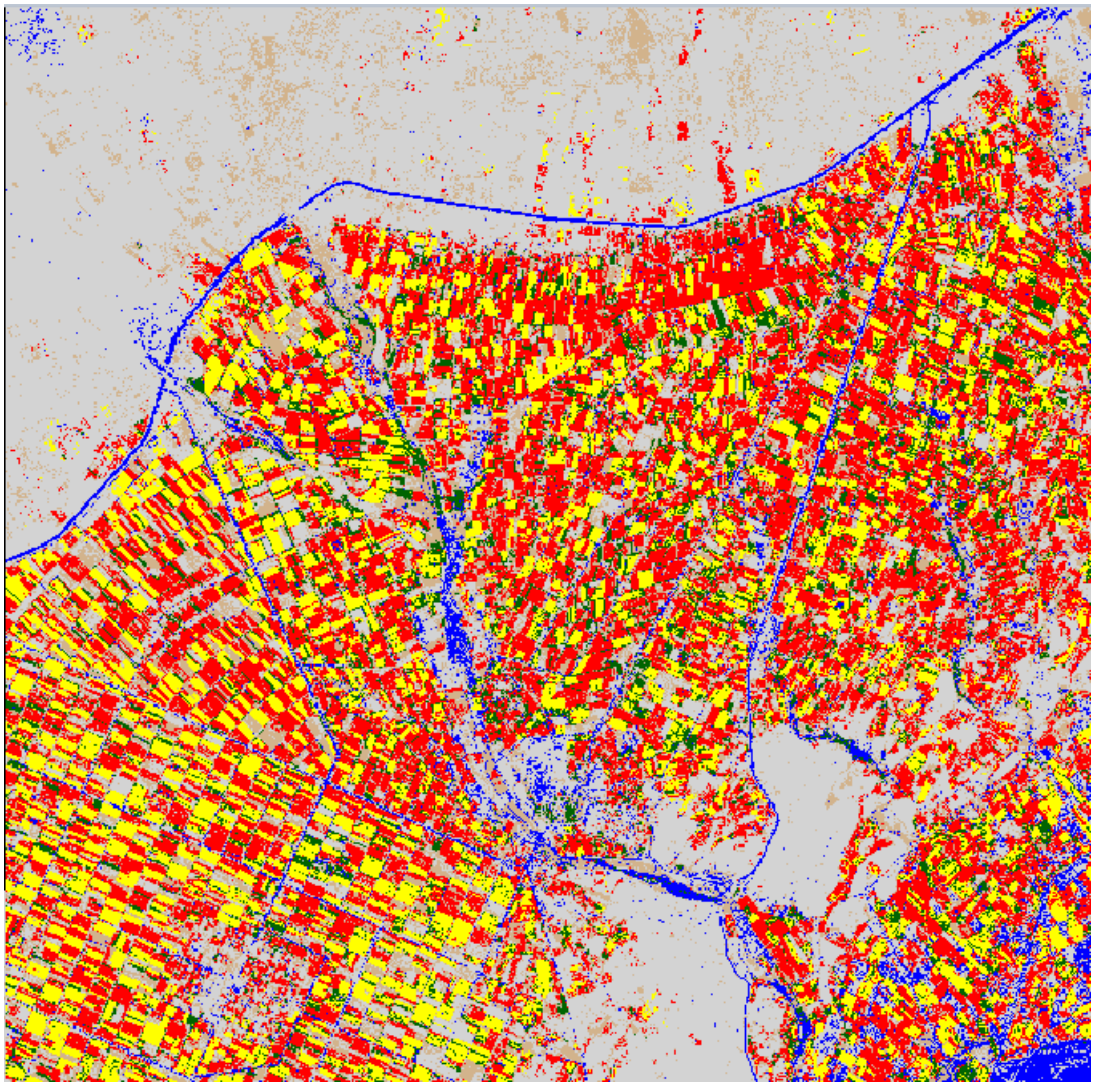

Key
Poppy
Wheat
Trees
Bare
House
Water

Held87 Two-date Classification - 16 Feb and 21 Mar 05

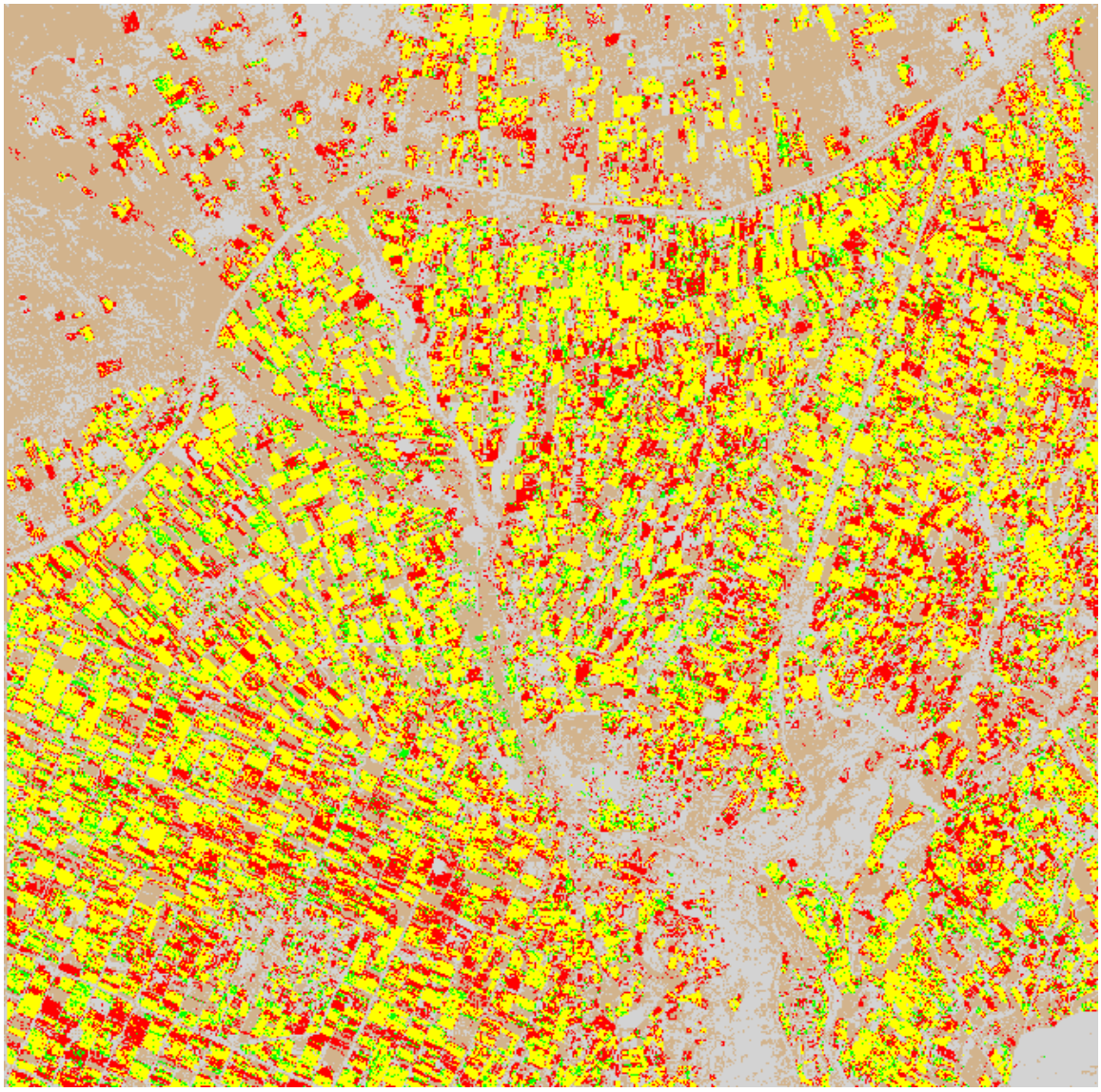

Key
Poppy
Wheat
Trees
Bare
House
Water

Held57 Two-date Classification - 28Apr 04 and 20 May 04

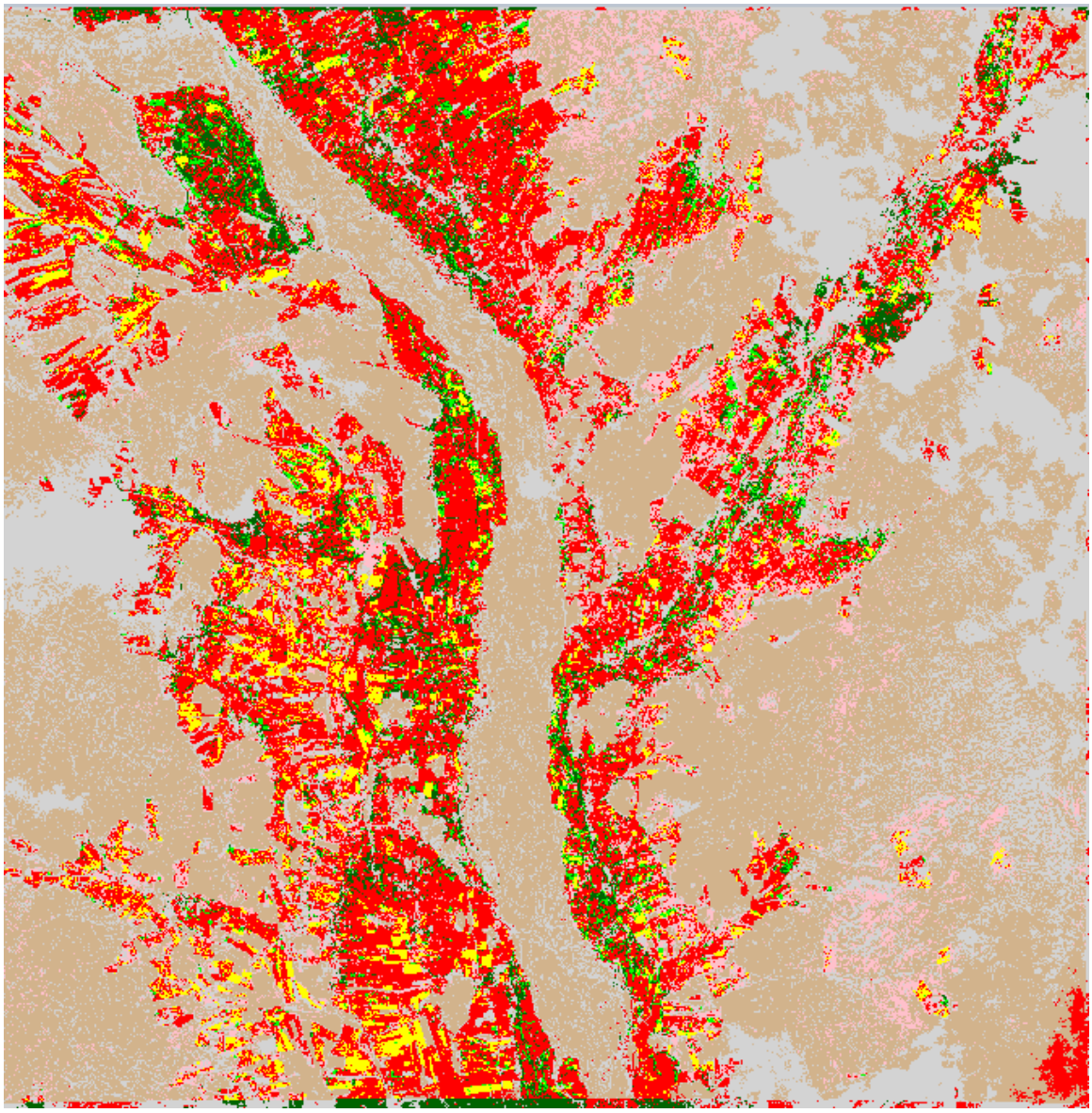

Key
Poppy
Wheat
Alfalfa
Trees
Bare
Non Agri Veg
House

Held57 Two-date Classification - 19 Feb 05 and 29 Mar 05

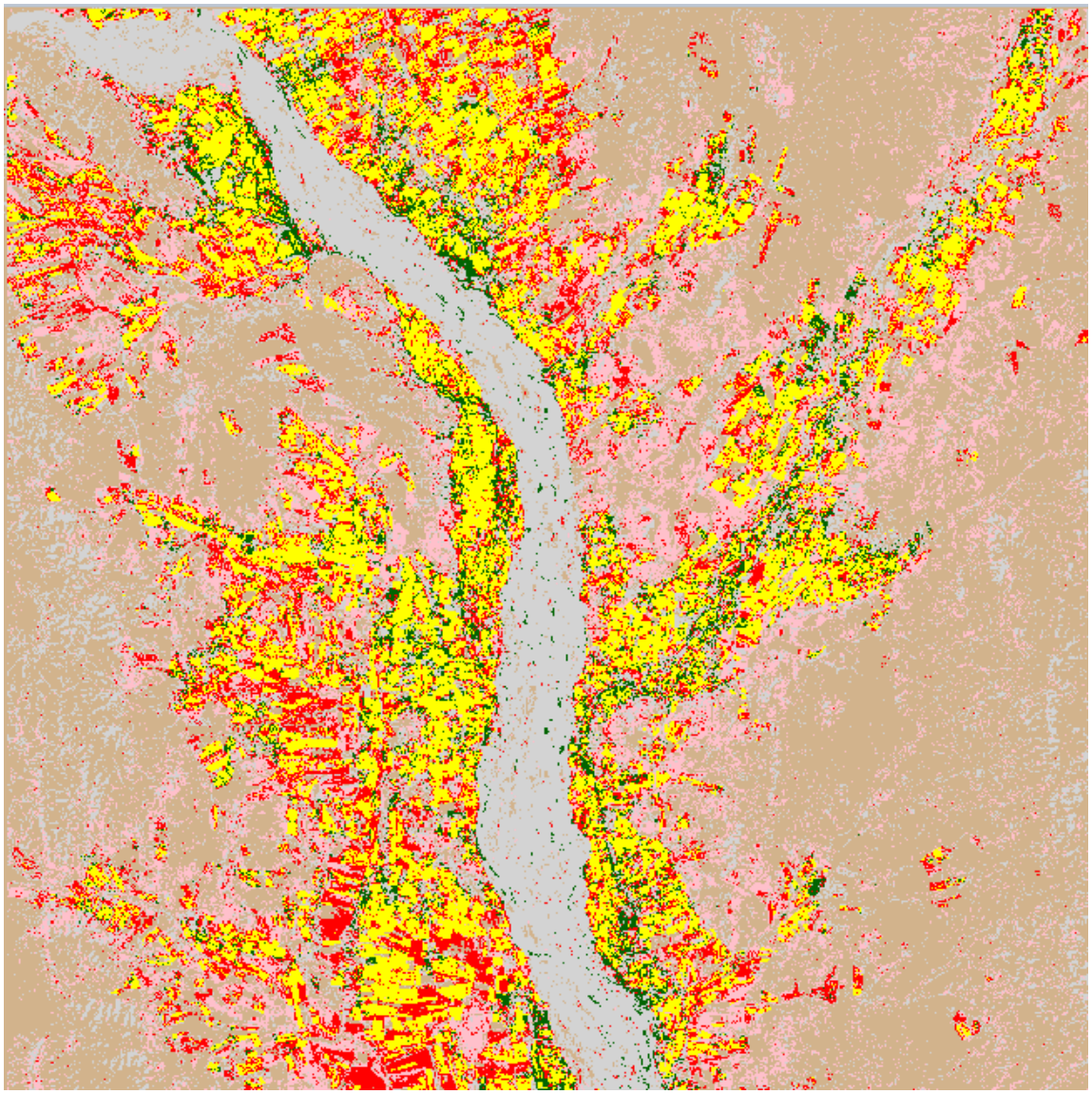

Key
Poppy
Wheat
Alfalfa
Trees
Bare
Non Agri Veg
House

Held115 Two-date Classification - 29 Apr 04 and 17 May 04

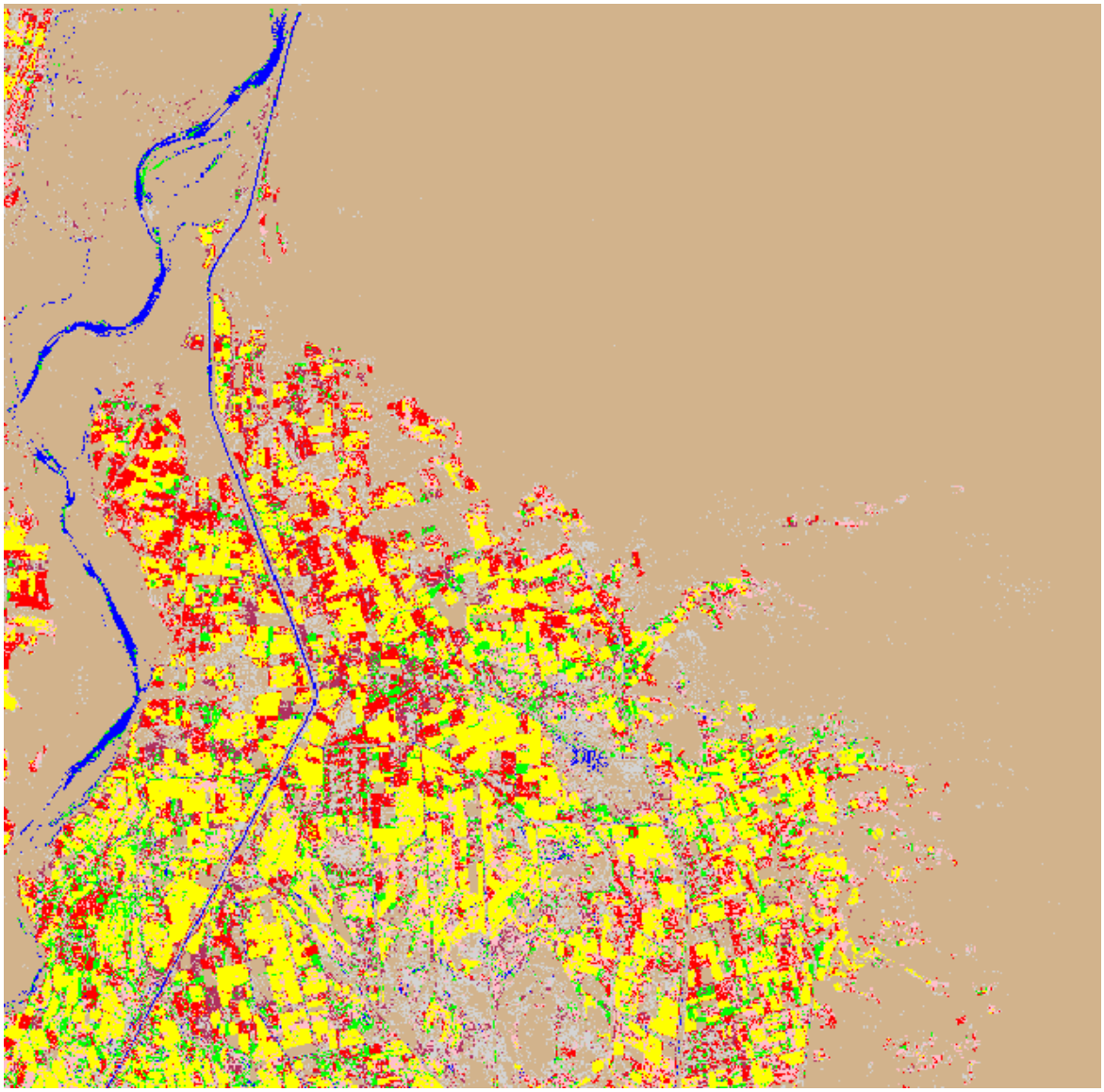

Key
Poppy
Wheat
Alfalfa
Trees
Bare
Vineyard
Non Agri Veg
House
Water

Appendix E Classification Accuracy

Cover Sheet